Paternal *Grb10* in Brain and Behaviour

Kira Dena Anne Rienecker

Submitted for consideration for award of PhD

School of Medicine

Cardiff University

2018

Declaration

DECLARATION

This work has not been submitted in substance for any other degree or award at this or any other university or place of learning, nor is being submitted concurrently in candidature for any degree or other award.

Signed ……..…… (candidate) Date ……..……

STATEMENT 1

This thesis is being submitted in partial fulfillment of the requirements for the degree of PhD.

Signed ……..…… (candidate) Date ……..……

STATEMENT 2

This thesis is the result of my own independent work/investigation, except where otherwise stated, and the thesis has not been edited by a third party beyond what is permitted by Cardiff University's Policy on the Use of Third Party Editors by Research Degree Students. Other sources are acknowledged by explicit references. The views expressed are my own.

Signed ……..…… (candidate) Date ……..……

STATEMENT 3

I hereby give consent for my thesis, if accepted, to be available online in the University's Open Access repository and for inter-library loan, and for the title and summary to be made available to outside organisations.

Signed ……..…… (candidate) Date ……..……

STATEMENT 4: PREVIOUSLY APPROVED BAR ON ACCESS

I hereby give consent for my thesis, if accepted, to be available online in the University's Open Access repository and for inter-library loans **after expiry of a bar on access previously approved by the Academic Standards & Quality Committee.**

Signed ……..…… (candidate) Date ……..……

Said Conrad Cornelius o'Donald o'Dell,
My very young friend who is learning to spell:
"The A is for Ape. And the B is for Bear.
"The C is for Camel. The H is for Hare.
"The M is for Mouse. And the R is for Rat.
"I know *all* the twenty-six letters like that…

"…through to Z is for Zebra. I know them all well."
Said Conrad Cornelius o'Donald o'Dell.
"So now I know everything *anyone* knows
"From beginning to end. From the start to the close.
"Because Z is as far as the Alphabet goes."

Then he almost fell flat on his face on the floor
When I picked up the chalk and drew one letter more!
A letter he never had dreamed of before!
And I said "*You* can stop, if you want, with the Z.
"Because most people stop with the Z
"*But not me!*

"In the places I go there are things that I see
"That I *never* could spell if I stopped with the Z.
"I'm telling you this 'cause you're one of my friends.
"*My* alphabet starts where *your* alphabet ends!"

…..

When you go beyond Zebra,
Who knows..?
There's no telling
What wonderful things
You might find yourself spelling!

Like QUAN is for Quandary, who lives on a shelf
In a hole in the ocean alone by himself
And he worries, each day, from the dawn's early light
And he worries, just worries, far into the night.
He just stands there and worries. He simply can't stop…
Is his top-side his bottom? Or bottom-side top?

-Dr. Seuss
On Beyond Zebra
(Seuss, 1955)

Acknowledgements

First and foremost, thank you to Anthony for his encouragement and support in all the projects I got excited about in the last four years. I have truly enjoyed this PhD, and I have really valued the opportunity to jump headfirst into these challenges. I also owe him a great debt for his editing expertise, which has many times made sense of my (hopefully) exuberant drafts. It would be yet another trial of his patience to elaborate further, and so I must simply say **thank you** again. Clearly words cannot cover it.

Thank you to my second supervisor, Matt Hill, for enabling me when I got stars in my eyes over targeted epigenetic editing tools. Thank you to everyone in HEB (especially Emma, Trudy, Niels, and Craig) and BioSi (Ros' lab and Bridget) for answering a million questions and for your time. Thank you to the basement staff (especially Rhys, Jenny, and Nicole!) for keeping things bright and sunny in an underground tunnel network. None of us could do this without you. Thank goodness we escaped to underground tunnel networks with ziplines at least once.

I would like to thank Rae and Manni for being phenomenal support; for being there to ruminate with, celebrate with, vent to, and process Marvel movies with me. Rae, you have been my rock in a foreign land! (#suspiciouslyclose) To Oly, Lee, Rachael, Jon, Ellen, and Aurelien–you guys are family. Rachael, we've gotten through this writing thing together! Additional thanks to Ellen, Oly, and Jon for GMing–we needed the escape!

Rae and I have told Matt Richardson nearly every week for three years that we would not be able to do our PhDs without his weight lifting programs. Thank you so much for enduring frustration, blood, sweat, tears, swearing, and more. Matt & Verity and everyone at SYNERGI–you are mental health heroes. Thank you to No Fit State, for getting me off the ground, and feeding the temptation to run away with the Circus.

I want to thank every dog who has ever lived, but I will pick out some particularly: Thank you to Griff, who never failed to improve my day by reminding me throwing sticks for him is the most important thing. Thank you to Holly. No gym is complete without a dog interrupting you with a ball. Thank you to Willow, who was the perfect thesis-writing teddy bear. Thank you to Riley, Zoey, Holly, Cody, and Atka. Dogs are good.

Thank you to alt rock as a genre, for providing manic energy, including Andy Black, Palaye Royale, Black Veil Brides, MCR, All Time Low, Halestorm, Imagine Dragons, Fall Out Boy, Barns Courtney, and the Goo Goo Dolls.

I need to thank my family for putting up with me moving 5000 miles away for four years. I have missed you acutely. I am extraordinarily lucky to have an overabundance of unconditional support. Special thanks to Jeff, for Calvin and Hobbes and rock climbing and the extra mile. Special thanks to Erica, for Girl Scout cookies and adaptability and 80s movies. Special thanks to Dad, for Dr. Seuss and Bishop Pines and Dad Jackets and the ocean. Special thanks to Mom for reading and Space and the constellation Orion and for being my Wonder Woman. I am surrounded by passionate, driven people and they galvanize me every day. Finally, thank you to my high school science teacher, Mr. Zaccheo. You started this.

Acknowledgements of Assistance

Mentoring, training and/or consultation in techniques & laboratory practice
Prof. Anthony Isles: general advice and discussion of neuroscience, imprinting, behavioural neuroscience, behavioural genetics, experimental design, laboratory training, and manuscript editing.
Dr. Matthew Hill: advice, discussion, and laboratory training with respect to CRISPR/dCas9 constructs, cloning, and transfection.
Dr. Gráinne McNamara: general discussion, pyrosequencing assistance, advice on behavioural testing and analysis
Dr. Trevor Humby: advice and assistance with setting up behavioural tasks
Dr. Laura Westacott: advice and assistance with setting up behavioural tasks
Dr. Niels Haan: general advice on laboratory techniques and training on brain sectioning, IHC, and imaging.
David Harrison: training in stereology
Bridget Allen: training in mESC derivation
Ngoc-Nga Vinh: assistance on IHC techniques
Dr. Greg Parker: training on MRI processing
Dr. Craig Joyce: cell culture advice, training on laboratory equipment (slide scanner etc)
Manal Adam: general discussion, statistics advice
Emily Baker: statistics advice

Data obtained from a technical service provider
Andrew Stewart, EMRIC, Cardiff University: MRI scans
Dr. Greg Parker, CUBRIC, Cardiff University: MRI brain mask and coregistration programs
Source Biosciences: Sanger Sequencing

Data produced jointly
Prof. Anthony Isles: brain weight data
Alexander Chavasse, School of Medicine, Cardiff University: behavioural data for 6 and 10 month female cohorts
Matthew Bosworth, Schools of Psychology and Medicine, Cardiff University: barbering monitoring
Simona Zahova, School of Medicine, Cardiff University: perfusion dissections

Data/materials provided by someone else
Kim Moorwood, Ward Lab, University of Bath: *Grb10KO* mice (via embryo transfer)

Funding
This work was made possible by the generous support of the Wellcome Trust.

Summary

Imprinted genes are highly expressed in the brain and have a role in adult behaviour. Additionally, madumnal and padumnal genomes contribute disproportionately to certain brain regions. Previous research has shown paternal *Grb10* is expressed in mid and hind brain regions, with high expression in monoaminergic systems, and is not expressed in the cortex. This thesis demonstrates $Grb10^{+/p}$ mouse brains are overgrown in both weight and volume, and their postnatal allometry differs from wildtype and $Grb10^{+/m}$ controls. Using longitudinal MRI, I found both cortical and subcortical volumes are larger in $Grb10^{+/p}$ than wildtypes, in contrast previous studies using Nissl-staining, which reported overgrowth only in subcortical regions. I also used IHC to investigate total cell and neuronal counts in the caudate putamen, where paternal *Grb10* is expressed, and found no difference between $Grb10^{+/p}$ and wildtype brains.

$Grb10^{+/p}$ male mice are also reported to have enhanced social dominance. I next investigated social dominance behaviours to determine if their emergence or severity correlated with brain allometry. We found $Grb10^{+/p}$ mice of both sexes were no more likely to win social dominance encounters under social housing conditions. Under social isolation stress, $Grb10^{+/p}$ males were *less* likely to win (in contrast to previously published work), while $Grb10^{+/p}$ females were *more* likely to win. We also found no consistent correlation in cage rank measured by social tube test, urine marking, and barbering. This suggests $Grb10^{+/p}$ mice may display a social instability phenotype, and begs comparison to $Cdkn1c^{BACx1}$ mice.

Finally, I constructed a CRISPR/dCas9 based epigenome editor to make targeted changes to the imprinting control region for functional studies. These tools will aid causal studies of imprinting regulatory mechanisms and will avoid the problems associated with classical approaches such as direct manipulation of the DNA sequence (deletion studies) or widespread manipulation of epigenetic readers, writers, erasers, and marks.

Common Abbreviations

˚C	Degrees Celsius
5-Aza	5-azacytidine
5-HT	5-hydroxytryptamine
Ag	Androgenetic
Akt	Serine-Threonine kinase
ANCOVA	Analysis of covariance
ANOVA	Analysis of variance
AS	Angelman Syndrome
BL	Benjamini-Liu method
BPS	Between PH and SH2 domain
BS	Bisulfite
Cdkn1c	cyclin dependent kinase inhibitor 1c
cDNA	complementary DNA
CGI	CpG Island
ChAT	Choline Acetyltransferase
CNS	Central Nervous System
CRISPR	Clustered Regularly Interspersed Short Palindromic Repeats
CTCF	CCCTC–Binding Factor
DA	Dopamine
DAPI	4',6-diamidino-2-phenylindole
DAT	Dopamine Active Transporter
DBD	DNA binding domain
dCas9	dead Cas9
DHS	DNase Hypersensitive sites
DMEM	Dulbecco's Modified Eagle Media
DMR	Differentially Methylated Region
DMSO	Dimethyl Sulfoxide
DMT	DNA methyltransferase
DNA	Deoxyribonucleic acid
DNMTs	De Novo Methyl Transferase
dNTPs	deoxy-ribonucleotide-triphosphates
DPX	Di-N-Butyle Phthalate in Xylene
DRN	Dorsal Raphe Nucleus
EPM	Elevated Plus Maze
ERK	Extracellular signal-regulated kinase aka MAPK
FBS	Fetal Bovine Serum
FDR	False Discovery Rate
gDMR	germline DMR
gDNA	genomic DNA
GFP	Green Fluorescent Protein
GM	Grbs and Mig region (RA, PH, and BPS domains)
Grb10Δ2-4	*Grb10* KO model, 36kb deletion by *LacZ* insert between exons 2 and 4

***Grb10*$^{+/m}$**	*Grb10* maternal knockout, 12bp deletion by *LacZ* insert exon 7
***Grb10*$^{+/p}$**	*Grb10* paternal knockout, 12bp deletion by *LacZ* insert exon 7
H3K27me3	Histone 3 Lysine 27 trimethylation
H3K4me3	Histone 3 Lysine 4 trimethylation
H3K9ac	Histone 3 Lysine 9 acetylation
H4K20me3	Histone 4 Lysine 30 trimethylation
HAT	Histone acetyltransferase
HDAC	Histone deacetylase
HEK	Human Embryonic Kidney
IC	Imprinting Centre
ICR	Imprinting Control Region
IGF1	Insulin like growth factor
IGF1R	Insulin Like Growth Factor 1 Receptor
IGs	Imprinted Genes
IHC	Immunohistochemistry
IR	Insulin Receptor
IRS	insulin receptor substrate
KO	Knockout
LacZ	*Lac* operon Z
LC	Locus Coeruleus
lncRNA	long noncoding RNA
LOI	Loss of imprinting
MAPK	Mitogen activated protein kinase aka ERK
mESC	murine Embryonic Stem Cell
mPFC	medial Prefrontal Cortex
MRI	Magnetic Resonance Imaging
mTORC1/2	mammalian target of rapamycin complex 1 or 2
NAc	Nucleus Accumbens
NACWO	Named Animal Care and Welfare Officer
NaOAc	Sodium Acetate
ncRNA	noncoding RNA
Nesp	Neuroendocrine secretory protein
NeuN	Neuronal Nuclear Protein
OCD	Obsessive compulsive disorder
OCT	Optimal cutting temperature compound
PBS	Phosphate-buffered saline
PCR	Polymerase Chain Reaction
PFC	Prefrontal Cortex
Pg	parthenogenetic
PH	Pleckstrin Homology domain
PI3K	Phosphoinositide 3-kinase
PR	Proline Rich region
PWS	Prader-Willi Syndrome
RA	Ras-Associating domain
RES	Residuals

RNA	Ribonucleic acid
ROI	Region of Interest
RTK	Receptor Tyrosine Kinase
SDS	Sodium dodecyl sulfate
SEM	Standard error of the mean
sgRNA	single guide RNA
SH2	Carboxy-terminal src-homology 2 domain
SN	Substantia nigra
SNC	Substantia nigra pars compacta
snoRNA	small nucleolar RNA
SPSS	Statistical Package for Social Sciences
SRE	Studentized Residuals
SRS	Silver Russel Syndrome
TBST	Tris-Buffered Saline and Tween
TE	Tris-EDTA
TET2	TET methylcytosine dioxygenase 2
TET2(CD)	TET2 Catalytic Domain
TRIS	Tris(hydroxymethyl)aminomethane
TSS	transcription start site
VTA	Ventral Tegmental Area
WT	Wild Type
ZFP	Zinc Finger Protein

Table of Contents

1 General Introduction

1.1 Why it is important to link imprinted genes and social behaviours

1.1.1 Brain Expression and Behavioural Phenotypes

Imprinted Genes are highly expressed in the brain and KOs generate a range of behavioural phenotypes

The classic defining feature of imprinted genes (IGs) is their parent-of-origin dependent monoallelic expression, mediated by epigenetic instructions differentially prescribed by the parental germ cells (Ferguson-Smith, 2011). But why is genomic imprinting of such interest to neuroscientists? Largely, it is because a limited genome relies on mechanisms like imprinting to generate the functional flexibility and myriad cell types necessary for brain development and activity. Behaviour itself is an emergent property of an organism–a special phenotype mediated by the brain. It allows organisms to react and adapt to environmental change, coordinate and compete with other organisms, and access resources and reproductive opportunities. Genetic knockout models of imprinted genes present a wide range of behavioural phenotypes, revealing their contribution to these processes. However, imprinted knockout models reveal layers of information surpassing the contribution of a gene product alone. Parent-of-origin dependent phenotypes of imprinted genes highlight how alternative epigenetic architectures can specify the application of gene products by regulating expression timing, splicing, dosage, and tissue and cell-specificity. Genes, as replicating units under evolutionary pressures and in competition with their alternatives at their genomic loci, seize the functional

variability in dosage generated by epigenetic regulatory mechanisms as a competitive opportunity. Thus, imprinting evolved as an intra-locus competition by parent of origin to manipulate the functional use of certain genes.

Several evolutionary hypotheses attempt to justify the cost incurred by the apparent haploidy resulting from imprinting. These hypotheses highlight situations in which parental genomes experience a difference in context or a conflict of interest affecting their optimal strategy for inheritance. Work describing the role of IGs in placental development, fetal growth, metabolism, and mother-offspring interactions have provided robust evidence for evolution through competition for and coordination of maternal resources via the placenta and perinatal care (Charalambous, da Rocha, & Ferguson-Smith, 2007; Cowley et al., 2014; Haig, 2014; Wilkins & Haig, 2003). However, a large proportion of identified imprinted genes are also highly expressed in the central nervous system (CNS), indicating a significant role in brain development and adult behaviour (Davies, Isles, Humby, & Wilkinson, 2008; Davies, Isles, & Wilkinson, 2005). The evolutionary relationship between adult post-natal social behaviour and imprinting has proved more refractory to attempts to generate testable hypotheses. However, the imprinted gene *Grb10* (growth factor receptor bound protein 10) was directly linked to a post-weaning social behaviour phenotype in 2011, and provides a cornerstone example supporting behaviour as a substrate for imprinting evolution, with some criticisms (Curley, 2011; Garfield et al., 2011; Haig, 2006; Isles, Davies, & Wilkinson, 2006). It is necessary to explore examples of imprinted genes

impacting social behaviour to understand how this complex property of an organism in group contexts can emerge from genetic, epigenetic, and neurodevelopmental mechanisms.

1.1.2 Non-equivalence and the Extended Phenotype

Parental contributions are not equivalent, and genes don't necessarily work for the 'good of the organism'

To understand the impact of imprinting mechanisms on social behaviour, we must consider the action of evolution not only upon the individual's phenotypes, mediated by their genome, but also upon the relationships the individual has with kin sharing portions of the same genome. Gene expression and function can be finely tuned to reflect the competitive strategies employed by these special hereditary units (IGs) to manipulate the 'extended phenotype' shared within a social group containing both potential relatives and competitors (Dawkins, 1999). To wit, "an offspring's mother and father will usually have different sets of collateral kin" (Haig, 2006). Thus, benefits of social relationships conferred upon the mother's kin improve the inclusive fitness of the maternal but not paternal genome and vice versa. In social groups with different dispersal patterns of maternal and paternal kin, imprinted genes can mediate coordination and competition between individuals to promote the 'optimal' strategy for maternally and paternally inherited genes (Haig, 2006; Úbeda & Gardner, 2011). Imprinting and epigenetic regulatory architectures enrich the adaptability of the genome to

engender the range behavioural phenotypes which impact fitness within the shifting context of natural selection.

1.1.3 Functional imprinting and behavioural regulation

Imprinting models and their evolutionary theories help us understand the functional contribution of epigenetic regulation to behavioural variability

Importantly, understanding how gene expression can be modulated through imprinting will also give us a better holistic understanding of healthy brain development, and may also offer insight into treatments for behavioural disorders. Aberrant social functioning is a symptom of many neurologic and psychiatric disorders, and some, such as Prader–Willi Syndrome (PWS) and Angelman Syndrome (AS), directly implicate imprinted genes (McNamara & Isles, 2013, 2014; van den Berg, Lamballais, & Kushner, 2015). While this thesis does not focus on the etiology of a syndrome or disease associated with *Grb10*, the methodology linking the molecular mechanisms of imprinting with its functional impact on cellular, anatomical, and behavioural phenotypes provides an example of how an integrative approach to behavioural neuroepigenetics can illuminate the functional impact of imprinting architecture in regulating a behaviourally-linked gene.

1.2 *Grb10* phenotypes

Murine growth factor receptor bound protein 10 (*Grb10)* is an imprinted gene directly linked to an adult inter-individual, postnatal social behaviour phenotype (Garfield et al., 2011). The *Grb10KO* mutant mouse strain was

generated by insertion of a *LacZ:neomycin*^{r} gene trap cassette within *Grb10* exon 7, deleting 12 base pairs (Cowley et al., 2014; Garfield et al., 2011). This knockout model generates two distinct lines by parent-of origin inheritance of the KO allele: the maternal (*Grb10KO*$^{+/m}$), and the paternal (*Grb10KO*$^{+/p}$) knockout. The *Grb10KO*$^{+/p}$ model is the main investigative subject of this thesis and is referred to as *Grb10*$^{+/p}$.

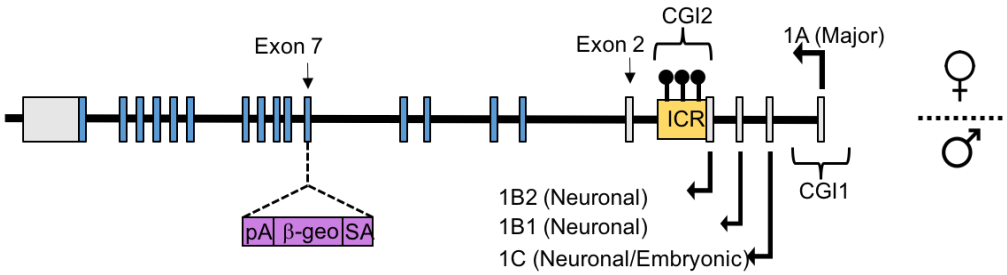

Figure 1.1 Grb10 Gene, Transcript, and LacZ insert Annotations

Figure: Based on diagrams from (Garfield et al., 2011; Plasschaert & Bartolomei, 2015). *Not to scale.*

1.2.1 *Grb10* protein

Murine *Grb10* lies on proximal chromosome 11 and encodes a cellular adapter protein which belongs to a small family including Grb7 and Grb14 (Charalambous et al., 2003; Han, Shen, & Guan, 2001). This family shares a well-conserved sequence and protein architecture. Important structural features in both human and mouse Grb7/10/14 family proteins include, in order, an amino-terminal proline rich region (PR), a Ras-Associating (RA) domain, a pleckstrin homology (PH) domain, a short functional region called BPS (between the PH and SH2 domain), and finally a carboxy-terminal src-homology 2 (SH2) domain (Han et al., 2001; Kabir & Kazi, 2014). The RA, PH, and BPS domains are grouped as a central segment termed the GM (Grbs and

Mig) region (Holt & Siddle, 2005). The SH2 domain mediates interactions with receptor tyrosine kinases (RTKs) and tyrosine-phosphorylated signaling molecules. This region holds the highest sequence identity between members of the Grb7/10/14 family (60-70%), indicating its central function (Desbuquois, Carré, & Burnol, 2013). The BPS domain mediates Grb7/10/14 inhibition of the RTKs insulin receptor (IR) and insulin-like growth factor receptor (IGFR) (Desbuquois et al., 2013). This domain only acquires structure when bound to the phosphorylated receptor (Depetris et al., 2005; Desbuquois et al., 2013). The PH domain binds phosphoinositides and the RA domain targets Grb7/10/14 to insulin-activated GTPases at the plasma membrane (Depetris, Wu, & Hubbard, 2009). The RA and PH domains, connected by a short linker, associate as a unit which dimerizes at the PH domain to position the RA domain for binding membrane-associated GTPases. Although Grb10 RA-PH dimerizes only weakly in solution, SH2 dimerization enhances formation of the RA-PH dimer (Depetris et al., 2009; Stein, Ghirlando, & Hubbard, 2003). Finally, the N-terminal region mediates binding with Grb10-interacting glycine-tyrosine-phenylalanine (GYF) proteins. Grb10 isoforms are most variable at the N-terminal (Desbuquois et al., 2013).

Figure 1.2 Domain Architecture of Grb10 protein (Depetris et al., 2009, Figure 1a)

Figure 1.2: *Diagram adapted from Depetris et al 2009. Abbreviations are P (Proline rich, aka PR), RA (Ras-associating), PH (pleckstrin-homology), BPS*

(between PH and SH2), SH2 (Src-homology-2). Light gray section is a short linker between RA and PH domains.

Grb10 interacts with many tyrosine kinases, including the epidermal growth factor receptor (EGFR), hepatocyte growth factor (c-Met), c-kit/stem cell factor receptor (SCFR) and platelet–derived growth factor *beta* receptor (PDGFβR) (Han et al., 2001; Holt & Siddle, 2005; Ooi et al., 1995; J. Wang et al., 1999). The Grb7/10/14 family also partners with docking proteins for IR/IGFR signaling, including IRS1, Shc, and p85/PI3K, as well as serine/threonine kinases and Nedd4 (ubiquitin ligase neuronal precursor cell-expressed developmentally down-regulated 4). While not generally a direct RTK substrate, Grb10 is tyrosine-phosphorylated by Tec, Src, and Fyn kinases and undergoes growth factor/cytokine-stimulated serine/threonine phosphorylation. In cell lines, Grb10 is associated with the cytoplasm and membranes, but has also been found in mitochondria in association with Raf1 kinase (Desbuquois et al., 2013). Through these interactions the Grb7/10/14 family is positioned to regulate cell proliferation, apoptosis, and metabolism (Han et al., 2001; Holt et al., 2009; Plasschaert & Bartolomei, 2015). The Grb10 protein itself is firmly established as a potent growth suppressor at cellular and physiological levels (Charalambous et al., 2003; Plasschaert & Bartolomei, 2015). *Grb10* may also have a role in stem cell self-renewal and regeneration (Yan et al., 2016).

Pursuant to this, Grb10's most well-characterized molecular role is as an inhibitor of insulin receptor (IR) and insulin-like growth factor 1 receptor

(IGF1R) signaling to growth and metabolic pathways (M. Liu et al., 2014; Vecchione, Marchese, Henry, Rotin, & Morrione, 2003; Yan et al., 2016). When signaling activates autophosphorylation of these receptors, the Grb10 SH2 and BPS domains bind noncompetitively to the receptor's core kinase domain (Plasschaert & Bartolomei, 2015; F. M. Smith et al., 2007; Yan et al., 2016). Sequence variants in the BPS domain enhance binding specificity, distinguishing the activity of each of the Grb7 family proteins (Desbuquois et al., 2013; Han et al., 2001). Grb10 is thought to block signaling between activated tyrosine kinase receptors and downstream cascades including the Raf/Mek/ERK and Akt pathways (Jahn, Seipel, Urschel, Peschel, & Duyster, 2002; Lim, Mei, 2004; Nantel, Mohammad-Ali, Sherk, Posner, & Thomas, 1998). Depletion of Grb10 by small interfering RNA (siRNA) increases insulin-dependent phosphorylation of Shc, Akt and IGF-dependent Akt, and MAPK/ERK1/ERK2 (Desbuquois et al., 2013; Langlais et al., 2004). Conversely, overexpression of Grb10 and Grb14 inhibits the activation of IRS/PI3K/Akt (metabolic actions of insulin) and Mek/ERK (cell proliferation and differentiation) signaling downstream of IR and IGFR (Shiura et al., 2005; Wick et al., 2003). Grb10 inhibition of the PI3K/Akt pathway occurs through a negative feedback loop on growth factor signaling. This function depends upon the phosphorylation of the Grb10 proline-rich (PR) and BPS domains by mTORC1. mTORC1 phosphorylation activates and stabilizes Grb10 while chronic mTOR inhibition decreases Grb10 abundance (Hsu et al., 2011). Stabilized Grb10 disrupts IR phosphorylation of IRS1/IRS2, inhibiting signal transmission along the PI3K/Akt pathway (Wick et al., 2003). Thus, while the

multiprotein complexes mTORC1 and mTORC2 within the PI3K/Akt pathway promote and regulate cell growth and proliferation, mTORC1 simultaneously activates a negative feedback loop which relies on Grb10 inhibition at the growth factor receptors (Hsu et al., 2011).

1.2.2 The *Grb10*KO model

The paternal allele of *Grb10* is implicated in the regulation of social dominance behaviour and delay discounting (Dent et al., 2018). *Grb10*$^{+/p}$ mice are reported to be more likely to initiate allogrooming, and to win encounters in the Lindzey tube test more frequently than wild-type controls (Garfield et al., 2011). Both tests are considered measurements of social dominance (Lindzey, Winston, & Manosevitz, 1961; Strozik & Festing, 1981; F. Wang, Kessels, & Hu, 2014). The formation of social hierarchies is an evolutionarily conserved phenomenon which influences health, disease, and access to resources and reproductive opportunities (Cheung et al., 2010; Lardy, Allainé, Bonenfant, & Cohas, 2015; Saavedra-Rodríguez & Feig, 2013; van den Berg et al., 2015). *Grb10*$^{+/p}$ mice also persist longer in choosing the large, delayed reward in a delayed-reinforcement task (Dent et al., 2018). This is interpreted as a demonstration of less impulsive choice. Comparison with the opposite phenotype of maternally imprinted *Nesp*$^{+/m}$ mice provides evidence that parental conflict influences adult decision making independently from the confounds of *in utero* or pre-weaning growth (Dent et al., 2018). Both the social dominance and delay discounting phenotypes reported in *Grb10*$^{+/p}$ mice

support adult behaviour as a substrate for the evolution of imprinting (Haig, 2006).

Curiously, the maternal knockout (*Grb10*$^{+/m}$) mice demonstrate their own distinct phenotype, in contrast to many other imprinting models in which an altered phenotype is associated with deletion of one parental allele but not the other. *Grb10*$^{+/m}$ mice do not show the behavioural phenotype described in paternal knockouts (Garfield 2011, supplementary Fig 5i), but they do show significant and well-characterized fetal and placental overgrowth (Charalambous et al., 2003; Garfield et al., 2011). Notably, and to be discussed on later in this thesis, the fetal brain is spared the increase in size observed in *Grb10* maternal knockout pups (Charalambous et al., 2003; F. M. Smith et al., 2007). Loss of maternally-derived Grb10 results in increased placental efficiency and a 50% expansion of the labyrinthine compartment (Charalambous et al., 2010). Maternal knockout has also revealed complementary roles for *Grb10* in mediating the nutrient supply and demand between mother and pup. Mothers (F1) deficient in maternally (F0) inherited Grb10 have an increased brood (F2) size and concomitant decrease in embryonic and placental weight (Charalambous et al., 2010). Cross fostering experiments demonstrated *Grb10*$^{m/+}$ pups exhibit increased demand for nutrients, to which WT but not *Grb10*$^{m/+}$ nurses respond with increased provisioning (Cowley et al., 2014). *Grb10* also influences adult body composition, as *Grb10* expressed in the mother's tissues affects offspring adiposity while *Grb10* expressed in the offspring influences lean mass (Cowley et al., 2014). Disruption of maternal *Grb10* continues impact phenotype in

adulthood through glucose homeostasis and insulin signaling (F. M. Smith et al., 2007). Thus, maternal *Grb10* regulation of growth and metabolism demonstrates a clear role in the prenatal parental conflict in the placenta and maternal-offspring coordination of postnatal nutrients (Haig, 2014; Wolf & Hager, 2006). Comparison of the *Grb10KO* models prompts us to discuss how genomic imprinting achieves divergent functional roles for the parental alleles, and the evolutionary drives which may have established this unique regulatory mechanism.

1.3 Genomic Imprinting Theory

1.3.1 Parental genomes are not equivalent

The distinct parent-of-origin phenotypes of *Grb10KO* mice highlight an important concept for imprinted genes: the maternal and paternal genomes are not equivalent. *Grb10* gene dosage is the subject of parent-of-origin conflict in multiple tissues (brain, skeletal muscle, adipocytes, placenta), where imprinting allows the parental alleles to adopt context-sensitive 'stances'. While most imprinted genes universally silence one allele, at *Grb10*, both parental genomes achieve discrete monoallelic expression. In placenta, maternal expression is favoured while paternal is silenced, but in brain, the reverse 'stance' is adopted. The epigenetic regulation of *Grb10* expression responds to context-specific factors to switch expression profiles and silence or promote context-specific transcription start sites. *Grb10* imprinting architecture is discussed in section 1.4. Here I will introduce imprinting, its evolutionary theories, and basic mechanisms.

The non-equivalence of the maternal and paternal genomes was first revealed by uniparental mouse embryos modeled in the 1980s (Barton, Surani, & Norris, 1984; McGrath & Solter, 1984). While control embryos containing transplanted nuclei of paired maternal and paternal origin were viable, androgenetic (paternally diploid; Ag) and parthenogenetic (maternally diploid; Pg) embryos died during the early post-implantation period (McGrath & Solter, 1984). Additionally, androgenetic embryos developed substantial extraembryonic tissues, particularly the placental trophoblast, but had very retarded embryo growth (Barton et al., 1984). Reciprocally, parthenogenetic embryos developed further, but had very restricted extraembryonic tissues (Barton et al., 1984; M. A. H. Surani & Barton, 1983). These initial experiments concluded the content of parental nuclear contributions may be equivalent, but their functional contribution is not.

Chimeric mice revealed maternal and paternal genomes have partially dissociable contributions to brain development and function (Perez, Rubinstein, & Dulac, 2016). By using chimeras with <40% Ag/Pg cells, these models circumvented the mid-gestation lethality limiting analysis of fully Ag/Pg embryos and the mice survived to adulthood. 'Ag chimeras' with a mix of androgenetic and normal cells displayed a relatively small brain:body size ratio while 'Pg chimeras' with a parthenogenetic and normal cell mix displayed a larger brain:body size ratio. This indicated the combined effect of maternally expressed genes enhanced brain size while the paternally expressed genes restricted brain growth (Davies et al., 2008; Keverne, Fundele, Narasimha,

Barton, & Surani, 1996). This is consistent with the predicted growth restriction role of paternal *Grb10* expressed in the brain.

Additionally, Pg and Ag cell distribution in chimeric brains was reciprocal. Pg cells (maternal origin) contributed mainly to the neocortex while Ag cells contributed to hypothalamic, septal, and preoptic areas (Keverne, 1997; Keverne et al., 1996). This indicates distinct roles for the parental genomes in various brain regions (Perez et al., 2016). This pattern also appears consistent with the exclusion of paternal *Grb10* expression from cortical regions and its strong expression in midbrain regions, detailed in Section 1.5. However, this division could be driven by a few key genes with large effects. The maternally expressed *Nesp55* is among the many exceptions to the pattern, as its expression extensively overlaps with paternal *Grb10*, as discussed later (Davies et al., 2005; Dent & Isles, 2014).

1.3.2 Evolutionary theory, Asymmetry of relatedness, and Grb10

Nonequivalence of parent-of-origin arises in contexts where maternal and paternal genomes have different optimal solutions to selection pressures and adaptive problems. These solutions must be disparate enough to justify pseudo-haploidy incurred by imprinting. Imprinting effectively silences one allele in all or some tissues, giving up the benefits of diploidy in alleviating the load of partially recessive somatic mutations (Orr, 1995). Here, I will discuss two evolutionary theories that attempt to predict the contexts in which this asymmetry of selection pressure is sufficient to justify imprinting. The two standards of imprinting evolution are the parental conflict or kinship theory

and the maternal-offspring coadaptation theory. While both theories identify conflict during nutrient allocation and maternal care in prenatal and pre-weaning periods, the parental conflict/kinship theory also predicts conflict in adult behaviours when sex-biased dispersal from a social group creates asymmetry of relatedness (Isles et al., 2006). Post hoc interpretation of various Grb10 phenotypes shows similarities to the predictions of both theories. I will describe the predictions of these theories to help us interpret social behaviours impacted by Grb10.

1.3.2.1 Parental Conflict/Kinship

The Parental Conflict theory and its extension, the Kinship theory, implicate differential inclusive fitness for maternally (madumnal) and paternally (padumnal) inherited alleles as the evolutionary driver of imprinting (Trivers, 1974; Wilkins & Haig, 2003). Popularly, the parental conflict theory contextualizes this pressure as a conflict between maternal and paternal fitness where multiple paternity is possible. Maternal resources are assumed to be allocated equally between all offspring over the maternal reproductive lifetime, regardless of paternal relation, while the paternal genome can be propagated by multiple mothers. Kinship theory extends this conflict beyond the individual offspring to its relatives by calculating inclusive fitness based on the coefficient of relatedness of individuals.

A major site of action of this theory is the allocation of resources acquired from the mother by the fetus. Resources the fetus acquires involve an indirect cost to other offspring sharing the same madumnal or padumnal

alleles. Selection pressures weigh the direct benefit to the fetus against the probability and magnitude of the cost to the residual fitness of the mother or father (parental conflict). This may also be phrased as the cost to the residual fitness of the shared madumnal or padumnal allele in other individuals (inclusive fitness). While the mother can guarantee one of her two alleles are present in any offspring she carries, the father (or the padumnal allele) cannot guarantee relationship between the individual offspring and any future offspring the mother carries. In other words, offspring sharing maternal resources are more likely to carry the same copy of the madumnal allele (one of two allelic possibilities) than to carry the same copy of the padumnal allele because of the possibility of multiple paternity. This differential probability weights the calculation differently for maternal and paternal alleles, providing substrate for the evolution of imprinting. For a growth restrictor such as Grb10 acting in the placenta, it is of greater benefit to the residual fitness of the padumnal allele to acquire more maternal resources immediately, lest maternal resources be acquired by an unrelated allele (multiple paternity). In contrast, it is of greater benefit to the residual fitness of the madumnal allele to restrict access to maternal resources, allowing the mother to parse these resources out among offspring. Thus in the placenta, *Grb10* is maternally expressed, acting as a potent growth restrictor, and paternally repressed, limiting its efficacy in restricting growth (Charalambous et al., 2010, 2003). Similar conflicts may be found within postnatal competition for maternal care.

Beyond growth and maternal care, the kinship theory also explains the pressures of selection in post-weaning social interactions among individuals

with different probabilities of sharing madumnal and padumnal alleles (Isles et al., 2006). Asymmetry of relatedness is particularly applicable to social groups affected by sex-biased dispersal and inbreeding. Two classic scenarios of asymmetrical relatedness are multiple paternity (discussed above), and sex-biased dispersal, such as that observed in a pride of lions, where there is more madumnal allelic diversity than padumnal in the group (Haig, 2006; Isles et al., 2006). In social contexts, inclusive fitness extends indefinitely to more distant relations (aunts/uncles, cousins etc) with smaller coefficients of relatedness for the madumnal/padumnal allele in question, as the likelihood of sharing the allele diminishes (Haig, 2006; Wilkins & Haig, 2003). Social behaviours such as 'altruism', 'cooperation', and 'selfishness' are commonly cited in kinship theory. Hypothetically, natural selection could favor imprinting of genes impacting altruism where social groups contain asymmetrical relatedness. The active allele of such an imprinted gene would be the one more likely to be shared among individuals (higher relatedness probability), based on group composition. The silent allele would be the one more likely to be in competition with other alternatives (lower relatedness probability).

The link between *Grb10* and post-weaning social dominance supports adult social behaviour as another substrate (besides placental growth) driving the emergence of imprinting at this locus. However, the evolutionary theory is unclear on the direction of effect predicted for madumnal and padumnal alleles impacting social dominance (Garfield et al., 2011; Úbeda & Gardner, 2010). Further characterization of the *Grb10*$^{+/p}$ social dominance phenotype

may help refine our understanding of the selective pressures acting on behaviour which are sufficient to justify the costs of imprinting.

1.3.2.2 Maternal-Offspring co-adaptation

The maternal-offspring coadaptation model describes how imprinting may have evolved as a method of coordinating expressed alleles in mothers and offspring to impact offspring fitness (Wolf & Hager, 2006). The mammary gland is the major site of nutrient provisioning from mother to offspring, and provisioning is optimal when mother and offspring are of the same genotype (Hager & Johnstone, 2003). Imprinting in the mammary tissue however, is not fully explained by coordination by allelic matching, as the mother has an equal chance of passing either allele to the offspring. For example, the mother may express her madumnal allele, but pass on her padumnal allele.

Maternally expressed *Grb10* provides support to the mother-offspring coadaptation model. *Grb10* is maternally expressed in the mammary epithelium during lactation and promotes postnatal nutrient supply from the mother, influencing offspring adiposity. In the offspring, the maternally expressed allele suppresses nutrient demand and influences lean mass. (Note that these madumnal alleles need not be identical in mother and offspring– the mother can pass on either of the grandparental alleles.) Thus, the complementary functions of the maternal and offspring madumnal alleles together coordinate lean/fat proportions during developmental programming (Cowley et al., 2014).

While this coadaptation model has been treated as a different solution to imprinting evolution, Haig (2014) argues parental conflict theory also defines conditions for cooperation in coadaptation (Haig, 2014). In the mammary epithelium, the genome of the father is not present to directly influence allocation of resources. The impact of the padumnal allele on maternal provisioning is instead mediated through successful resource-seeking behaviour in the pre-weaning offspring or programming of maternal care behaviours via the placenta (Creeth et al., 2018). Thus, parental conflict might be extended into the balance of postnatal supply and demand.

The selective pressures of parental conflict and maternal-offspring coadaptation need not be mutually exclusive sources for the evolution of imprinting at *Grb10*. The distinct physiological and behavioural processes impacted by *Grb10* expression suggest an initial selective pressure leading to imprinting could be built upon by other pressures in other tissues facilitating novel functions. For example, imprinted expression early in development could be extended to facilitate functions in adult tissues, which might require the acquisition of somatic DMRs or additional modifications to the imprinting architecture. The bivalent chromatin domain regulating paternal *Grb10* expression from CpG island 2 (discussed in Section 1.4.5.2) may be an example architectural feature for an investigation of imprinting elaboration.

1.4 Imprinting mechanisms and Grb10

1.4.1 Epigenetic Discrimination of Parent-of-Origin

As both parents contribute a full, matching complement of genes to the zygote, functional difference must arise from a difference in gene expression (dosage, tissue-specificity, and timing) prescribed by imprinted regulation. In early experiments, Surani & Barton suggested "specific imprinting of the paternal and maternal genomes occurs during gametogenesis" by epigenetic mechanisms (Barton et al., 1984; M. A. H. Surani & Barton, 1983). Complementary silencing or expression of genes required for one parental role or the other generates a need for both sets for normal development. Again, however, while many imprinted genes are active from a single allele in parent-of origin specific manner, uniform and complementary expression and silencing is insufficient to characterize imprinting. In the mouse, both parental *Grb10* alleles are required for a wild-type phenotype and demonstrate complementary tissue-specific expression (Garfield et al., 2011). Many human tissues also feature biallelic *Grb10* expression, limiting imprinted expression patterns to key tissues such as the placental trophoblast and brain (Monk et al., 2009). So, what defines an imprinted gene and what is the mechanism of imprinting?

1.4.2 Imprinting Control Regions

Genomic imprinting is an epigenetic phenomenon which regulates the transcriptional activity of a gene or cluster of genes in a parent-of-origin specific manner (John & Lefebvre, 2011). Currently, 151 genes are identified as imprinted in the mouse, and many are conserved in the human as well

(Arnaud, 2010; Williamson et al., 2013). As suggested by Surani & Barton, imprinting occurs when one parental allele is epigenetically marked by methylation during embryogenesis, creating the basis for allele-specific regulatory differences (Barton et al., 1984; M. A. H. Surani & Barton, 1983; M.Azim Surani, 1998). These marks, called differentially methylated regions (DMRs), are established in the parental germlines and are protected from genome-wide demethylation during embryogenesis (Bartolomei & Ferguson-Smith, 2011; M A Surani, 2001). These differences are reiterated in later developmental stages as further modifications maintain and elaborate the imprinting mark to create the imprinting center (IC) or imprinting control region (ICR). (John & Lefebvre, 2011).

An imprinting centre (IC) or imprinting control region (ICR) is the minimal functional region, as defined by targeted deletions, which regulates an imprinted locus *in cis* (John & Lefebvre, 2011). This includes a section of DNA and its epigenetic modifications (both DNA methylation and histone marks). While some ICRs regulate imprinted domains extending over large regions of DNA and require complex and extensive epigenetic architecture to regulate a cluster of genes, others regulate a single imprinted protein-coding gene (Ideraabdullah, Vigneau, & Bartolomei, 2008; A. J. Wood & Oakey, 2006). A typical imprinted cluster contains 3-12 genes spread over 20-3700 kb of DNA, but not all genes within a given cluster are necessarily expressed from the same parental chromosome (Barlow, 2011; Lee & Bartolomei, 2013). For example, at the imprinted PWS/AS locus on human chromosome 15q11-q13, one ICR regulates maternally and paternally expressed genes interspersed

with biallelically expressed genes (McNamara & Isles, 2013). Furthermore, imprinting architecture can vary between tissues and developmental stages, resulting in differing expression patterns in abundance and splice variants. This variation is the result of tissue- and stage-specific epigenetic modification at the locus, subsequently maintained through several rounds of DNA replication (John & Lefebvre, 2011).

Grb10 is an imprinted gene on murine chromosome 11, and human chromosome 7, and is immediately flanked by imprinted *Ddc/DDC* (*Dopa Decarboxylase*) and biallelically expressed *Cobl/COBL* (*Cordon-bleu*) (Hitchins et al., 2002, 2001; Menheniott et al., 2008; Monk et al., 2003). There is some evidence *Grb10* and *Ddc* form an imprinting cluster regulated by an ICR on *Grb10*, though the mechanism by which *Ddc* is regulated by this ICR is not fully described (See section 1.4.5.3 for further elaboration on this imprinting cluster) (Menheniott et al., 2008). The ICR on both murine *Grb10* and human *GRB10* is a maternally methylated CpG island, designated CGI2 in mice and CGI-2 in humans (Arnaud et al., 2003; Monk et al., 2009). This ICR achieves tissue-specific *Grb10* expression from different transcription start sites (TSS) on each parental allele. In mice, the paternal allele is transcribed from the downstream TSS at CpG island 2 (CGI2, Exons 1B1 and 1B2) and CGI3 (Exon 1C). Expression from Exons 1B1 and 1B2 at CGI2 is exclusive to neurons in the CNS. The maternal allele, on the other hand, is expressed from a general upstream TSS at CGI1 (Exon 1A) in all tissues excepting the CNS (Hikichi, Kohda, Kaneko-Ishino, & Ishino, 2003; Sanz et al., 2008; Yamasaki-Ishizaki et al., 2007). In humans, *GRB10* is expressed biallelically in most tissues, maternally expressed

in the placental villous trophoblast, and paternally expressed in the brain (Blagitko et al., 2000; Hikichi et al., 2003; Monk et al., 2009). During the development of mESCs to motor neurons, the expressed isoform and allele undergoes a switch–the maternal isoform expression declines and the paternal isoforms gains traction (Plasschaert & Bartolomei, 2015). Paternal deletion of the *Grb10* ICR in mice results in biallelic maternal expression of the major *Grb10* isoform in all tissues, including brain. This maternalization results in severe pre- and post-natal growth retardation. While this deletion included at least one paternal-specific promoter, occluding expression of this isoform, the deletion study also reveals the paternal ICR normally represses the major promoter *in cis* (Plasschaert & Bartolomei, 2015; Shiura et al., 2009). In contrast, maternal deletion of the ICR produced no observable growth phenotype. The distinction of maternal and paternal ICRs and their divergent consequences begins with the establishment of the CGI2 DMR in the separate germlines.

1.4.3 Establishing germline DMRs

Imprinting begins by establishing germline differentially methylated regions (gDMRs). Oogenesis and spermatogenesis create diverging conditions under which germline methylation is established in the haploid cell and then maintained in the fertilized zygote. In both germlines, differential methylation may depend on interactions between transcriptional events, de novo methylation machinery, and chromatin status. Importantly, the specificity of genomic imprinting seems to be determined by targeted maintenance of

differential marking after fertilization, rather than by the initial acquisition of marks in the haploid germ cells (Kelsey & Feil, 2013).

At the onset of gametogenesis, primordial germ cells have undergone extensive DNA demethylation, including erasure of pre-existing parental-allele-specific methylation, and are ready for the re-establishment of parent-specific gDMRs (Guibert, Forné, & Weber, 2012). In oogenesis, female germ cells arrest in the diplotene of prophase I in meiosis until after fetal birth, when they are incorporated into primordial follicles. Follicle activation in turn stimulates a growth phase during which the oocyte acquires methylation in a progressive manner dependent on oocyte size. Different gDMRs acquire full imprinting at different rates during oocyte growth. In this non-dividing haploid cell, there is no competing demethylation or modification by maintenance complexes (Kelsey & Feil, 2013). In contrast, prospermatogonia begin to acquire methylation prior to the onset of meiosis. Thus, paternal germ cells go through multiple rounds of cell division between the onset of methylation and the production of mature sperm. These rounds of cell division present multiple opportunities for initial methylation patterns to be modified through maintenance and potentially accumulate epimutations (Kelsey & Feil, 2013).

Maternal and paternal gDMRs have characteristics which reflect their differential mechanisms for methylation in germ cells and maintenance in the fertilized zygote. While the known paternal gDMRs (paternally methylated: *H19/Igf2, Dlk1-Gtl2,* and *Rasgrf1*) are intergenic CG-rich elements, maternal gDMRs (maternally methylated) are intragenic CpG islands that comprise promoters (Kelsey & Feil, 2013). These maternal gDMRs are fully protected

against DNA methylation in male germ cells. While gDMRs are established in both oocytes and sperm, the majority are acquired in the female germline (Arnaud, 2010; Ferguson-Smith, 2011). Regardless, approximately half of imprinted genes are expressed from the maternal allele and half from the paternal allele (Arnaud, 2010).

Kelsey & Feil predict a model of *de novo* maternal gDMR methylation at intragenic CGIs which relies on transcription status and histone modification state in oocytes. First, an active oocyte-specific upstream transcription site acquires active histones marks by binding activating histone-modifying enzymes and recruits the elongating RNA Pol II complex. Repressive histone-modifying enzymes associated with RNA Pol II add silencing marks to the gene body downstream as the gene is transcribed. This reinforces silencing at inactive intragenic transcription start sites downstream. The DNMT3A/DNMT3L de novo methylation complex recognizes accumulating repressive histone modifications at inactive transcription start sites and adds *de novo* DNA methylation (Hata, Okano, Lei, & Li, 2002; Kaneda et al., 2004). This establishes an intragenic maternal gDMR methylated in oocytes. The *Snrpn* DMR is an example of a maternal DMR corresponding to a silent CpG island promoter located within active transcription units in oocytes (E. Y. Smith, Futtner, Chamberlain, Johnstone, & Resnick, 2011). Additionally, at the *Gnas* locus, truncating transcripts from the furthest upstream *Nesp* promoter disrupts oocyte-derived gDMRs (Chotalia et al., 2009). Other oocyte-expressed sites downstream escape the addition of silencing marks by binding chromatin-modifying complexes themselves and continuing active expression (Kelsey &

Feil, 2013; Smallwood & Kelsey, 2012). Complementing the maternal model, several promoters associated with maternally methylated gDMRs are actively transcribed and are marked by H3K4me3 (active mark) in male foetal germ cells, indicating active transcription and histone marks may protect these sites from *de novo* methylation in male germ cells (Henckel, Chebli, Kota, Arnaud, & Feil, 2012). Kelsey & Feil's model suggests intragenic maternal gDMRs could be established by general processes such as gene body methylation, and then selectively maintained after fertilization.

There is less evidence of a common mechanism for *de novo* methylation of gDMRs in male germ cells, particularly as few paternally methylated gDMRs are known. Transcripts traversing the paternal gDMRs in male germ cells late in gestation could be consistent with a transcription-dependent methylation mechanism (Henckel et al., 2012). However, paternal gDMRs are intergenic, suggesting general mechanisms of gene body methylation may be unlikely. Kelsey and Feil also suggest noncoding RNAs could recruit histone modifiers to paternal gDMRs to guide methylation, considering imprinted loci retain nucleosomal organization in mature sperm, but provide no evidence for this possibility.

1.4.4 Targeted maintenance of germline DMRs

In both oocytes and sperm, many more CpG islands are initially fully methylated than known imprinting gDMRs. Imprinting specificity may be best attributed to a process of general (though differential) methylation in oocytes and sperm, with a selective maintenance of methylation status after

fertilization–especially during the genome-wide demethylation period in the pre-implantation diploid embryo (Kelsey & Feil, 2013). Following fertilization, the paternal genome loses a large part of its DNA methylation through active demethylation. The maternal genome loses DNA methylation more gradually (Reik, 2007). The protein stella, or DPPA3, is highly expressed in oogenesis and persists in the pre-implantation embryo. DPPA3 protects maternally methylated genes *Peg1* and *Peg5*, as well as paternally methylated genes *H19* and *Rasgrf1* from active DNA methylation (Nakamura et al., 2007). DPPA3 might accomplish this via a wider role in protecting the maternal genome from 5mC to 5hmC conversion, an intermediate in demethylation (Wossidlo et al., 2011).

Targeted zinc finger proteins bound to imprinted gDMRs may also maintain methylation status during the post-fertilization demethylation period. ZFP57 (Krüppel-associated box-containing zinc-finger protein 57) binds the methylated allele of almost all imprinted gDMRs in ES cells (Quenneville et al., 2011). It is essential for the de novo methylation of *Snrpn* and is also capable of faithfully maintaining methylated or unmethylated status of transgenic ICRs (Anvar et al., 2016; Li et al., 2008). Another zinc-finger protein, CTCF, or CCCTC–Binding Factor, is a multi-functional transcriptional regulator protein that binds unmethylated DNA sequences. Mutation of CTCF binding sites at *H19* leads to aberrant gain of maternal methylation during post-implantation development (Engel, Thorvaldsen, & Bartolomei, 2006). Continual binding of factors such as ZFP57 and CTCF could protect the unmethylated gDMR against post-fertilization methylation. As CTCF is a

transcriptional regulator at several loci, this protection may reflect elements of the maternal gDMR mechanism modeled in Kelsey & Feil and described above (Kelsey & Feil, 2013). However, the ubiquity of CTCF excludes it as a sufficient source of specificity in gDMR maintenance.

Chromatin marks are another possible source of specificity in gDMR preservation. As imprinted loci are among the few regions that retain nucleosomal organization in mature sperm, both the male and female germline could contribute to gDMR–specifying histone modifications. Additionally, DNA methylation, while associated with repressed promoters, is not necessary to silence them–mouse mutants lacking DNA methylation retain their repression of imprinted protein coding genes. This supports a role for heterochromatic histone modifications in maintaining repressed promoters (Barlow, 2011). Interestingly, there is a lack of widespread heterochromatin in imprinting clusters (Barlow, 2011). In fact, at the *Igf2r/Air* locus, 19 DNase Hypersensitive Sites (DHS) indicating open chromatin are present across both alleles indicating transcriptional competence over the locus (Pauler, Stricker, Warczok, & Barlow, 2005). Repressive histone modifications cluster around the ICR, rather than spreading across a silenced allele. The DNA methylated alleles of gDMRs are focally enriched for heterochromatic marks such as H3K9me3 and H4K20me3 (Barlow, 2011; Henckel et al., 2009; Regha et al., 2007). Heterochromatic histone modifications may be more important for maintaining differential DNA methylation post-fertilization than for providing a mechanism for repressing an imprinted allele. A discussion of specific histone modifications relevant to imprinted gene silencing may be found in Barlow

2011. Conversely, enrichment of activating marks H3K4me2 and H3K4me3 at unmethylated gDMRs correlates with promoter activity and prevents the binding of DNMT3A and DNMT3B/DNMT3L *de novo* methylation complexes (Zhang et al., 2010). This is consistent with the previously described model in which active transcription prevented *de novo* methylation in the oocyte (Kelsey & Feil, 2013).

1.4.5 Regulatory mechanisms after fertilization

The tissue-specific expression of *Grb10* isoforms relies on more than differential methylation of the parental alleles at the ICR, as there are no tissue-specific differences in DNA methylation at CGI2 between villous trophoblast, brain, and placenta. Differential methylation in CGI2 and biallelic hypomethylation of CGI1 is maintained across murine tissue and developmental stages, regardless of expression (Yamasaki-Ishizaki et al., 2007). In humans as well, the CGI-2 DMR is present in both 'imprinted' (such as the CNS) and 'unimprinted' tissues (where *Grb10* is biallelically expressed) (Monk et al., 2009). Likewise, CpG Island 1 (CGI-1 in humans, CGI1 in mice) is ubiquitously unmethylated. However, CGI3 is paternally hypomethylated in mouse brain, suggesting DNA methylation is involved in regulating brain-specific expression from Exon 1C (Arnaud et al., 2003). Regardless, additional epigenetic modifications and regulatory mechanisms are necessary to direct the tissue-specific imprinted expression of *Grb10*/*GRB10* post-fertilization.

1.4.5.1 CTCF as an insulator

One model of imprinting regulation depends on CTCF binding sites within the ICR. We previously referenced CTCF as a ZFP which protects its binding sites from methylation during the post-fertilization period. CTCF binding to the ICR can also block interaction with insulators and enhancers in a methylation-sensitive fashion. For example, CTCF binding on the unmethylated maternal allele of the *Igf2/H19* ICR prevents shared enhancers from activating *Igf2* expression, deflecting their activity to promote exclusive *H19* expression. Conversely, paternal methylation prevents CTCF binding, allowing *Igf2*–enhancer interaction and paternal-specific *Igf2* expression. This in turn leads to secondary methylation and silencing of the paternal *H19* promoter (Lee & Bartolomei, 2013).

Murine *Grb10* regulation also employs CTCF, although the mechanism used here is less clear. While the regions between promoters in murine *Grb10* and human *GRB10* are highly homologous, a mouse-specific tandem repeat region allows CTCF binding to the unmethylated paternal allele in all tissues (Hikichi et al., 2003; Plasschaert & Bartolomei, 2015). Deletion of the *Grb10* ICR in mice results in biallelic expression of the major *Grb10* isoform in all tissues, suggesting a reactivation or release of the major promoter (Shiura et al., 2009). Additionally, depletion of CTCF results in modest but significant upregulation of the major *Grb10* isoform, but does not impact expression of the neuron-specific transcript in mESCs (Plasschaert & Bartolomei, 2015). The *Grb10* paternal ICR is therefore thought to repress the major promoter through the paternal recruitment of CTCF, though it is unclear whether this

acts through direct repressor activity or as an enhancer blocker, as at the *Igf2/H19* locus. In human tissues, the absence of the CTCF binding site found in mouse and biallelic expression from the major promoter suggests a different regulatory mechanism (Hikichi et al., 2003).

1.4.5.2 Bivalent chromatin domain

The murine *Grb10* unmethylated paternal ICR at CGI2 features a monoallelic bivalent chromatin domain enriched for both repressive (H3K27me3) and permissive (H3K4me2) marks in somatic tissues. H3K27me3 is found along the whole 5' UTR on the paternal unmethylated allele, but H3K4me2 enrichment is specific to CGI2 (Sanz et al., 2008; Yamasaki-Ishizaki et al., 2007). This 'primed' bivalent state is resolved during neuronal differentiation, where repressive H3K27me3 is lost, permissive H3K4me2 remains, and H3K9ac and H3K27ac marks are enriched (Sanz et al., 2008). Resolution of the bivalent domain correlates with reactivation of paternal expression in differentiating neurospheres and cultured motor neurons (Plasschaert & Bartolomei, 2015; Sanz et al., 2008). Loss of H3K27me3 alone is likely insufficient to trigger de-repression of the paternal-specific promoters at CGI2. Global loss of H3K27me3 in $EED^{-/-}$ embryos (lacking the Embryonic Ectoderm Development polycomb group protein which adds H3K27me3) fails to activate widespread *Grb10* paternal expression. Analysis of differentiating neurospheres suggests glial cells also lose H3K27me3 at CGI2, though they do not express paternal *Grb10* (Sanz et al., 2008). Neuronal-specific factors are likely required to extend H3K27me3 loss into active gene expression, probably

by recruiting histone acetyltransferases. The monoallelic bivalent chromatin domain is likely established in the pre-implantation embryo and is maintained in somatic tissues excepting the brain, as maternal expression is found in undifferentiated ES and trophoblast cells (Sanz et al., 2008). The bivalent domain and its resolution are conserved at the human ICR, where accumulating activating histone modifications like H3K9ac and H3K27ac presumably allow paternal expression of brain-specific transcript from exon UN2 (Monk et al., 2009).

In contrast to the paternal bivalent chromatin domain, the murine DNA methylated maternal CGI2 ICR is enriched for repressive histone marks H3K9me3 and H4K20me3. These marks likely maintain maternal silencing of the CGI2 promoters. In tissues and cultured cells, the promoter for the major maternal transcript, CGI1, is enriched for H3K4me2 and H3/4 pan-acetyl marks (Sanz et al., 2008; Yamasaki-Ishizaki et al., 2007). Additionally, CGI1, CGI2, and CGI3 are maternally enriched for H3K27me1, which has been linked to active transcriptional start sites (Sanz et al., 2008). These active marks likely contribute to exon 1A transcription from the major promoter in glial cells and fibroblasts, and are not found in neurons. In primary neuronal culture, CGI1 is biallelically enriched for H3K27 methylation and the major transcript is likewise biallelically silenced. In fibroblasts which express the maternal major transcript, CGI1 is enriched for H3K27 methylation only on the silent paternal allele. CGI3 is biallelically hypoacetylated at H3/4 and hypomethylated at H3K4 in cultured cells (Yamasaki-Ishizaki et al., 2007).

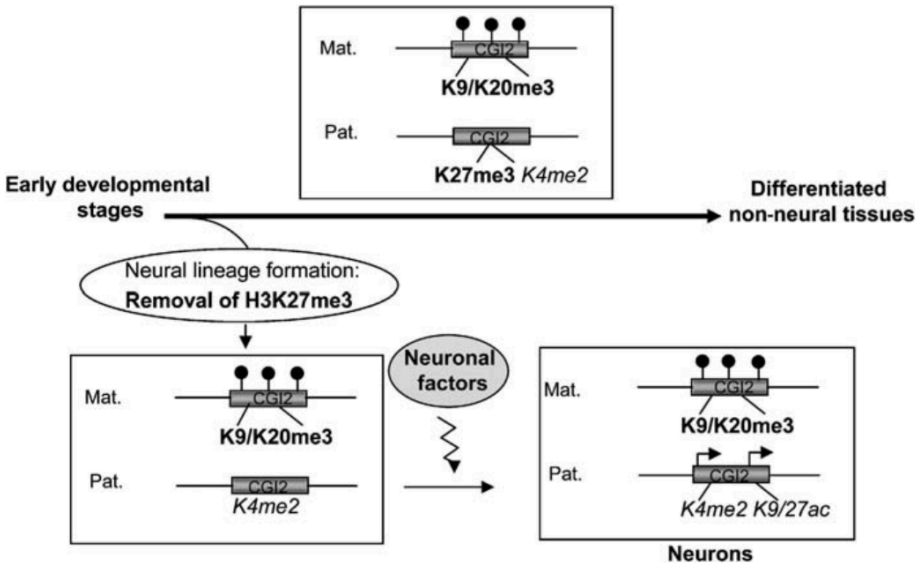

Figure 1.3 Model for Brain-Specific Expression of Paternal Grb10–Adapted from Sanz 2008, Figure 5

Parent- and tissue-specific expression of *Grb10* relies on marks which elaborate on the differentially methylated ICR at CGI2 and which are remodeled by tissue-specific factors. The main model for imprinted regulation of paternal-specific transcripts initiating from CGI2 relies on the bivalent chromatin domain present in somatic tissues and resolved in neurons (Sanz et al., 2008). A model for regulation of maternal-specific transcripts initiating from the major promoter at CGI1 relies on tissue-specific histone marks at CGI1 and potentially involves the binding of CTCF to the unmethylated paternal CGI2 as either a direct repressor or enhancer blocker to CGI1 (Hikichi et al., 2003).

1.4.5.3 Grb10 and Dopa Decarboxylase– an imprinting cluster

The *Grb10* ICR at CGI2 also appears to regulate the imprinted expression of its neighbor *Dopa Decarboxylase (Ddc*) (Menheniott et al., 2008).

In mice, *Ddc* is ~25 kb from *Grb10* on proximal chromosome 11. In humans, *DDC* and *GRB10* are in a conserved linkage region on chromosome 7p12.2 (Hitchins et al., 2001). Dopa decarboxylase (DDC), aka Aromatic L-Amino Acid Decarboxylase (AADC), plays an essential role in the biosynthesis of catecholamine neurotransmitters and serotonin (Christenson, 1972). DDC is expressed not only in dopaminergic and serotonergic neurons in the CNS and PNS, but also in nonneuronal tissues including liver, pancreas, kidney, intestine, and heart. Perturbations of *DDC* expression have been associated with neurodegenerative and psychiatric disorders including Parkinson's Disease, Bipolar Affective Disorder, and Attention Deficit Hyperactivity Disorder (Børglum et al., 2003; Ichinose et al., 1994; Kirley et al., 2002). *DDC* (alongside *GRB10*) is also within a chromosome region (7p12.2) associated with Silver–Russell Syndrome (Hitchins et al., 2001). Tissue-specific expression of *Ddc/DDC* in neuronal and nonneuronal lineages is directed by promoter switching and alternative splicing (Ichinose et al., 1992; Le Van Thai, Coste, Allen, Palmiter, & Weber, 1993).

While *Ddc* is biallelically expressed in the newborn brain, one transcriptional variant, *Ddc_exon1a*, is expressed exclusively from the paternal allele in the developing embryonic heart (Menheniott et al., 2008). Despite this tissue-specific imprinted expression pattern, *Ddc* does not appear to have a DMR in its promoter region. Instead, $Dnmt3^{mat-/+}$ embryos, in which maternal DMRs are lost, implicate a shared imprinting mechanism between *Grb10* and *Ddc_exon1a*. Maternal *Grb10* is significantly downregulated in $Dnmt3L^{mat-/+}$ embryos at e8.5, consistent with a loss of methylation at CGI2, while *Ddc* was

two-fold overexpressed, consistent with reactivation of a maternally repressed imprinted allele (Arnaud et al., 2006; Menheniott et al., 2008). The neighboring genes *Fidgetin-like 1* (*Fignl1*) and *Cobl* were not differentially expressed in *Dnmt3L*$^{mat-/+}$ nor uniparental duplication embryos (Hitchins et al., 2002; Menheniott et al., 2008). This evidence suggests *Grb10* and *Ddc* are reciprocally regulated by *Dnmt3L*-dependent maternal methylation of a shared ICR at *Grb10* CGI2, and that this imprinting cluster excludes neighboring *Fignl1* and *Cobl*.

Reciprocal expression of *Grb10* (maternal) and *Ddc_exon1a* (paternal) in the heart could be achieved by a mechanism resembling that at the *H19/Igf2* cluster. There, CTCF binds to a maternally unmethylated element in the ICR and blocks enhancer interaction with *Igf2*, allowing interaction with *H19* instead (Hark et al., 2000). CTCF sites in mouse CGI2 may play a similar role in activating paternal expression of *Ddc_exon1a* in the presence of heart-specific transcription factors and continuous blocking of paternal *Grb10* expression from the major promoter. However, these CTCF sites are absent in human CGI-2 at *GRB10*, and specific characterization of *DDC* expression in human fetal heart is as yet insufficient (Menheniott et al., 2008). If the biallelic *DDC* expression reported in homogenized fetal tissues also extends to the heart, the absence of CTCF binding sites may be the cause of differential imprinting of *Ddc/DDC* between mouse and human (Hitchins et al., 2002).

The overlap of functional niches, with high paternal *Grb10* expression in monoaminergic neurons and the role of *Ddc* in catecholamine production in dopaminergic and serotonergic neurons is also a point of curiosity. These

imprinted genes do not share overlapping imprinted tissue-specific expression, as *Ddc* is biallelically expressed in the embryonic brain and *Grb10* is paternally silent in the heart. Nevertheless, the proximity of these genes may have aided the selective pressures of imprinting in conferring imprinting control on *Ddc* through mechanisms already present at *Grb10* CGI2. Far from passive acquisition by proximity however, Menheniott et al. note the well characterized effects of catecholamine neurotransmitters upon cardiac development suggest an active acquisition of imprinting at *Ddc* (Menheniott et al., 2008).

1.4.5.4 Other post-fertilization mechanisms of imprinting regulation

Grb10, as an imprinted gene regulated by a tissue-sensitive and monoallelic bivalent chromatin domain and expressed from both alleles in complementary patterns, is unique locus. Here, I will briefly describe a few additional mechanisms of imprinting regulation, not used at *Grb10*, but relevant to imprinted clusters in general.

Noncoding RNAs (ncRNAs) are a recognized regulatory mechanism at established imprinted loci. Most imprinting clusters contain a variety of ncRNAs (microRNAs, snoRNAs, lncRNAs) with *cis*-regulatory functions. Long noncoding RNAs (lncRNAs), for example, have multiple proposed roles in imprinting regulation. Code overlap with adjacent imprinted genes could create sense-antisense transcriptional interference, where the transcription of the lncRNA kicks RNA polymerase II off the imprinted gene. This mechanism is proposed for the regulation of *Igf2r* (imprinted) by the lncRNA Airn. *Igf2r* is

initially bialleleically expressed, but the initiation of *Airn* expression from the paternal allele repulses RNA Pol II and silences *Igf2r* expression *in cis* (Latos et al., 2009; Lee & Bartolomei, 2013). lncRNAs may also directly recruit repressive chromatin proteins to form repressive complexes. Examples include lncRNAs Gtl2 and Nespas, which appear to associate with polycomb repressive proteins. Our previous example, *Airn,* is also suggested to actively recruit G9a, a histone H3 lysine 9 methyltransferase, to regulate paternal-specific silencing of the gene *Slc22a3* in the placenta (Lee & Bartolomei, 2013; Nagano et al., 2008). Another variety of ncRNAs, small nucleolar lncRNAs (sno-lncRNAs), may regulate imprinting through alternative splicing. Sno-lncRNAs from the PWS region accumulate near their site of synthesis and strongly associate with Fox family splicing regulators, possibly acting as a molecular sink. This action alters splicing patterns in a localized fashion (Lee & Bartolomei, 2013; Yin et al., 2012).

Imprinting regulatory mechanisms may also intervene after the initiation of transcription but before elongation. The sense-orientated retrogene *Mcts2* is located within an intron of imprinted *H13 (*minor histocompatibility antigen *H13*). Expression of *Mcts2* silences paternal *H13* expression *in cis* by causing *H13* mRNA to use upstream polyadenylation sites. This produces shortened transcripts lacking enzymatic activity. On the maternal chromosome, DNA methylation silences the *Mcts2* promoter, allowing the full-length, functional expression of *H13*. RNA Polymerase II is recruited to both alleles, regardless of the final transcriptional product (Barlow, 2011; A. J. Wood et al., 2008).

Imprinted genes rely on additional epigenetic remodeling and tissue-specific factors to achieve their final expression profiles. These include methylation sensitive factors such as CTCF, tissue-specific remodeling of histone marks, expression of various noncoding RNAs, and interference with transcription initiation and elongation.

1.5 Consequences of Imprinting–Grb10 expression

Grb10 was first identified as a maternally expressed imprinted gene in a cDNA subtractive hybridization study using normal and androgenetic (paternal diploid genome only) fertilized mouse embryos (Miyoshi et al., 1998). Its role as an inhibitor of the growth promoting IR and IGF1R pathways flagged it as a candidate gene for Silver-Russell syndrome (SRS). Seven-10% of SRS cases are caused by maternal uniparental duplication (UPD) of human chromosome 7, where *GRB10* localizes, causing pre- and postnatal growth retardation (Kotzot & Utermann, 2005). No pathogenic mutations have been identified for genes in the duplicated region, suggesting an imprinted dosage problem (Eggermann et al., 2008). However, biallelic expression of *Grb10* from the major promoter in human tissues (notably excepting the CNS) discounts a major role in the etiology of SRS (Blagitko et al., 2000). Additionally, several SRS patients have segmental maternal UPD restricted to the long arm of chromosome 7 (UPD(7q)mat), which also contains imprinted loci, indicating aberrant imprinting of *GRB10* (on 7p) is not required (Eggermann et al., 2008). While *Grb10* has been discounted in explaining the phenotypes of SRS, it does have distinct parent-of-origin phenotypes (previously described), that rely on

and reflect its imprinted expression patterns. Here I will describe the unique expression patterns achieved by the *Grb10* imprinting architecture in the embryo and adult mouse to contextualize the expectations and aims of experiments in this thesis.

1.5.1 Expression in Embryo

The *LacZ* reporter cassette in the *Grb10*KO model used in this thesis and that of A. Garfield allows clear visualization of reciprocal parent-of-origin *Grb10* expression in the whole embryo. Maternal inheritance of the *LacZ* reporter cassette interrupting *Grb10* shows widespread expression throughout the e10.5 embryo, excepting the CNS. Almost all endoderm- and mesoderm-derived tissues reported maternal expression (Garfield, 2007). In keeping with this, *Grb10* and *Grb14* mRNA and protein are detectable in skeletal muscle and white adipose tissue, both major insulin targets, as well as the heart and kidney (Desbuquois et al., 2013; Laviola et al., 1997; Ooi et al., 1995). In the CNS at e10.5, maternal *Grb10* expression was limited to the roof plate of the metencephalon and the surfaces of the lateral and fourth ventricles. At e14.5, CNS expression of maternal *Grb10* is restricted to the choroid plexi of the lateral and fourth ventricles, the ependymal layers of the ventricles, and the meninges of the brain and spinal cord–all non-neuronal regions (Garfield, 2007). The *Grb10Δ2-4* model demonstrated maternal expression in the trophoblast and foetal endothelium of mature (e14.5 and e17.5) placenta (Charalambous et al., 2010). Overall, expression of maternal *Grb10* declines during growth deceleration in late gestation, possibly as part

of an imprinted gene network that controls mammalian somatic growth (Al Adhami et al., 2015; Desbuquois et al., 2013). Maternal expression persists postnatally in only a subset of insulin responsive tissues (Desbuquois et al., 2013; F. M. Smith et al., 2007).

Reciprocally, paternal inheritance of the *Grb10*KO *LacZ* cassette shows expression is restricted to the CNS. Paternal expression in the brain is absent at e9.5, but emerges with scattered staining in the rhombencephalon at e10.5, and is more noticeable by e11.5. At e14.5, expression becomes clear in the differentiated medulla oblongata and caudally along the ventral spinal cord. Additionally, staining is found in the mesencephalon, thalamic and hypothalamic regions of the diencephalon, and the olfactory lobes (Garfield, 2007). *Grb10* expression is completely absent from cortical structures and the cerebellum. The emergence of reporter expression between e.11.5 and e14.5 suggests the paternal-specific brain promoter is activated after the commencement of neurogenesis and depends on neuron-specific transcriptional regulators (Garfield, 2007; Garfield et al., 2011; Hikichi et al., 2003; Sanz et al., 2008).

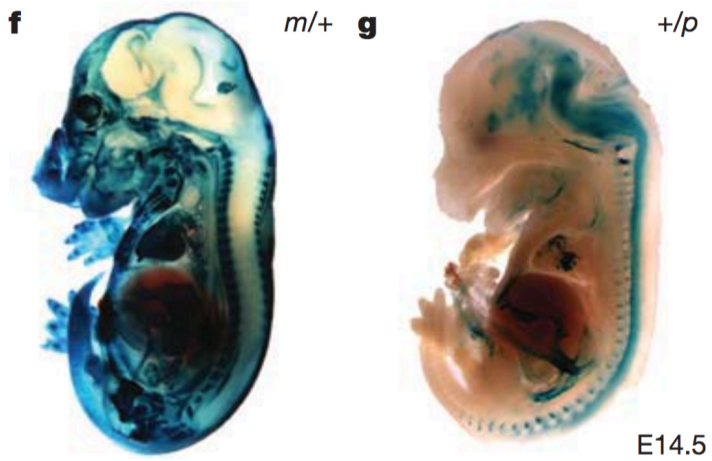

Figure 1.4 Reciprocal Reporter Expression in Grb10KO models–Adapted from Garfield 2011, Figure 1

1.5.2 Expression in Adult Brain

In the adult *Grb10*$^{+/p}$ brain (murine, 3 months of age), the paternally inherited *LacZ* cassette reports *Grb10* expression via β-galactosidase (Garfield, 2007). β-galactosidase staining is evident in the thalamus, hypothalamus, midbrain, and hindbrain but is excluded from the cortex, cerebellum, and medulla oblongata (Garfield, 2007; Garfield et al., 2011). Expression in LHPA-related (limbic-hypothalamic-pituitary axis) brain regions marks *Grb10* for a potential function in stress-related signaling (Plasschaert & Bartolomei, 2015). Notably, the imprinted gene *Nesp*, which has a role in novel exploration behaviour, has overlapping expression with *Grb10* in LHPA related brain regions (Dent & Isles, 2014). *Nesp* and *Grb10* are highly expressed in the hypothalamus, dorsal raphe nucleus, locus coeruleus, and Edinger-Westphal nucleus (Dent & Isles, 2014; Plagge et al., 2005).

Paternal *Grb10* expression is also neuron-specific and is found in almost all monoaminergic cell populations (Garfield et al., 2011; Yamasaki-Ishizaki et

al., 2007). Fluorescent co-localization demonstrated paternal *Grb10* expression in cholinergic (ChAT) interneurons neurons of caudate putamen, dopaminergic (DAT) neurons of the substantia nigra pars compacta, and serotonergic (5-HT) neurons of the dorsal raphe nucleus. Both *LacZ* reporter expression and *in situ* hybridization analysis of endogenous *Grb10* mRNA are in concordance with this expression profile (Garfield et al., 2011). The strongest sites of β-galactosidase activity in the paternal knockout are the substantia nigra pars compacta and the ventral tegmental area, respectively identifying the A9 and A10 dopaminergic cell body populations. The adjacent substantia nigra pars reticulata, from which GABAergic neurons project, is completely excluded from reporter expression (Garfield, 2007). Maternal *Grb10* expression is almost completely absent from *Grb10KO*$^{+/p}$ brains, though low levels are detectable in a few regions including the median preoptic nucleus, medial habenular, medial amydaloid nuclei, and ventromedial hypothalamus (Garfield et al., 2011).

1.5.3 Midbrain monoaminergic expression and social behaviour

The strong midbrain monoaminergic expression of paternal *Grb10* is a good place to begin investigating how paternal expression (and not the maternal) impacts the behavioural phenotypes found in this model. Monoaminergic signaling in the midbrain mediates aggressive, impulsive, fearful, and stress-responsive behaviours relevant to social contexts (Audero et al., 2013; F. Wang et al., 2011). Reciprocally, social hierarchies impact individual experience of stress via dopaminergic signaling (Matthews et al.,

2016). Modulation of serotonin and dopamine can influence dominant and submissive behaviour (Qu, Ligneul, Van der Henst, & Dreher, 2017). The relationship between the midbrain and social dominance behaviours is discussed in more detail in Chapter 5.

There is evidence to suggest monoaminergic brain regions may mediate the impact of paternal *Grb10* knockout on social behaviour. Compellingly, Garfield found *Grb10*$^{+/p}$ mice 3 months of age have significantly larger subcortical areas at Bregma +0.26 to +0.38 and Bregma -1.46 to -1.72 compared to wildtype controls, whereas cortical areas in the same regions were not significantly different. In parallel, total wet brain to body weight ratios at 84 days (3 months) and 308 days (10 months) were significantly higher than wildtype controls, whereas this difference did not exist at D1 (Garfield, 2007). This suggests paternal *Grb10* knockout removed a growth restrictor which acts in subcortical brain regions during adulthood or primes brain maturation protocols in adulthood. This phenotype warranted further characterization and is the basis of Aim (1) of this thesis. However, macro-dissected brain regions of *Grb10*$^{+/p}$ showed no change in the levels of dopamine, serotonin, noradrenalin, and acetylcholine (Garfield et al., 2011). If subcortical overgrowth in *Grb10*$^{+/p}$ mice induces changes in social behaviour by impacting monoaminergic signaling in the midbrain and hindbrain, it may not be mediated by global changes in the level of these neurotransmitters. We determined further characterization of brain growth allometry and social behaviour in the *Grb10*$^{+/p}$ mouse was required to understand the role of paternal *Grb10* in brain and behaviour. I describe the aims of this thesis below.

1.6 Aims

1.6.1 Aim (1) Characterize Midbrain Overgrowth in *Grb10*$^{+/p}$ mice (Chapters 3, 4)

To address how brain growth changes over time I took two approaches. Firstly, I set up a cross-sectional study of three cohorts tested at 2 months, 6 months, and 10 months to investigate the development of midbrain overgrowth. I used histology (Nissl staining) to compare midbrain area to cortical area in brain sections across all three time points. In addition to investigating subcortical area, I also sought to identify the cause of the increase. Three possibilities are increased proliferation of neuronal or glial cells, increase in cell size or lower cell density, and aberrant pruning or decreased cell death/apoptosis. Therefore, we investigated neuron to total cell ratios and densities via fluorescent antibody staining for NeuN and DAPI to determine whether loss of paternal *Grb10* in neurons impacted their numbers or density within the expanded midbrain (Histology and IHC–Chapter 3). My second approach was to examine brain growth in a longitudinal cohort using MRI scanning at 2 months, 6 months, and 10 months of age. This group provides a longitudinal, within-subjects measure of brain maturation to integrate the correlations between brain morphology made during our cross-sectional study (MRI–Chapter 4).

1.6.2 Aim (2) Examine key behaviours over time and correlate with any changes in brain growth (Chapters 5, 6)

Behavioural testing was conducted as part of the cross-sectional study described above. Animals underwent overlapping social dominance measurements, including the Taylor tube test (stranger encounter and within-cage encounters) and urine marking at 2 months, 6 months, and 10 months of age. In addition, I monitored degree of whisker barbering in behavioural cohorts (Social Dominance–Chapter 5). Marble burying and elevated plus maze were included as additional tests to exclude alternative explanations of social dominance test results (Compulsivity and Anxiety–Chapter 6) (Curley, 2011). After behavioural testing within a restricted 4-week window, several animals were selected for perfusion and sectioning for Aim (1).

1.6.3 Aim (3) Construct a CRISPR/dCas9 epigenetic editing tool to probe the functional role of the *GRB10/Grb10* DMR (Chapter 7)

Our third aim was to use targeted epigenetic editing to probe the functional role of the *Grb10* imprinting mark. We created a novel CRISPR/dCas9 based epigenome editing tool with a TET2 catalytic domain for targeted erasure of the differential methylation at CpG2. We aimed to test our construct in HEK cells before expanding applications to wildtype mESCs derived from our colony. Targeted manipulations allow us to explore the functional role of the imprinting mark, independently of changes made to the DNA sequence of *Grb10*. Previous models have relied on deletion of crucial DNA by the insertion of reporter cassettes (Charalambous et al., 2003; Garfield

et al., 2011). The *Grb10Δ2-4* model deletes 36 kb of endogenous sequence from before exon 2 to after exon 4, while *Grb10KO* deletes 12 bp of exon 7 (Cowley et al., 2014). The *Grb10Δ2-4* model deleted a paternal promoter and failed to recapitulate the whole paternal expression profile, while the *Grb10*KO model inserted a *LacZ* cassette into exon 7, disrupting the transcript (Garfield et al., 2011). The first deletion model raises a confounding variable (the loss of the promoter) in analysis of the functional role of epigenetic marks. The insertion of *LacZ* cassette in both models alters the length of the gene, potentially dysregulating spatially- or sequence-driven mechanisms. It is important to develop targeted epigenetic editors for functional investigation of imprinting marks independent of gene sequence, as functional difference by parent-of-origin arises within the imprinting architecture and not within sequence.

2 General Methods

2.1 General Molecular Methods

2.1.1 Polymerase Chain Reaction (PCR) protocol

Basic reaction mixtures and thermocycling programmes are described in the following tables. Primers and alternative annealing temperatures are specified in the thesis where relevant or in Appendix V for mESCs. Primers were designed using the NCBI Primer-BLAST tool with default preference settings. Pyrosequencing primers were designed using the Pyromark Assay Design 2.0 software. PCR reactions were carried out in MicroAmp 8-Tube strips (Applied Biosystems).

Table 2.1 PCR Reaction Mix

Reaction	Supplier	Reaction Volume
ddH20	–	To 10 µl total volume
10x Buffer	Qiagen	1 µl
$MgCl_2$	Qiagen	0.8 µl
dNTPs (2 µM)	Bioline	0.8 µl
F primer (10 µM)	Sigma	0.3 µl
R_1 primer (10 µM)	Sigma	0.3 µl
R_2 primer (10 µM)	Sigma	0.3 µl
HotStar Taq	Qiagen	0.125 µl
DNA template	–	1-2 µl

Table 2.2 HotStar Taq Thermocycling PCR protocol

HotStar Taq Thermocycling PCR Protocol
1. 95˚C for 10 minutes
2. 95˚C for 30 sec
3. 50 – 60˚C for 30 sec
4. 72˚C for 45 sec
5. Stages 2-4, 30-34 cycles
6. 72˚C for 5 min
7. 4˚C forever

2.1.2 Gel Electrophoresis

PCR products were separated on 1-2% agarose gels (1.5% standard) in 0.5% TBE buffer. Gels were run at 100V for 50 minutes, unless otherwise specified by the protocol.

2.2 Animal Husbandry

2.2.1 Subjects: *Grb10KO* B6CBAF1

*Grb10*KO mice were previously created as described in Garfield et al (2011) using a LacZ:neomycin gene-trap cassette interrupting exon 7, and were maintained on a C57BL/6:CBA mixed genetic background through breeding to F1 mates (Garfield, 2007; Garfield et al., 2011). The mouse colony used in this thesis was derived from eight KO females born in Cardiff after embryo transfer from a colony in Bath, courtesy of the Andrew Ward lab and Kim Moorwood. This line was maintained by crossing with a wildtype "B6CBAF1/crl" line from Charles River (aka C57BL/6J:CBA/CaCrl F1 mice, the first generation progeny of a cross between female C57BL/6J and male CBA/CaCrl mice) or in house on wildtype mice with the mixed genetic background of the Bath mice. These animals were maintained on a non-inbred background to avoid the problem of an inverted vagina, which occurs frequently on inbred strain backgrounds in *Grb10KO* mice (personal communication with Andrew Ward). Experimental animals were of mixed C57BL/6:CBA genetic background; generated by crossing wildtype (WT) "B6CBAF1/crl" or C57BL/6:CBA mixed background breeding stock with the desired parent of origin heterozygous *Grb10*KO animal, also on a mixed background as in Garfield 2011.

Paternal (*Grb10*$^{+/p}$) and maternal (*Grb10*$^{+/m}$) knockouts are distinguished because the alleles of this imprinted gene show tissue-specific and complementary expression patterns. In mouse, the maternal allele alone is expressed in peripheral tissues. Conversely, the paternal allele alone is expressed in the CNS. Each parent-of-origin specific heterozygous knockout thus constitutes a separate model. *Grb10*$^{+/p}$ mice have a loss of *Grb10* expression in the CNS only, while *Grb10*$^{+/m}$ mice have a loss of *Grb10* expression in the peripheral tissues but *not* in the CNS. While the paternal KO (*Grb10*$^{+/p}$) mice are the primary focus of this thesis, the maternal KOs (*Grb10*$^{+/m}$) and wildtype (WT) littermates were used as controls. These littermate controls possessed the same mixed genetic background as our *Grb10*$^{+/p}$ mice, thereby avoiding potential behavioural variability due to strain, cross, or generation (F1, F2, etc) differences.

2.2.2 Animal Husbandry

All mice were housed in single-sex, environmentally enriched cages (cardboard tubes, shred-mats, chew sticks) of 1-5 adult mice per cage. Cages were kept in a temperature and humidity controlled animal holding room (21 $\pm$ 2˚C and 50 $\pm$ 10% respectively) on a 12-hour light-dark cycle (lights on at 7:00 hours, lights off at 19:00 hours). Breeding animals were held in a smaller, quieter breeding room at the same temperature and humidity as the holding room. All subjects had *ad libitum* access to standard rodent laboratory chow and water. Cages were cleaned and changed once a week at a regular time and

day of the week for minimal disruption. Changes to the cleaning schedule dictated by the behavioural testing are indicated below in Section 1.3.4.

Behavioural groups were housed in cages of four containing two wildtype (WT) and two knockout (KO) animals from the same type of parent-of-origin cross (maternal or paternal). Where possible, animals of the same birth litter were kept together. Male mice were genotyped from identification ear clips prior to weaning to enable the cage set-up. Females were weaned prior to genotyping and re-sorted into the appropriate set-up. Mice were weaned between P19 and P28.

Breeding animals were paired two females to one male for two weeks. After the two week period, the male was removed. Dams were placed in individual housing the week prior to full term. This measure was necessary to aid pre-weaning ear clip identification and genotyping of the behavioural cohort. This ensured the behavioural cohorts could be weaned into balanced genotype groups (2 WT, 2 *Grb10*$^{+/p}$ per cage) and ensured exact lineage and litter groups were known for the stranger encounter tube tests. Any impact of maternal isolation in the final week of gestation would have applied to both WT and *Grb10*$^{+/p}$ mice of both sexes. Some, but not all, mothers showed signs of self-over-grooming. These mice were monitored by the researcher and NACWO.

All mice were monitored by the experimenter and staff for signs of ill health. Mice showing signs of illness were assessed by the NACWO, and were culled if necessary. During colony maintenance, two virgin *Grb10*KO$^{+/m}$ mice from different parental crosses were culled due to swollen vulvas.

2.2.3 Genotyping

Initial genotyping was carried out on DNA extracted from excess tissue from identification ear clips. At end-of-life, genotype was re-confirmed from tail biopsies. Ear clips and tail biopsies were digested overnight at 55˚C in Tail Lysis buffer (100 mM Tris-HCl, 5 mM EDTA, 0.2% SDS, 200 mM NaCl) with proteinase K (20 µg/ml). Samples were spun for 10 minutes at 13,000 rpm and the supernatant was tipped into a new tube. After Ice-cold isopropanol was added, samples were inverted and stored in a -80 freezer for 10 minutes. Samples were spun for 2 minutes at 13,000 rpm and isopropanol supernatant was poured off. Ice cold 70% ethanol was added, the samples were vortexed, and were spun for 2 minutes at 13,000 rpm. The ethanol was poured off and the samples were air dried before being resuspended in TE buffer. Samples were heated at 50˚C for ~20 minutes before being stored or used in a genotyping PCR reaction. The genotyping PCR reaction used components described in the molecular methods section and the following three primers. A band at 393 bp indicated a WT allele while a band at 177bp indicated a KO allele.

Table 2.3 Genotyping Primers

Primer Name	**Direction**	**Sequence**	**Annealing**	**Notes**
Grb10_SetBFor	Forward	CCAAGTGGAGAG TACCATGCC	60˚C	Murine *Grb10* exon 8
Grb10_SetBRev	Reverse	TCACCTGACAGGC ACCTCCCC	60˚C	Murine *Grb10* WT allele

Grb10_KO_KM4Rev	Reverse	CACAACGGGTTCT TCTGTTAGTCC		Murine *Grb10* KO allele

2.3 Behavioural methods

2.3.1 Handling

Behavioural cohorts were weaned at P19-P28 days. Subsequently, mice were handled as little as possible up until one week prior to the start of behavioural testing. One week out, the researcher who would perform the behavioural tests handled the mice daily for 5 days, recording weight and barbering status. Kira Rienecker conducted behavioural testing for male mice 2, 6, and 10 months of age and tube testing for female mice 2 months of age. Alexander Chavasse conducted behavioural testing for female mice 6 and 10 months of age.

2.3.2 Measurement of bodyweight

Bodyweight was measured at weaning, at each behavioural testing session, and after culling. This data was used as an index of growth and development and as a measure of general health.

2.3.3 Observed Home Cage Behaviour

As previously observed in the Garfield thesis (p 224), the *Grb10*KO colony showed unusual home cage behaviour (Garfield, 2007). Cages generated from paternal transmission demonstrated highly excitable behaviour and frequent cage lid climbing. On removal of the lid, mice rapidly circled the cage to avoid the handler, and made multiple escape attempts by springing up at the corners

of the cages. Younger animals (pre-weaning) were more excitable, particularly at 3 weeks of age but not at 2 weeks of age. Excitable young mice also demonstrated tail-rattling. Older mice were less excitable, particularly experienced wild-type mothers. On one occasion, one male was separated from his cage mates due to excessive aggression/fighting with cage mates.

2.3.4 Order of Experiments

The 8-10 week, 6 month, and 10 month cohorts (but not the isolation cohorts) underwent behavioural testing, in order, for: stranger tube test, social tube test, urine marking (except females), marble burying, and elevated plus maze (EPM). Each mouse experienced a maximum of one test per day. Details of each test are found in Chapters 5 and 6. Cages were not cleaned during multiple day testing of the same dominance test, and were half-cleaned between tube testing and urine marking blocks. Mice were transferred to fresh cages following urine marking, and normal cleaning schedules resumed for marble burying and EPM.

Mice from the behavioural cohort were perfused for immunohistochemistry and Nissl-staining experiments in Chapter 3. Cage rank from the social tube test was used to select animals for perfusion. Mice were selected in cage mate pairs containing one wildtype and one *Grb10*$^{+/p}$ also holding the top two ranks in the cage. Rank 1 was alternated between wildtype and *Grb10*$^{+/p}$ where possible. *Grb10*$^{+/m}$ mice did not undergo tube testing and were selected randomly. For logistical reasons, transcardiac perfusions of

terminally anesthetized mice occurred after marble burying. The remaining cohort continued with the EPM. Further details are available in Chapter 3.

Five cages of mice from the 10 month behavioural cohort were scanned in a longitudinal MRI study at 10 weeks, 6 months, and 10 months of age. These mice were handled for scanning but not prior to or between scanning sessions. These mice were incorporated into the behavioural testing program for the rest of the cohort at 10 months of age, including the 5-day pre-behaviour handling period. MRI scanning at 10 months of age took place after urine marking and before marble burying and the EPM.

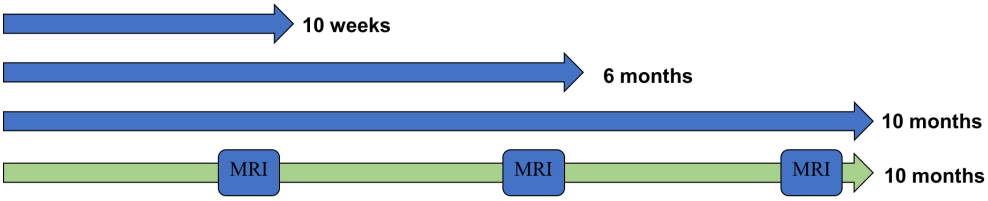

Figure 2.1 Overview of Experimental Cohorts

2.3.5 Behavioural Testing Environments

Three rooms were reserved for behavioural testing for all three cohorts. Temperature and humidity in the behavioural rooms were identical to the holding rooms. All tube testing and urine marking was performed in a quiet room lit by a single indirect lamp bulb between 25 and 60 W. All mice experienced stranger- and social-encounter tube testing in only one room, but male and female mice underwent testing in separate rooms when both Kira Rienecker (male mice) and Alex Chevasse (female mice) performed testing at 6 and 10 months. For urine marking, cohorts were divided as whole cages between two rooms, such that two urine marking tests could occur simultaneously, but all four mice in a cage underwent testing in the same

room. All marble burying and EPM testing occurred in the “Ethovision” room, which was lit by an overhead fluorescent light. The overhead fluorescent light was required to achieve minimum sensitivity for Ethovision tracking, and did not appear to affect results.

2.3.6 Ethovision Tracking

Marble burying and the EPM used the EthoVision Observer video tracking software (version 3.0.15, Noldus Information Technology, Netherlands). EthoVision identifies the boundaries of the subject’s body (body fill) and tracks the subject’s movement from a center point in the body fill. Tracking is confined to predefined zones within the total arena, which are customized to each task. Once these zones are defined for the task, the behavioural apparatus is not moved, for consistency between trials. The EthoVision tracking system calculates quantitative descriptors about the subject’s movement over a series of frames collected at 12 frames/sec. Tracking was calibrated for the test prior to testing using non-experimental mice from the same colony as the experimental subjects.

2.3.7 Culling Protocol

Aside from mice culled by terminal anesthesia for transcardiac perfusion, all mice for these experiments and the supporting colony were culled by cervical dislocation. Mice from the behavioural cohorts and the supporting colony (where possible) were also dissected for brain weight data, presented in Chapter 3.

2.4 Statistics and Data Presentation

Specific statistical analyses are detailed in each chapter. Data analysis was performed using SPSS (versions 23 and 25). Laerd Statistics guides were followed for all procedures and reporting, where possible (https://statistics.laerd.com/premium/index.php). Chapter results sections first present the data screening summary, followed by a "Summary" section with generalized results, and finally the detailed "Reports" sections. Data in diagrams are presented as mean ± standard error of the mean, unless otherwise stated. Specifics are detailed in chapter methods. Statistical significance underwent False Discovery Rate (FDR) corrections using the Benjamini-Liu (BL) method (Y Benjamini & Liu, 1999; Yoav Benjamini, Drai, Elmer, Kafkafi, & Golani, 2001). FDR corrections were performed on all reported measures belonging to one task or overarching heading, and FDR corrections were separate between different tasks/headings. Abridged tables presented in the chapters extend to the critical significance value. Full tables of the BL FDR corrections are available in the appendix. FDR corrections were not carried out for groups of less than 5 statistical tests. Graphs and figures were created using Excel (version 15.32) and Powerpoint (version 15.32).

3 Histology

3.1 Introduction

Preliminary data from Garfield's thesis suggested male *Grb10*$^{+/p}$ brains show a subcortical overgrowth phenotype. Compared to WT brains in both raw brain weight and as a proportion of body weight, *Grb10*$^{+/p}$ were no different at P0, but were heavier at D84 (3 months) and D308 (10 months). Between D84 and D308, *Grb10*$^{+/p}$ brains continued to gain mass while WT brains showed no significant change. Additionally, Garfield measured cortical, subcortical, and total area in Nissl-stained brain sections between Bregma +0.26 mm to +0.38 mm and Bregma -1.46 mm to -1.72 mm from male mice 3 months of age. Subcortical and total area at both positions was significantly larger in *Grb10*$^{+/p}$ brains than wildtypes. Cortical area was comparable to wildtype controls (Garfield, 2007). The objective of this chapter and the next (MRI – Chapter 4) was to systematically examine brain growth in *Grb10*$^{+/p}$ mouse brain. To do this we used histology and immunohistochemistry (this Chapter) and MRI techniques (Chapter 4).

3.1.1 Chapter Aims

Aim (1) Confirm and expand data on increased wet brain weight with age in Grb10$^{+/p}$ mice

We measured whole wet brain weight from as many wildtype, *Grb10*$^{+/m}$, and *Grb10*$^{+/p}$ mice in the colony as possible, and plotted the data

against age to gain a qualitative description of brain growth allometry. For analysis, these data were broken into discrete age bins to determine the effects of GENOTYPE, SEX, and AGE on brain weight.

Aim (2) Measure nested areas in Nissl-stained sections of *Grb10*$^{+/p}$, *Grb10*$^{+/m}$, and wildtype brains at 10 weeks, 6 months, and 10 months of age.

We complimented weight data with area measurements of Nissl-stained brains at 10 weeks, 6 months, and 10 months. Area measurements were nested into subsections to gain information about the specific regions most affected by subcortical overgrowth. We focused on the caudate putamen at Bregma +0.74mm, where we expect paternal *Grb10* expression in cholinergic inter-neurons (Garfield et al., 2011). This cross-sectional Nissl-stained area data was intended to confirm Garfield's findings in both male and female mice, create a profile over three age groups, and provide a point of reference for total cell and neuron density in Aim (3).

Aim (3) Determine neuron density in putative regions of *Grb10*$^{+/p}$ subcortical overgrowth at 10 months of age.

We determined neuron density in putative regions of *Grb10*$^{+/p}$ subcortical overgrowth at 10 months of age. Immunofluorescent staining for β-galactosidase expressed from the paternal *Grb10* allele in *Grb10*$^{+/p}$ mice co-localizes with markers specific for dopaminergic neurons within the substantia

nigra pars compacta, serotonergic neurons within the dorsal raphe nucleus, and cholinergic inter-neurons within the caudate putamen (Garfield et al., 2011). We stained brain slices from male and female mice 10 months of age for total (DAPI) and neuronal (NeuN) cell counts to gain a measure of total cell and neuron density the caudate putamen. The cell counting series was parallel to the 10 month Nissl-stained series used for area measures. We used stereology as a systematic random sampling method (Schmitz et al., 2014). This method accounted for cell orientation and diameter, randomized counting frames in the regions of interest, and allowed us to use the same counting frames for both DAPI and NeuN sampling. Together, Aims (1), (2), and (3) intended to describe the growth allometry of *Grb10*$^{+/p}$ brains.

3.2 Methods

3.2.1 Whole Wet Brain dissection

Whole brains were dissected from freshly culled animals in the colony and weighed. Measurements included whole animal body weight, whole brain wet weight, and whole brain wet weight minus olfactory bulbs (in case we were unable to retrieve intact olfactory bulbs from a sufficient proportion of the population). Approximately 70% of data points fall within three 20-day age bins centered around systematic points in time. These age bins represent the large cross sectional cohorts used in our histology and behavioural studies. The remaining 30% of data points were taken whenever culling occurred during colony maintenance. *Grb10*$^{+/m}$ data in our whole wet brain weight analysis represents only those individuals remaining after meeting our goals for

histology. No *Grb10*$^{+/m}$ cages were bred specifically for behavioural studies or the whole wet brain weight data set.

3.2.2 Perfusions

Brain tissue was preserved by transcardiac perfusions of mice terminally anesthetized with sodium pentobarbital. Animals were first perfused with PBS (~25 ml), and then with ~15 ml neutral buffered Formalin solution (10%, Sigma HT5014-1CS). Brains were removed whole and placed in Formalin at 4˚C for 24-48 hours. They were then washed in PBS and submerged in 30% sucrose in PBS at 4˚C at least overnight or until they sank. Sucrose solution was refreshed following this treatment, and brains were stored at 4˚C until sectioning. For long term storage, brains were embedded in OCT, frozen over dry ice, and stored at -80˚C. If needed, rostral and caudal halves of the brain were manually separated by razor blade at approximately Bregma -1.58 prior to freezing.

3.2.3 Sectioning

Sectioning was carried out on a Leica Small Cryostat at -24˚C. Brain were mounted by freezing in a base of OCT over dry ice with the axial plane perpendicular to the chuck. Sections of 15 µm were mounted directly onto Poly-L-Lysine Hydrobromide (Sigma P1399) coated glass slides and were dried at room temperature, dried overnight, and optionally stored at 4˚C until Nissl staining. Sections of 30 µm were deposited free floating in PBS and were stored at 4˚C until used for immunohistochemistry or mounted for Nissl staining.

3.2.4 Nissl Staining

Staining was performed at room temperature. Sections on glass slides were washed briefly in PBS before undergoing staining for Nissl substances. Slides were washed 2 minutes each in descending ethanol washes (100, 100, 90, 70%), followed by 2 min in deionized water and 3 minutes in fresh Nissl stain (0.05% Cresyl fast violet w/v in 1% sodium acetate, 5% Formic acid solution, and H_2O). Slides were rinsed 30 seconds in deionized water, followed by an ascending ethanol series 3 minutes each (70, 90) and 2 minutes each (100, 100%). Slides were finished with 5 min in xylene and were transferred to fresh xylene to await mounting. Slides were mounted in DPX under coverslips. Nissl stained slides were imaged under bright field at 10x magnification using the Zeiss Axioscan Slide Scanner. Section area was measured using ImageJ software. Sections were compared to a mouse brain atlas (Franklin & Paxinos, 2007).

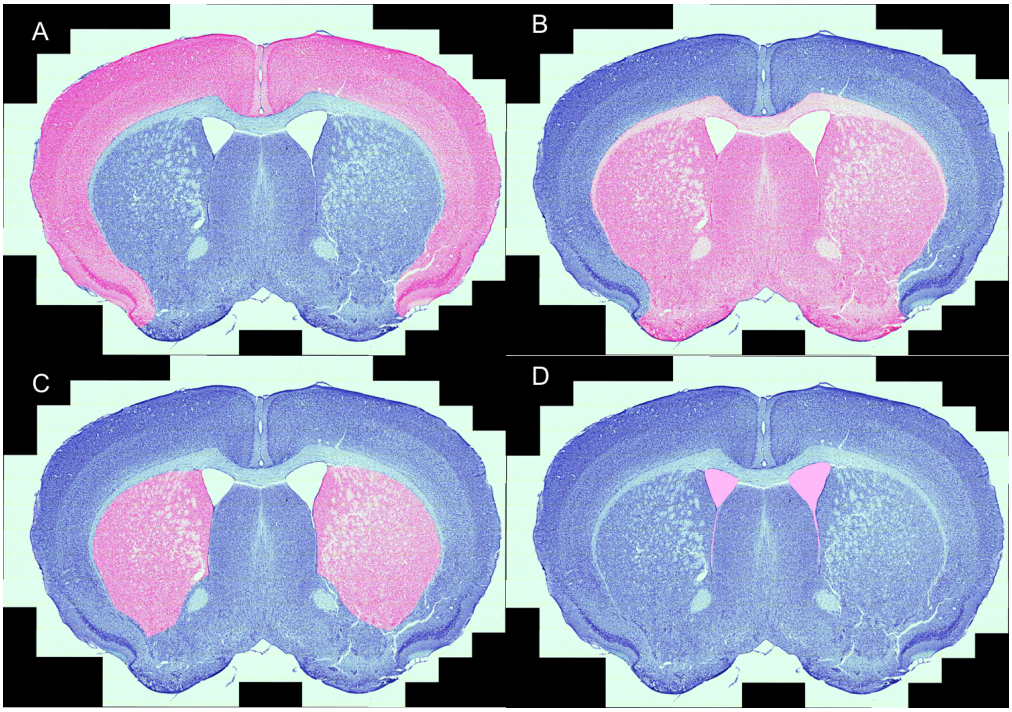

Figure 3.1 Nissl Staining Bregma 0.74mm Area Measures–Example A100 P (female WT)

Figure 3.1: Areas (in pink) defined as being representative of A–Cortex, B–Sub-cortex, C–Caudate Putamen, D–Ventricles

3.2.5 Immunohistochemistry

Free floating sections of 30 µm were stained for NeuN under the following protocol. Sections were transferred from PBS to a blocking solution of 3% donkey serum (DS) solution in 1% Triton X-100 in PBS for 2 hours at room temperature with mild shaking. Blocking solution was removed and sections were covered in a 1˚ antibody solution containing Anti-NeuN (aka Anti-Fox3 Biolegend 835401, Formerly SIG–39860) at 1:500 dilution in 0.2% DS in 0.1% Triton X-100 in PBS. Sections were covered and incubated in 1˚ antibody overnight at 4˚C. Sections were then washed 3 times for 10 minutes each in

0.2% DS in 0.1% Triton X-100. Washes were replaced with a 2˚ antibody solution containing Alexa Fluor Donkey Anti-Mouse (Thermofisher A31570) at 1:1000 dilution in 0.2% DS in 0.1% Triton X-100 in PBS. Sections were covered with aluminum foil and incubated in 2˚ antibody solution for 2 hours at room temperature with mild shaking. Following 2˚ antibody, sections were washed 2 times in PBS before counterstaining with 300 nm DAPI in PBS for 5 minutes at room temperature. DAPI solution was removed and the sections were rinsed in PBS. Finally, free floating sections were mounted on Poly-L-Lysine Hydrobromide (Sigma P1399) coated glass slides, dried briefly, and finished with Fluorescence mounting medium (Dako S3023) and a coverslip. Finished fluorescent slides were dried overnight in the dark at room temperature and were finally stored at 4˚C.

3.2.6 Stereology

Fluorescent slides were counted using the Visiopharm stereology software. Sections of 30 µm were counted at a frequency of 1:3, and fell between Bregma regions 0.74 to 0.38. Counts covered six regions of interest consisting of the right and left caudate putamen for three sections. Cells were counted at 40x magnification under oil using a frame size of 483.31 μm^2. The step length of the random grid was 482.55 µm and counting frames were excluded if they fell outside the pre-defined region of interest (ROI). DAPI was counted first, and the same counting frames were repeated to count NeuN staining. Cell diameter measurements were taken in the first or last frame of

each ROI using the cell closest to the upper right hand corner. The cell count estimate was calculated using the equation:

$$C = \Sigma c^* (\Sigma A / \Sigma(a^*n)) * f *(M/(M+D))$$

Where "C" is the estimate for total number of cells (with the Abercrombie correction), "A" is the area of the region of interest (ROI) for each section, "a" is the area of the sampling frame, "n" is the number of sampling frames allocated to each ROI), "c" is the number of cells counted in each sampling frame, "M" is the thickness of the section, "D" is the mean cell diameter, and "f" is the sectioning frequency.

3.2.7 Statistics

Prior to analysis, the data were screened for outliers most probably caused by experimenter or measurement error. Shapiro-Wilk's test was used to assess the normality of the data, and outliers were identified as measurements with studentized residuals more extreme than ±3 SD. Analyses were conducted first with any outliers included and were then compared to analyses excluding the outliers to determine their impact on results. Graphs display descriptive means ± standard error of the descriptive mean unless otherwise stated. Graphs of the main effects and simple main effects show estimated mean ± standard error of the estimated mean.

The Benjamini-Liu (BL) procedure was used to correct for false discovery rate (FDR) of 5% over the entirety of related analyses for a data sets. The BL procedure requires no assumptions about independence or dependence (positive or negative), and thus was judged to be the most appropriate FDR

correction for the nested area measures (Yoav Benjamini et al., 2001). Where there were no significant effects, FDR was not applied.

3.3 Results

1.1.1 Allometric Brain Growth

Figure 3.2 Colony Wet Brain Weight by Age

Table 3.1 Colony Wet Brain and Body Weight–Total "N" Summary

	Female	Male	Total
WT	96	128	224
Grb10$^{+/m}$	19	27	46
Grb10$^{+/p}$	73	81	154
Total	188	236	424

Data Screening

Table 3.2 Binned Whole Brain and Body Weight 3-way ANOVA–Data Counts

SEX	AGE	WT	Grb10+/p	Grb10+/m	Totals
Female	**305 to 325 Days**	14	11	0	*25*
	185 to 205 Days	22	20	5	*47*
	75-95 Days	28	18	4	*50*
	Total	*64*	*49*	*9*	*122*
Male	**305 to 325 Days**	25	15	4	*44*
	185 to 205 Days	32	23	9	*64*
	75-95 Days	33	25	5	*63*
	Total	*90*	*63*	*18*	*171*
Total	***305 to 325 Days***	*39*	*26*	*4*	*69*
	185 to 205 Days	*54*	*43*	*14*	*111*
	75-95 Days	*61*	*43*	*9*	*113*
	Total	*154*	*112*	*27*	*293*

A three-way ANOVA was conducted to examine the effects of between-subjects factors GENOTYPE, AGE, and SEX on whole wet brain weight in our colony. GENOTYPE was considered at three levels (wildtype, *Grb10^{+m}*, and *Grb10$^{+/p}$*), AGE was considered at three levels (75-95 days, 185-205 days, and

305-325 days of age), and SEX was considered at two levels (Females and Males). We also considered and rejected several ANCOVA models incorporating BODY WEIGHT for our analysis. First, we considered including the transformed variable "BODY WEIGHT SQUARED" as a covariate, but the main effect of this variable was not significant in our preliminary models, and was therefore excluded from our analysis. "BODY WEIGHT" did have a significant main effect in preliminary models, but in the three-way ANCOVA, there was a significant two-way interaction between the covariate "BODY WEIGHT" and the independent variables GENOTYPE and AGE. Therefore, the assumption of homogeneity of regression slopes was violated, and we could not continue with the three-way ANCOVA. We proceeded with a three-way ANOVA (below), and analyzed body weight separately.

Shapiro-Wilk's test indicated the data were normally distributed for all cells of the design ($p > 0.05$), except for female *Grb10*$^{+/m}$ at 185-205 days of age ($p = 0.014$). The Q-Q plot of the data for this cell shows positive skew. The studentized residuals (SREs) identified two outliers: 14 (SRE = 3.30, Male WT 185-205 days), and T12 (SRE = 3.01, Female *Grb10*$^{+/m}$ 185-205 days). There was homogeneity of variance for the data, as assessed by Levene's test ($p = 0.271$).

Summary

The three-way interaction between GENOTYPE, SEX, and AGE was not statistically significant, nor were the two-way interactions between GENOTYPE and SEX, or SEX and AGE. The two-way interaction between GENOTYPE and

AGE was statistically significant, and we followed up with simple main effects analyses.

Both the simple main effects of GENOTYPE and AGE on whole wet brain weight were significant. *Grb10*$^{+/p}$ brains were heavier than wildtype brains at 75-95 days and 185-205 days, and heavier than both wildtypes and *Grb10*$^{+/m}$ brains at 305-325 days of age. *Grb10*$^{+/m}$ brain weight was not significantly different from wildtypes in any age bin. Wildtype brains were heavier at 185-205 days than 75-95 days and 305-325 days. *Grb10*$^{+/m}$ brains were heavier at 185-205 days than 305-325 days. Unlike wildtype and *Grb10*$^{+/m}$, which appear to peak in weight at 185-205, *Grb10*$^{+/p}$ brains maintained weight between the latter age bins. *Grb10*$^{+/p}$ brains at 305-325 days and 185-205 days were heavier than at 75-95 days, and there was no significant difference between 305-325 days and 185-205 days. When the whole brain weight and body weight outliers (14, T12, A71P, A53P, C134P, and C39 P) were removed, the results of the analysis did not change.

Report

The three-way interaction between GENOTYPE, SEX, and AGE was not statistically significant, $F(3,276) = 0.584$, $p = 0.626$, partial $\eta^2 = 0.006$. The two way interaction between GENOTYPE and SEX was not statistically significant, $F(2,276) = 0.965$, $p = 0.382$, partial $\eta^2 = 0.007$. The two way interaction between SEX and AGE was also not significant, $F(2,276) = 0.787$, $p = 0.456$, partial $\eta^2 = 0.006$. There was a statistically significant two way interaction

between AGE and GENOTYPE F(4,276) = 4.685, p = 0.001, partial η^2 = 0.064. Therefore, we ran simple main effects analyses.

*Table 3.3 Estimated Marginal Means AGE*GENOTYPE for Whole Wet Brain Weight*

AGE	GENOTYPE	Mean	Std. Error
305 to 325 Days	WT	469.323	4.224
	Grb10+/p	509.412	5.023
	Grb10+/m	439.750[a]	12.654
185 to 205 Days	WT	489.049	3.504
	Grb10+/p	506.711	3.869
	Grb10+/m	500.328	7.058
75-95 Days	WT	461.694	3.251
	Grb10+/p	492.05	3.911
	Grb10+/m	475.265	8.488

a– based on modified population marginal mean.

The simple main effect of GENOTYPE on whole wet brain weight was significant for mice 75-95 days of AGE (F(2,276) = 17.819, p < 0.001, partial η^2 = 0.114), 185-205 days of AGE (F(2,276) = 5.822, p = 0.003, partial η^2 = 0.040), and 305-325 days of AGE (F(2,276) = 24.908, p < 0.001, partial η^2 = 0.153). Estimated marginal means are summarized in the table "Estimated Marginal Means AGE*GENOTYPE for Whole Wet Brain Weight". All pairwise comparisons were made using the Bonferroni adjustment. Data are presented as mean difference with the 95% confidence interval.

At 75-95 days of AGE, *Grb10$^{+/p}$* brains were significantly heavier than WT brains by 6.575% (30.356 (95%CI 18.105 to 42.607) mg, p < 0.001). No other pairwise comparisons were significant. At 185-205 days of AGE, *Grb10$^{+/p}$* brains were significantly heavier than WT brains by 3.611% (17.662 (95%CI 5.089 to 30.236) mg, p = 0.002). No other pairwise comparisons at 185-205 days of AGE were significant. At 305-325 days of AGE, *Grb10$^{+/p}$* brains were

significantly heavier than WT by about 8.542% (40.089 (95%CI 24.282 to 55.897) mg, $p < 0.001$) and *Grb10*$^{+/m}$ brains by 15.841% (69.662 (95%CI 36.870 to 102.454) mg, $p < 0.001$). Wildtype and *Grb10*$^{+/m}$ brains were not significantly different.

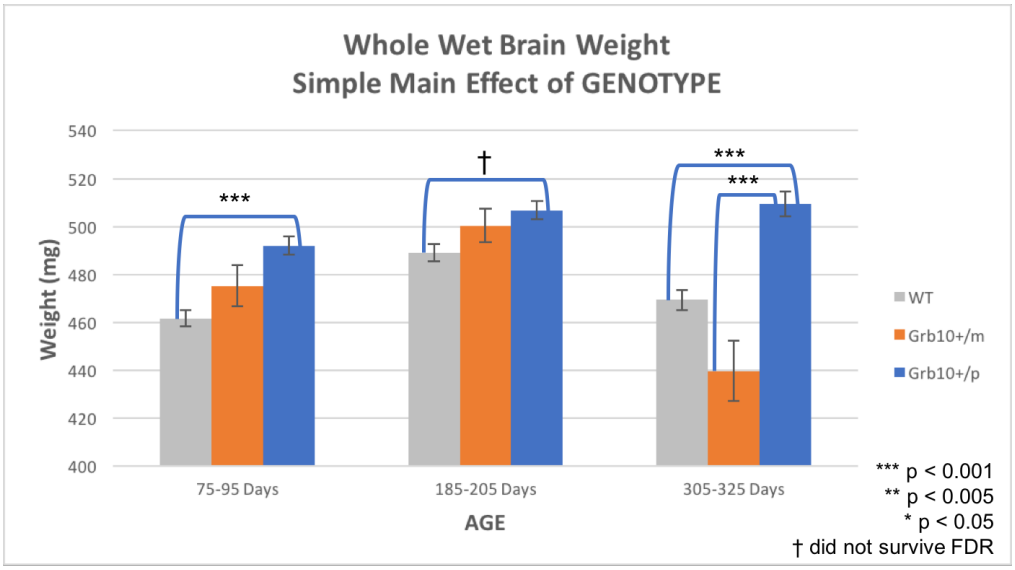

Figure 3.3 Whole Wet Brain Weight–Pairwise Comparisons of Simple Main Effect of GENOTYPE

The simple main effect of AGE on whole wet brain weight was significant for wildtype ($F(2,276) = 16.909$, $p < 0.001$, partial $\eta^2 = 0.109$), *Grb10*$^{+/m}$ ($F(2,276) = 9.259$, $p < 0.001$, partial $\eta^2 = 0.063$), and *Grb10*$^{+/p}$ mice ($F(2,276) = 5.060$, $p = 0.007$, partial $\eta^2 = 0.035$). Estimated marginal means are summarized in the table "Estimated Marginal Means AGE*GENOTYPE for Whole Wet Brain Weight".

Wildtype brains at 185-205 days were significantly heavier than brains at 305-325 days (19.726 (95%CI 6.506 to 32.945) mg, $p = 0.001$) and brains at 75-95 days (27.355 (95%CI 15.840 to 38.869) mg, $p < 0.001$). Wildtype brains at 305-325 days and 75-95 days were not statistically different. *Grb10*$^{+/m}$ brains

at 185-205 days were significantly heavier than brains at 305-325 days (60.578 (95%CI 25.679 to 95.476) mg, p < 0.001). No other pairwise comparisons for *Grb10*$^{+/m}$ brains were significant. *Grb10*$^{+/p}$ brains at 305-325 days were significantly heavier than brains at 75-95 days (17.362 (95%CI2.028 to 32.696) mg, p = 0.020). *Grb10*$^{+/p}$ brains at 185-205 days were also significantly heavier than brains at 75-95 days (14.661 (95%CI 1.409 to 27.912) mg, p = 0.024). *Grb10*$^{+/p}$ brains at 185-205 and 305-325 days of AGE were not statistically significantly different in weight.

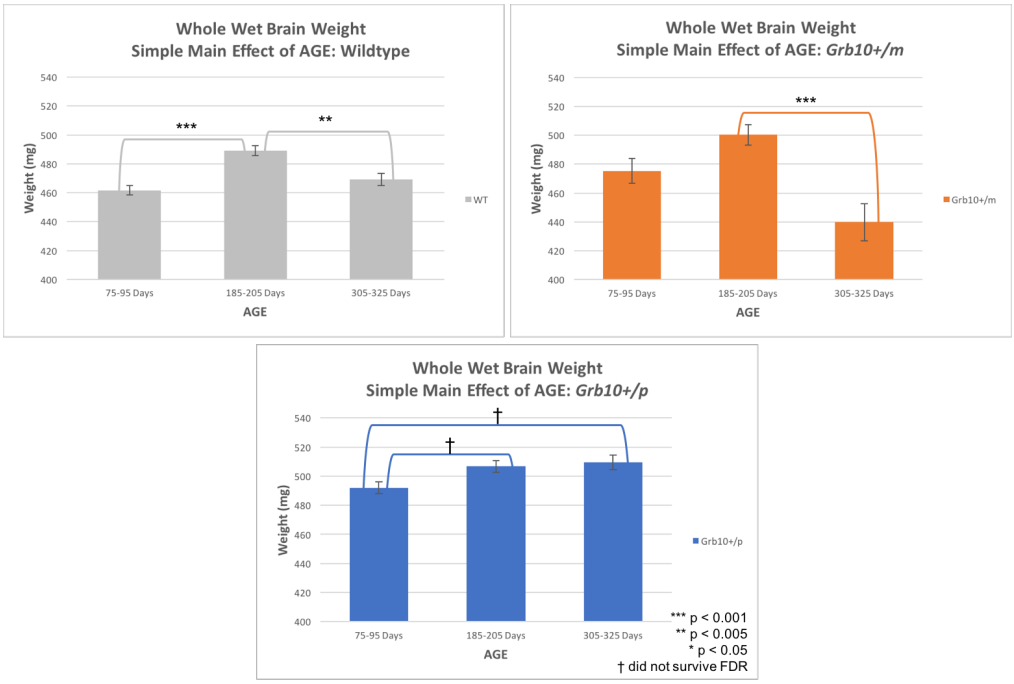

Figure 3.4 Whole Wet Brain Weight–Pairwise Comparisons of Simple Main Effect of AGE

3.3.1 Allometric Body Weight

A three-way ANOVA was conducted to examine the effects of between-subjects factors GENOTYPE, AGE, and SEX on body weight in our colony. GENOTYPE was considered at three levels (wildtype, *Grb10*$^{+m}$, and *Grb10*$^{+/p}$), AGE was considered at three levels (75-95 days, 185-205 days, and 305-325

days of age), and SEX was considered at two levels (Females and Males). Shapiro-Wilk's test indicated the data were normally distributed for all cells ($p > 0.05$) except for *Grb10*$^{+/p}$ females 185-205 days of age ($p = 0.001$), WT females 75-95 days of age ($p = 0.041$), and WT males 75-95 days of age ($p = 0.027$). Q-Q plots showed positive skew for all three groups. Studentized residuals of the data revealed four outliers: A71 P (SRE = 4.58, WT male 305-325 days of age), A53 P (SRE = 3.50, WT male 305-3025 days of age), C134 P (SRE = 3.28, *Grb10*$^{+/p}$ female 185-205 days of age), and C39 P (SRE = 3.00, WT male 185-205 days of age). Levene's test indicated the assumption of homogeneity of variances was violated ($p < 0.001$). Transforming the data for body weight did not resolve the violation. Therefore, we also split our data by AGE and ran two-way ANOVAs for GENOTYPE and SEX. Levene's test indicated there was homogeneity of variances for the two-way ANOVA at 305-325 days ($p = 0.664$) and 185-205 days ($p = 0.068$), but the assumption was violated at 75-95 days ($p = 0.008$). The results of the three-way ANOVA (GENOTYPE*AGE*SEX) are reported below, and the results of the two-way ANOVA are described in the summary, where the outcome differs from the three-way ANOVA.

Summary

The three-way interaction between GENOTYPE, SEX, and AGE was not statistically significant, nor was the two-way interaction between SEX and AGE. The two-way interactions between GENOTYPE*SEX and AGE*GENOTYPE were statistically significant, and we followed up with simple main effects analysis.

For GENOTYPE*SEX, the simple main effect of GENOTYPE was not significant for male or female mice separately, but there was a significant main effect of SEX for wildtype, *Grb10*$^{+/m}$, and *Grb10*$^{+/p}$ mice individually. Male body weights were consistently heavier than female body weights for all three genotype groups. For AGE*GENOTYPE, the simple main effect of AGE was significant for each genotype group individually. Wildtype and *Grb10*$^{+/p}$ mice weighed significantly more at each consecutive age group (75-95 days < 185-205 days < 305-325 days), while *Grb10*$^{+/m}$ mice weighed more at 305-325 days than at 185-205 and 75-95 days, but were not significantly different between 75-95 days and 185-205 days. The simple main effect of GENOTYPE for AGE*GENOTYPE was significant for 305-325 days and 75-95 days, but not 185-205 days of age. No pairwise comparisons between the genotype groups at 305-325 days survived Bonferroni correction. At 75-95 days, *Grb10*$^{+/m}$ mice were significantly heavier than both wildtype and *Grb10*$^{+/p}$ mice, and there was no significant difference between wildtype and *Grb10*$^{+/p}$ body weights. Overall, male mice weighed more than female mice. All genotype groups increased in body weight with age, except *Grb10*$^{+/m}$ mice between 75-95 days and 185-205 days of age. There were no genotype differences in body weight within each sex or any age bin, except for *Grb10*$^{+/m}$ mice (pooled sexes) at 75-95 days of age, which were heavier than both wildtype and *Grb10*$^{+/p}$ mice.

We removed the six outliers for whole wet brain weight and body weight to determine whether they impacted the analysis. The outliers removed were: 14, T12, A71P, A53P, C134P, and C39 P. The assumption of homogeneity of variances was still violated for the three-way ANOVA. For

GENOTYPE*SEX, there was a significant simple main effect of GENOTYPE. Male, but not female, *Grb10*$^{+/p}$ mice overall weighed more than wildtypes. For GENOTYPE*AGE, there was also a simple main effect of GENOTYPE. At 305-325 days, *Grb10*$^{+/p}$ mice weighed more than wildtypes, and at 75-95 days (as in the outliers-included analysis) *Grb10*$^{+/m}$ mice weighed more than wildtype or *Grb10*$^{+/p}$ mice. All other outcomes were the same as in the outliers-included analysis.

Report

The three-way interaction between GENOTYPE, SEX, and AGE was not statistically significant, $F(3,276) = 0.199$, $p = 0.897$, partial $\eta^2 = 0.002$. The two way interaction between SEX and AGE was not significant, $F(2,276) = 2.275$, $p = 0.105$, partial $\eta^2 = 0.016$. The two way interaction between GENOTYPE and SEX was statistically significant, $F(2,276) = 3.134$, $p = 0.045$, partial $\eta^2 = 0.022$. There was also a statistically significant two way interaction between AGE and GENOTYPE $F(4,276) = 4.141$, $p = 0.003$, partial $\eta^2 = 0.057$. Therefore, we ran simple main effects analyses for GENOTYPE*SEX and AGE*GENOTYPE. All pairwise comparisons were made using the Bonferroni adjustment. Data are presented as mean difference with the 95% confidence interval.

*Table 3.4 Estimated Marginal Means GENOTYPE*SEX for Body Weight*

GENOTYPE	SEX	Mean	Std. Error
WT	FEMALE	26.41	0.504
	MALE	33.502	0.411
***Grb10*$^{+/p}$**	FEMALE	26.136	0.572
	MALE	34.471	0.500
***Grb10*$^{+/m}$**	FEMALE	27.266[a]	1.298
	MALE	32.768	0.966

a–Based on modified population marginal mean

For GENOTYPE*SEX, estimated marginal means are summarized in the table "Estimated Marginal Means GENOTYPE*SEX for Body Weight". The simple main effect of GENOTYPE on body weight was not significant for female ($F(2,276) = 0.326$, $p = 0.722$, partial $\eta^2 = 0.002$) or male mice ($F(2,276) = 1.733$, $p = 0.179$, partial $\eta^2 = 0.012$). The simple main effect of SEX on body weight was significant for all three GENOTYPEs: wildtypes ($F(1,276) = 118.944$, $p < 0.001$, partial $\eta^2 = 0.301$), *Grb10*$^{+/m}$ ($F(1,276) = 11.564$, $p = 0.001$, partial $\eta^2 = 0.040$), and *Grb10*$^{+/p}$ ($F(1,276) = 120.489$, $p < 0.001$, partial $\eta^2 = 0.304$). Male body weight was significantly heavier than female body weight for wildtype (7.091 (95%CI 5.811 to 8.371) g, $p < 0.001$), *Grb10*$^{+/m}$ (5.502 (95%CI 2.317 to 8.687) g, $p = 0.001$), and *Grb10*$^{+/p}$ mice (8.335 (95%CI 6.840 to 9.830) g, $p < 0.001$).

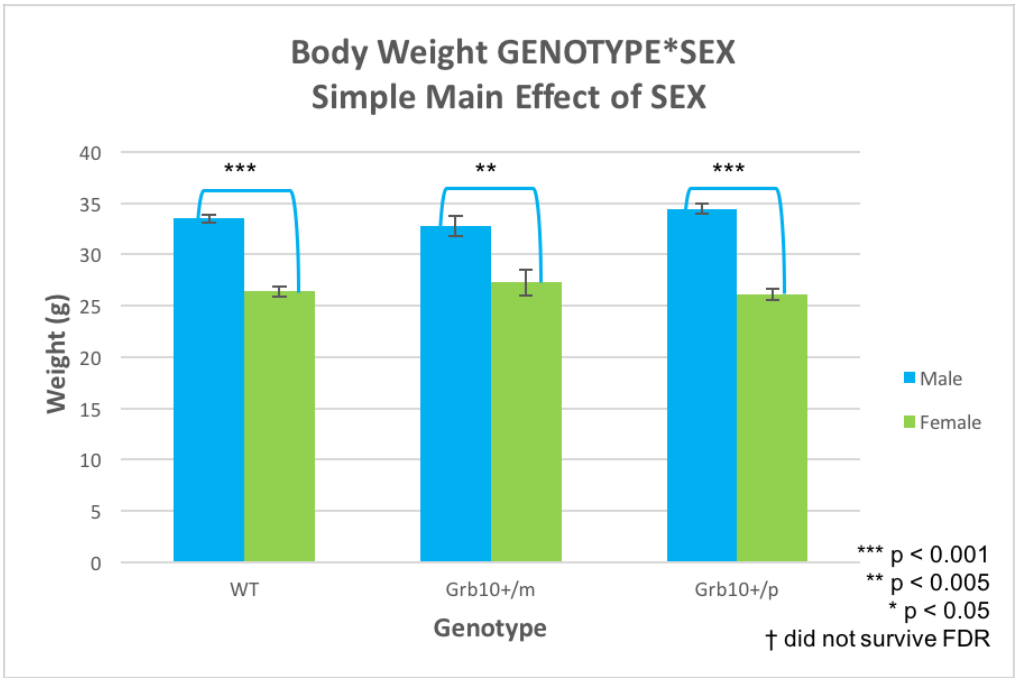

*Figure 3.5 Body Weight GENOTYPE*SEX–Simple Main Effect of SEX*

*Table 3.5 Estimated Marginal Means AGE*GENOTYPE for Body Weight*

AGE	GENOTYPE	Mean	Std. Error
305 to 325 Days	WT	34.28	0.646
	Grb10+/p	36.543	0.768
	Grb10+/m	37.682[a]	1.935
185 to 205 Days	WT	31.545	0.536
	Grb10+/p	30.582	0.592
	Grb10+/m	29.593	1.079
75-95 Days	WT	24.044	0.497
	Grb10+/p	23.784	0.598
	Grb10+/m	27.984	1.298

a–Based on modified population marginal mean

For AGE*GENOTYPE, estimated marginal means are summarized in the table "Estimated Marginal Means AGE*GENOTYPE for Body Weight". The simple main effect of AGE was significant for wildtype ($F(2,276) = 94.297$, $p < 0.001$, partial $\eta^2 = 0.406$), *Grb10*$^{+/m}$ ($F(2,276) = 9.087$, $p < 0.001$, partial $\eta^2 = 0.062$), and *Grb10*$^{+/p}$ mice ($F(2,276) = 89.337$, $p < 0.001$, partial $\eta^2 = 0.393$). Wildtype mice weighed significantly more at 305-325 days compared to 185-

205 days (2.735 (95%CI 0.714 to 4.756) g, p = 0.004) and to 75-95 days (10.236 (95%CI 8.273 to 12.199) g, p < 0.001). Wildtype mice also weighed significantly more at 185-205 days than at 75-95 days (7.501 (95%CI 5.741 to 9.261) g, p < 0.001). *Grb10*$^{+/m}$ mice weighed significantly more at 305-325 days compared to 185-205 days (8.090 (95%CI 2.754 to 13.425) g, p = 0.001) and to 75-95 days (9.698 (95%CI 4.087 to 15.310) g, p < 0.001). Body weight for *Grb10*$^{+/m}$ mice was not significantly different between 185-205 days and 75-95 days (1.609 (95%CI -2.457 to 5.674) g, p = 1.000). *Grb10*$^{+/p}$ mice weighed significantly more at 305-325 days compared to 185-205 days (5.961 (95%CI 3.626 to 8.296) g, p < 0.001) and to 75-95 days (12.759 (95%CI 10.414 to 15.103) g, p < 0.001). *Grb10*$^{+/p}$ mice also weighed significantly more at 185-205 days than 75-95 days (6.798 (95%CI 4.772 to 8.824) g, p < 0.001).

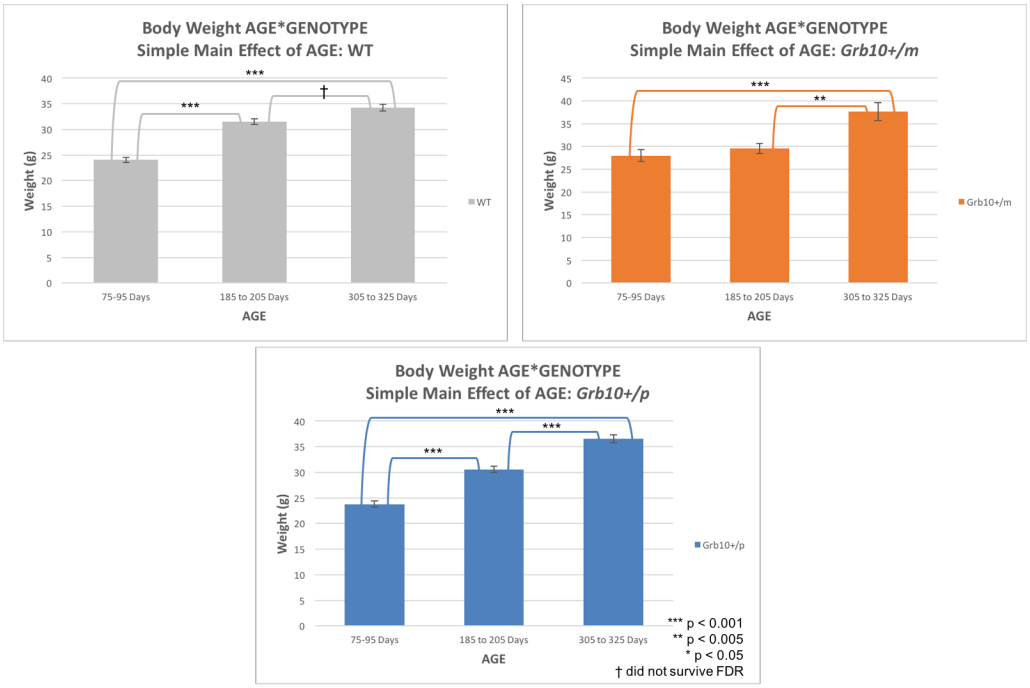

*Figure 3.6 Body Weight AGE*GENOTYPE–Simple Main Effect of AGE*

For AGE*GENOTYPE, the simple main effect of GENOTYPE was not significant for 185-205 days ($F(2,276) = 1.599$, $p = 0.204$, partial $\eta^2 = 0.011$).

The simple main effect of GENOTYPE was significant for 305-325 days (F(2,276) = 3.307, p = 0.038, partial η^2 = 0.023) and for 75-95 days (F(2,276) = 4.529, p = 0.012, partial η^2 = 0.032). At 305-325 days, no pairwise comparisons survived Bonferroni adjustment. There was no significant difference between wildtype and *Grb10*$^{+/m}$ (-3.403 (95%CI -8.316 to 1.510) g, p = 0.289), wildtype and *Grb10*$^{+/p}$ (-2.264 (95%CI -4.680 to 0.153) g, p = 0.075), or *Grb10*$^{+/m}$ and *Grb10*$^{+/p}$ body weights (1.139 (95%CI -3.874 to 6.153) g, p = 1.000). At 75-95 days, *Grb10*$^{+/m}$ body weight was significantly higher than wildtype (3.941 (95%CI 0.593 to 7.288) g, p = 0.015) and *Grb10*$^{+/p}$ (4.200 (95%CI 0.758 to 7.642) g, p = 0.011). There was no significant difference between wildtype and *Grb10*$^{+/p}$ body weights at 75-95 days (0.259 (95%CI -1.614 to 2.132) g, p = 1.000).

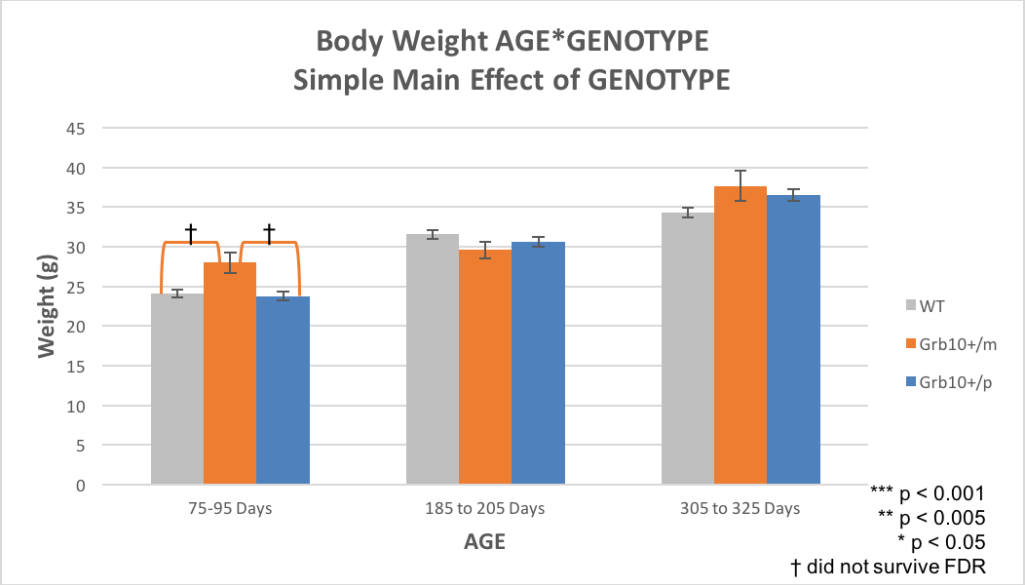

*Figure 3.7 Body Weight AGE*GENOTYPE–Simple Main Effect of GENOTYPE*

3.3.2 False Discovery Rate Corrections–Allometric Growth

The Benjamini-Liu (BL) procedure was used to correct for false discovery rate (FDR) of 5% over all significance tests in the three-way ANOVAs used to analyze Whole Wet Brain Weight and Body Weight. Bonferroni adjusted

pairwise corrections were included in the FDR tables. Of 36 originally significant results, 24 survived FDR correction. The two-way interactions GENOTYPE*SEX and AGE*GENOTYPE for body weight analysis were among the tests that became non-significant. In the table below, BW is Body Weight and WWB is Wet Brain Weight.

Table 3.6 Abridged FDR Corrections–Whole Wet Brain and Body Weights

Variable	P value	Rank (m = 67)	B-L: (min, 0.05, 0.05*(m/(m+1-i)^2)	Difference
BW Simple Main Effect of AGE (AGE*GENOTYPE)–WT	6.16E-32	1	7.46E-04	7.46E-04
BW Simple Main Effect of AGE (AGE*GENOTYPE)–*Grb10+/p*	1.21E-30	2	7.69E-04	7.69E-04
BW Simple Main Effect of AGE (AGE*GENOTYPE)–*Grb10+/p* 305-325 vs 75-95	2.28E-30	3	7.93E-04	7.93E-04
BW Simple Main Effect of AGE (AGE*GENOTYPE)–WT 305-325 vs 75-95	1.91E-28	4	8.18E-04	8.18E-04
BW Simple Main Effect of SEX (GENOTYPE*SEX)–*Grb10+/p*	1.68E-23	5	8.44E-04	8.44E-04
BW Simple Main Effect of SEX (GENOTYPE*SEX)–WT	2.90E-23	6	8.71E-04	8.71E-04
BW Simple Main Effect of AGE (AGE*GENOTYPE)–WT 185-205 vs 75-95	1.15E-20	7	9.00E-04	9.00E-04
BW Simple Main Effect of AGE	6.05E-14	8	9.31E-04	9.31E-04

(AGE*GENOTYPE)–*Grb10+/p* 185-205 vs 75-95				
WWB Simple Main Effect of GENOTYPE–305 to 325 Days	1.14E-10	9	9.62E-04	9.62E-04
BW Simple Main Effect of AGE (AGE*GENOTYPE)–*Grb10+/p* 305-325 vs 185-205	8.15E-09	10	9.96E-04	9.96E-04
WWB Simple Main Effect of GENOTYPE–305 to 325 Days WT vs *Grb10+/p*	1.02E-08	11	1.03E-03	1.03E-03
WWB Simple Main Effect of GENOTYPE–75 to 95 Days WT vs *Grb10+/p*	2.20E-08	12	1.07E-03	1.07E-03
WWB Simple Main Effect of GENOTYPE–75 to 95 Days	5.27E-08	13	1.11E-03	1.11E-03
WWB Simple Main Effect of AGE–WT 185-205 vs 75-95	8.20E-08	14	1.15E-03	1.15E-03
WWB Simple Main Effect of AGE–Wildtype	1.18E-07	15	1.19E-03	1.19E-03
WWB Simple Main Effect of GENOTYPE–305 to 325 Days *Grb10+/p* vs *Grb10+/m*	2.00E-06	16	1.24E-03	1.24E-03
WWB Simple Main Effect of AGE–*Grb10+/m* 305-325 vs 185-205	0.000117	17	1.29E-03	1.17E-03
BW Simple Main Effect of AGE (AGE*GENOTYPE)–*Grb10+/m* 305-325 vs 75-95	0.000126	18	1.34E-03	1.21E-03
WWB Simple Main Effect of AGE–*Grb10+/m*	0.000128	19	1.40E-03	1.27E-03
BW Simple Main Effect of AGE	0.000151	20	1.45E-03	1.30E-03

(AGE*GENOTYPE)–*Grb10+/m*				
BW Simple Main Effect of SEX (GENOTYPE*SEX)–*Grb10+/m*	0.000772	21	1.52E-03	7.45E-04
BW Simple Main Effect of AGE (AGE*GENOTYPE)–*Grb10+/m* 305-325 vs 185-205	0.000934	22	1.58E-03	6.49E-04
Whole Wet Brain Weight AGE*GENOTYPE	0.001129	23	1.65E-03	5.25E-04
WWB Simple Main Effect of AGE–WT 305-325 vs 185-205	1.16E-03	24	1.73E-03	5.70E-04
WWB Simple Main Effect of GENOTYPE–185 to 205 Days WT vs *Grb10+/p*	0.002458	25	1.81E-03	-6.46E-04

3.3.3 Nissl Staining–Bregma 0.74mm

Data Screening

Three-way ANOVAs were conducted to examine effects of GENOTYPE, AGE, and SEX on area measurements of Nissl-stained brain slices at Bregma 0.74 mm. Areas measured included “whole brain”, “cortical”, “subcortical”, “caudate putamen”, and “ventricles”. Measures for bilateral structures (caudate putamen and ventricles) represent the summed area of both sides. Each AGE bin represents a separate cohort of mice.

Table 3.7 Nissl Staining Cases–Bregma 0.74 mm

	Age	Genotype	N
Males	10 weeks	WT	3
		Grb10$^{+/p}$	3
		Grb10$^{+/m}$	2
	6 months	WT	3
		Grb10$^{+/p}$	3
		Grb10$^{+/m}$	4
	10 months	WT	3
		Grb10$^{+/p}$	4
		Grb10$^{+/m}$	3
Females	10 weeks	WT	3
		Grb10$^{+/p}$	3
		Grb10$^{+/m}$	2
	6 months	WT	3
		Grb10$^{+/p}$	4
		Grb10$^{+/m}$	3
	10 months	WT	3
		Grb10$^{+/p}$	3
		Grb10$^{+/m}$	3

Data reported for main effects analyses are estimated marginal mean ± standard error, unless otherwise stated. Shapiro-Wilk's test indicated the data were normally distributed for all cells of the analysis ($p > 0.05$) except WT male ventricles at 6 mo ($p = 0.040$), WT female whole brain area at 10 weeks ($p = 0.033$), *Grb10*$^{+/p}$ male subcortical area at 6 mo ($p = 0.036$), and *Grb10*$^{+/m}$ female whole brain area ($p = 0.046$) and subcortical area ($p = 0.005$) at 10 months. *Grb10*$^{+/m}$ data at 10 weeks had $n = 2$ samples, so normality could not be calculated. There was homogeneity of variance for all dependent variables, as assessed by Levene's test ($p > 0.05$), except for "ventricles area" ($p < 0.001$). Ventricles area was analyzed with the three-way ANOVA and the outcome was checked against alternative analyses, detailed in the "Ventricles Area" report below. There were three outliers with an SRE more extreme than ± 3SD in one

measure: A83 P (*Grb10*$^{+/p}$ male 10 months, caudate putamen SRE = -3.05), A4 P (WT male 10 months, ventricles SRE = 3.45), A134 P (*Grb10*$^{+/m}$ female 10 months, ventricles SRE = 3.09).

Summary

There were no significant three-way interactions between GENOTYPE, SEX, and AGE for any area measures. The two-way interactions GENOTYPE*SEX and GENOTYPE*AGE were not significant, nor was the main effect of GENOTYPE. There was a significant two-way interaction between SEX and AGE for cortical area. There was no simple main effect of AGE on cortical area, but there was a simple main effect of SEX at 6 months–cortical area for males was significantly smaller than for females. For all instances with no significant interactions, the main effect of SEX was also not significant. There was a significant main effect of AGE on whole brain, subcortical, caudate putamen, and ventricle area. Whole brain area was larger at 10 months than 10 weeks. Subcortical area was larger at 10 months than at 6 months and 10 weeks. Caudate putamen area was larger at 10 months and 6 months than at 10 weeks. Ventricle area was larger at 10 months than at 6 months and 10 weeks. No other comparisons were significant.

The outliers A83 P, A4 P, and A134 P were removed from the data set to determine if they impacted the outcome of the analysis. When these outliers were removed, there was also significant two-way SEX*AGE interaction for whole brain area. There was a significant simple main effect of SEX at 6 months, with whole brain area for males being significantly smaller

than females. There was also a significant simple main effect of AGE. Whole brain area for males was larger at 10 months than 6 months, and was no different for any other pairwise comparisons. Whole brain area for females was larger at 6 months than at 10 weeks, and no other pairwise comparisons were significant. There were no other differences in the outcome of the analysis.

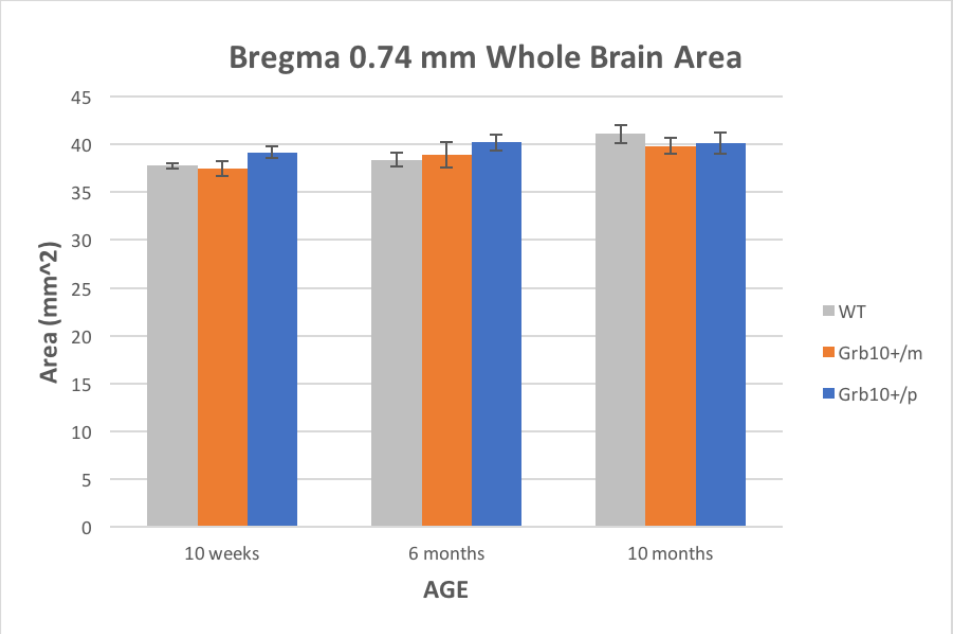

Figure 3.8 Bregma 0.74 mm Whole Brain Area

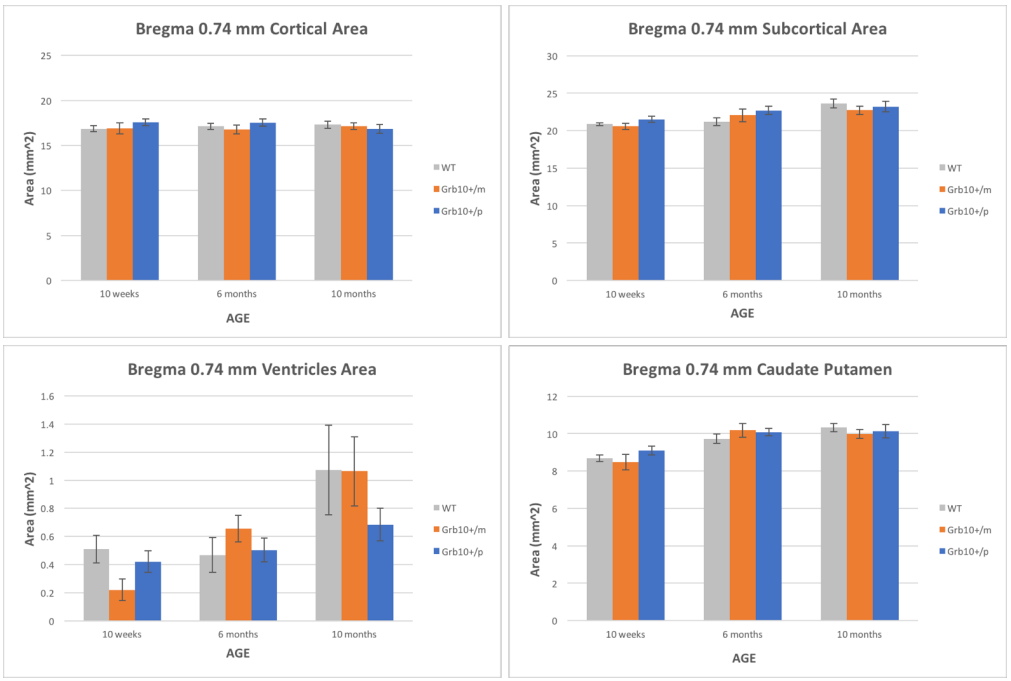

Figure 3.9 Bregma 0.74 mm Subdivision Areas

Reports

"Whole Brain Area"

The three-way interaction between GENOTYPE, SEX, and AGE was not significant for whole brain area, $F(4,37) = 1.241$, $p = 0.311$, partial $\eta^2 = 0.118$. The two way interactions SEX*AGE ($F(2,37) = 2.979$, $p = 0.063$, partial $\eta^2 = 0.139$), GENOTYPE*AGE ($F(4,37) = 0.732$, $p = 0.576$, partial $\eta^2 = 0.073$), and GENOTYPE*SEX ($F(2,37) = 1.320$, $p = 0.279$, partial $\eta^2 = 0.067$) were also not significant. There were no significant main effects of GENOTYPE ($F(2,37) = 1.120$, $p = 0.337$, partial $\eta^2 = 0.057$) or SEX ($F(1,37) = 3.209$, $p = 0.081$, partial $\eta^2 = 0.080$). There was a significant main effect of AGE on whole brain area, $F(2,37) = 4.811$, $p = 0.014$, partial $\eta^2 = 0.206$. We performed all pairwise comparisons with the Bonferroni adjustment. Data are reported as mean difference with the 95% confidence interval. Whole brain area increased significantly between 10 months (40.295 ± 0.493 mm^2) and 10 weeks (38.125

± 0.544 mm^2), mean difference 2.269 (95%CI 0.429 to 4.110) mm^2, p = 0.011. There was no significant difference between 10 months and 6 months (39.221 ± 0.482 mm^2), mean difference 1.174 (95%CI -0.555 to 2.903) mm^2, p = 0.291. There was also no significant difference between 6 months and 10 weeks (1.096 (95%CI -0.727 to 2.918) mm^2, p = 0.421).

"Cortical Area"

The three way interaction between GENOTYPE, SEX and AGE was not significant for cortical area, F(4,37) = 1.592, p = 0.197, partial η^2 = 0.147. The two-way interactions GENOTYPE*AGE (F(4,37) = 0.626, p = 0.647, partial η^2 = 0.063) and GENOTYPE*SEX (F(2,37) = 2.207, p = 0.124, partial η^2 = 0.107) were not significant. The main effect of GENOTYPE was not significant, F(2,37) = 0.674, p = 0.516, partial η^2 = 0.035. There was a significant two-way interaction for SEX and AGE, F(2,37) = 3.331, p = 0.047, partial η^2 = 0.153. We performed simple main effects analysis. All pairwise comparisons were made using the Bonferroni adjustment. Data are presented as mean difference with the 95% confidence interval.

For the two-way interaction SEX*AGE, there was no significant simple main effect of AGE for male (F(2,37) = 1.441, p = 0.250, partial η^2 = 0.072) or female (F(2,37) = 1.907, p = 0.163, partial η^2 = 0.093) mice. The simple main effect of SEX was not significant at 10 weeks (F(1,37) = 0.383, p = 0.540, partial η^2 = 0.010) or 10 months of age (F(1,37) = 1.548, p = 0.221, partial η^2 = 0.040). There was a significant simple main effect of SEX on cortical area at 6 months of age, F(1,37) = 10.146, p = 0.003, partial η^2 = 0.215. Cortical area at 6 months

was significantly smaller for males (16.496 ± 0.300 mm^2) than for females (17.847 ± 0.300 mm^2), mean difference -1.351 (95%CI -2.211 to -0.492) mm^2, p = 0.003. There was no significant difference in cortical area between males (16.872 ± 0.300 mm^2) and females (17.411 ± 0.313 mm^2) at 10 months, mean difference -0.540 (95%CI -1.418 to 0.339) mm^2, p = 0.221. There was no significant difference between males (17.262 ± 0.338 mm^2) and females (16.996 ± 0.338 mm^2) at 10 weeks, mean difference 0.296 (95%CI -0.673 to 1.266) mm^2, p = 0.540.

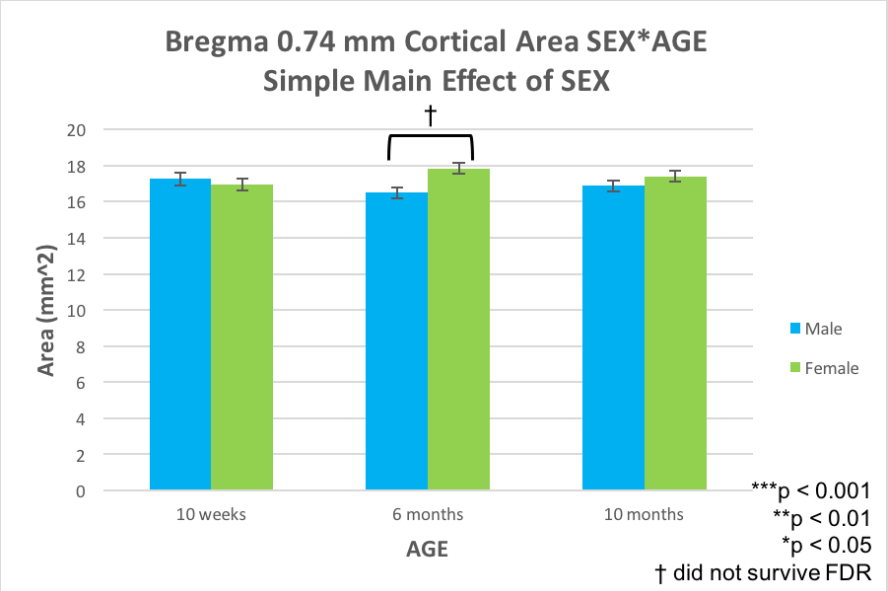

*Figure 3.10 Bregma 0.74 mm Cortical Area (SEX*AGE) Simple Main Effect of SEX*

"Subcortical Area"

There was no significant three way interaction between GENOTYPE, SEX, and AGE for subcortical area, F(4,37) = 0.867, p = 0.493, partial η^2 = 0.086. The two-way interactions SEX*AGE (F(2,37) = 2.056, p = 0.142, partial η^2 = 0.100), GENOTYPE*AGE (F(4,37) = 0.924, p = 0.461, partial η^2 = 0.091), and

GENOTYPE*SEX (F(2,37) = 0.651, p = 0.528, partial η^2 = 0.034) were not significant. There was no significant main effect of GENOTYPE (F(2,37) = 1.070, p = 0.353, partial η^2 = 0.055) or SEX (F(1,37) = 1.639, p = 0.208, partial η^2 = 0.042). There was a significant main effect of AGE on subcortical area, F(2,37) = 10.045, p < 0.001, partial η^2 = 0.352. All pairwise comparisons were performed using the Bonferroni correction. Data are presented as estimated marginal mean ± standard error with the mean difference and 95% confidence interval.

Subcortical area at 10 months (23.214 ± 0.334 mm^2) was significantly greater than at 6 months (22.029 ± 0.327 mm^2), mean difference 1.185 (95%CI 0.012 to 2.358) mm^2, p = 0.047). Subcortical area at 10 months was also significantly greater than at 10 weeks (20.992 ± 0.369 mm^2), mean difference 2.221 (95%CI 0.972 to 3.470) mm^2, p < 0.001). There was no significant difference between 6 months and 10 weeks, mean difference 1.036 (95%CI -0.200 to 2.273) mm^2, p = 0.127.

“Caudate Putamen”

There was no significant three way interaction between GENOTYPE, SEX, and AGE for caudate putamen area, F(4,37) = 0.543, p = 0.705, partial η^2 = 0.055. The two-way interactions for SEX*AGE (F(2,37) = 1.066, p = 0.355, partial η^2 = 0.054), GENOTYPE*AGE (F(4,37) = 1.047, p = 0.396, partial η^2 = 0.102, and GENOTYPE*SEX (F(2,37) = 0.234, p = 0.792, partial η^2 = 0.012) were not significant. There was no significant main effect of GENOTYPE (F(2,37) = 0.486, p = 0.619, partial η^2 = 0.026) or SEX (F(1,37) = 3.645, p = 0.064, partial

η^2 = 0.090). There was a significant main effect of AGE, F(2,37) = 20.630, p < 0.001, partial η^2 = 0.527. All pairwise comparisons were performed using the Bonferroni adjustment. Data are presented as estimated marginal mean ± standard error with the mean difference and 95% confidence interval.

Caudate Putamen area at 10 months (10.155 ± 0.159 mm^2) was significantly larger than at 10 weeks (8.762 ± 0.175 mm^2), mean difference 1.393 (95%CI 0.800 to 1.986) mm^2, p < 0.001). Area at 6 months (10.028 ± 0.155 mm^2) was also significantly larger than at 10 weeks, mean difference 1.266 (95%CI 0.678 to 1.853) mm^2, p < 0.001. There was no significant difference between area at 10 months and 6 months, mean difference 0.127 (95%CI -0.430 to 0.684) mm^2, p = 1.000.

"Ventricles Area"

The assumption of homogeneity of error variances was violated for ventricle area (Levene's test p < 0.001). Nevertheless, we proceeded with the three-way ANOVA. We performed two-way and one-way ANOVAs on the data for comparison; these alternative analyses are summarized in the Appendix. None of the alternative analyses showed a significant effect of GENOTYPE on ventricle area. In one-way ANOVAs for AGE, only *Grb10*$^{+/m}$ males showed a difference– area at 10 months was larger than at 10 weeks.

There was no significant interaction between GENOTYPE, SEX, and AGE for ventricle area, F(4,37) = 1.169, p = 0.340, partial η^2 = 0.112. The two-way interactions SEX*AGE (F(2,37) = 0.576, p = 0.567, partial η^2 = 0.030), GENOTYPE*AGE (F(4,37) = 1.024, p = 0.408, partial η^2 = 0.100), and

GENOTYPE*SEX (F(2,37) = 1.616, p = 0.212, partial η^2 = 0.080) were not significant. The main effects of GENOTYPE (F(2,37) = 0.681, p = 0.512, partial η^2 = 0.036) and SEX (F(1,37) = 0.306, p = 0.583, partial η^2 = 0.008) were not significant. There was a significant main effect of AGE on ventricle area, F(2,37) = 9.840, p < 0.001, partial η^2 = 0.347. All pairwise comparisons were performed using the Bonferroni adjustment. Data are presented as estimated marginal mean ± standard error with the mean difference and 95% confidence interval.

Ventricle area was 0.949 ± 0.091 mm^2 at 10 months, 0.533 ± 0.089 mm^2 at 6 months, and 0.384 ± 0.100 mm^2 at 10 weeks. Area at 10 months was significantly larger than at 6 months (0.416 (95%CI 0.098 to 0.734) mm^2, p = 0.007) and at 10 weeks (0.566 (95%CI 0.227 to 0.904) mm^2, p < 0.001). There was no significant difference between area at 6 months and 10 weeks, mean difference 0.149 (95%CI -0.185 to 0.484) mm^2, p = 0.811.

3.3.4 False Discovery Rate Corrections–Bregma 0.74 mm

The Benjamini-Liu (BL) procedure was used to correct for false discovery rate (FDR) of 5% over the entirety of area measures for Nissl stained brain slices at Bregma 0.74 mm. Of 13 originally significant tests, 7 survived FDR correction. The main effect of AGE on caudate putamen area was significant. Caudate putamen area at 10 months and 6 months was significantly larger than at 10 weeks. The main effect of AGE on subcortical area also survived. Subcortical area was larger at 10 months than 10 weeks. Finally, the main effect of AGE on ventricle area survived. Ventricle area at 10 months was larger than at 10 weeks.

Table 3.8 Abridged FDR Corrections–Nissl Bregma 0.74 mm

Variable	P value	Rank (m = 48)	B-L: (min, 0.05, 0.05*(m/(m+1-i)^2)	Difference
Caudate Putamen AGE	9.58E-07	1	1.042E-03	1.041E-03
Caudate Putamen (AGE) 10 mo vs 10 wks	3.000E-06	2	1.086E-03	1.083E-03
Caudate Putamen (AGE) 6 mo vs 10 wks	1.200E-05	3	1.134E-03	1.122E-03
Subcortical (AGE) 10 mo vs 10 wks	2.210E-04	4	1.185E-03	9.642E-04
Subcortical AGE	3.280E-04	5	1.240E-03	9.117E-04
Ventricles AGE	3.740E-04	6	1.298E-03	9.240E-04
Ventricles (AGE) 10 mo vs 10 wks	4.940E-04	7	1.361E-03	8.665E-04
Cortical (SEX*AGE) SEX 6 mo	2.933E-03	8	1.428E-03	-1.505E-03

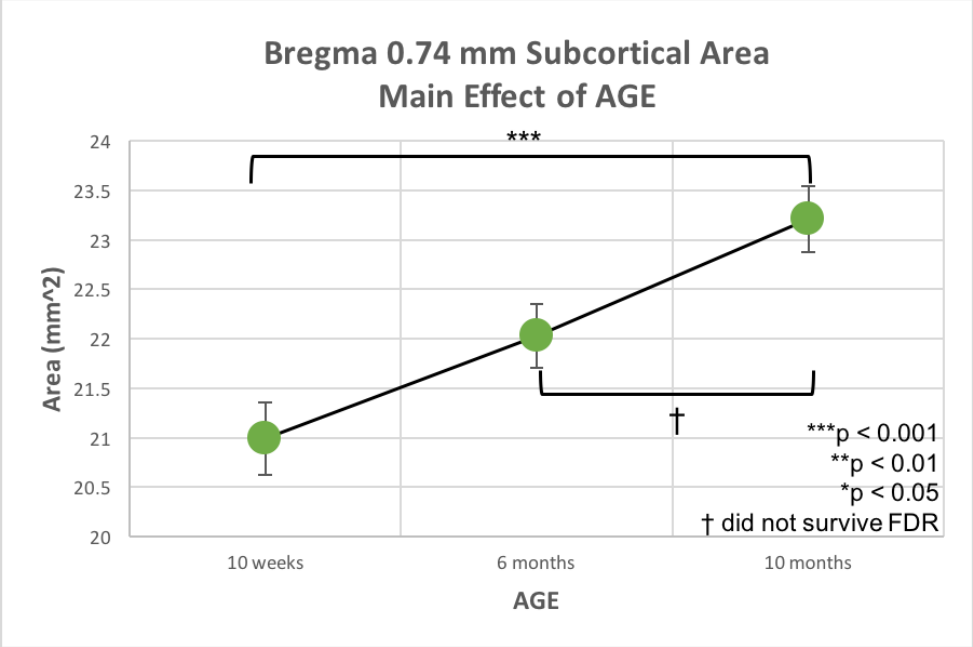

Figure 3.11 Bregma 0.74 mm Subcortical Area Main Effect of AGE

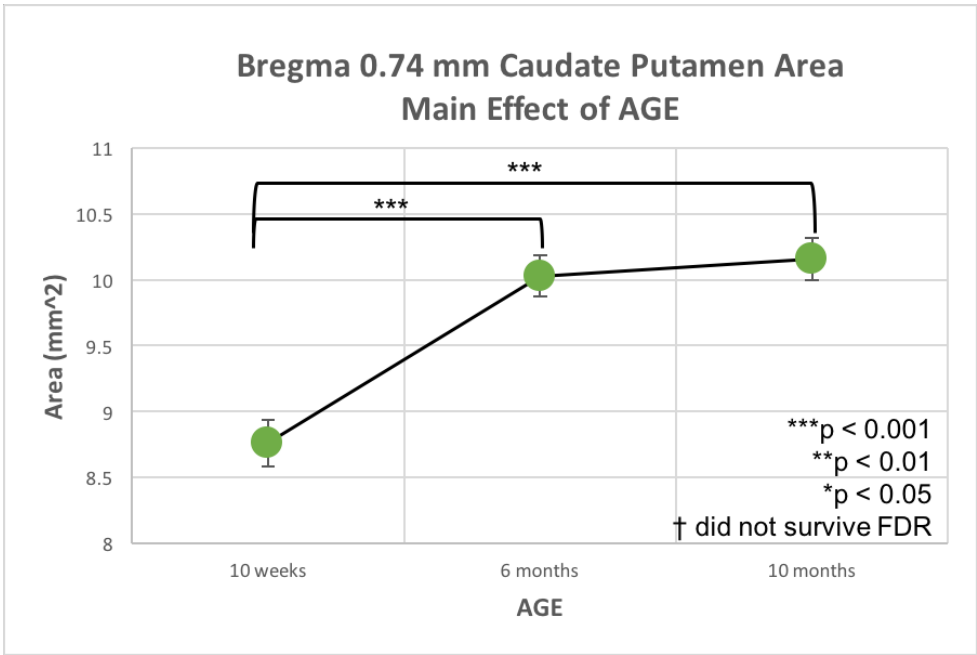

Figure 3.12 Bregma 0.74 mm Caudate Putamen Main Effect of AGE

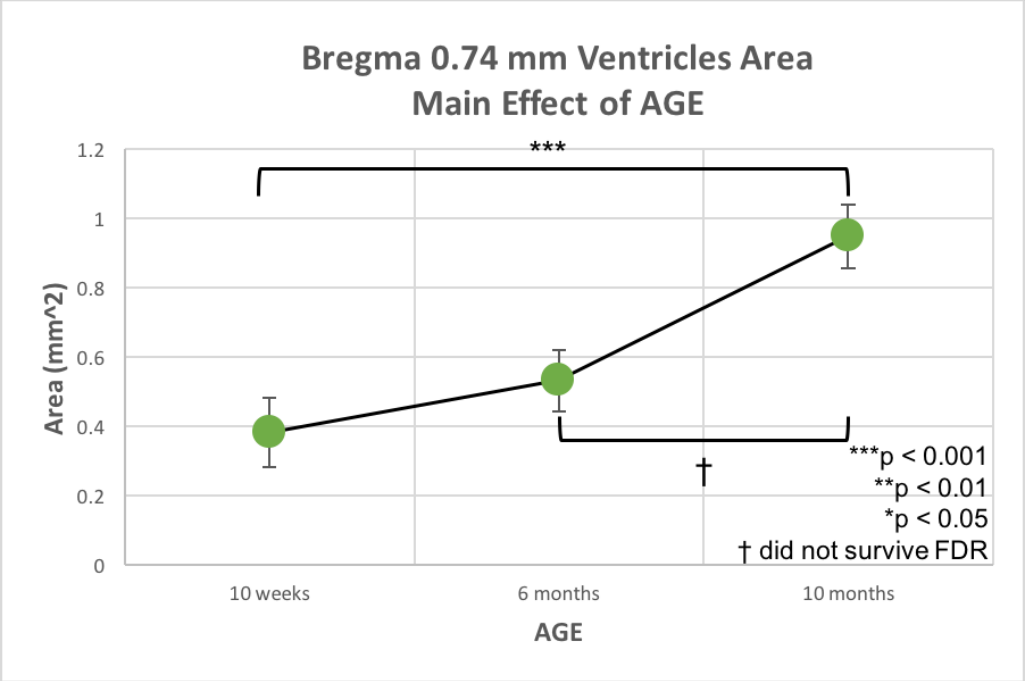

Figure 3.13 Bregma 0.74 mm Ventricles Area Main Effect of AGE

3.3.5 Neuron Density–10 mo cohort

Summary

Sections from brains 10 months of age were counted for DAPI and NeuN staining by stereology. There were three brains for each combination of GENOTYPE and SEX (total n = 18). Cells were counted over three 30 µm sections of caudate putamen spaced at a 1:3 ratio between Bregma regions 0.74 to 0.38. Counting frames were identical for DAPI and NeuN counts. The total estimated cell counts for the target volume were analyzed by two-way or one-way ANOVA for the effect of GENOTYPE and/or SEX. There was no significant main effect of GENOTYPE or SEX on DAPI counts. NeuN counts were analyzed separately by SEX. There was no significant effect of GENOTYPE on NeuN count for either SEX.

When individual ratios of NeuN:DAPI counts for each sample were analyzed using two-way ANOVA, there was still no significant interaction between GENOTYPE and SEX, nor any significant main effects.

Reports

DAPI stain

A two-way ANOVA was conducted to examine the effects of GENOTYPE and SEX on the stereology-estimated counts of DAPI stained cells in the caudate putamen. The sample sizes were 3 brains each for the six combinations of SEX (male and female) and GENOTYPE (WT, *Grb10*$^{+/m}$, *Grb10*$^{+/p}$). Residual analysis was used to test the assumptions of the two-way ANOVA. There were no outliers, as assessed by inspection of box plots of the

residuals. The residuals were normally distributed, as assessed by Shapiro-Wilk's test ($p > 0.05$). Levene's test indicated there was homogeneity of variance in the data ($p = 0.079$). Data are presented as estimated marginal mean ± standard error, unless otherwise stated.

The interaction between GENOTYPE and SEX was not statistically significant, $F(2,12) = 0.156$, $p = 0.857$, partial $\eta^2 = 0.025$. The main effect of GENOTYPE was not statistically significant, $F(2,18) = 0.150$, $p = 0.863$, partial $\eta^2 = 0.024$. The estimated mean DAPI cell count was 4.060E5 ± 2.096E4 cells for wildtype, 4.221E5 ± 2.096E4 cells for *Grb10*$^{+/m}$, and 4.121E5 ± 2.096E4 cells for *Grb10*$^{+/p}$ brains. The main effect of SEX was also not statistically significant, $F(1,12) = 0.156$, $p = 0.857$, partial $\eta^2 = 0.025$. The estimated mean DAPI cell count was 4.179E5 ± 1.712E4 cells for male and 4.089E5 ± 1.712E4 cells for female brains.

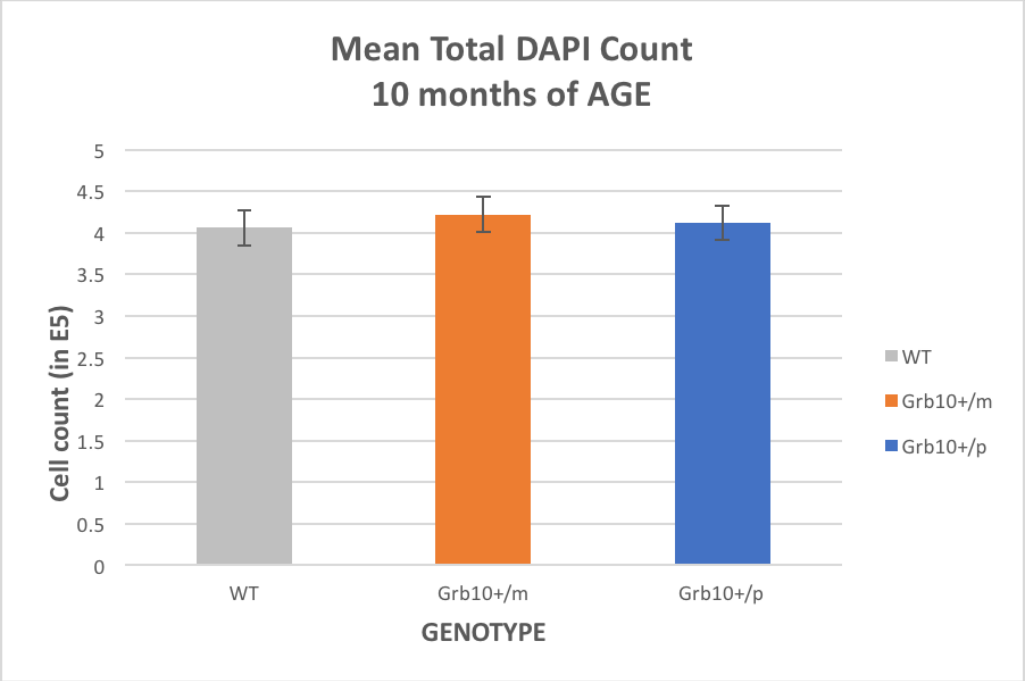

Figure 3.14 Estimated Marginal Mean Total DAPI Count–10 months

NeuN stain

A two-way ANOVA could not be conducted to examine the effects of GENOTYPE and SEX on the stereology estimated counts of NeuN stained cells in the caudate putamen, because the data violated the assumption of homogeneity of error variances (Levene's test p = 0.016). Therefore, male and female counts were analyzed separately using one-way ANOVAs. The sample sizes were 3 brains for each GENOTYPE (WT, *Grb10*$^{+/m}$, *Grb10*$^{+/p}$) for each sex (male and female).

Shapiro-Wilk's test indicated NeuN data for male brains were normally distributed for all three genotypes (WT p = 0.408, *Grb10*$^{+/m}$ p = 0.306, *Grb10*$^{+/p}$ p = 0.468). There were no outliers with studentized residuals more extreme than ±3 SD. There was homogeneity of error variances, as assessed by Levene's test (p = 0.391). Data are presented below as descriptive mean ± standard deviation. There was no significant effect of GENOTYPE on NeuN count in male brains, F(2,6) = 0.081, p = 0.923, partial η^2 = 0.026. The mean NeuN counts for male brains 10 months of age were 2.453E5 ± 1.628E4 cells for wildtype, 2.526E5 ± 3.115E4 cells for *Grb10*$^{+/m}$, and 2.466E5 ± 2.097E4 cells for *Grb10*$^{+/p}$ brains.

Shapiro-Wilk's test indicated NeuN data for female brains were normally distributed (p > 0.05). There were no outliers with studentized residuals more extreme than ±3 SD. The assumption of homogeneity of variances was violated, as assessed by Levene's test (p = 0.036). Therefore, we have interpreted Welch's F. Data are presented below as descriptive mean ± standard deviation. There was no significant effect of GENOTYPE on NeuN

count, F(2,3.203) = 0.109, p = 0.900. The mean NeuN counts were 2.427E5 ± 7.419E4 cells for wildtypes, 2.499E5 ± 3.954E4 cells for *Grb10*$^{+/m}$, and 2.561E5 ± 1.089E4 cells for *Grb10*$^{+/p}$ brains.

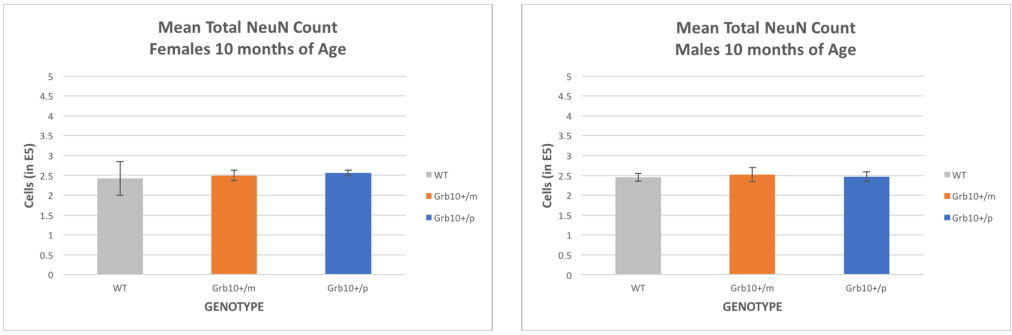

Figure 3.15 Mean Total NeuN Counts–Males & Females 10 months

Ratio

Individual brain ratios between NeuN and DAPI counts were analyzed for the effects of GENOTYPE and SEX using a two-way ANOVA. Studentized residuals (SRE) of the data were normally distributed (Shapiro-Wilk's $p > 0.05$), and there were no outliers more extreme than ±3 SD. There was homogeneity of variance (Levene's test, $p = 0.101$). There was no significant interaction between GENOTYPE and SEX, $F(2,12) = 0.047$, $p = 0.954$, partial $\eta^2 = 0.008$. The main effects of GENOTYPE ($F(2,12) = 0.299$, $p = 0.747$, partial $\eta^2 = 0.047$) and SEX ($F(1,12) = 0.930$, $p = 0.354$, partial $\eta^2 = 0.072$) were not significant. The ratios of the NeuN:DAPI counts presented are descriptive mean ± standard deviation.

Table 3.9 NeuN:DAPI Ratio–Descriptives

GENOTYPE	SEX	Mean Ratio	Std. Deviation	N
WT	Male	0.591	0.055	3
	Female	0.611	0.034	3
	Total	0.601	0.042	6
PAT KO	Male	0.605	0.029	3
	Female	0.614	0.004	3
	Total	0.610	0.019	6
MAT KO	Male	0.587	0.025	3
	Female	0.603	0.031	3
	Total	0.595	0.027	6
Total	Male	0.594	0.034	9
	Female	0.609	0.023	9
	Total	0.602	0.030	18

3.4 Discussion

Although there were specific cohorts of animals taken at 10-weeks, 6-months and 10- months, I sampled brain weight in all animals available throughout the project. Subsequently, brain and body weight samples were grouped into three separate 20-day BINS (75-95, 185-205 and 305-325 days). Analysis of these data indicated *Grb10*$^{+/p}$ brains were generally heavier than both wildtype (by 6.575% at 75-95 and 8.542% at 305-325 days) and *Grb10*$^{+/m}$ brains (by 15.841% at 305-325 days). A key difference between *Grb10*$^{+/p}$ and both wildtype and *Grb10*$^{+/m}$ brains was the pattern of change over time, as reflected in a significant interaction between GENOTYPE and AGE. Unlike wildtype and *Grb10*$^{+/m}$ brains, which were heaviest at 185-205 days (~6-7 months) and then decreased at 305-325 days (~10-11 months), *Grb10*$^{+/p}$ brains maintained weight between 185-205 days and 305-325 days (and weight at 75-95 days < 185-205 days and 305-325 days). In fact, the wildtype and *Grb10*$^{+/m}$ decline in brain weight survived FDR correction, while the increase in *Grb10*$^{+/p}$ brain weight between 75-95 days and the later age bins did not. We conclude *Grb10*$^{+/p}$ brains are generally heavier than controls and maintain this weight with age, where control brains decline in weight at later ages. These results were not due to overall differences in body weight, as there were no differences in body weight between the three genotype groups after FDR correction. Prior to FDR correction, *Grb10*$^{+/m}$ body weight at 75-95 days was heavier than wildtypes and *Grb10*$^{+/p}$ mice, and was no different at other ages, consistent with previous findings that *Grb10*$^{+/m}$ mice start heavier but normalize with age (Garfield, 2007).

Our wet weight brain data confirmed and elaborated Garfield's finding that adult *Grb10*$^{+/p}$ brains generally weigh more than wildtypes (Aim 1). Our experimental design did not examine brain weight at birth, and therefore we could not address Garfield's finding that this difference in brain weight does not exist at P0 (Garfield, 2007). Our data confirmed *Grb10*$^{+/p}$ postnatal brain allometry differs from wildtypes, but disagrees with Garfield on the pattern. Garfield's *Grb10*$^{+/p}$ brain mass increased significantly between D84 and D308, where wildtype brain mass did not significantly change (Garfield, 2007). In contrast, we concluded *Grb10*$^{+/p}$ display a pattern of weight maintenance rather than continuous weight increase, and both wildtype and *Grb10*$^{+/m}$ controls displayed a decline in brain weight in later life.

Having clearly demonstrated the brains of *Grb10*$^{+/p}$ mice are heavier than control groups, my next aim was to examine the morphology in more detail. I used histological techniques to examine regional differences in brain size in parallel with immunohistochemistry to assess total cell and neuronal counts in relevant regions of *Grb10*$^{+/p}$ reporter expression.

In Aim (2), we used nested area measures to pursue Garfield's observations of subcortical overgrowth and to investigate this effect in more specific regions. We focused on brain slices at Bregma +0.74 mm, where paternal *Grb10* is expressed in the caudate putamen, but not the cortex (Garfield, 2007). This was more rostral, but still adjacent to Garfield's measures at +0.26 mm to +0.38 mm. We sought to add to the total coverage in the characterization of brain slice area. In our three-way ANOVA for the effects of GENOTYPE, SEX, and AGE, we found no significant interactions or main effects

of GENOTYPE or SEX. The exception was a significant simple main effect of SEX at 6 months of age, where males had smaller cortical area than females, but this did not survive FDR correction. The main effects of AGE on subcortical, caudate putamen, and ventricle area survived FDR correction. All three area measures increased between 10 weeks and 10 months of age, and caudate putamen area also increased between 10 weeks and 6 months of age. We therefore did not confirm Garfield's observations, despite doubling the sample size at each age group by using male and female brains.

In Aim (3), we measured total cell count and neuronal cell count in 10-month-old brain slices between +0.74 mm to +0.38 mm. The stained series used for cell counting was parallel to the series used to measure area of 10-month-old brains in Aim (2). There were no significant differences by SEX or GENOTYPE on DAPI count or GENOTYPE differences in NeuN count in individual analyses of each sex. There was also no significant difference in the direct neuron to total cell count ratio.

3.4.1 Experimental Sensitivity Analysis

Although our Nissl-stained area and cell count experiments used similar sample sizes for each group as compared to Garfield's pilot study on Nissl-stained area, we did not find significant differences in these experiments. One possible explanation is that we lacked the power to adequately detect an effect. However, calculating observed power, from the observed means and variances in our experiment is based on the questionable assumption that sample effect size is identical to the effect size in the population. This assumption can bias the power calculation (Faul, Erdfelder, Lang, & Buchner,

2007). Therefore, I performed a sensitivity analysis to assess the minimum population effect size we could detect in each comparison of our experiment, based on our experimental parameters. For each calculation of effect size using G*Power 3.1 (Faul et al., 2007), I used $\alpha = 0.05$ (as used in my statistical analyses) and power $(1- \beta) = 0.80$. My output was Cohen's f, which I converted to omega squared (ω^2) as a measure of relative effect magnitude in the population. Cohen's f was converted to effect size ω^2 using the equation:

$$\omega^2 = f^2 / (1 + f^2)$$

Cohen's values for small ($\omega^2 = 0.01$) , medium ($\omega^2 = 0.6$), and large effects ($\omega^2 \geq 0.15$) were used to assess effect size (Cohen, 1988; Field, 2013; Keppel, 1991).

Nissl Stained Area

I performed a sensitivity analysis for each measure of area, including "whole brain", "cortical", "subcortical", "caudate putamen", and "ventricles", with a unique numerator degrees of freedom. As these measures represented subsets of the same samples, analyzed using three-way ANOVAs, the parameters of the sensitivity analysis are common between them. For all calculations, $\alpha = 0.05$, power $(1-\beta) = 0.80$, total sample size = 55, and # of groups = 18.

For the three-way interactions for GENOTYPE*SEX*AGE, the numerator df = 4, resulting in a Cohen's f = 0.496 and $w^2 = 0.198$. According to Cohen's

classifications, this was a large effect size ($\omega^2 > 0.15$). For the two-way interactions for SEX*AGE and GENOTYPE*SEX, as well as for the main effects of GENOTYPE and AGE, the numerator df = 2. Cohen's f = 0.436 and $\omega^2 = 0.160$, a large effect size ($\omega^2 > 0.15$). For the main effect of SEX, the numerator df = 1. Cohen's f = 0.388 and $\omega^2 = 0.131$, a medium effect size ($0.06 < \omega^2 < 0.15$).

Garfield's area measures compared only WT and *Grb10*$^{+/p}$ male mice at 3 months of age. These data were analyzed with a 2-tailed t-test. My sensitivity analysis parameters were tails = 2, $\alpha = 0.05$, power = 0.80, sample size group 1 = 3, sample size group 2 = 3 (Garfield, 2007). The effect size Cohen's d = 3.077. We converted d using the equation:

$$f = d * \text{square root} (1 / (2*a))$$

where a = the number of groups (2 for Garfield's experiment)

For Garfield's experiment, Cohen's f = 1.539 and $\omega^2 = 0.703$. While our analysis was unable to detect differences in area between our groups, Garfield's experiment, which did find a difference in subcortical and whole area between genotype groups was less sensitive than our own experiment. Regardless, both experiments were underpowered to detect anything less than a large effect.

Cell Counts

I performed sensitivity analysis for DAPI cell count interactions and main effects. For all calculations, $\alpha = 0.05$, power ($1- \beta$) = 0.80, total sample size = 18, and # of groups = 6. For the two-way interaction GENOTYPE*SEX and

the main effect of GENOTYPE, the numerator df = 2, Cohen's f = 0.833, and ω^2 = 0.410. For the main effect of SEX, the numerator df = 1, Cohen's f = 0.720, and ω^2 = 0.341. These are both very large effect sizes ($\omega^2 > 0.15$).

I performed sensitivity analysis for the one-way ANOVAs for male and female NeuN counts by GENOTYPE. For both analyses (male and female), α = 0.05, power (1- β) = 0.80, total sample size = 9, # of groups = 3, and the numerator df = 2. Cohen's f = 1.357, and ω^2 = 0.648 for both males and females by GENOTYPE. This was a very large effect size ($\omega^2 > 0.15$).

The DAPI:NeuN ratio was analyzed with a two-way ANOVA for GENOTYPE and SEX. In the sensitivity analysis, α = 0.05, power (1- β) = 0.80, total sample size = 18, # of groups = 6. For the two-way interaction GENOTYPE*SEX and the main effect of GENOTYPE, the numerator df = 2, Cohen's f = 0.833, and ω^2 = 0.410. For the main effect of SEX, the numerator df = 1, Cohen's f = 0.720, and ω^2 = 0.341. This experiment was only powered to detect large and very large effects. Further investigation should expand the sample size in each group.

3.4.2 Integrating Brain Weight, Area, and Cell Counts

We face a dilemma in proposing an integrated interpretation of the brain weight data, Nissl-stained area measurements, and total cell and neuronal count data. *Grb10* may regulate cell proliferation, neuronal survival, and/or apoptotic mechanisms to regulate brain growth (Kebache et al., 2007; Morrione, Valentinis, Resnicoff, Xu, & Baserga, 1997; Werner & LeRoith, 2014). Cell density provides clues as to the mechanism of *Grb10*$^{+/p}$ brain overgrowth. If we wish to calculate the total cell and neuronal density in our *Grb10*$^{+/p}$ and

wildtype brains, we need to determine whether our Nissl-stained area measures (1) truly lack difference in the samples and the population, (2) truly lack difference in the samples but not the population, or (3) artificially lack difference in the samples. In the first instance, we might conclude there is no population genotype difference in total and neuronal cell density in the caudate putamen between Bregma +0.74 mm and +0.38 mm. The observed increase in weight in *Grb10*$^{+/p}$ brains compared to wildtypes at 10 months might therefore be the result of (1a) differences in cell density in other brain regions, but not the caudate putamen, or (1b) no difference in cell density or area measures in any region, but increased length/volume of the brain. In the second instance, we may have by chance selected samples with similar areas. In other words, the sampled *Grb10*$^{+/p}$ brains may be on the lower end of possible sizes, and/or the sampled wildtype brains may be on the higher end of possible sizes. Because this would be a true lack of difference in the sample, we might assume cell counts and density information would scale up or down appropriately with brain area. We could therefore conclude (2a) there is no population genotype difference in total and neuronal cell density in the caudate putamen. Therefore, if the *Grb10*$^{+/p}$ population has larger areas overall, the population difference in brain weight might be explained by more total tissue of the same cell density in *Grb10*$^{+/p}$ brains. In the third instance, where the lack of difference between our wildtype and *Grb10*$^{+/p}$ Nissl-stained slices is artificial, and *Grb10*$^{+/p}$ subcortical area is larger than wildtypes (as observed in Garfield 2007), total cell and neuronal density could be lower in *Grb10*$^{+/p}$ than wildtype brains. Therefore, the increase in brain weight might

be due to (3a) increased connectivity between cells. None of these cases suggest a difference in non-neuronal glial populations, as total cell counts were identical between genotypes. However, we have not reported a direct test for this measure. No true conclusions may be made if our area measures are artificially altered by experimental processing. However, it is unlikely that option (3) is the case, as brains of all genotypes and sexes underwent the same fixation processes.

We conclude the increase in wet weight in *Grb10*$^{+/p}$ brains is real and present in both sexes. *Grb10*$^{+/p}$ brains maintain weight with age, where wildtype and *Grb10*$^{+/m}$ brain weights peak at 185-205 days and decline by 305-325 days of age. We did not measure an effect of GENOTYPE or SEX on section area at Bregma +0.74mm. There seems to be no difference between GENOTYPES in raw total or neuronal cell counts, nor a difference in the ratio of neuronal to total cell staining. The ambiguity incited by the discrepancy between Garfield's Nissl-staining data and our own called for a more sensitive measure of *Grb10*$^{+/p}$ brain dimensions. We used MRI volumetric data in the next chapter to supplement our data on the putative subcortical overgrowth phenotype in *Grb10*$^{+/p}$ (male) mice.

4 MRI

4.1 Introduction

4.1.1 Longitudinal MRI

Evidence from the previous chapter and from Garfield 2007 indicate *Grb10*$^{+/p}$ brains weigh more than those of wildtype and *Grb10*$^{+/m}$ mice. The expression profile of the *LacZ* cassette in Grb10$^{+/p}$ mice provides a clue to the brain regions which may contribute most to this phenotype. Macroscopically, *Grb10*$^{+/p}$ paternal expression is absent from the cortex and highly expressed in subcortical regions including the monoaminergic systems of the midbrain and the cholinergic interneurons of the caudate putamen (Garfield et al., 2011). Nissl stained sections in Garfield 2007 showed *Grb10*$^{+/p}$ brains had larger total and subcortical areas than wildtypes, but cortex area was not significantly different (Garfield, 2007). In our study however, Nissl stained sections somewhat more rostral to those in Garfield 2007 did not show this effect of GENOTYPE at 10 weeks, 6 months, or 10 months of age.

To gain a more nuanced insight into the differences in *Grb10*$^{+/p}$ brain, we conducted a longitudinal MRI study to track brain volume data in individual adult animals over time. *Grb10*$^{+/p}$ and wildtype mice in mixed genotype housing were subjected MRI scans at 10 weeks, 6 months, and 10 months of age, and underwent behavioural testing at 10 months of age, for integration with our cross-sectional behavioural study. The longitudinal MRI study provided a more sensitive comparison between brain morphology at different ages than afforded by Nissl stained brain slices. While perfusion and Nissl

staining samples different mice for each age group investigated, MRI reduces variance by sampling the same individuals at multiple ages.

We were also able to test the significance of the interaction of the between-subjects variable GENOTYPE and the within subjects variable AGE. In the previous chapter, we demonstrated a significant two-way interaction between GENOTYPE and AGE (as between-subjects factors) for the dependent variable "whole wet brain weight". We found *Grb10*$^{+/p}$ brains were significantly heavier at each age bin than at the age bin before. Wildtype and *Grb10*$^{+/m}$ in our study gained mass between bin 75-95 days (2-3 months) and 185-205 days (6 -7 months), but lost mass between 185-205 days and 305-325 days. Garfield's Student T-test comparisons also indicated *Grb10*$^{+/p}$ brains continue to gain mass into 10 months of age, where wildtype brains do not (Garfield, 2007). The longitudinal MRI study reduces inter-individual noise which could interfere with our description of brain growth allometry.

4.1.2 Chapter Aim

Aim (1) Describe "whole brain", "subcortical", and "cortical" volumes in *Grb10*$^{+/p}$ and wildtype male mice at 10 weeks, 6 months, and 10 months of age.

Anatomical MRI scans at 10 weeks, 6 months, and 10 months were analyzed to investigate the interaction and main effects of GENOTYPE and AGE in the cohort. Volumes measured were comparable to areas measured in the Nissl staining experiments in the previous chapter and in Garfield 2007.

4.2 Methods

4.2.1 Subjects

Five cages of four mice in mixed genotype housing (2 wildtype, 2 *Grb10*$^{+/p}$) were scanned in a longitudinal MRI study at 10 weeks, 6 months, and 10 months of age. Three mice were initially mis-genotyped as *Grb10*$^{+/p}$ instead of wildtypes (A64 P, A70 P, A71 P), and therefore, two cages were not equally balanced between *Grb10*$^{+/p}$ and wildtype cage mates. Genotypes were corrected for analysis.

4.2.2 Scanning

MRI scans were conducted by Andrew Stewart in the Experimental MRI Center (EMRIC) at Cardiff University. Mice were anesthetized using 3% isoflurane in 30% O_2 with a flow rate of 1 liter/minute. Once anesthetized, the mouse was placed in the prone position on a heating pad on the scanner bed and was stabilized at 80-90 breaths per minute by reducing isoflurane to approximately 1%. Animals were taped down and a tooth bar was fixed to minimize motion. MRI was performed on a Bruker 9.4 Tesla (400MHz) scanner, with a bore size of 20 cm. Paravision Version 6.0.1 software combined with Avance II electronics was used to collect the data. RF volume coil (72 mm diameter) was used as a transmitter with a 4-channel phased array receive coil (Bruker Biospin, Part No T11071). A localizer scan was used to position the mouse appropriately. A Bruker shimming procedure was used to optimize the magnetic field homogeneity. Anatomical data was collected using a T2 weighted scan (TR = 2500 ms, echo spacing =11 ms, TE = 22 ms, averages = 8, rare factor = 4, FOV = 25.6 x 25.6 mm, matrix = 128 x 128 x 40 mm). Voxel

dimensions were 0.200 x 0.200 mm with 0.400 mm slice thickness. Diffusion Tensor Imaging (DTI) data was collected following the anatomical scan, but these data are not analyzed here. Each scanning session (per mouse) lasted approximately 1 hour.

4.2.3 Data Processing

Data processing was performed on MATLAB R2015a. Raw T2 scans were trimmed on ExploreDTI v.4.8.6 (© Alexander Leemans) and exported as NIfTI(nii) files. Scans at 10 weeks were used to create a study-specific template brain (Dr. Greg Parker, CUBRIC, Cardiff University) on which template masks were manually drawn. “Whole brain volume” was measured from the beginning of the olfactory bulbs to the end of the cerebellum, not including any brain stem. “Cortical” and “subcortical” volumes were manually drawn to be complementary, starting from Bregma +1.98 mm to include the caudate putamen and ending at Bregma -4.24 mm to include the dorsal raphe nucleus. Cortical masks included the hippocampus, and excluded the corpus callosum, external capsule, alveus, and third ventricle. Subcortical masks included all area below the cortical mask, but excluded the ventricles. Template masks were co-registered to the individual brain scans at each of the three time points and were manually tailored to the individual scan to calculate volumes.

4.2.4 Statistics

Shapiro-Wilk’s test was used to assess normality, and was followed up with examination of the histogram of the data where needed. Outliers were identified as data points with studentized residuals (SREs) more extreme than

±3 SD. Graphs depict descriptive mean ± standard error of the descriptive mean unless otherwise stated. Data for main effects are presented as estimated marginal mean ± standard error of the estimated mean. Significant main effects are followed by post hoc analysis with the Bonferroni adjustment for all pairwise comparisons. Mean difference is presented with the 95% confidence interval.

The BL procedure requires no assumptions about independence or dependence (positive or negative), and thus was judged to be the most appropriate FDR correction for the statistical tests of volume (Yoav Benjamini et al., 2001).

4.3 Results

4.3.1 Whole Brain Volume

Whole brain volume was collected from 20 male mice (13 wildtype, 7 *Grb10*$^{+p}$) at three ages (10 weeks, 6 months, 10 months) in a longitudinal study. The data were analyzed using a 2-way mixed ANOVA, with the between subjects variable GENOTYPE, the within-subjects variable AGE, and the dependent variable “whole brain volume”.

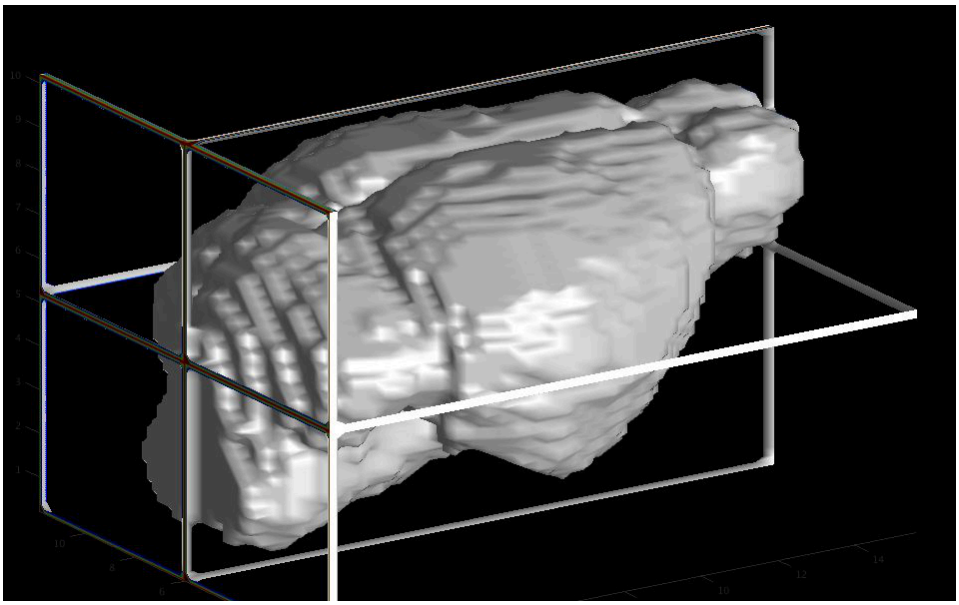

Figure 4.1 Whole Brain Mask Example (A49 P, wildtype)

Data Screening

Two subjects were excluded from the analysis because whole brain volumes at 6 months were incomplete (A50 P and A64 P– both wildtype). The final cases analyzed were wildtype (n = 11) and *Grb10*$^{+/p}$ (n = 7). Shapiro-Wilk's test indicated the data were normally distributed for all cells of the design ($p > 0.05$). There were no outliers with studentized residuals more extreme than ± 3SD. There was homogeneity of variance and covariance, as assessed by Levene's test ($p > 0.05$) and Box's M ($p = 0.614$) respectively. Mauchly's test of sphericity indicated the assumption of sphericity was met, $\chi^2(2) = 2.098$, $p = 0.350$.

Report

The interaction between AGE and GENOTYPE was not statistically significant for whole brain volume, $F(2,32) = 2.355$, $p = 0.111$, partial η^2 =

0.128. The main effect of GENOTYPE was statistically significant, $F(1,16) = 6.719$, $p = 0.020$, partial $\eta^2 = 0.296$. The main effect of AGE was also statistically significant, $F(2,32) = 90.437$, $p < 0.001$, partial $\eta^2 = 0.850$.

The estimated mean whole brain volume by GENOTYPE was 509.401 ± 10.761 mm^3 for *Grb10*$^{+/p}$ mice and 473.722 ± 8.584 mm^3 for wildtypes, a statistically significant mean difference of 35.680 (95%CI 6.499 to 64.860) mm^3, $p = 0.020$. This was a 7% increase in brain volume for *Grb10*$^{+/p}$ mice compared to wildtypes, estimated across all ages. The estimated mean whole brain volume by AGE was 476.047 ± 6.533 mm^3 at 10 weeks, 494.839 ± 7.115 mm^3 at 6 months, and 503.798 ± 7.296 mm^3 at 10 months. Volume statistically significantly increased from 10 weeks to 6 months (18.792 (95%CI 12.773 to 24.812) mm^3, $p < 0.001$), 10 weeks to 10 months (27.751 (95%CI 21.544 to 33.959) mm^3, $p < 0.001$), and from 6 months to 10 months (8.959 (95%CI 4.451 to 13.467) mm^3, $p < 0.001$).

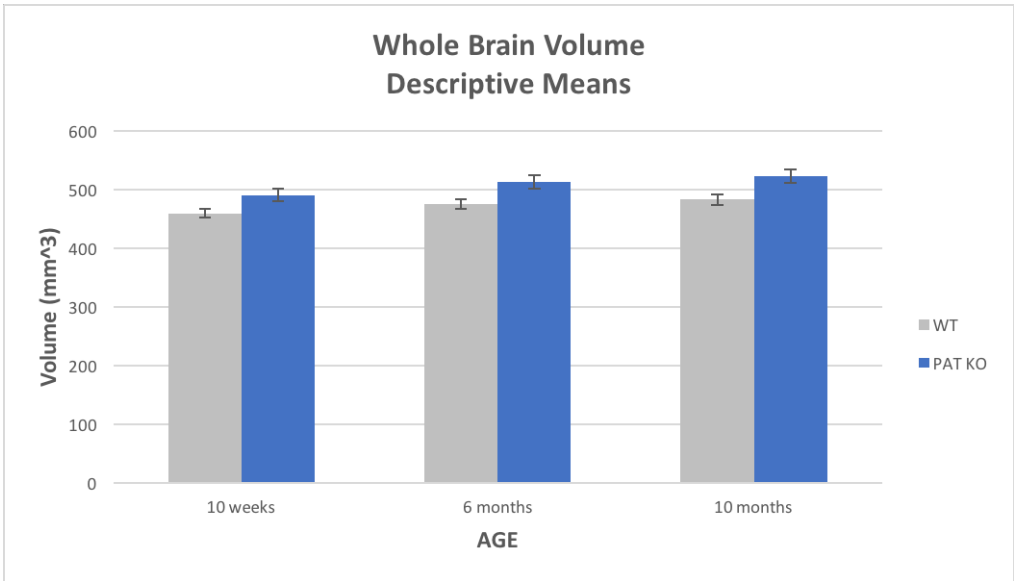

Figure 4.2 Whole Brain Volume Descriptive Means

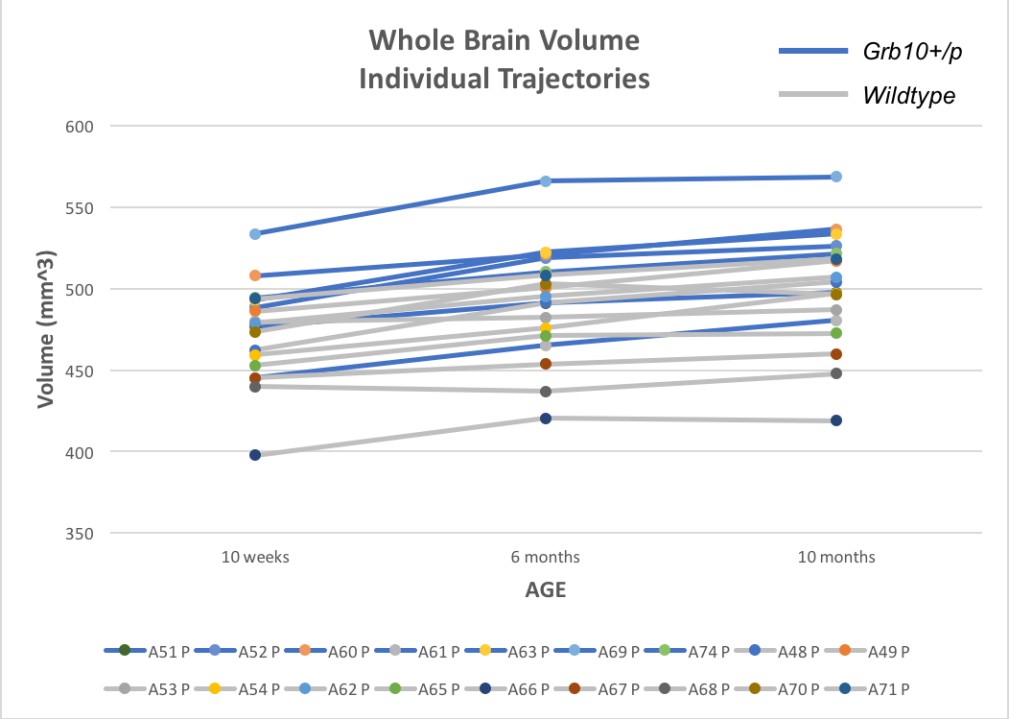

Figure 4.3 Whole Brain Volume Individual Trajectories

4.3.2 Subcortical Volume

Subcortical volume was collected from 20 male mice (13 wildtype, 7 *Grb10*$^{+p}$) at three ages (10 weeks, 6 months, 10 months) in a longitudinal study. Data are analyzed here at 10 months, where there was the largest overall

difference in whole brain volume. We used a one-way ANOVA with the between-subjects factor GENOTYPE and the dependent variable “subcortical volume”. Volumes for all 20 mice scanned are included at 10 months.

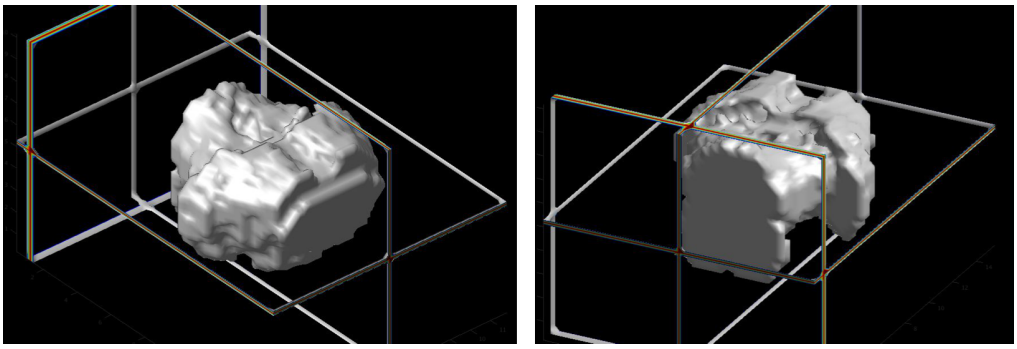

Figure 4.4 Subcortical Mask Example (A49 P, wildtype)

Data Screening and Report

Shapiro-Wilk’s test indicated the data were normally distributed for *Grb10*$^{+/p}$ brains (p = 0.868) but non-normally distributed for wildtypes (p = 0.008). The histogram of the wildtype data showed negative skew. There were no outliers with studentized residuals more extreme than ± 3SD. There was homogeneity of variance, as assessed by Levene’s test (p = 0.433). There was a significant effect of GENOTYPE on subcortical volume at 10 months: 162.539 ± 3.649 mm^3 for *Grb10*$^{+/p}$ and 149.234 ± 2.678 mm^3 for wildtypes, a statistically significant mean difference of 13.305 (95%CI 3.797 to 22.813) mm^3, F(1,18) = 8.642, p = 0.009, partial η^2 = 0.324.

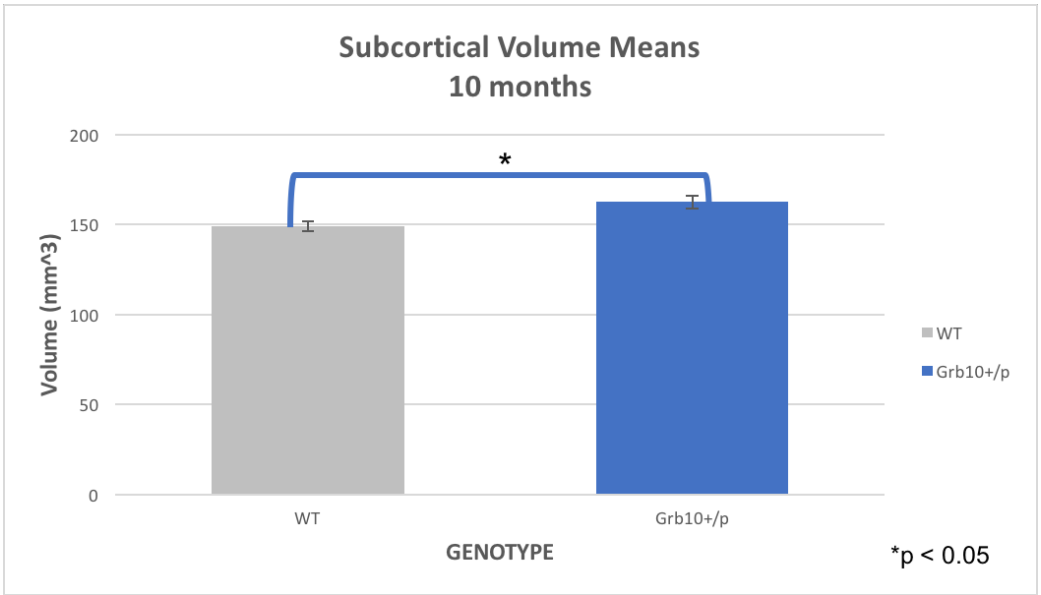

Figure 4.5 Subcortical Volume Means–10 months

4.3.3 Cortical Volume

Cortical volume was collected from 20 male mice (13 wildtype, 7 *Grb10*$^{+p}$) at three ages (10 weeks, 6 months, 10 months) in a longitudinal study. Data are analyzed here at 10 months, where there was the largest overall difference in whole brain volume. We used a one-way ANOVA with the between-subjects factor GENOTYPE and the dependent variable "Cortical volume". Volumes for all 20 mice scanned are included at 10 months.

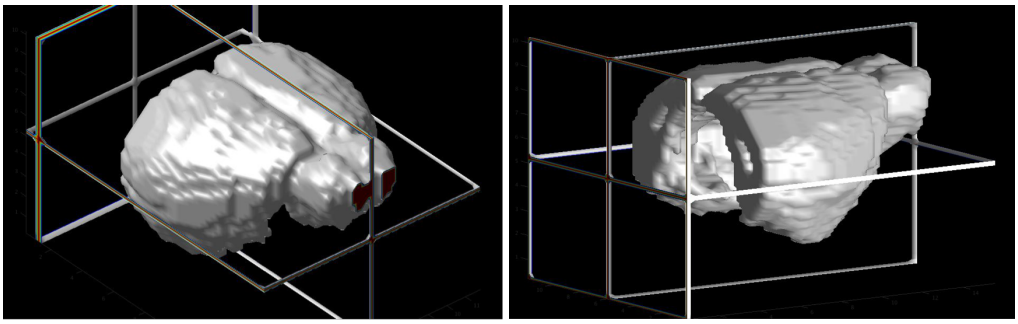

Figure 4.6 Cortical Mask Example (A49 P, wildtype)

Data Screening and Report

Shapiro-Wilk's test indicated the cortical volume data were normally distributed for both wildtype (p = 0.298) and *Grb10*$^{+/p}$ brains (p = 0.359). There were no outliers with studentized residuals (SREs) more extreme than ± 3SD. There was homogeneity of variance, as assessed by Levene's test (p = 0.662). There was a significant effect of GENOTYPE on cortical volume at 10 months: 189.998 ± 4.197 mm^3 for *Grb10*$^{+/p}$ and 177.463 ± 3.080 mm^3 for wildtype brains, a mean difference of 12.534 (95%CI 1.597 to 23.472) mm^3, F(1,18) = 5.797, p = 0.027, partial η^2 = 0.244.

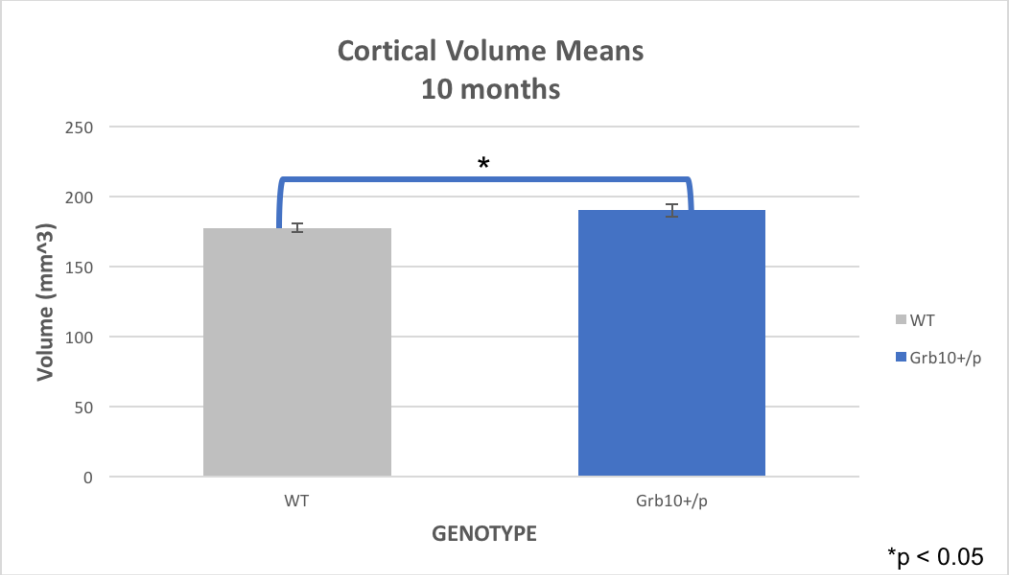

Figure 4.7 Cortical Volume Means–10 months

4.3.4 False Discovery Rate Corrections

The Benjamini-Liu (BL) procedure was used to correct for a false discovery rate (FDR) of 5% over the entirety of volumetric measures. Of eight

statistical tests, seven were originally found to be statistically significant and remained significant after FDR correction.

Table 4.1 FDR Corrections–MRI Volumes

Variable	P value	Rank (m = 8)	BL = (min 0.05, 0.05*m/(m+1-i)^2	Difference
Whole Brain Main Effect of AGE	6.80E-14	1	6.250E-03	6.25E-03
Whole Brain 10 weeks to 10 months	6.55E-09	2	8.163E-03	8.16E-03
Whole Brain 10 weeks to 6 months	9.58E-07	3	0.011	0.011
Whole Brain 6 months to 10 months	2.10E-04	4	0.016	0.016
Subcortical Volume Effect of GENOTYPE	8.76E-03	5	0.025	0.016
Whole Brain Main Effect of GENOTYPE	0.020	6	0.044	0.025
Cortical Volume Effect of GENOTYPE	0.027	7	0.050	0.023
Whole Brain Interaction–AGE*GENOTYPE	0.111	8	0.050	-0.061

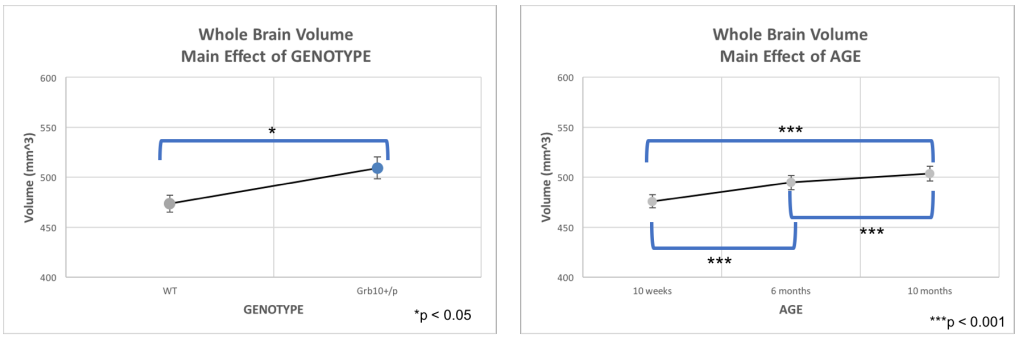

Figure 4.8 Whole Brain Volume Significant Main Effects

4.4 Discussion

Our longitudinal MRI study found whole, subcortical, and cortical brain volumes in *Grb10*$^{+/p}$ mice were consistently larger than wildtypes. We did not find evidence of an interaction between GENOTYPE and AGE for whole brain volume, though the main effects of both were significant individually. There was a 7% increase in *Grb10*$^{+/p}$ whole brain volume for compared to wildtypes across all ages. In Chapter 3, we found *Grb10*$^{+/p}$ brains weighed 6.575% more than wildtypes at 75-95 days and 8.542% more at 305-325 days. At 75-95 and 305-325 days of age, total *Grb10*$^{+/p}$ increase in weight and volume is comparable, but at 185-205 days, *Grb10*$^{+/p}$ brains had significantly larger volumes but were not significantly heavier after FDR correction. Taken together, the data in Chapters 3 and 4 indicate that *Grb10*$^{+/p}$ brains are generally larger and weigh more than wildtypes.

In Chapter 3, the discrepancy between our Nissl-stained area measurements and Garfield's called for MRI volumetric data as a more sensitive measure of *Grb10*$^{+/p}$ brain dimensions. We hoped this data would give us a better idea of neuronal and total cell density in *Grb10*$^{+/p}$ brains. Stereology estimates from parallel brain sections in our study indicated no difference in neuronal or total cell count estimates in the caudate putamen. However, in our Nissl-stained samples of 10-month-old brains we also did not find a genotype difference in total, subcortical, or cortical area. We presented multiple possible conclusions about cell density in the caudate putamen. In this chapter, we demonstrated *Grb10*$^{+/p}$ brain volumes are consistently larger

than wildtypes. It is entirely possible our Nissl-stained area results fail to show a true population difference due to low power. Alternatively, *Grb10*$^{+/p}$ brains are no different in sectional area, but instead have larger volumes because they are longer. Regardless, our MRI results show there is a true difference in volume the population, and this appears to be proportional to the increase in brain weight. Therefore, we suggest *Grb10*$^{+/p}$ brains have more tissue of the same neuronal and total cell density as wildtypes. Further analysis is required to determine what dimensions gain this extra tissue.

In this longitudinal MRI study, we found cortical volume at 10 months of age (like total and subcortical volumes) was significantly greater in *Grb10*$^{+/p}$ mice. This contrasts with Garfield's original report that cortical area in Nissl-stained sections was comparable between *Grb10*$^{+/p}$ and wildtype brains. Interpretation of these results must first consider how each study has defined "cortical" and "subcortical" divisions. Specifically, Garfield 2007 included hippocampus in subcortical and not cortical area. We include hippocampus in cortical and not subcortical area for both Nissl areas and volume measurements. We do not expect the hippocampus to be a focal area for volumetric change in *Grb10*$^{+/p}$ mice, as paternal *Grb10* is not highly expressed there. In fact, *LacZ* staining in *Grb10*$^{+/p}$ mice indicated paternal *Grb10* is absent from the cortex and did not show notable staining in the hippocampus (Garfield, 2007). Regardless, further analysis should compare hippocampal volume between wildtype and *Grb10*$^{+/p}$ brains to account for the possibility that respective inclusion or exclusion of hippocampal volume explains the difference between our finding (significantly increased *Grb10*$^{+/p}$ cortical

volume) Garfield's finding (no significant difference in cortical area). A comparison of cortical thickness between genotype groups may also be a useful measure to assess whether cortical morphology has responded proportionally to the subcortical growth, or has been disproportionately distorted.

The absence of paternal *Grb10* expression in the cortex raises the question of how paternal knockout might effect a change in cortical growth. Paternal *Grb10* is normally highly expressed in subcortical regions and starts between E11.5 and E14.5, concurrent with the onset of neurogenesis (Garfield et al., 2011). We might therefore expect paternal knockout to remove a growth restrictor involved in subcortical brain development, in parallel with maternal knockout models which feature placental overgrowth (Charalambous et al., 2010). Indeed, we found subcortical volume was significantly larger in $Grb10^{+/p}$ brains at 10 months. However, we can expect no such direct consequence in the cortex, where the *LacZ* reporter of the $Grb10^{+/p}$ model is not detectable (Garfield et al., 2011). One potential explanation for increased cortical volume in $Grb10^{+/p}$ brains might be increased innervation of the cortex by midbrain structures with high paternal *Grb10* expression–for example, the mediodorsal thalamic input (thalamic paternal *Grb10* expression) to the dorsomedial prefrontal cortex or dopaminergic projections from the ventral tegmental area (dopaminergic paternal $Grb10^{+/p}$ expression) to the nucleus accumbens and medial prefrontal cortex (van der Kooij et al., 2018; Zhou et al., 2017). An investigation of this possibility would require a calculation of neuron density

in the cortex and an analysis of white matter volume from the acquired DTI scans, not presented in this thesis.

Finally, whole wet brain weight data but not whole brain volumetric data describe a significant interaction between GENOTYPE and AGE. Both Garfield's study and our own report *Grb10*$^{+/p}$ brains continue to increase in wet weight between 3 (Garfield) or 6 (Rienecker) and 10 months of age where wildtypes do not. In Chapter 3, we report a peak in wet brain weight for both wildtype and *Grb10*$^{+m}$ controls at ~6 months and a decrease at ~10 months. However, *Grb10*$^{+/p}$ MRI whole brain volumes were consistently larger than wildtypes, and in both genotypes, volume increased at each subsequent age measured. This suggests a difference in brain density with age, as wildtypes gain volume but not weight between 6 and 10 months and *Grb10*$^{+/p}$ continue to gain weight and volume. We also note we find *Grb10*$^{+/p}$ mice score consistently higher in both wet brain weight and volume than wildtype mice, even at our earliest time point of 10 weeks. Garfield 2007 reported no difference in wet brain weight between *Grb10*$^{+/p}$ and wildtypes at birth, P0. While we cannot extend a prediction to brain weight and volume and birth based on our own data, we do suggest further studies re-examine brain weight and volume at P0 to determine whether the differences we report here arise from prenatal development or are induced by postnatal mechanisms.

5 Social Dominance Behaviour

5.1 Introduction

Paternal *Grb10* is well known for its impact on social dominance as described in Nature in 2011 (Garfield et al., 2011). We were interested in how *Grb10*, as an adapter protein and potent growth suppressor, might be connected to this social dominance phenotype through its impact on the brain morphology described in Chapters 3 and 4 of this thesis. Therefore, our primary aim in this chapter was to investigate social dominance through a cross sectional study over 8 weeks, 6 months, and 10 months of age, and to compare our findings with our investigation of brain overgrowth in $Grb10^{+/p}$ mice. We hypothesized the social dominance phenotype described in Garfield 2011 would become more pronounced as the difference in subcortical growth between wildtypes and $Grb10^{+/p}$ mice became greater. As the surprising results of our cross-sectional study emerged, we acquired a second aim of replicating and dissecting Garfield's original social dominance findings for comparison to our own work. In these tests, we focused on social isolation as a factor potentially impacting a social dominance phenotype.

5.1.1 The midbrain and social dominance

The prefrontal cortex (PFC) is central to the processing of information related to hierarchies and to the top-down control of subcortical structures involved in dominance behaviours (J. Chen et al., 2011; F. Wang et al., 2014). The medial PFC (mPFC) is particularly well connected to social dominance, as several papers have demonstrated direct manipulations of neural activity here

can cause rank change (F. Wang et al., 2011; Zhou et al., 2017). While paternal *Grb10* expression is entirely absent from cortical structures, it is highly expressed in regions to which the mPFC projects, including the dorsal raphe nucleus, the ventral tegmental area, the amygdala, the thalamus, the hypothalamus, and the striatum (Garfield, 2007; Garfield et al., 2011). The regulation of serotonin and dopamine release in some of these regions mediates the expression of aggressive, impulsive, fearful, and stress responsive behaviours (F. Wang et al., 2011). For example, the suppression of serotonin neuron firing in the dorsal raphe nucleus is associated with increased impulsive and aggressive behaviour (Audero et al., 2013). Monoaminergic neurotransmission and the midbrain dopaminergic system are also particularly targeted by parentally biased and monoallelically imprinted genes, including *Dlk1, Cdkn1c,* and *Ube3a* in addition to *Grb10* (Jacobs et al., 2009; McNamara et al., 2017; Mulherkar & Jana, 2010; Perez et al., 2016). Dysmorphia in the subcortical regions of high paternal *Grb10* expression, particularly monoaminergic nuclei, could alter the response of these regions to mPFC control. This could be mediated through altered connectivity to the mPFC, which has already been shown to impact social dominance related behaviour. For example, the strength of the mediodorsal thalamus to dorsomedial PFC circuit (MDT-dmPFC) shows synaptic weakening during repeated defeat-induced social avoidance, and conversely, repeated winning strengthened MDT-dmPFC synapses (Zhou et al., 2017).

We pursued the social dominance phenotype observed in Garfield 2011 aiming to better characterize the impacted dominance-related

behaviours and to contextualize our observations in the subcortical overgrowth described in Chapters 3 and 4. The following experiments promised a better understanding of how imprinted gene expression in subcortical nuclei impact the neural circuits involved in social dominance. This will elucidate what systems and behaviours mediated selection the program of imprinting regulation in brain tissues.

5.1.2 Study Design– Investigating social dominance phenotypes

We designed our behavioural study to dissect different elements of social dominance phenotypes and to draw converging evidence from different testing methods. Testing for each cohort was restricted to a four-week window to avoid significant differences in brain growth morphology between the beginning and end of the behavioural testing period. The cross-sectional study primarily allowed us to obtain representative samples of brains from each age group, and secondarily avoided learning effects over time, which might confound comparisons of the behaviours at different ages.

We chose age groups 8 weeks (2 months), 6 months, and 10 months to space testing between the earliest time at which we could obtain meaningful behavioral data (8 weeks) and the age of testing in the Garfield paper (Garfield et al., 2011). This spacing also aided our coverage of brain growth measurements in Chapters 3 and 4.

The *stranger* encounter Lindzey tube test, the *social* encounter Lindzey tube test, the urine marking test, and observations of whisker barbering were

employed to generate converging evidence about social dominance in our mice. Here, we will discuss the reliability of these tests and the social dominance strategies they assess.

The Lindzey tube test is an accepted measure of social dominance in mice (Lindzey et al., 1961). Wang et al. 2011 assessed the reliability of this method for describing within-cage hierarchies using three criteria since employed in other social dominance studies: transitivity, stability over time, and consistency with other dominance measures (van den Berg et al., 2015; F. Wang et al., 2011). The tube test was used to describe the general assessment criteria for social dominance tests and as a reference against which to compare other dominance tests.

Dominance tests with high transitivity (criterion 1) generate a high incidence hierarchies in which, if mouse A is dominant over mouse B and mouse B is dominant over mouse C, then mouse A will also be dominant over mouse C. In the Wang 2011 paper, the tube test generated transitive ranks in 95% of cases, and linear hierarchies in 89% of four mouse cages. This paper also deemed the tube test ranking stable over time (criterion 2), with mice adopting the same rank as the previous day in 59% of comparisons generated over 7 days of daily assessments (F. Wang et al., 2011).

Consistency with other dominance tests (criterion 3) is particularly important in demonstrating the test measures social dominance as an underlying dependent variable, rather than measuring differences in the sensorimotor skills required to undertake the test. Convergent and correlating evidence from tests requiring different performances strengthens the

description of a robust dominance hierarchy and the characterization of a social dominance phenotype. In Wang et al 2011, the tube test was compared to five additional dominance measures, including the visible burrow system, the antagonistic behaviour test, ultrasonic vocalization toward females, the barbering assay, and the urine marking assay. Dominance ranking in each of the five tests was consistent with the tube test ranking and significantly correlated among themselves (F. Wang et al., 2011). Our behavioural study assesses our *Grb10*$^{+/p}$ mice on the criterion of consistency by employing two versions of the tube test, the urine marking test, and the barbering assay.

The urine marking test quantifies the area covered by territorial scent marks during a social encounter between two mice in a novel territory (Desjardins, Maruniak, & Bronson, 1973; McNamara, John, & Isles, 2018). These scent marks/urine drops delineate territorial boundaries and contain chemical cues of social status (Ralls, 1971). Compared to subordinates, dominant mice deposit a greater number of marks and cover areas closer to the wire partition separating opponents. While the dominant-subordinate distinction is more apparent in single-housed mice than in group-housed mice, there is still a trend for mice ranked highly in the tube test to also mark more territory in the urine test (F. Wang et al., 2014, 2011). This difference is presumably due to social behavioural plasticity, which adjusts social strategies in single housing or low density populations compared to group housing or high density populations. Wild mice in less dense populations adopt territorial defensiveness, while mice in more dense populations must be more socially

tolerant and adapt to a hierarchical system which reduces costly conflicts (Singleton & Krebs, 2007; F. Wang et al., 2014).

The Dhalia Effect, or the whisker barbering effect, describes the tendency for the dominant mouse in the cage to trim the whiskers from subordinates, resulting in cages with just one unbarbered mouse (Strozik & Festing, 1981). In Wang 2011, whisker barbering strongly correlated with tube test rank, satisfying consistency between dominance tests (criterion 3) (F. Wang et al., 2011). However, this consistency seems to be dependent on the tube testing protocol. Studies in which mice are trained to pass through the tube prior to encountering conflict situations and are tested for stable rank on consecutive days show strong correlation between barbering (the Dahlia effect) and tube test rank (F. Wang et al., 2014, 2011). Conversely, studies that have not included training and in which testing is limited to a single one-day session (opposed to showing rank stability over time) lack this correlation between barbering rank and tube test rank (Garner, Dufour, Gregg, Weisker, & Mench, 2004).

5.1.3 Important caveats to the Garfield 2011 study

In Garfield et al. 2011, the enhanced social dominance phenotype was originally identified using the Lindzey tube test without training, and the finding was supported by an elevated incidence of barbering in cages containing *Grb10*$^{+/p}$ mice (Garfield et al., 2011). The testing cohort consisted

of isolated male mice aged 10-11 months, who had previously been housed in unbalanced litter groups.

Training prior to the tube test

In our study, we wished to remain consistent with the original observation conditions of *Grb10*$^{+/p}$ social dominance in Garfield 2011, which used a tube testing paradigm without training. This decision requires consideration as the use or absence of tube test training impacts correlation with the whisker barbering effect, as described in Section 1.1.2. Contrary to this division in the literature between tests including training which correlate strongly with whisker barbering and tests without training which do not, the Garfield 2011 paper reported a whisker barbering effect consistent with the tube test results, despite an absence of training (Garfield et al., 2011).

One potential issue with using training is the possible interference of a learning effect. If WT and *Grb10*$^{+/p}$ mice acquire this training differently, or are differentially persistent in this training, a learning effect may obscure the underlying dominance measure. This concern may be ameliorated using multiple types of dominance measures employing different sensorimotor and cognitive mechanisms.

The impact of prior social experience on dominance testing

Wang 2011, the order in which the tube test and other social dominance assessments were performed did not impact the correlations between them (F. Wang et al., 2011). The authors suggested the performance

of the tube test did not induce an artificial hierarchy (F. Wang et al., 2014). However, there is a concern that male mice employ prior social experience in the establishment of stable social hierarchies (van den Berg et al., 2015). An *a priori* random assignment of linear hierarchy on Day 1 during tube test matches of unfamiliar mice remained stable on Day 2 under natural match conditions. While these assigned hierarchies remained stable within consecutive days of testing of the tube test, the van den Berg (2015) paper did not test whether this hierarchy carried over to other measures of social dominance.

Social isolation

Tube testing in the Garfield 2011 paper took place after mice were isolated to determine whether the barbering was self-inflicted. Social isolation impacts midbrain function, aggression, and dominance-related behaviours, often through alterations in monoaminergic signaling (Valzelli & Bernasconi, 1979). Tyrosine Hydroxylase (TH) mRNA transiently increases in the midbrain during social isolation, peaking at 34% elevation in the VTA and 48% elevation in the substantia nigra (SN) after 14 days of isolation before returning to control levels by 28 days. Simultaneously, proenkephalin (PE) mRNA levels transiently decrease in the striatum, where they are known to be tonically inhibited by dopaminergic activity from midbrain projections (Angulo, Printz, Ledoux, & McEwen, 1991).

Adult social isolation over 3 months induces changes in epigenetic marks and epigenetic writer/eraser activity in the midbrain. This includes

increased global DNA methylation and enhanced DNA methyltransferase (DMT) activity, increased H3K4me/me2 and enhanced H3K4 histone methyltransferase (HMT) activity, and increased H3K9ac and activation of histone acetyltransferase (HAT) and histone deacetylase (HDAC). Additionally, mRNA levels of serotonin transporter Slc6a4 are reduced and *Slc6a4* promoter methylation is increased (Siuda et al., 2014). This disruption of an essential component of serotonin homeostasis reflects other research in which reduction in the turnover rate of brain serotonin is implicated in behavioural changes induced by isolation (Valzelli & Bernasconi, 1979).

Short periods of isolation can also impact synaptic function in the midbrain. Acute social isolation over 24 hours potentiates synapses onto dopamine neurons in the dorsal raphe nucleus (DRN), which represents the aversive state of social isolation. These dopamine neurons project to the mPFC, the lateral hypothalamus, and the central amygdala, among other regions. Not only does the AMPA receptor/ NMDA receptor ratio in DRN neurons change after acute isolation, the subunit composition at these synapses changes, with implications for neuron excitability and synaptic efficacy (Matthews et al., 2016). The subjective experience of isolation also differs based on social rank. Dominant mice were more sensitive to the behavioural effects of manipulating DRN dopaminergic activity through optogenetic activation and inhibition (Matthews et al., 2016).

Given the extensive changes to midbrain synaptic function, monoaminergic signaling, and epigenetic regulation induced by social isolation, we saw a need to determine whether the isolation period in the

Garfield et al experiment impacted the dominance phenotype observed in *Grb10*$^{+/p}$ mice. We assessed the potential impact of social isolation by replicating the Garfield study and comparing it to results from our socially housed cohort.

Matches against strangers vs cage mates

Additionally, isolated *Grb10*$^{+/p}$ mice in the original study faced individually housed wildtype strangers (Garfield, 2007; Garfield et al., 2011). Dominance hierarchies are a means of social organization impacting access to essential resources with consequences for health, survival, and reproductive success. Stable hierarchies can minimize conflict between group members and lower associated risks. Behaviours which contribute to establishing, maintaining, and moving within dominance hierarchies directly relate to the relationship of the individual to the group or to a stranger/intruder (Singleton & Krebs, 2007; F. Wang et al., 2014). Therefore, our study design sought to differentiate between social dominance within-cage and in encounters with an unfamiliar mouse. Our cross-sectional cohorts were socially housed in genotype balanced cages (to avoid biased weighting of within-cage hierarchies by any potential dominance phenotype). The stranger encounter tube test preceded the round robin social encounter tube test to avoid any impact of learning effects over repeated testing on the stranger encounter test.

Sex

The Garfield et al. 2011 study used only male mice. Female mice are commonly excluded from social dominance assessments as they do not share some of the behaviours used to assess male social hierarchies, such as territorial marking and vocalizations to a potential mate. However, female mice can establish stable linear hierarchies in the Lindzey tube test. While test outcomes for male mice are strongly influenced by prior social experience, female mice primarily rely on intrinsic attributes to establish a hierarchy. Manipulation of testosterone levels in both sexes can induce a reversal of social strategy (van den Berg et al., 2015).

We included female mice in all possible behavioural tests. They were excluded from the urine marking test as we did not expect to obtain useful territorial marking. We recorded oestrus status and considered it in our statistical analyses. We initially considered social dominance data separately for each sex but subsequently pooled data for certain analyses.

5.1.4 Chapter Aims

Aim (1) Investigate social dominance in *Grb10*$^{+/p}$ mice through a cross sectional study over 8 weeks, 6 months, and 10 months of age.

Our primary aim was to draw converging evidence from the stranger-encounter and social-encounter Lindzey tube test, the urine marking test, and whisker barbering observations to assess social dominance in *Grb10*$^{+/p}$ adult mice over time. We wished to correlate this data with observations of brain

weight, morphology, and histology at the same age bins in Chapters 3 and 4. The experimental set up considered sex, unfamiliar vs familiar encounters, group hierarchies, within-cage genotype balance, and learning effects from repeated testing.

Aim (2) Assess the impact of social isolation on social dominance in *Grb10*$^{+/p}$ mice compared to group housing.

The impact of social isolation on the midbrain and monoaminergic signaling warranted specific consideration of whether the isolation period contributed to the original observation of enhanced social dominance in *Grb10*$^{+/p}$ mice in Garfield et al. 2011. For instance, *Grb10*$^{+/p}$ and wildtype mice could potentially react differentially in social dominance tests after exposure to the stress of extended social isolation, but not in the absence of this stress.

5.2 Methods

5.2.1 Subjects

Animals were housed in genotype-balanced social cages of 4 mice: 2 wildtypes, 2 *Grb10*$^{+/p}$. The 8-10 week, 6 month, and 10 month cohorts (but not the isolation cohorts) underwent testing, in order, for: stranger tube test, social tube test, and urine marking (except females). Females 8-10 weeks of age did not undergo testing for marble burying or elevated plus mage. Unfiltered match and cage numbers for each behavioural test are reported in the tables below. A "match" constitutes a *Grb10*$^{+/p}$ vs wildtype encounter.

These represent overall cases considered in the analyses, and further filtering is detailed in the respective results sections.

Socially housed mice 9 months of age were placed in fresh individual housing for 30 days. Immediately following this isolation period, these mice, now 10 months of age, underwent five days of handling, in concordance with typical behavioural testing procedures, and then dominance testing in the stranger encounter tube test. Cage bedding was not changed during the testing period.

Table 5.1 Unfiltered Match and Cage Numbers–Males

Age	Stranger Tube Matches	Social Tube Cages	Urine Marking Cages	Social Isolation Matches
8 weeks	28	15	11	—
6 months	23	13	13	—
10 months	23	12	12	10

Table 5.2 Unfiltered Match and Cage Numbers–Females

Age	Stranger Tube Matches	Social Tube Cages	Social Isolation Matches
8 weeks	20	10	—
6 months	21	12	—
10 months	13	8	15

5.2.2 Handling

Mice were handled as little as possible up until one week prior to the start of behavioural testing; then they were handled daily for 5 days before beginning testing. See General Methods for pre-testing handling procedures. For cohorts 6 months of age and 10 months of age, Kira Rienecker conducted

behavioural testing for male mice while Alexander Chavasse conducted behavioural testing for female mice under the supervision of Kira Rienecker.

5.2.3 Tube Test

The stranger encounter and social encounter tube tests were conducted under identical conditions. Unfamiliar opponents were chosen from different home cages and different litters. Any socially housed wildtype opponents were housed in genotype-balanced (2 WT, 2 *Grb10*$^{+/p}$) cages. Opponent mice were simultaneously presented to either end of a Perspex tube (30.5 cm x 3.5 cm or 30 cm x 2.5 cm depending on weight class) in a quiet behavioural testing room in dim light (an indirect lamp bulb between 25 to 60 W). Opponents met in the middle of the tube and outcome was scored when one animal was forced to back out of the tube. Losers were counted as the first animal with all four feet out of the tube. No time limit was imposed. Trials in which either opponent turned around in the tube, both mice backed out without confrontation, or both mice squeezed past each other were not counted (all instances of trial "failure"). In the stranger encounter tube test, animals were completely naïve to the test and mistrials were not re-run. These instances are detailed in Table 5.3. In the social encounter tube test, mistrials were re-run on a separate day to complete the within-cage hierarchy, but each opponent pair only underwent one successful trial. These paradigms were adopted to avoid any learning effects. Each animal completed only one tube test per day. Testing was arranged to ensure genotype groups and individual mice underwent trials balanced by side of entry.

In the stranger encounter tube test (for socially housed and isolated male and female cohorts), opponents were weight matched to minimize differences across the whole cohort. To maximize trial numbers, no trials were eliminated based on weight. In approximately 77% of encounters, the heavier mouse was less than 15% heavier than the lighter mouse. In approximately 86% of encounters, the heavier mouse was less than 20% heavier than the lighter mouse. In Chapter 3, we demonstrated there were no significant genotype differences in body weight between *Grb10*$^{+/p}$ and wildtype controls in our colony.

Table 5.3 Stranger Encounter Tube Test–Trials Not Counted Due to Failure

Totals	F Failed	F Attempted	M Failed	M attempted
Cohort D	0	24	0	28
Cohort C	3	24	3	26
Cohort A	3	16	0	26
Isolation Day 1	4	15	2	10
Isolation Day 2	2	15	1	10
Isolation Day 3	0	15	0	10

5.2.4 Urine Marking

Urine marking tests were conducted in a quiet behavioural testing room in dim light (one indirect lamp bulb between 25 to 60 W). Mice were simultaneously placed in one compartment of a 30 x 30 x 30 cm box divided by a metal grid through which they could see, hear, and smell the opponent mouse but not physically interact. A clear, smooth barrier was placed on top of the grid to prevent climbing out of the box or into the other compartment. Each compartment contained a 14cm by 29.5 cm sheet of Whatman chromatography paper (3 mm, GE Healthcare UK Limited CAT No 3030-2221).

Each trial lasted 1 hour, at the end of which both mice were removed and the cages cleaned with 70% alcohol wipes.

Following the trials, chromatography paper was left to dry before staining with Ninhydrin spray reagent (Sigma-Aldrich N1286). Stained papers were scanned to pdfs and were scored in Image J. To score, each paper was overlaid with a grid of 1cm^2 squares. All squares containing a sent mark were counted and used in a ratio against usable grid (total grid squares minus shredded sections and urine marks covering more than 4 consecutive squares). The winner of each encounter possessed the higher ratio of squares containing sent marks to usable grid.

5.2.5 Statistics

Likelihood of winning a social dominance match– Binomial Test

The binomial test was conducted to determine if the proportion of *Grb10*$^{+/p}$ wins in '*Grb10*$^{+/p}$' versus 'familiar wildtype' matches in the social tube and urine tests differed significantly from chance (0.5). Each match included in the analysis was unique, but most individual mice were involved in two matches against cage mates of the opposite genotype. For example, "*Grb10*$^{+/p}$ A vs WT B" and "*Grb10*$^{+/p}$ A vs WT C" would be included in the analysis as independent matches.

Within-cage rank–Related Samples Sign Test and Wilcoxon Signed Rank Test

The related samples sign test and the Wilcoxon signed-rank test were used to compare the difference in cage rank between the genotype groups for

hierarchies generated during the social tube and urine tests. Rank hierarchies were also established in each cage, with rank scored between 0 (least dominant) to 1 (most dominant), based on the number of wins divided by possible matches against cage mates. Data were ordered as matched pairs, with the average of the two *Grb10*$^{+/p}$ mice paired with the average of the two wildtypes in the cage. Differences were calculated by subtracting the average wildtype rank within the cage from average *Grb10*$^{+/p}$ rank within the cage. If the distribution of differences was found to be asymmetric, the related samples sign test was employed; if symmetric, the Wilcoxon signed-rank test was used. Data about differences and average genotype rank were presented as medians.

False Discovery Rate Corrections

Statistical significance underwent False Discovery Rate (FDR) corrections using the Benjamini-Liu (BL) method (Y Benjamini & Liu, 1999; Yoav Benjamini et al., 2001). FDR corrections were performed on all reported analyses belonging to one task (ie, “marble burying task” or “EPM”), and FDR corrections were separate between different tasks. Abridged tables extend to the critical significance value. Full tables of the BL FDR corrections are available in the appendix. FDR corrections were not carried out for groups of less than 5 statistical tests.

5.3 Results

5.3.1 Oestrus in the Tube Test

Socially housed wildtype mice aged 8 weeks, 6 months, and 10 months faced familiar wildtype cage mates during the social tube test. In 16 of the matches pooled across these cohorts, a wildtype mouse judged to be in oestrus faced a wildtype mouse not in oestrus. A binomial test indicated the proportion of wins for wildtype females in oestrus (0.44) was not significantly different from chance (0.5), p = 0.804 (2-tailed).

Socially housed mice aged 8 weeks, 6 months, and 10 months faced unfamiliar mice of the opposing genotype in the stranger encounter tube test. In 18 matches pooled across these cohorts, a mouse judged to be in oestrus by swab or by visual assessment faced a mouse judged not to be in oestrus. In 9 matches, the mouse in oestrus was *Grb10*$^{+/p}$, and in the remaining 9 the mouse in oestrus was wildtype. A binomial test indicated the proportion of wins for mice in oestrus (0.33), regardless of genotype, was not significantly different from chance (0.5), p = 0.238 (2-tailed). In combination with the analysis of familiar wildtype vs wildtype encounters above, we justify ignoring oestrus stage in the statistical analysis of both stranger encounter and social encounter tube tests in the following sections.

5.3.2 Barbering

The barbering proportions for each genotype within the three cohorts are depicted qualitatively below. As mice were housed in balanced genotype

cages (2 *Grb10*$^{+/p}$ and 2 WT), barbering status is not independent between genotype groups, precluding a chi-square test for homogeneity.

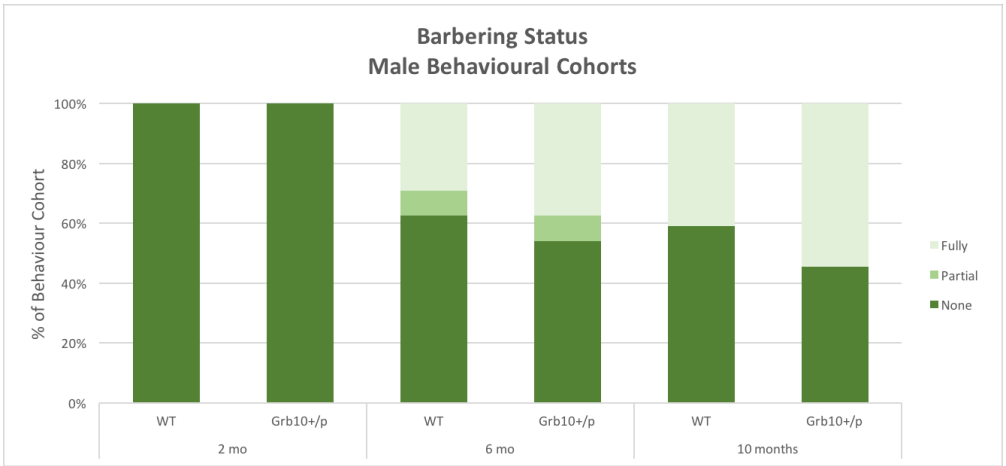

Figure 5.1 Male Behavioural Cohorts–Barbering Status

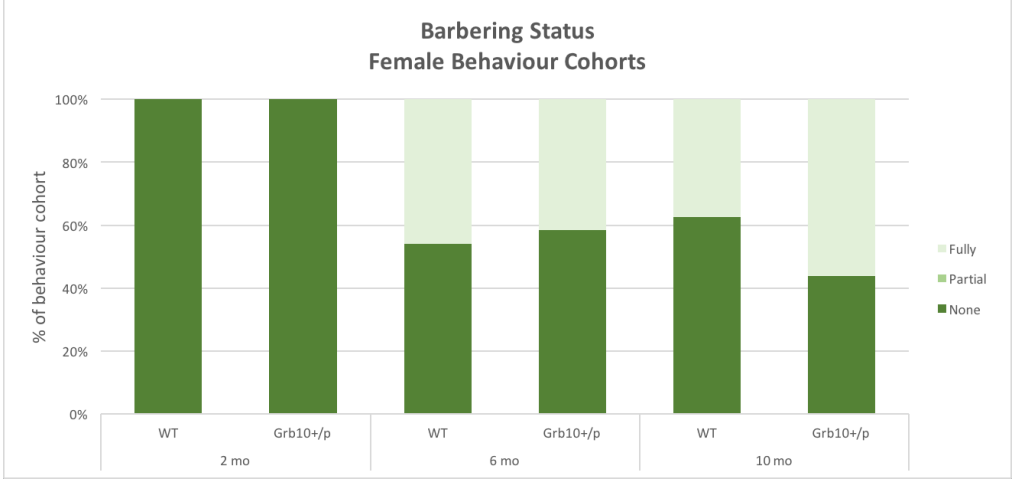

Figure 5.2 Female Behavioural Cohorts–Barbering Status

Table 5.4 Male Cage Barbering Counts

Cohort Age	Identifiable Barber	Total Observed Mice
8 weeks	0 cages of 12 cages	48
6 months	6 of 12 cages	48
10 months	3 of 11 cages	44

In three cages of the 10 month male behavioural cohort, all four mice were fully barbered.

Table 5.5 Female Cage Barbering Counts

Cohort Age	Identifiable Barber	Total Observed Mice
8 weeks	0 of 10 cages	40
6 months	7 of 12 cages	48
10 months	5 of 8 cages	32

Behavioural cages at 6 months and 10 months with identifiable barbers were pooled to analyze the proportion of *Grb10*$^{+/p}$ vs WT barbers. Binomial tests indicated the proportion of barbers who were *Grb10*$^{+/p}$ was not statistically different from chance (0.5) in cages of either sex.

Table 5.6 Barber Genotype in Behavioural Cohorts

Sex	Barbered Cages (pooled)	WT Barbers	*Grb10*$^{+/p}$ Barbers	Sig.
Male	9 cages	0.78	0.22	0.180
Female	12 cages	0.58	0.42	0.774

5.3.3 Stranger Tube Test

Summary

Socially housed Grb10$^{+/p}$ mice aged 8 weeks, 6 months, and 10 months faced unfamiliar socially housed wildtype mice in the tube test (N for each group indicated in the table). Mice were naïve to the test to avoid learning effects. Binomial tests indicated the proportion of wins for Grb10$^{+/p}$ in all three age groups for both sexes were not significantly different to chance (0.5). P

values in the table are 2-tailed. Analysis did not include barbering or oestrus status.

Table 5.7 Stranger Tube Test Grb10$^{+/p}$ Proportion wins and P-values

Age	Male matches (N)	Males proportion wins	Males p value	Female matches (N)	Females proportion wins	Females p value
8 weeks	28	0.320	0.087	20	0.350	0.263
6 months	23	0.522	1.000	21	0.619	0.383
10 months	23	0.430	0.678	13	0.462	1.000

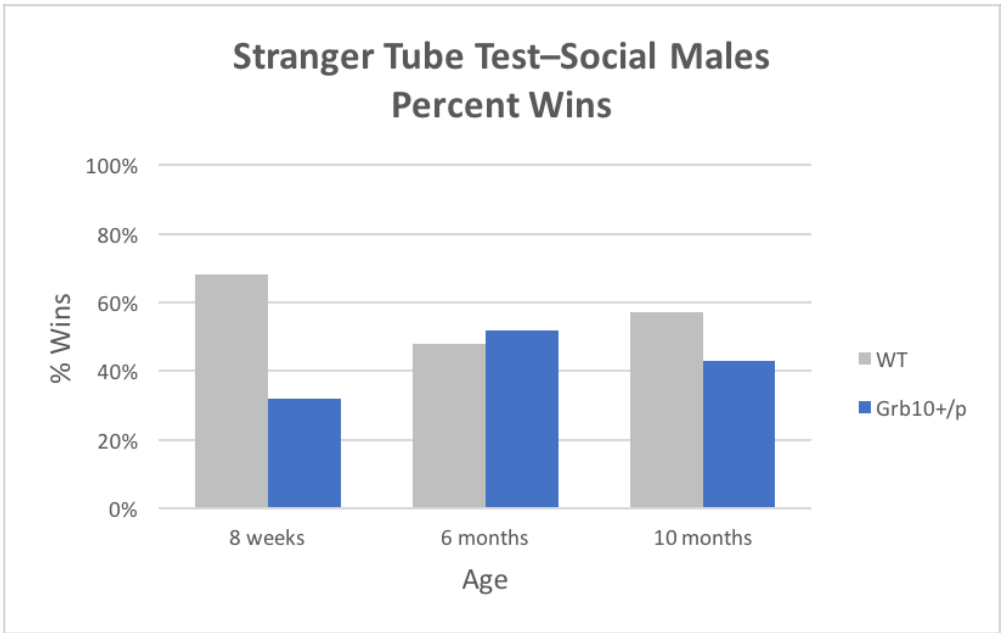

Figure 5.3 Males Stranger Tube Test Percent Wins

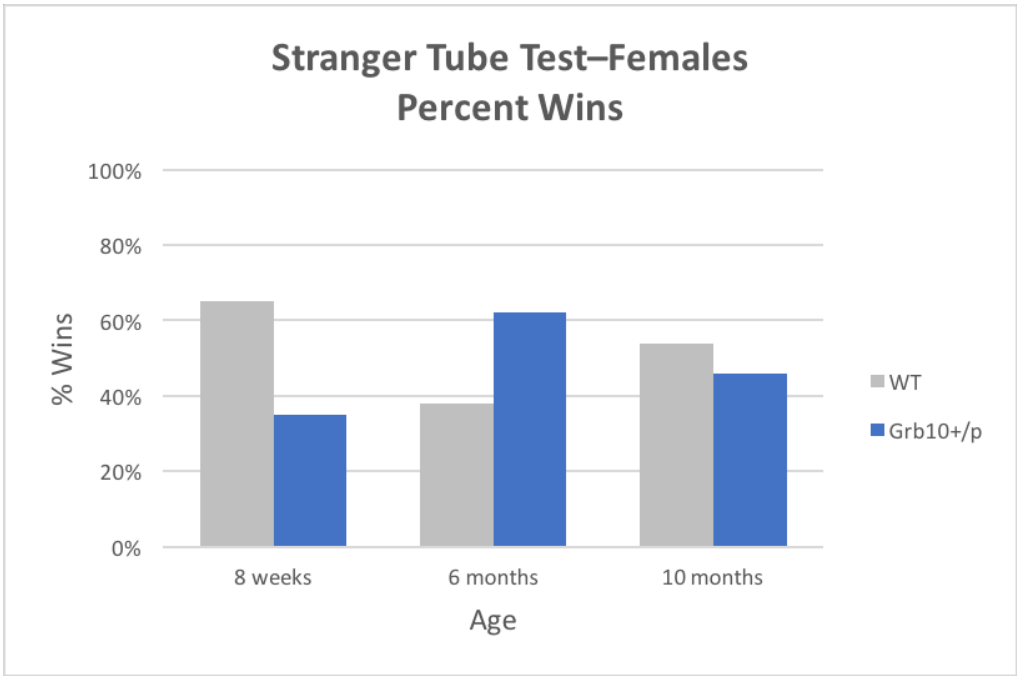

Figure 5.4 Females Stranger Tube Test Percent Wins

8-10 week cohort

Socially housed Grb10$^{+/p}$ males aged 8 weeks faced unfamiliar socially housed wildtype males in the tube test (N = 28 matches). A binomial test indicated the proportion of wins for Grb10$^{+/p}$ males (0.32) was not significantly different from chance (0.5), p = 0.087 (2-tailed).

Socially housed Grb10$^{+/p}$ females aged 8 weeks faced unfamiliar socially housed wildtype females in the tube test (N = 20 matches). A binomial test indicated the proportion of wins for Grb10$^{+/p}$ females (0.35) was not significantly different from chance (0.5), p = 0.263 (2-tailed).

6 mo cohort

Socially housed Grb10$^{+/p}$ males aged 6 months faced unfamiliar socially housed wildtype males in the tube test (N = 23 matches). A binomial test

indicated the proportion of wins for Grb10$^{+/p}$ males (0.522) was not significantly different from chance (0.5), p = 1.000 (2-tailed).

In 9 of these matches, a barbered mouse faced an unfamiliar, un-barbered mouse (of a different genotype, as per the set up). In 5 matches, the barbered mouse was *Grb10*$^{+/p}$, and in 4 matches, the barbered mouse was wildtype. A binomial test indicated the proportion of wins for barbered mice (0.78), regardless of genotype, was not statistically different from chance (0.50), p = 0.180 (2-tailed).

Socially housed Grb10$^{+/p}$ females aged 6 months faced unfamiliar socially housed wildtype females in the tube test (N = 21). A binomial test indicated the proportion of wins for Grb10$^{+/p}$ females (0.619) was not significantly different from chance (0.5), p = 0.383 (2-tailed).

In 16 of these matches, a barbered female mouse faced an unfamiliar, un-barbered female mouse (of a different genotype, as per the set up). In 8 of these matches, the barbered mouse was *Grb10*$^{+/p}$, and in the other 8 matches, the barbered mouse was wildtype. A binomial test indicated the proportion of wins for barbered female mice (0.88), regardless of genotype, was statistically different from chance (0.5), p = 0.004 (2-tailed).

10 mo cohort

Socially housed Grb10$^{+/p}$ males aged 10 months faced unfamiliar socially housed wildtype males in the tube test (N = 23 matches). A binomial test indicated the proportion of wins for Grb10$^{+/p}$ males (0.43) was not

significantly different from chance (0.5), p = 0.678 (2 tailed). Barbering status of the opponents was excluded from this analysis.

In 19 of these matches, a barbered male mouse faced an unfamiliar, un-barbered male mouse (of a different genotype, as per the set up). In 11 of these 19 matches, the barbered mouse was *Grb10*$^{+/p}$, and in the remaining 8 matches, the barbered mouse was wildtype. A binomial test indicated the proportion of wins for barbered male mice (0.37), regardless of genotype, was not statistically different from chance (0.5), p = 0.359 (2-tailed).

Socially housed Grb10$^{+/p}$ females aged 10 months faced unfamiliar socially housed wildtype females in the tube test (N = 13 matches). A binomial test indicated the proportion of wins for Grb10$^{+/p}$ females (0.46) was not significantly different from chance (0.5), p = 1.000 (2 tailed). Barbering and oestrus status have been excluded from this analysis.

In 8 of these matches, a barbered female mouse faced an unfamiliar, un-barbered female mouse (of a different genotype, as per the set up). In 5 of these matches, the barbered mouse was *Grb10*$^{+/p}$, and in the remaining 3 matches, the barbered mouse was wildtype. A binomial test indicated the proportion of wins for barbered female mice (0.63), regardless of genotype, was not statistically different from chance (0.5), p = 0.727 (2-tailed).

5.3.4 False Discovery Rate Corrections– Stranger Encounter Tube Test

The Benjamini-Liu (BL) procedure was used to correct for false discovery rate (FDR) of 5% over the entirety of statistical tests for the stranger

encounter tube test. Of the 10 tests, only "Stranger tube test 6 months–Barbered Female mice" (wins in the stranger tube test by barbered female mice 6 months of age) was originally found to be significant. This result survived FDR correction.

Table 5.8 Abridged FDR Corrections–Stranger Encounter Tube Test

Finding	P value	Rank (m=10)	BL = (min 0.05, 0.05*m/(m+1-i)^2	(BL) – P value
Stranger Tube Test 6 months–Barbered Female Mice	4.181E-03	1	5.000E-03	0.001
Stranger Tube Test 8-10 weeks–Males	0.087	2	6.173E-03	-0.081

5.3.5 Social Tube Test

Summary

The social tube test followed the stranger tube test. Genotype-balanced cages containing 4 mice (2 WT, 2 PAT KO) 8 weeks, 6 months, and 10 months of age each completed the social tube test to determine cage hierarchy. The binomial test was conducted to determine if the proportion of *Grb10*$^{+/p}$ wins in '*Grb10*$^{+/p}$' versus 'familiar wildtype' matches differed significantly from chance (0.5). Each match included in the analysis was unique, but most individual mice were involved in two matches against cage mates of the opposite genotype (See Section 1.2.6 on Statistical Methods).

Binomial tests indicated the proportion of wins for Grb10$^{+/p}$ in all three age groups and for both sexes were not significantly different to chance (0.5) in the social tube test. P values in the table are 2-tailed. Analysis did not include

barbering or oestrus status. Oestrus was excluded after analysis of social tube tests between wildtype females in oestrus vs familiar wildtype not in oestrus (see Section 5.3.1). Barbering was ignored because it is not independent of the social hierarchy measurement made using the social tube test.

Rank hierarchies were also established in each cage, with rank scored between 0 (least dominant) to 1 (most dominant), based on the number of wins divided by possible matches against cage mates. The related samples sign test was used to compare differences in average cage rank between genotype groups. For each cage, the averaged wildtype ranks within cage (n=2 per cage) were compared as paired samples to the averaged *Grb10*$^{+/p}$ ranks within cage (n=2 per cage).

The difference between average within-cage rank for *Grb10*$^{+/p}$ and wildtypes at 8-10 weeks, 6 months, or 10 months of age for males and females was not statistically significant.

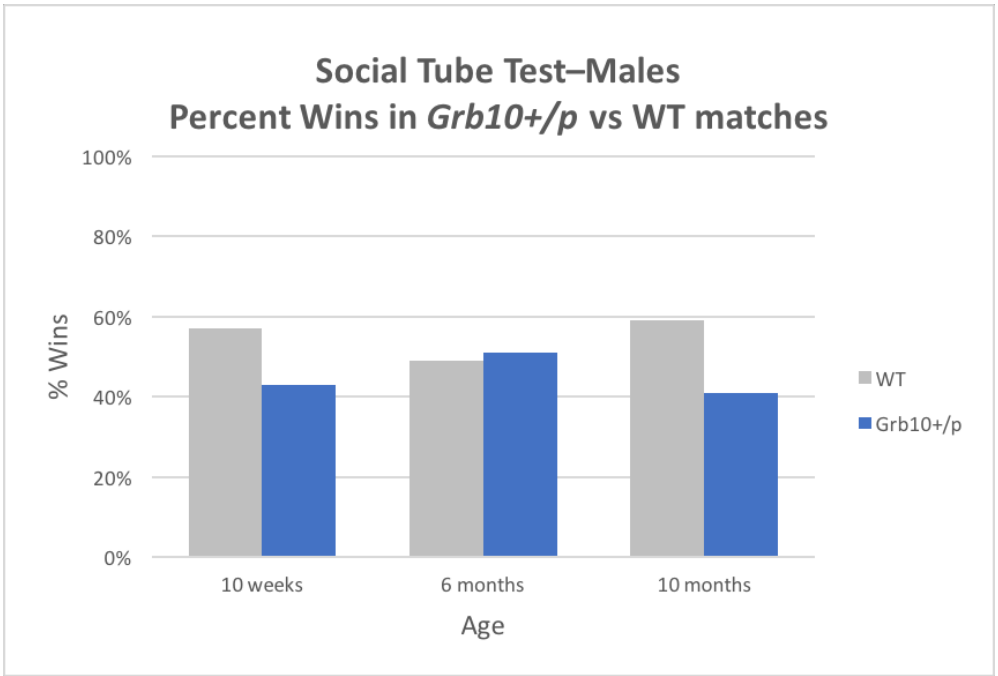

Figure 5.5 Males Social Tube Test Percent Wins in Grb10+/p vs WT matches

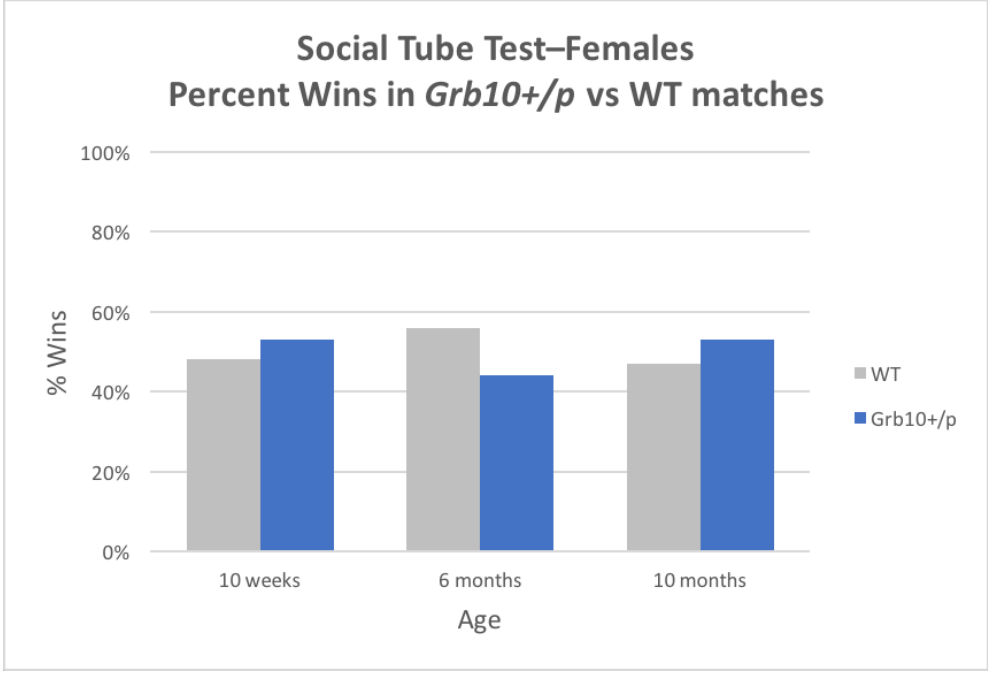

Figure 5.6 Females Social Tube Test Percent Wins in Grb10+/p vs WT matches

Table 5.9 Males Social Tube Test Grb10+/p vs WT Binomial Analysis

Age	Male matches (N)	Males proportion wins Grb10 +/p	Males p value	Linear Hierarchy
8 weeks	56	0.43	0.350	11/12
6 months	51	0.51	1.000	8/12
10 months	46	0.41	0.302	9/11

Table 5.10 Females Social Tube Test Grb10+/p vs WT Binomial Analysis

Age	Female matches (N)	Females proportion wins Grb10 +/p	Females p value	Linear Hierarchy
8 weeks	40	0.53	0.875	5/10
6 months	48	0.44	0.471	10/12
10 months	32	0.53	0.860	4/8

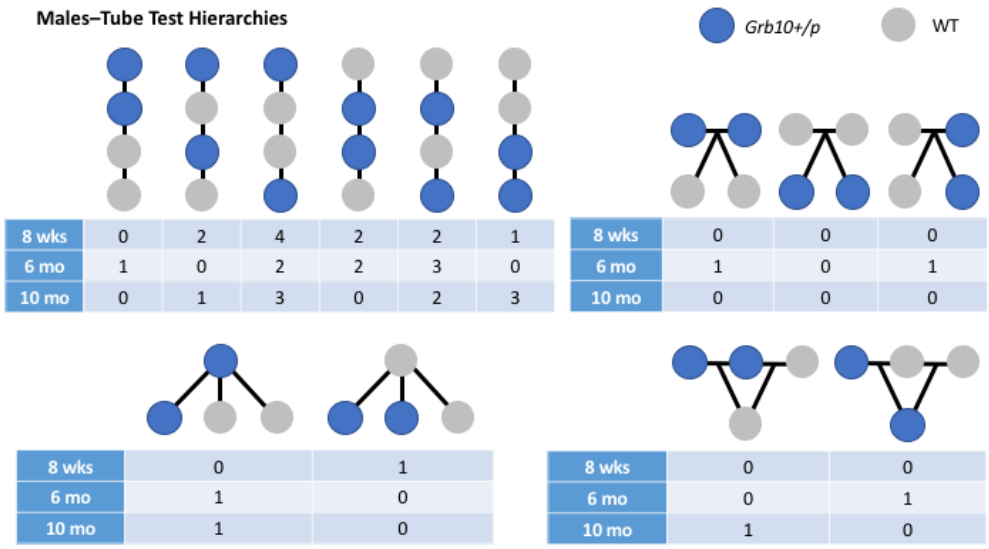

Figure 5.7 Male Tube Test Hierarchies

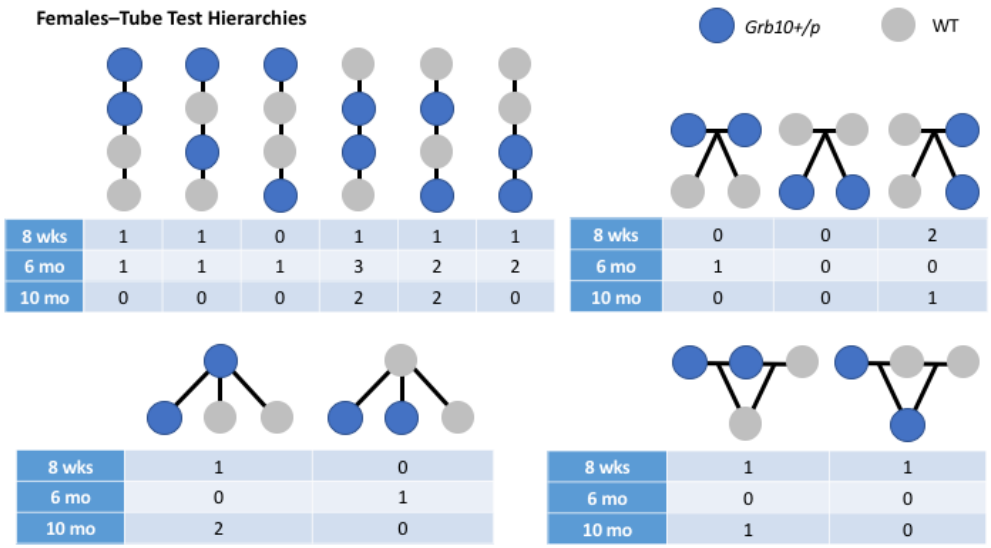

Figure 5.8 Female Tube Test Hierarchies

8-10 week cohort

Males

Twelve genotype-balanced cages containing 4 male mice 2 months of age each completed the within-cage social tube test (WT n=24, *Grb10*$^{+/p}$ n=24). Eleven of twelve male cages demonstrated a linear hierarchy. Three additional cages completed some, but not all matches in the round-robin. Fifty-six *Grb10*$^{+/p}$ vs familiar wildtype matches were used to examine the frequency of *Grb10*$^{+/p}$ wins. The proportion of *Grb10*$^{+/p}$ wins (0.43) at 8-10 weeks of age was not statistically significantly different from chance (0.5), p = 0.350 (2-tailed).

The related samples sign test was used to compare the difference in average cage rank between genotype groups. The distribution of differences was not symmetrical. Of the twelve cages, two had higher average rank for

Grb10$^{+/p}$ mice, four had lower average rank for *Grb10*$^{+/p}$ mice, and in 6, *Grb10*$^{+/p}$ tied with wildtype average rank. Median average cage rank in the social tube test was equivalent for WT (0.500) and *Grb10*$^{+/p}$ (0.500) mice; median difference (0.000). There was no statistically significant difference between genotypes in average within-cage rank, z = -0.408, p = 0.688.

Females

Ten genotype-balanced cages containing 4 female mice each completed the within-cage tube test (WT n=20, KO n= 20). Female cage hierarchies were less consistent than males, with 5 cages demonstrating a linear hierarchy, and 5 demonstrating non-linear hierarchy. Forty *Grb10*$^{+/p}$ vs familiar wildtype matches were used to examine the frequency of *Grb10*$^{+/p}$ wins. The proportion of *Grb10*$^{+/p}$ wins (0.53) at 8-10 weeks of age was not significantly different from chance (0.5), p = 0.875 (2-tailed).

The related samples sign test was used to compare the difference in cage rank between genotype groups. The distribution of differences was bimodal. Of the ten cages, four had higher average rank for *Grb10*$^{+/p}$ mice, three had lower average rank for *Grb10*$^{+/p}$ mice, and in three, *Grb10*$^{+/p}$ and wildtype average rank were tied. Median average cage rank in the social tube test was equivalent for WT (0.500) and *Grb10*$^{+/p}$ mice (0.500); median difference (0.000). There was no statistically significant difference between genotypes in average within-cage rank, z = 0.000, p = 1.000.

6 mo cohort

Males

Twelve genotype-balanced cages containing 4 male mice 6 months of age each completed the within-cage tube test (WT = 24, PAT KO =24). Eight of twelve cages demonstrated a linear hierarchy. One additional cage completed some but not all matches. In total, fifty-one *Grb10*$^{+/p}$ vs WT matches were used to examine the frequency of *Grb10*$^{+/p}$ wins. The proportion of *Grb10*$^{+/p}$ wins (0.51) was not statistically different from chance (0.50), p = 1.000 (2-tailed).

The related samples sign test was used to compare differences in cage rank between genotype groups. The distribution of differences was not symmetrical. Of the twelve cages, three had higher average rank for *Grb10*$^{+/p}$ mice, four had lower average rank for *Grb10*$^{+/p}$ mice, and in 5, *Grb10*$^{+/p}$ and wildtype average rank was tied. Median average cage rank in the social tube test was equivalent for WT (0.500) and *Grb10*$^{+/p}$ (0.500) mice; median difference (0.000). There was no statistically significant difference between genotypes in average within-cage rank, z = 0.000, p = 1.000.

Females

Twelve genotype balanced cages containing 4 female mice 6 months of age each completed the within-cage tube test (WT = 24, PAT KO = 24). Ten of twelve cages demonstrated a linear hierarchy. Forty-eight *Grb10*$^{+/p}$ vs WT matches were used to examine the frequency of *Grb10*$^{+/p}$ wins. The proportion of female *Grb10*$^{+/p}$ wins (0.44) was not statistically different from chance (0.5), p = 0.471 (2-tailed).

The related samples sign test was used to compare differences in cage rank between genotype groups. The distribution of differences was not symmetrical. Of the twelve cages, *Grb10*$^{+/p}$ mice had higher average rank than wildtypes in three, lower average rank in five, and tied with wildtype average rank in four. Median average cage rank in the social tube test was equivalent for WT (0.500) and *Grb10*$^{+/p}$ (0.500) mice; median difference (0.000). There was no statistically significant difference between genotypes in average within-cage rank, z = -0.354, p = 0.727.

10 month cohort

Males

Eleven genotype balanced cages containing 4 male mice 10 months of age each completed the within-cage tube test. One additional cage was unbalanced (3 WT, 1 *Grb10*$^{+/p}$). The total counts were WT n = 24, *Grb10*$^{+/p}$ n = 23. Nine of eleven balanced cages displayed a linear hierarchy. In total, forty-six *Grb10*$^{+/p}$ vs familiar wildtype matches were used to examine the frequency of *Grb10*$^{+/p}$ wins. The proportion of *Grb10*$^{+/p}$ wins (0.41) was not statistically different from chance (0.50), p = 0.302 (2-tailed).

The related samples sign test was used to compare differences in average cage rank between genotype groups. The distribution of differences was mildly negatively skewed. Of the eleven genotype-balanced cages, *Grb10*$^{+/p}$ mice had higher average rank than wildtypes in three, lower average

rank in five, and tied with wildtype average rank in three. Median average cage rank in the social tube test was equivalent for WT (0.500) and *Grb10*$^{+/p}$ (0.500) mice; median difference (0.000). There was no statistically significant difference between genotypes in average within-cage rank, z = -0.354, p = 0.727.

Females

Eight genotype balanced cages containing 4 female mice 10 months of age each completed the within-cage tube test (WT = 16, PAT KO = 16). Four of eight cages displayed a linear hierarchy. Thirty-two *Grb10*$^{+/p}$ vs WT matches were used to examine the frequency of *Grb10*$^{+/p}$ wins. The proportion of *Grb10*$^{+/p}$ wins (0.53) was not statistically different from chance (0.5), p = 0.860 (2-tailed).

The distribution of differences between genotype group average ranks was approximately symmetrical, so the Wilcoxon signed-rank test was run instead of the related samples sign test. Of the eight cages, *Grb10*$^{+/p}$ average within-cage rank was higher than wildtype in three, lower than wildtype in two, and tied with wildtype within-cage rank in three. Median average cage rank in the social tube test was equivalent for WT (0.500) and *Grb10*$^{+/p}$ (0.500) mice; median difference (0.000). There was no statistically significant difference between genotypes in average within-cage rank, z = 0.966, p = 0.334.

5.3.6 False Discovery Rate Corrections–Social Tube Test

The Benjamini-Liu (BL) procedure was used to correct for false discovery rate (FDR) of 5% over the entirety of statistical measures for the social tube test. Of 12 tests, none were found to be significant before or after FDR corrections.

Table 5.11 Abridged FDR Corrections–Social Tube Test

Finding	**P value**	**Rank (m=12)**	**BL = (min 0.05, 0.05*m/(m+1-i)^2**	**(BL) – P value**
Social Tube Test 10 months–Males	0.302	1	4.17E-03	-0.298

5.3.7 Urine Marking

Summary

The social urine marking test followed the social tube test. Genotype-balanced cages containing 4 mice (2 WT, 2 PAT KO) 8 weeks, 6 months, and 10 months of age each completed the social tube test to determine cage hierarchy.

The binomial test was conducted to determine if the proportion of *Grb10*$^{+/p}$ wins in '*Grb10*$^{+/p}$' versus 'familiar wildtype' matches differed significantly from chance (0.5). Each match included in the analysis was unique, but most individual mice were involved in two matches against cage mates of the opposite genotype (See Section 5.2.5 on Statistical Methods). At 8-10 weeks, the proportion of *Grb10*$^{+/p}$ wins was statistically higher than chance. There was no significant difference at 6 or 10 months.

Rank hierarchies were also established in each cage, with rank scored between 0 (least dominant) to 1 (most dominant), based on the number of wins divided by possible matches against cage mates. The related samples sign test was used to compare differences in average cage rank between genotype groups. For each cage, the averaged wildtype ranks within cage (n=2 per cage) were compared as paired samples to the averaged *Grb10*$^{+/p}$ ranks within cage (n=2 per cage). At 8-10 weeks, the difference in rank between *Grb10*$^{+/p}$ mice (median average cage rank 0.667) and wildtypes (median average cage rank 0.333) was statistically significant. The difference in average cage rank between genotype groups was not significant at 6 months or at 10 months.

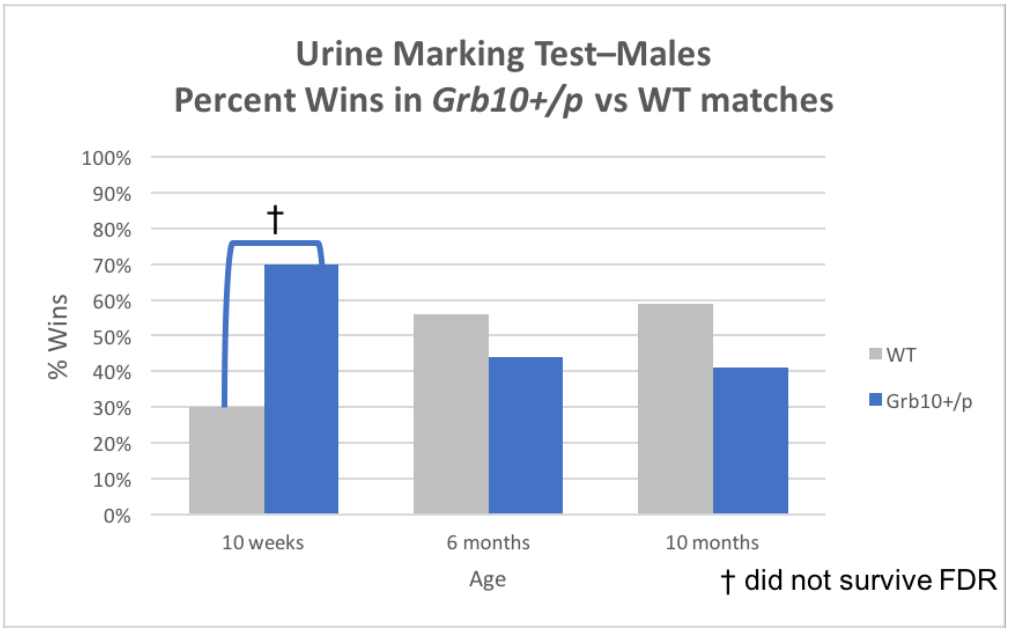

Figure 5.9 Urine Marking Percent Wins Grb10+/p vs WT matches

Table 5.12 Urine Marking Grb10+/p vs WT Binomial Analysis

Age	Male matches (N)	Males proportion wins Grb10 +/p	Males p value	Linear Hierarchy
8 weeks	44	0.70	0.01	8/11
6 months	52	0.56	0.488	9/12
10 months	46	0.41	0.302	8/11

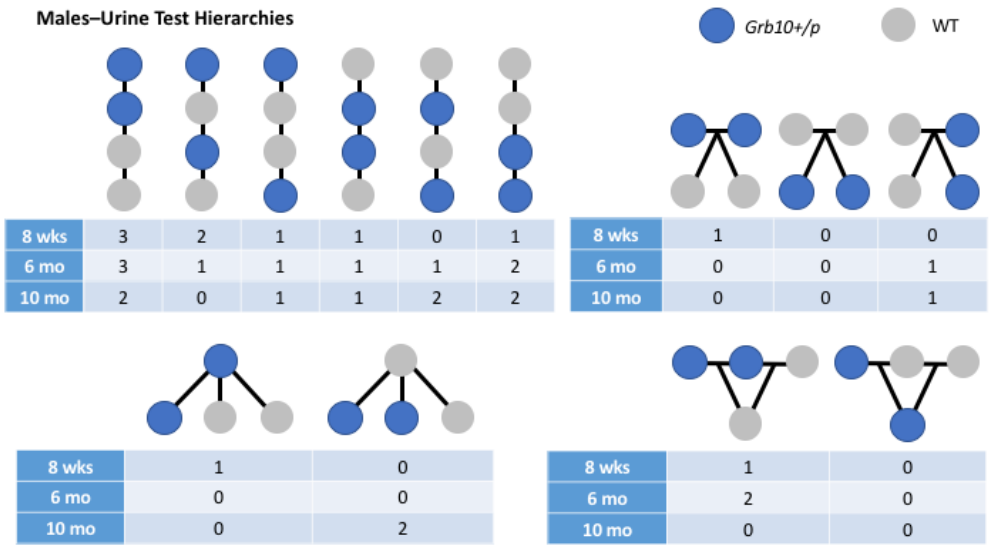

Figure 5.10 Male Urine Test Hierarchies

8-10 week cohort

Eleven genotype-balanced cages containing 4 male mice 8 weeks of age each completed the urine-marking test (WT n=22, *Grb10*$^{+/p}$ n = 22). Eight of eleven cages displayed a linear hierarchy. Forty-four *Grb10*$^{+/p}$ vs wildtype matches were used to examine the frequency of *Grb10*$^{+/p}$ wins. The proportion of *Grb10*$^{+/p}$ wins (0.70) was statistically higher than chance (0.05), p = 0.01 (2-tailed).

The related samples sign test was used to compare differences in average cage rank between genotype groups. The distribution of differences was not symmetrical. Of eleven cages, *Grb10*$^{+/p}$ average cage rank was higher than wildtypes in 8, lower in 1, and tied with wildtypes in 2. Overall, *Grb10*$^{+/p}$ average cage rank (median average cage rank 0.667) was higher than wildtype

(median 0.333), with a statistically significant rank increase of 0.333 (where 0 is most subordinate and 1 is most dominant), z = 2.000, p = 0.039.

6 month cohort

Twelve genotype-balanced cages containing 4 male mice (2 WT and 2 *Grb10*$^{+/p}$) 6 months of age each completed the urine-marking test (WT n=24, *Grb10*$^{+/p}$ n = 24). Nine of twelve cages displayed a linear hierarchy. One additional cage completed some, but not all matches. In total, fifty-two *Grb10*$^{+/p}$ vs wildtype matches were used to examine the frequency of *Grb10*$^{+/p}$ wins. The proportion of *Grb10*$^{+/p}$ wins (0.56) was not statistically different from chance (0.5), p = 0.488 (2-tailed).

The related samples sign test was used to compare differences in average cage rank between genotype groups. The distribution of differences was not symmetrical. Of twelve cages, *Grb10*$^{+/p}$ average cage rank was higher than wildtypes in 6, lower in 3, and tied with wildtypes in 3. Overall, the difference between *Grb10*$^{+/p}$ average cage rank (median average cage rank 0.583) and wildtype (median 0.417) was not statistically significant; median difference (0.167), z = 0.667, p = 0.508.

10 month cohort

Eleven genotype-balanced cages containing 4 male mice (2 WT and 2 *Grb10*$^{+/p}$) 10 months of age each completed the urine marking test. One additional cage was unbalanced (3 WT, 1 *Grb10*$^{+/p}$). The total counts were WT

n = 24, *Grb10*$^{+/p}$ n = 23. Eight of eleven genotype-balanced cages displayed a linear hierarchy. In total, forty-six *Grb10*$^{+/p}$ vs wildtype matches were used to examine the frequency of *Grb10*$^{+/p}$ wins. The proportion of *Grb10*$^{+/p}$ wins (0.41) was not statistically different from chance (0.5), p = 0.302 (2-tailed).

The distribution of differences was approximately symmetrical, so the related samples Wilcoxon-signed rank test was used to analyze average cage rank at 10 months. Of eleven cages, *Grb10*$^{+/p}$ average cage rank was higher than wildtypes in 2, lower in 6, and tied with wildtype average cage rank in 3. Overall, the difference between *Grb10*$^{+/p}$ average cage rank (median average cage rank 0.333) and wildtype (median 0.667) was not statistically significant; median difference (-0.333), z = -0.718, p = 0.473.

5.3.8 False Discovery Rate Corrections–Urine Marking Test

The Benjamini-Liu (BL) procedure was used to correct for false discovery rate (FDR) of 5% over the entirety of statistical measures in the urine marking test. Of 6 tests, 2 were originally found to be significant: “urine test 8-10 weeks–*Grb10*$^{+/p}$ wins” and “average cage rank 8-10 weeks”. These findings did not survive FDR correction.

Table 5.13 Abridged FDR Corrections–Urine Marking Test

Finding	**P value**	**Rank (m=6)**	**BL = (min 0.05, 0.05*m/(m+1-i)^2**	**(BL) – P value**
Urine Test 8-10 weeks–*Grb10+/p* wins	0.010	1	8.33E-03	-1.23E-03
Average Cage Rank 8-10 weeks	0.039	2	0.012	-0.027
Urine Test 6 months–*Grb10+/p* wins	0.488	3	0.019	-0.470

5.3.9 Rank Correlations

5.3.9.1 Social Tube Test and Urine Marking Correlations

The Mantel-Haenszel test of trends was run to determine if there was a linear association between social tube test rank and urine marking rank in total male mice at each age cohort. For this statistical analysis, rank was described between 0 (0 wins against cage mates in the dominance test) and 3 (three wins against cage mates in the dominance test) for both dominance tests.

Rank data was also broken into genotype groups to follow up the test of the total cohort rank associations. The aim was to examine association between social tube test rank and urine marking rank for each genotype group separately. However, the rank data for the genotype groups are not completely independent due to the balanced genotype cages, and this must qualify any interpretation of the separated analyses.

Summary

There was not a significant linear association between social tube test rank and urine marking rank in the behavioural cohorts 8-10 weeks of age and

6 months of age. There was a significant linear association overall at 10 months of age. When this cohort was broken down by genotype group, a significant linear association was found for *Grb10*$^{+/p}$ mice, but not for wildtypes. Linear association between these two measures of within cage rank for social dominance was not reliable.

Males 8-10 weeks

The Mantel-Haenszel test of trend showed there was not a significant linear association between tube test rank and urine marking rank, $\chi^2(1) = 0.696$, $p = 0.404$, $r = -0.134$. The dominance ranking results of the social tube test and urine marking test for mice 8-10 weeks of age were not associated (n = 40 mice).

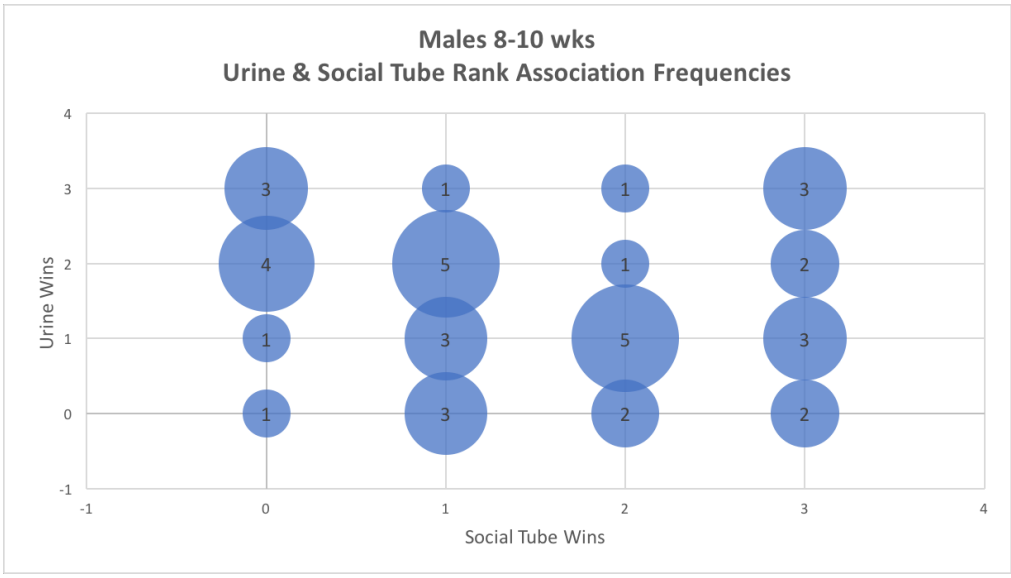

Figure 5.11 Males 8-10 weeks Urine & Social Tube Rank Association Frequencies

The Mantel-Haenszel test of trend showed there was not a significant linear association between tube test rank and urine marking rank for wildtype mice 8-10 weeks of age, $\chi^2(1) = 0.035$, $p = 0.852$, $r = -0.043$. There was also no linear association for *Grb10*$^{+/p}$ mice 8-10 weeks of age, $\chi^2(1) = 0.514$, $p = 0.474$, $r = -0.164$. Tube test rank and urine marking rank were not associated in either WT (n = 20) or *Grb10*$^{+/p}$ (n = 20) groups.

Males 6 months

The Mantel-Haenszel test of trend showed there was not a significant linear association between tube test rank and urine marking rank, $\chi^2(1) = 0.301$, $p = 0.583$, $r = -0.080$. The dominance ranking results of the social tube test and urine marking test for mice 6 months of age were not associated (n = 48 mice).

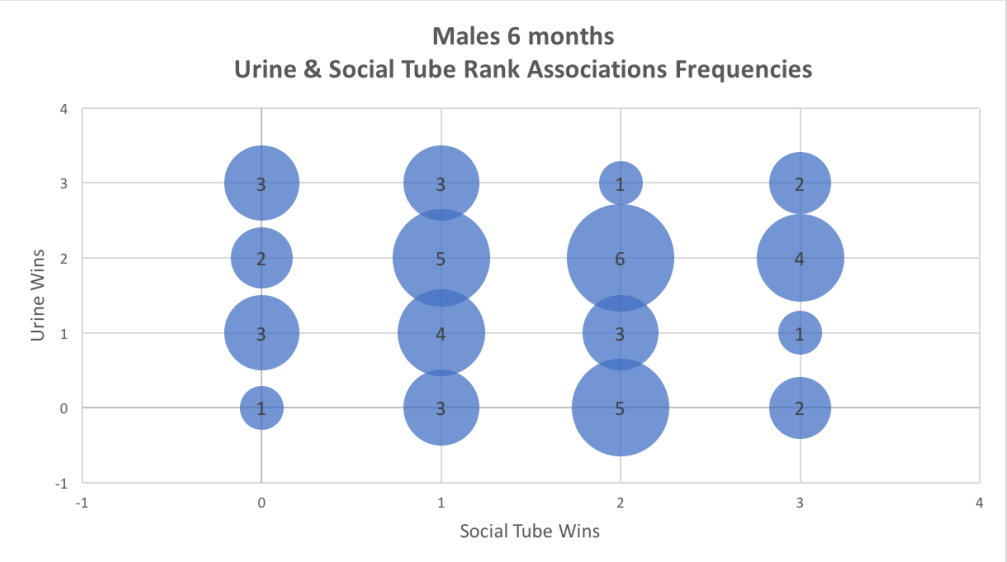

Figure 5.12 Males 6 mo Urine & Social Tube Rank Association Frequencies

The Mantel-Haenszel test of trend showed there was not a significant linear association between tube test rank and urine marking rank for wildtype mice 6 months of age, $\chi^2(1) = 0.038$, $p = 0.845$, $r = -0.041$. There was also no significant linear association between tube test rank and urine marking rank for *Grb10*$^{+/p}$ mice, $\chi^2(1) = 0.341$, $p = 0.559$, $r = -0.122$. Social tube test rank and urine marking rank were not associated in either WT (n = 24) or *Grb10*$^{+/p}$ (n = 24) groups.

Males 10 months

The Mantel-Haenszel test of trend showed a significant linear association between tube test rank and urine marking rank, $\chi^2(1) = 7.176$, $p = 0.007$, $r = 0.409$. Social tube test rank and urine marking rank for male mice 10 months of age were associated (n = 44).

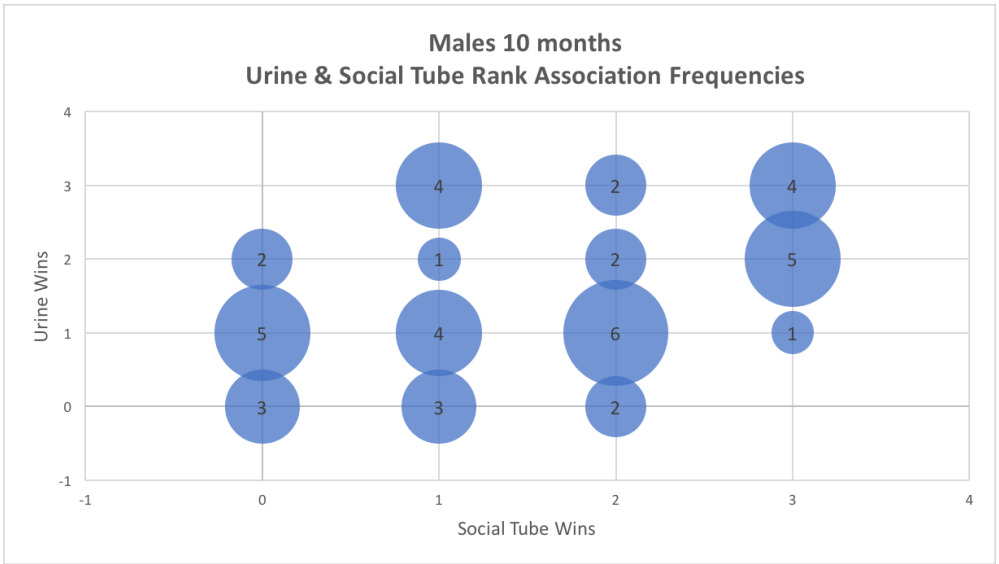

Figure 5.13 Males 10 mo Urine & Social Tube Rank Association Frequencies

The Mantel-Haenszel test of trend showed a there was not a significant linear association between social tube rank and urine marking rank in wildtype males 10 months of age, $\chi^2(1) = 1.196$, $p = 0.274$, $r = 0.239$. However, there was a significant linear association in *Grb10*$^{+/p}$ males 10 months of age, $\chi^2(1) = 5.706$, $p = 0.017$, $r = 0.521$.

5.3.9.2 Barbering and Social Tube Test Correlations/Social Urine Correlations

The Mantel-Haenszel test of trend was used to measure barbering and social dominance test correlations. Tube rank was scored from 0 to 3 wins, and barbering rank was scored from 0 (barbered subordinate) to 1 (unbarbered dominant). *Grb10*$^{+/p}$ and wildtype mice were considered together. Only cages with a clear barbering structure were analyzed.

Rank data was also broken into genotype groups to follow up the test of the total cohort rank associations. The aim was to examine association between barbering and the social tube or urine tests for each genotype group separately. However, the rank data for the genotype groups are not completely independent due to the balanced genotype cages, and this must qualify any interpretation of the separated analyses.

Summary

There was a significant linear association between tube test and barbering rank for male mice (pooled genotypes) 10 months of age. All other associations between barbering and social tube or urine ranking for male and female mice were not significant.

Males and Females 8-10 weeks

There were no barbered cages observed at 8-10 weeks.

Males 6 months

There were six cages of males (n = 24 mice) at 6 months of age with a clear 1:3 ratio of unbarbered to barbered mice. Cases considered were wildtype (n = 12 mice) and *Grb10*$^{+/p}$ (n = 12 mice). The Mantel-Haenszel test of trend showed there was not a significant linear association between tube test rank and barbering rank, $\chi^2(1) = 0.000$, $p = 1.000$, $r = 0.000$. There was also no significant linear association between urine test rank and barbering rank, $\chi^2(1) = 0.170$, p = 0.680, r = -0.086.

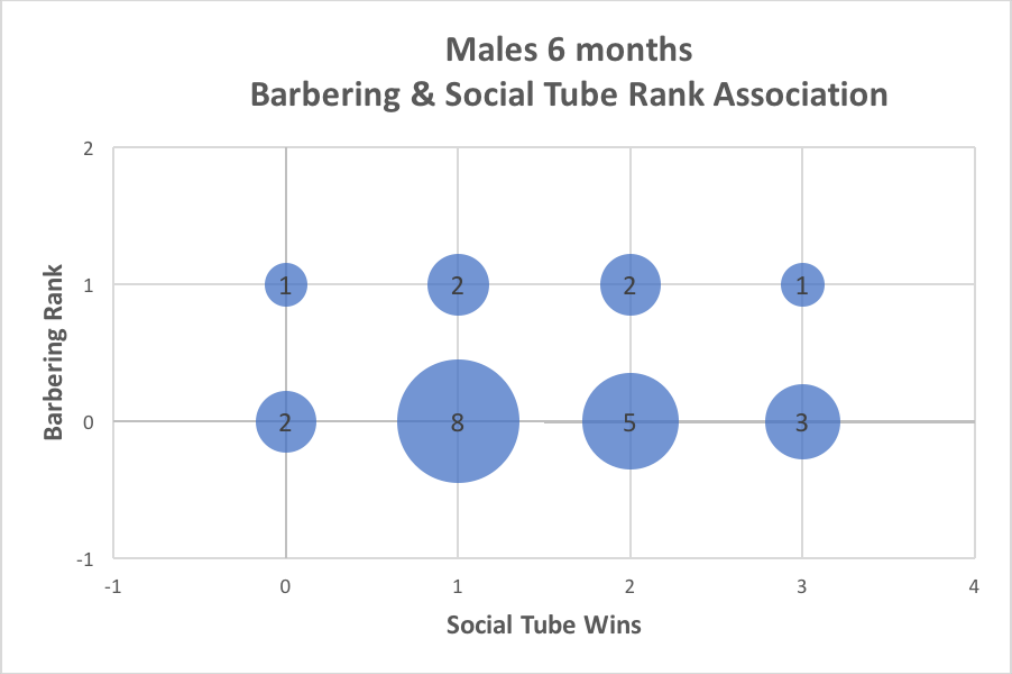

Figure 5.14 Males 6 months Barbering & Social Tube Rank Association

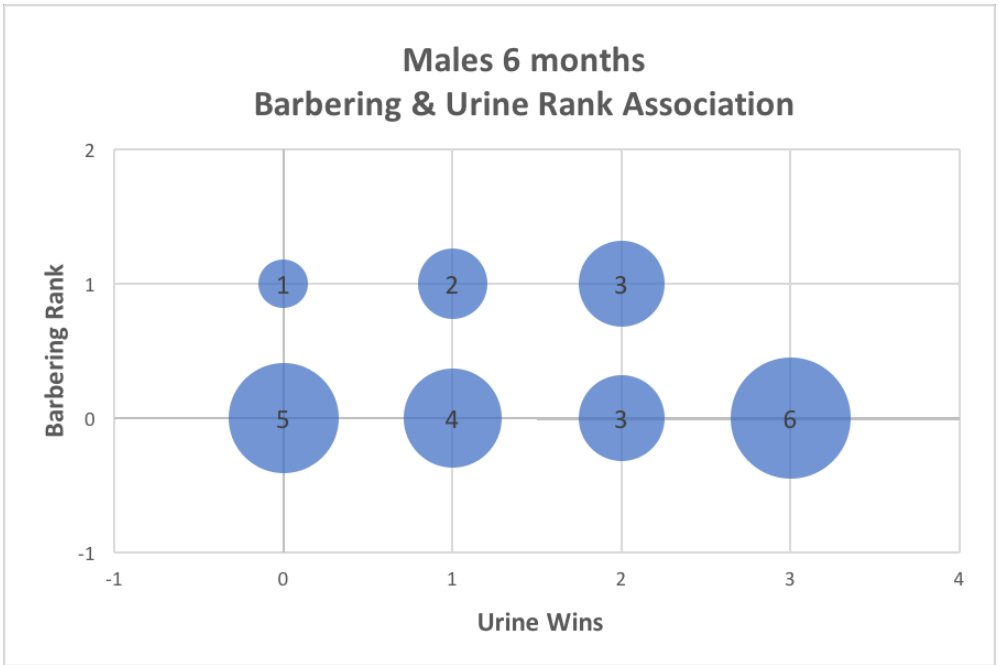

Figure 5.15 Males 6 months Barbering & Urine Rank Association

For wildtypes alone, there was no significant linear association between tube test and barbering rank ($\chi^2(1) = 1.719$, p = 0.190, $r = 0.395$), nor between urine test and barbering rank ($\chi^2(1) = 0.031$, p = 0.861, $r = -0.053$). For *Grb10*$^{+/p}$ alone, there was no significant linear association between tube test and barbering rank ($\chi^2(1) = 0.926$, p = 0.336, $r = -0.290$), nor between urine test and barbering rank ($\chi^2(1) = 0.307$, p = 0.579, $r = -0.167$).

Males 10 months

There were three cages of males at 10 months of age with a clear 1:3 ratio of unbarbered to barbered mice. In three additional cages, all four mice in the cage were barbered; these were not included in the analysis. Cases considered were wildtypes (n = 6), *Grb10*$^{+/p}$ (n = 6). The Mantel-Haenszel test of trend showed there was a significant linear association between tube test

rank and barbering rank, $\chi^2(1) = 3.993$, $p = 0.046$, $r = 0.602$. There was no significant linear association between urine test rank and barbering rank, $\chi^2(1) = 0.081$, p = 0.775, $r = -0.086$.

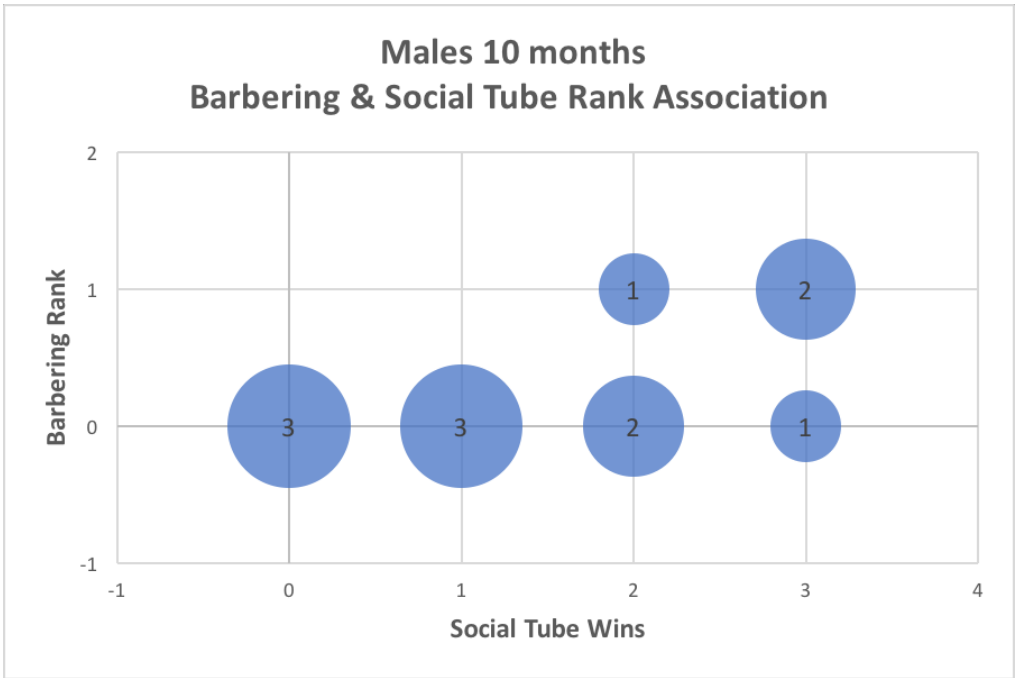

Figure 5.16 Males 10 months Barbering & Social Tube Rank Association

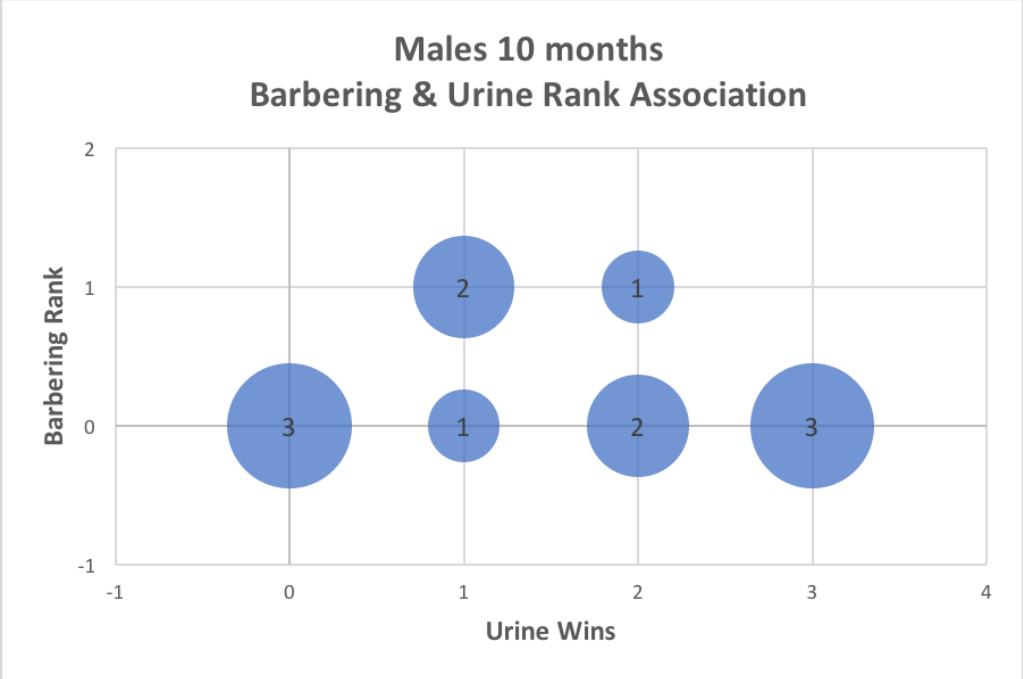

Figure 5.17 Males 10 months Barbering & Urine Rank Association

There was a significant linear association between tube rank and barbering rank for wildtypes, $\chi^2(1) = 4.091$, p = 0.043, *r* = 0.905. There was no significant linear association between urine rank and barbering rank for wildtypes, $\chi^2(1) = 3.333$, p = 0.068, *r* = -0.816. There were no *Grb10*$^{+/p}$ barbers, so the Mantel-Haenszel test could not be calculated for tube or urine rank association with barbering rank.

Females 6 months

There were seven cages of females at 6 months of age with a clear 1:3 ratio of unbarbered to barbered mice. Cases considered were wildtypes (n = 14 mice) and *Grb10*$^{+/p}$ mice (n = 14 mice). The Mantel-Haenszel test of trend showed there was no significant linear association between tube test rank and barbering rank, $\chi^2(1) = 0.918$, p = 0.338, r = 0.184.

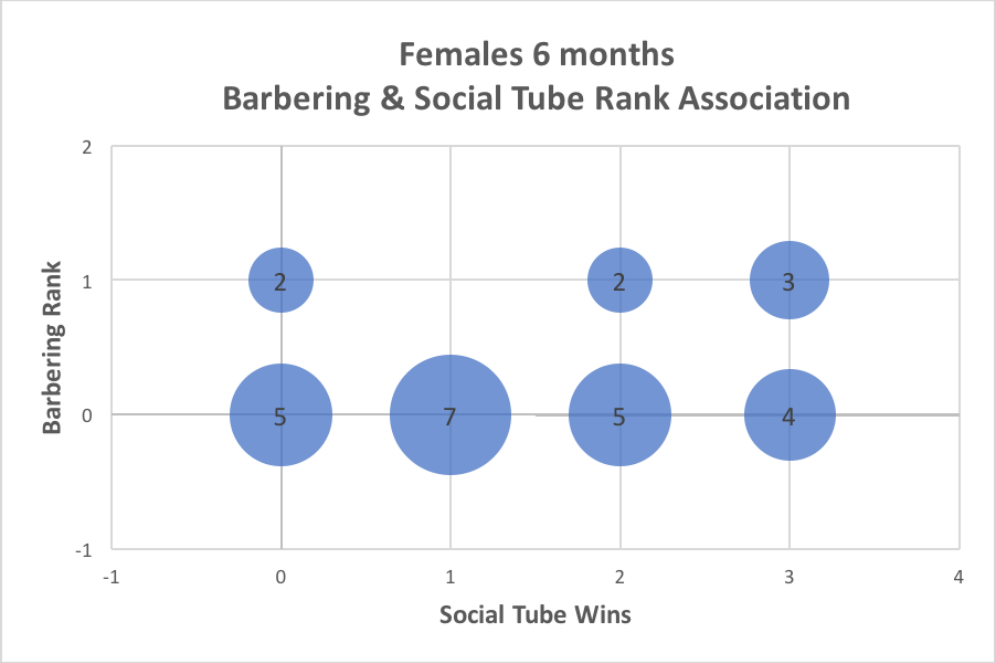

Figure 5.18 Females 6 months Barbering & Social Tube Association

There was no significant association between tube rank and barbering for wildtypes ($\chi^2(1) = 0.001$, p = 0.969, $r = 0.011$) or *Grb10*$^{+/p}$ mice ($\chi^2(1) = 1.977$, p = 0.160, $r = 0.390$).

Females 10 months

There were five cages of females at 10 months of age with a clear 1:3 ratio of unbarbered to barbered mice. Cases considered were wildtype (n = 10 mice) and *Grb10*$^{+/p}$ (n = 10 mice). The Mantel-Haenszel test of trend showed there was no significant linear association between tube test rank and barbering rank, $\chi^2(1) = 1.377$, p = 0.241, r = -0.269.

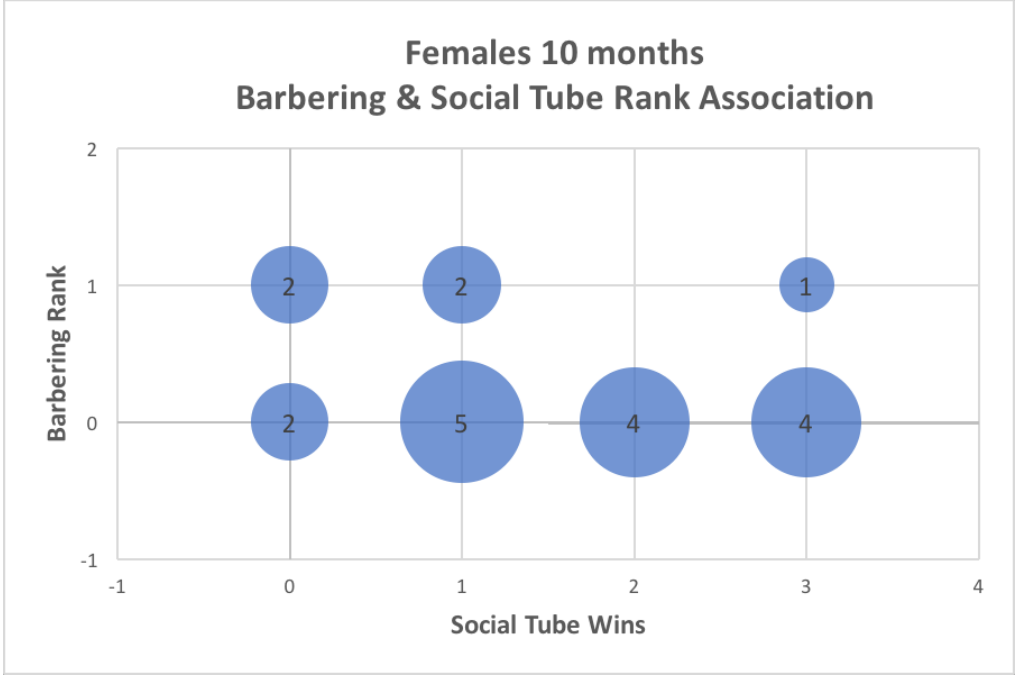

Figure 5.19 Females 10 months Barbering & Social Tube Association

There was no significant linear association between tube and barbering rank for wildtypes ($\chi^2(1) = 0.510$, p = 0.475, $r = -0.238$) or *Grb10*$^{+/p}$ mice ($\chi^2(1) = 2.333$, p = 0.127, $r = -0.509$).

5.3.10 False Discovery Rate Corrections–Social Dominance Correlations

The Benjamini-Liu (BL) procedure was used to correct for false discovery rate (FDR) of 5% over the entirety of social dominance correlations. Out of 25 tests, 4 were originally found to be significant, but none survived FDR correction.

Table 5.14 Abridged FDR Corrections–Social Dominance Correlations

Finding	**P value**	**Rank (m=25)**	**BL = (min 0.05, 0.05*m/(m+1-i)^2**	**(BL) – P value**
Males 10 months Urine vs Tube Association (Both Genotypes)	0.007	1	2.00E-03	-0.005

5.3.11 Social Isolation

Males

Isolated male mice 10 months of age underwent dominance testing in the stranger encounter tube test (*Grb10*$^{+/p}$ n = 10, WT n = 10). Isolated *Grb10*$^{+/p}$ mice faced one unfamiliar isolated wildtype each day for three days.

On Day 1, mice were naïve to the tube test. Of eight successful matches, *Grb10*$^{+/p}$ mice won 2. The binomial test determined the proportion of *Grb10*$^{+/p}$ wins (0.25) was not statistically significantly different to chance (0.5), p = 0.289 (2-tailed).

After three days of testing, all unique *Grb10*$^{+/p}$ vs unfamiliar wildtype matches were analyzed using the binomial test (n = 27). The proportion of *Grb10*$^{+/p}$ wins (0.22) over three days of stranger encounter tube tests was statistically significantly lower than chance (0.50), p = 0.006 (2-tailed). None of

the isolated male mice were barbered before or after isolation, or during testing.

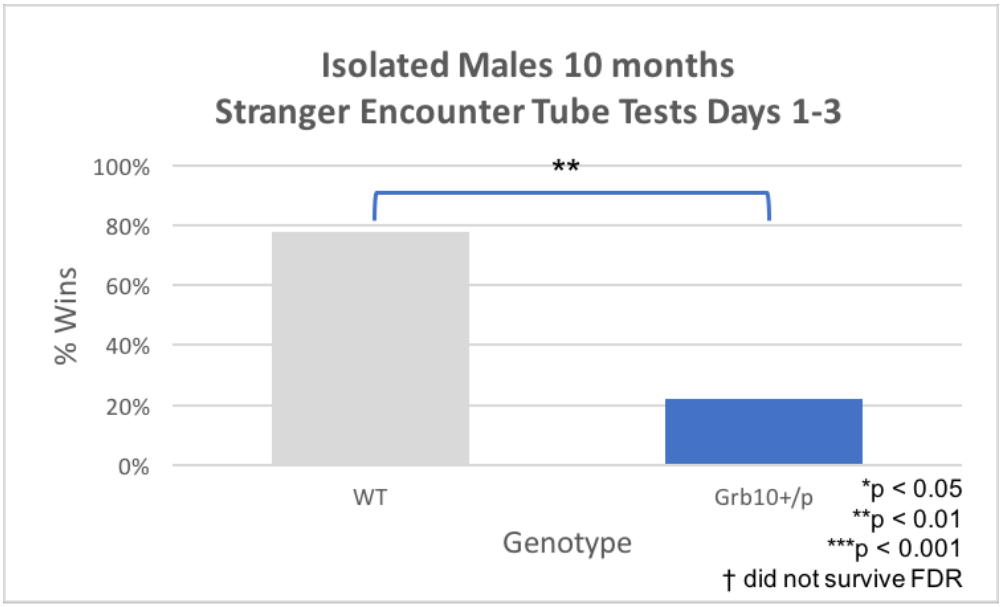

Figure 5.20 Isolated Males 10 months–Stranger Encounter Tube Test Days 1-3

Females

Isolated female mice underwent dominance testing in the stranger encounter tube test (*Grb10*$^{+/p}$ n = 15, WT n = 15). Isolated *Grb10*$^{+/p}$ mice faced one unfamiliar wildtype each day for three days.

On Day 1, mice were naïve to the tube test. Of eleven successful matches, *Grb10*$^{+/p}$ mice won 9. The binomial test determined the proportion of *Grb10*$^{+/p}$ wins (0.82) was not statistically significantly different to chance (0.5), $p = 0.065$ (2-tailed).

After three days of testing, all unique *Grb10*$^{+/p}$ vs unfamiliar wildtype matches were analyzed using the binomial test (n = 39). The proportion of *Grb10*$^{+/p}$ female wins (0.72) over three days of stranger encounter tube tests was significantly higher than chance (0.5), $p = 0.009$ (2-tailed).

Three cages of females displayed barbering prior to isolation. Two barbers were WT and one was *Grb10*$^{+/p}$. After 30 days of isolation and during tube testing, none of the female mice showed signs of whisker barbering.

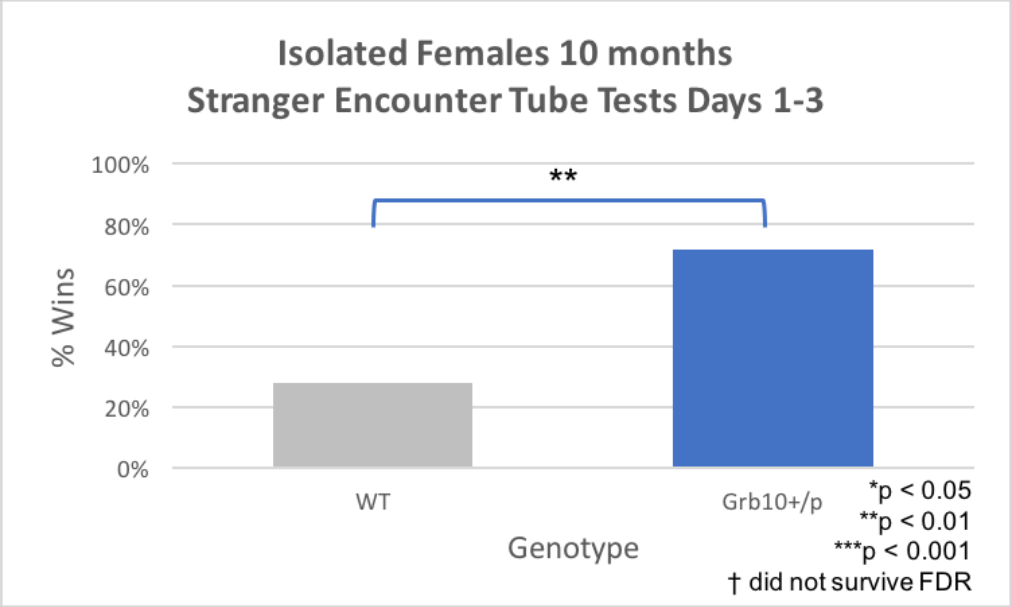

Figure 5.21 Isolated Females 10 months–Stranger Encounter Tube Test Days 1-3

Oestrus

All matches between isolated female mice in which a mouse in oestrus faced a mouse not in oestrus (determined visually or by oestrus swabbing) were pooled across days 1 to 3 (n = 13). The proportion of wins for mice in oestrus, irrespective of genotype, was compared to chance using the binomial test. The observed proportion of wins for mice in oestrus (0.69) was not statistically different to chance (0.5), p = 0.267 (2-tailed).

Males and Females

Considered together over the three-day trial period, the proportion of male and female *Grb10*$^{+/p}$ wins in unique matches (0.52) was not statistically significantly different to chance (0.5), p = 0.902 (2-tailed).

5.3.12 False Discovery Rate Corrections–Social Isolation Stranger Encounter Tube Test

The Benjamini-Liu (BL) procedure was used to correct for false discovery rate (FDR) of 5% over the entirety of measures in the social isolation stranger encounter tube tests. Of 6 tests, two were originally significant: "Isolated males–Stranger Encounter Days 1-3" and "Isolated Females–Stranger Encounter Days 1-3". Both findings survived FDR correction.

Table 5.15 Abridged FDR Corrections–Social Isolation Stranger Encounter Tube Test

Finding	P value	Rank (m=6)	BL = (min 0.05, 0.05*m/(m+1-i)^2	(BL) – P value
Isolated Males–Stranger Encounter Days 1-3	5.93E-03	1	8.33E-03	2.41E-03
Isolated Females–Stranger Encounter Days 1-3	9.48E-03	2	0.012	0.003
Isolated Females–Stranger Encounter Day 1	**0.065**	**3**	**0.019**	**-0.047**

5.4 Discussion

The primary goal of this chapter was to assess social dominance hierarchies over time in *Grb10*$^{+/p}$ mice in genotype-balanced group housed-animals. Group housing allowed us to assess dominance behaviours of socialized mice using overlapping social dominance tests. We compared this to the previously

reported enhanced dominance phenotype of isolated *Grb10*$^{+/p}$ mice in tube test matches against unfamiliar mice (Garfield et al., 2011). We hypothesized we would observe a correlation between the magnitude of the dominance phenotype and our brain overgrowth results from chapters 3 and 4.

Instead, in both sexes and at all three time points, we found no difference between *Grb10*$^{+/p}$ and wildtype socially housed mice in likelihood of winning matches in the familiar-encounter Lindzey tube test. We also found no differences in the social urine marking test, except at 8-10 weeks of age, where male *Grb10*$^{+/p}$ mice were more likely to urine mark than wildtype cage mates. This result did not survive FDR correction. In the stranger-encounter Lindzey tube test, we found no differences in the likelihood of a group-housed *Grb10*$^{+/p}$ win against an unfamiliar wildtype opponent.

Our second goal in this chapter was to assess the impact of social isolation stress on social dominance in *Grb10*$^{+/p}$ mice by replicating the conditions of the Garfield 2011 study. In our social isolation stress studies, *Grb10*$^{+/p}$ males were statistically significantly less likely to win in the stranger-encounter Lindzey tube test against an unfamiliar socially isolated wildtype opponent. This result was opposite to the finding reported in Garfield et al. 2011, although we replicated the conditions of testing and the power of the experiment (Garfield, 2007; Garfield et al., 2011). Notably, we chose not to use a statistical re-sampling technique such as the Monte Carlo permutation test, due to concerns about amplifying noise (Garfield et al., 2011). *Grb10*$^{+/p}$ females were statistically significantly more likely to win in the stranger-encounter Lindzey tube test. These opposing results between our study and the Garfield study

and between male and female cohorts suggest we are not observing a consistent enhanced social dominance phenotype. The low power of both the Garfield experiment (n = 7 WT and n = 8 *Grb10*$^{+/p}$ mice) and our own (n =10 WT and n = 10 *Grb10*$^{+/p}$) may demand additional testing in the context of new findings from social dominance tests of group-housed mice in this chapter.

We assessed the results of our social dominance hierarchies in group housed mice against criteria described in Wang et al. 2011, excepting stability over time (criterion 2), which was not tested in our experimental paradigm. Male cohorts had a higher absolute proportion of linear hierarchies than females, but both sexes showed evidence of transitivity (criterion 1). There was no correlation between tube test rank and urine marking rank (criterion 3) for males (pooled genotypes) at 8-10 weeks or at 6 months, though there was a statistically significant correlation at 10 months. When the analysis was separated by genotype, *Grb10*$^{+/p}$ but not wildtype mice showed a significant correlation between tube and urine rank at 10 months. These results did not survive FDR correction.

A higher proportion of barbers in our cohorts were wildtypes, rather than the *Grb10*$^{+/p}$ barbers reported in Garfield et al 2011. However, this proportion, pooled across all age groups, was not statistically significantly different from chance (0.50). Barbering was present in male and female cohorts at 6 and 10 months of age, but not at 8-10 weeks. At 10 months of age, but not 6 months, barbering rank (0 = barbered, 1 = barber) was significantly correlated with both social tube and urine rank in male mice (pooled genotypes). When genotypes were distinguished, barbering at 10 months correlated with urine rank for

Grb10$^{+/p}$ mice, but not wildtypes, and correlated with tube rank for wildtypes, but not *Grb10*$^{+/p}$ mice. These correlations did not survive FDR correction. Females did not show a significant correlation between barbering and social tube or urine rank at 6 or 10 months. Reports of barbering and tube test rank correlations in the literature suggest the use of training prior to the tube test results in correlation of between these dominance measures, whereas the absence of training does not result in correlation (F. Wang et al., 2014). To match the protocols reported in Garfield et al. 2011, and to avoid learning effects, we did not use tube test training, and this may be relevant to interpreting the absence of correlation between barbering and tube test results.

However, the additional lack of correlation between urine marking rank and either tube test rank or barbering status suggest signs of an unstable hierarchy. In Kalbassi 2017, *Nlgn3*$^{y/-}$ and wildtype males modified each other's behaviour in mixed group housing. Single genotype housing of either *Nlgn3*$^{y/-}$ or wildtype male mice showed the expected correlation between tube test ranking and courtship behaviours, but mixed genotype housing did not (Kalbassi, Bachmann, Cross, Roberton, & Baudouin, 2017; F. Wang et al., 2011). Female *Nlgn3*$^{-/-}$ mice were insensitive to mixed group housing but modified the behaviour of their *Nlgn3*$^{+/-}$ littermates (Kalbassi et al., 2017). This instability of rank in mixed genotype group housing and lack of correlation between dominance tests has also been observed in studies of *Cdkn1c*^{BACx1} mice, which overexpress the maternally imprinted *Cdkn1c* (McNamara et al., 2018). Oppositely imprinted maternal *Cdkn1c* and paternal *Grb10* have

overlapping functional relationships with the midbrain dopaminergic system, as *Cdkn1c* is key to appropriate proliferation and differentiation of midbrain dopaminergic neurons, paternal *Grb10* shows strong expression in these regions, and *Grb10*$^{+/p}$ brains show overgrowth. The stability of social hierarchies is a strong potential substrate for selection in the evolution of genomic imprinting in the brain. The results of this chapter call for further investigation of the impact of paternal *Grb10* on social stability and comparison with *Cdkn1c* overexpression. Such experiments should use a control cage set up to account for the impact of mixed-group housing.

6 Compulsivity and Anxiety Behaviours

6.1 Introduction

Although data from previous studies (Garfield et al., 2011) and our own (Chapter 5) suggest whisker barbering in *Grb10*$^{+/p}$ mice is not self-inflicted, multiple authors have questioned whether this phenotype is due to social dominance per se, or to alternative explanations such as compulsive-type behaviours or allogrooming (Curley, 2011; Haig & Úbeda, 2011). This chapter aims to systematically address this by examining compulsive and/or anxiety phenotypes in *Grb10*$^{+/p}$ mice.

6.1.1 Compulsivity

Elements of barbering in rodents, including features such as a focused affected area and onset during puberty, have been used to model trichotillomania and compulsive grooming (Kurien, Gross, & Scofield, 2005). For instance, SAPAP-3 is a post-synaptic density protein associated with obsessive compulsive disorder (OCD) and trichotillomania in human genetic studies. OCD is an anxiety disorder characterized by obsessive thinking and compulsive behaviour. Trichotillomania is characterized by compulsive hair plucking. SAPAP-3 knockout mice display facial over-grooming and anxiety phenotypes linked to monoaminergic dysregulation in the cortex and striatum (J. Wood, LaPalombara, & Ahmari, 2018). This link between compulsive and repetitive behaviour, and monoaminergic neurotransmitter systems is particularly relevant here. Paternal *Grb10* is highly expressed in monoaminergic regions including the striatum, and is detectable in serotonergic, dopaminergic, and cholinergic neurons (Garfield et al., 2011).

Serotonergic, dopaminergic, and glutamatergic neurotransmitter systems are implicated in the pathophysiology of OCD (Albelda & Joel, 2012).

The subcortical overgrowth described in our *Grb10*$^{+/p}$ mice in Chapters 3 and 4 may disrupt monoaminergic regulation in areas of high paternal *Grb10* expression. Given this and Garfield's reported incidence of whisker barbering, it is reasonable to screen our *Grb10*$^{+/p}$ mice for compulsive behaviour more generally before interpreting the barbering as a dominance behaviour. In this chapter, the marble burying test serves this purpose for our mixed-genotype, socially housed cohorts. The marble burying test has good face validity for repetitive and compulsive behaviour and detects differences between treatment conditions known to manipulate relevant neurotransmitter systems (Albelda & Joel, 2012). The main measure of this test is number of marbles buried, observed to increase with more compulsive behaviour. Marbles are often buried as a secondary result of digging and burrowing behaviour. In previous studies, marbles do not serve as an anxiety-producing stimulus and attempts to habituate mice to the marbles does not alter test results (Angoa-Pérez, Kane, Briggs, Francescutti, & Kuhn, 2013). However, there is some evidence sex hormones in both male and female rats modulate marble burying (Albelda & Joel, 2012).

While marble burying is a good initial screen for compulsive behaviours, there are some concerns over its predictive validity. First, marble burying may not be sensitive to all classes of anti-compulsive drugs, and therefore has restricted predictive value for human clinical study of OCD and compulsive behaviours. Second, marble burying alone cannot differentiate between

compulsive and anxiety behaviours. Drugs such as diazepam, which do not have anti-compulsive activity in humans, also reduce marble burying behaviour, but this suppressive effect disappears with repeated administration (Ichimaru, Egawa, & Sawa, 1995). In contrast, marble burying differences persist under repeated SSRI treatments (Albelda & Joel, 2012; Ichimaru et al., 1995). We considered anxiety when interpreting the results of the marble burying test.

6.1.2 Anxiety

The elevated plus maze is a long-standing measure of assessing unconditioned anxiety (Handley & Mithani, 1984). It has been used to screen pharmacological agents for anxiolytic and anxiogenic effects, to assess the impact of various stressors on anxiety, and to assess brain regions and mechanisms underlying anxiety behaviour (Walf & Frye, 2007). The main measure is the ratio of time spent on the open arms to time spent on the closed arms of the maze, and rodents spend most their time in the task in the closed arms, avoiding the open arms. Anxiogeneic drugs reduce time spent on open arms and anxiolytic drugs increase time spent on open arms (Pellow, Chopin, File, & Briley, 1985). Anxiety related behaviours such as freezing and risk assessment (stretch-attend postures) are increased on open arms under standard conditions. EPM results also predict behaviour in other anxiety measures such as the open field test (Frye, Petralia, & Rhodes, 2000; Walf & Frye, 2007). Our cohorts underwent a standard 5-minute trial on the EPM.

6.1.3 Chapter Aims

Aim (1) Screen *Grb10*$^{+/p}$ mice for compulsive behaviour to differentiate between interpretations of whisker barbering as a social dominance or trichotillomania-like phenotype.

Following social dominance testing in all three cohorts (10 weeks, 6 months, 10 months), *Grb10*$^{+/p}$ mice and wildtype cage mates underwent the 30–minute marble burying task. Marbles buried, half-buried, and displaced, were analyzed as the primary indicators of compulsivity, and were supplemented by time spent digging and grooming.

Aim (2) Screen *Grb10*$^{+/p}$ mice for anxiety phenotypes which might confound both compulsivity measures and social dominance competitions.

All three cohorts were screened for anxiety using the elevated plus maze as the final behaviour measure of the experimental program. This test enhances evidence from previous anxiety testing using the light/dark box and the open field paradigms, compares anxiety measures at each age tested, and provides a consistency check between the effects of Cardiff and Bath animal housing stressors.

6.2 Methods

6.2.1 Subjects

The same 8-10 week, 6 month, and 10 month cohorts were used for marble burying and EPM as for social dominance testing. Testing order was: stranger tube test, social tube test, urine marking (except females), marble burying, and elevated plus maze. For logistical purposes in this cross-sectional study, animals sacrificed for histology were perfused after the marble burying test but before the elevated plus maze. Therefore, complete trial numbers for marble testing and EPM differ.

6.2.2 Handling

Mice were handled as little as possible up until one week prior to the start of behavioural testing; then the researcher who would perform the behavioural tests handled the mice daily for 5 days, recording weight and barbering status.

6.2.3 Marble Burying

In the marble burying task, a box 40 cm (l) x 24 cm (w) x 11 cm (h) was ¾ filled with leveled sawdust and eight red marbles were placed in the "Marbles Zone" at the far end of the arena in a grid. The task was carried out in a quiet room with one overhead light (15 lux) using the Ethovision detection system (version 3.0.15, Noldus Information Technology, Netherlands). One cage of four mice was carried into the testing room at a time, and remained until all cage mates had individually completed the task. To begin the trial, mice were placed in the "Start Zone" and a clear lid was placed over the arena, with

narrow gaps on either 240mm end of the box. Mice were recorded in the arena for 30 minutes, with number of marbles displaced, half buried, and buried recorded manually on every 5-minute mark. Digging and grooming times were also manually scored throughout the trial.

Following the trial, the sawdust was turned over and fresh marbles were placed in the "Marbles Zone". Between cages, 1/3 of the sawdust was removed and replaced with fresh material. Marbles were cleaned with 70% alcohol wipes and dried before reuse.

6.2.4 Elevated Plus Maze (EPM)

The Elevated Plus Maze was carried out in a quiet room with overhead fluorescent lighting, which was necessary for Ethovision detection. The maze consisted of two bisecting white arms 80mm in width by 430mm in length and was elevated 45 cm above the foundation. The opposing pairs of arms were designated "Closed arms" (with 17cm high walls) and "Open arms" (without walls) respectively. The centre square of 80mm x 80mm was designated "Middle". One cage of four mice was carried into the testing room at a time, and remained until all cage mates had individually completed the task. To begin the 5-minute trial, mice were placed in Closed Arm 1. Movement was recorded by the Ethovision detection system, while time for grooming, stretch-attend, and head dips over the edge were scored manually. Between trials, the maze was cleaned with 70% alcohol wipes.

6.2.5 Statistical analysis

Prior to analysis, the data were screened for outliers obviously due to experimenter or measurement error. The Shapiro-Wilk's test was used to assess the normality of the data, and this was followed up with descriptions of the spread of data in histograms or the shape of the residuals (RES) in Q-Q plots. Outliers were further identified as trials with studentized residuals (SREs) more extreme than ±3 SD. All analyses were conducted first with these outliers included, and results were then compared to analyses with these outliers excluded. Results reported are for all outliers included, and differences created by removing the outliers are highlighted.

Data for Ethovision measures in the marble-burying and EPM tasks were analyzed using a two-way ANOVA, with AGE and GENOTYPE as between-subjects independent variables, and an Ethovision measures as the dependent variable. Marbles buried, half-buried, and displaced are analyzed for each cohort separately, using a two-way mixed ANOVA. The between-subjects variable is GENOTYPE, the within-subjects variable is TIME, and the dependent variable is marbles buried, half-buried, or displaced.

Data in main effects analyses are presented as estimated marginal mean ± standard error of the estimated marginal mean, unless otherwise stated. Graphs report descriptive means ± standard error of the descriptive mean, unless otherwise stated. This allows the data for GENOTYPE and AGE to be viewed independently. Where main effects are found to be significant and relevant to the aims of the chapter, the graph of the estimated marginal means ± standard error are also presented.

Statistical significance underwent False Discovery Rate (FDR) corrections using the Benjamini-Liu (BL) method (Y Benjamini & Liu, 1999; Yoav Benjamini et al., 2001). FDR corrections were performed on all reported analyses belonging to one task (ie, “marble burying task” or “EPM”), and FDR corrections were separate between different tasks. Abridged tables extend to the critical significance value. Full tables of the BL FDR corrections are available in the appendix.

6.3 Results

6.3.1 Marble Burying Ethovision Measures

A two-way ANOVA was conducted to determine the effects of GENOTYPE and AGE on ethovision measures during the marble burying task, including: “velocity”, “total time digging”, “total time grooming”, “percent time in ‘start’ zone”, “percent time in “marbles’ zone”, and “transitions”.

Data Screening

Socially housed male mice completed the marble burying task in three cohorts of different age groups (10 weeks, 6 months, and 10 months). Prior to carrying out the analysis, the data were screened for outliers. At 10 months, A17 P had an implausible number of zone transitions and was removed from the data set entirely. At 6 months, C52P had an implausible velocity and number of zone transitions and was removed from the data set entirely. At 8-10 weeks, D34 P had an error in measurement for time spent grooming, and

was removed from the data set entirely. The final trials included are summarized in the table.

Table 6.1 Marble Burying Trials Summary

Genotype	Age	N
WT	10 weeks	24
	6 months	24
	10 months	29
***Grb10*$^{+/p}$**	10 weeks	23
	6 months	23
	10 months	21

Shapiro-Wilk's test was used with the residuals (RES) to calculate normality for each cell for each measure ($p > 0.05$). Non-normal results were investigated with Q-Q plots. Outliers were identified using the studentized residuals (SRE).

Residuals (RES) for "velocity" were normally distributed for all cells except wildtype residuals at 6 months of age (Shapiro-Wilk's $p = 0.024$). The RES Q-Q plot for this cell showed some positive skew, largely due to an outlier. Studentized residuals identified this outlier as C19 P (SRE = 3.44). Residuals for all cells in "total time digging" were normally distributed. There was one outlier in "total time digging: C13 P (SRE = 3.64). None of the cells for "total time grooming" were normally distributed except for wildtype data at 6 months (Shapiro-Wilk's $p = 0.170$). The RES Q-Q plots for the non-normal cells were positively skewed. There were four outliers: D47 P (SRE = 3.79), C41 P (SRE = 3.40), A18 P (SRE = 3.30), and D15 P (SRE = 3.08). Residuals for all cells in "percent time in 'start' zone" were normally distributed. There were no

outliers with SRE more extreme than ± 3 SD. Likewise, residuals for all cells in "percent time in 'marbles' zone" were normally distributed, and there were no outliers. Residuals for all cells in "transitions" were normally distributed. There was one outlier: A53 P (SRE = 3.08). In summary, for ethovision measures across all cohorts, SRE for D15 P, C13 P, C19P, C41 P, C47 P, A18 P, and A53 P were more extreme than ± 3 SD. There was homogeneity of error variances for all measures except "total time grooming" (Levene's test p = 0.008). This measure was analyzed using separate one-way ANOVAs for each age group.

Outliers for marbles buried, half-buried, and displaced were considered separately for each age group because they required a two-way mixed ANOVA.

For 10 weeks of age, in marbles displaced, D21 P SRE was more extreme than $\pm$ 3 SD in three time bins, and D42 P was more extreme than $\pm$ 3 SD in one time bin. In marbles buried, D22P, D18 P, and D7 P were identified as outliers with SRE more extreme than $\pm$ 3 SD in at least one time bin. There were no outliers with SRE more extreme than $\pm$ 3 SD in marbles half buried.

For 6 months of age, there were two outliers in marbles buried: C60 P, and C3 P. In marbles displaced, there were three outliers: C40 P, C53 P, and C61 P. There were no trials with SREs more extreme than $\pm$ 3 SD in marbles half buried.

For 10 months of age, there were two outliers in marbles buried: A53 P, and A69 P. In marbles displaced, there were four outliers: A15 P, A18 P, A25 P, and A66 P. There were no trials with SREs more extreme that $\pm$ 3 SD in marbles half-buried.

The 21 total identified outliers related to marble burying measures (ethovision, marbles buried, half-buried, and displaced) from all cohorts were: D7 P, D15 P, D18P, D21 P, D22 P, D42 P, D47 P, C3 P, C13 P, C19 P, C40 P, C41 P, C53 P, C60 P, C61 P, A15 P, A18 P, A25 P, A53 P, A66 P, and A69 P.

Summary

There was no significant interaction between GENOTYPE and AGE for any measure analyzed with a two-way ANOVA. Time grooming was analyzed separately for each age bin, because it violated of the assumption of homogeneity of error variances in the two-way ANOVA. Additionally, time grooming was analyzed using a Mann-Whitney U test because it violated the assumption of normality for all but one cell of the design.

There was no significant difference in "velocity" by genotype or age. There was no significant main effect of GENOTYPE on "time spent digging", but there was a significant main effect of AGE: mice 10 weeks and 6 months of age both spent more time digging than mice 10 months of age, but there was no significant difference between mice 10 weeks and 6 months of age.

There was no significant difference between genotype groups in "time spent grooming" at any age bin. The main effects of GENOTYPE and AGE were not significant for "percent time spent in 'start' zone". Likewise, there were no significant differences for "percent time spent in 'marbles' zone". There was no significant main effect of GENOTYPE or AGE on transitions made between zones.

Twenty-one identified outliers were removed from the data set in a separate analysis to determine their impact on the statistical results. There were still no significant interactions between GENOTYPE and AGE for any measure analyzed with a two-way ANOVA. Time digging and time grooming data were analyzed separately for each age bin, due to violations of the assumption of homogeneity of error variances.

For "time spent digging", there was no difference between genotype groups at 6 or 10 months, but at 10 weeks, *Grb10*$^{+/p}$ mice spent significantly less time digging than wildtypes. There was still no significant effect of genotype group on number of transitions made between zones of the marble burying arena, but there was a significant effect of age: mice 6 months of age made more transitions than mice 10 months of age. There were no differences in transitions between any other pairwise comparisons of age. The outcomes of all other analyses were the same as in the original analyses including all trials.

Reports

"Velocity"

The interaction between GENOTYPE and AGE for "velocity" was not statistically significant, $F(2,138) = 1.051$, $p = 0.352$, partial $\eta^2 = 0.015$. Therefore, we conducted main effects analyses. The main effect of GENOTYPE was not statistically significant, $F(1,138) = 3.175$, $p = 0.077$, partial $\eta^2 = 0.022$. The main effect of AGE was also not statistically significant, $F(2,138) = 0.512$, $p = 0.600$, partial $\eta^2 = 0.007$.

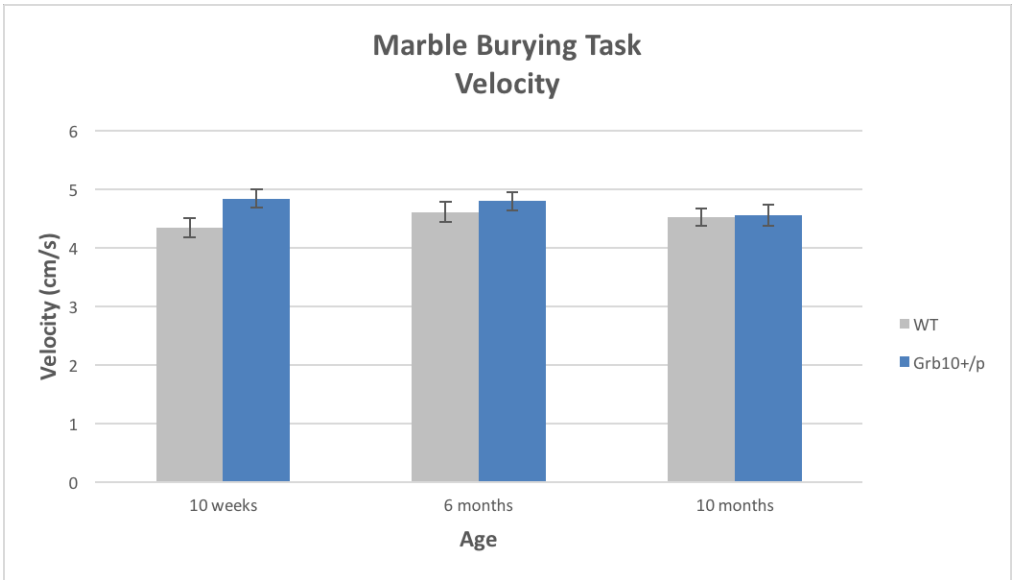

Figure 6.1 Marble Burying–Velocity

"Time spent digging"

The interaction between GENOTYPE and AGE for "total time spent digging" was not statistically significant, F(2,138) = 0.562, p = 0.571, partial η^2 = 0.008. Therefore, we conducted main effects analyses. The main effect of GENOTYPE was not statistically significant, F(1,138) = 0.412, p = 0.522, partial η^2 = 0.003.

There was a statistically significant main effect of AGE on "total time spent digging", F(2,138) = 11.813, p < 0.001, partial η^2 = 0.146. There was a statistically significant difference between time spent digging by mice 10 weeks of age (308.435 ± 18.905 s) and 10 months of age (211.083 ± 18.564 s), mean difference 97.352 (95%CI 33.138 to 161.566) s, p = 0.001. There was also a significant difference between time spent digging at 6 months (332.332 ± 18.905 s) and 10 months, mean difference 121.249 (95%CI 57.035 to 185.463)

s, p < 0.001. There was no significant difference between 10 weeks and 6 months, mean difference -23.897 (95%CI -88.693 to 40.899) s, p = 1.000.

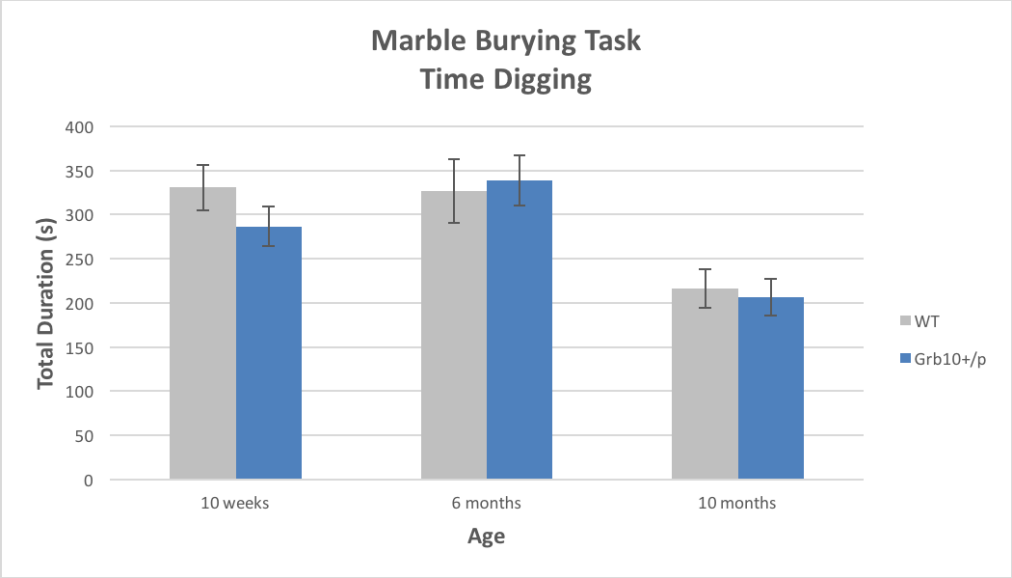

Figure 6.2 Marble Burying–Time Digging

"Time spent grooming"–separate nonparametric Mann-Whitney U tests

"Time spent grooming" violated the assumption of homogeneity of error variances, so each cohort was analyzed individually. Additionally, the residuals for all cells were non-normally distributed except wildtype data at 6 months. Therefore, "time spent grooming" was analyzed using the non-parametric Mann-Whitney U Test to determine if there was a difference between *Grb10*$^{+/p}$ and wildtype mice. For all time points, distributions of the measure for each genotype were determined similar by visual inspection, so medians are reported.

At 10 weeks, median time spent grooming for *Grb10*$^{+/p}$ mice (43.160 s) was not statistically different to wildtypes (46.640 s), U = 246.000, z = -0.638, p = 0.523. At 6 months, median time spent grooming for *Grb10*$^{+/p}$ mice (23.640

s) was not statistically different to wildtypes (33.120 s), U = 212.000, z = -1.362, p = 0.173. At 10 months, median time spent grooming for *Grb10*$^{+/p}$ mice (24.400 s) was not statistically different to wildtypes (32.880 s), U = 226.000, z = -1.543, p = 0.123.

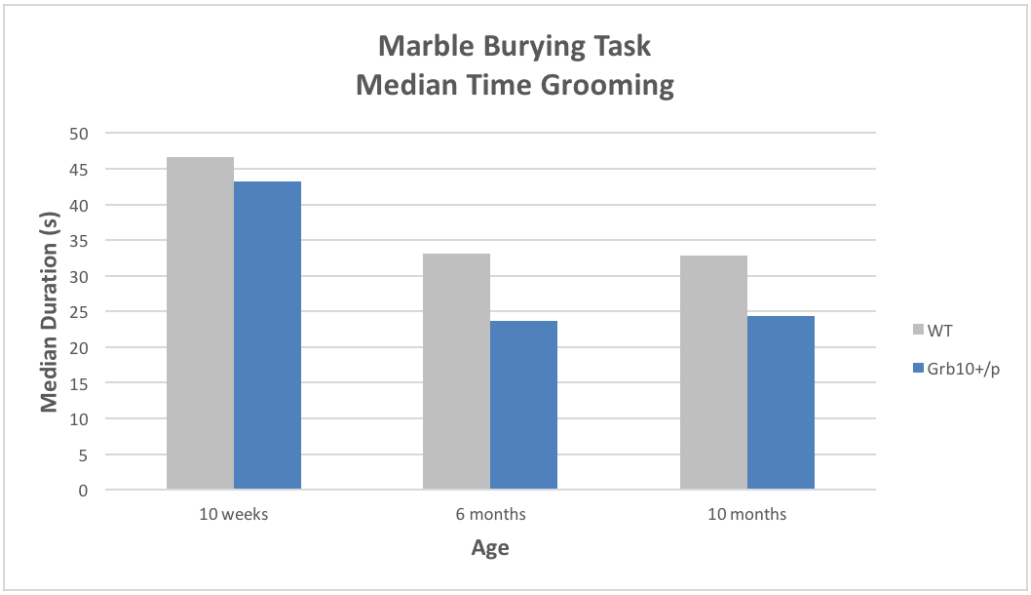

Figure 6.3 Marble Burying–Median Time Grooming

"Percent time in 'start' zone" and "Percent time in 'marbles' zone"

There was no statistically significant interaction between GENOTYPE and AGE in "percent time in 'start' zone", F(2,138) = 1.541, p = 0.218, partial η^2 = 0.022. Therefore, we performed main effects analyses. There was no significant main effect of GENOTYPE on percent time in the 'start' zone, F(1,138) = 0.887, p = 0.348, partial η^2 = 0.006. There was also no significant main effect of AGE on percent time in the 'start' zone, F(2,138) = 2.963, p = 0.055, partial η^2 = 0.041. Statistics for "percent time in 'marbles' zone" were identical (mean values were complementary).

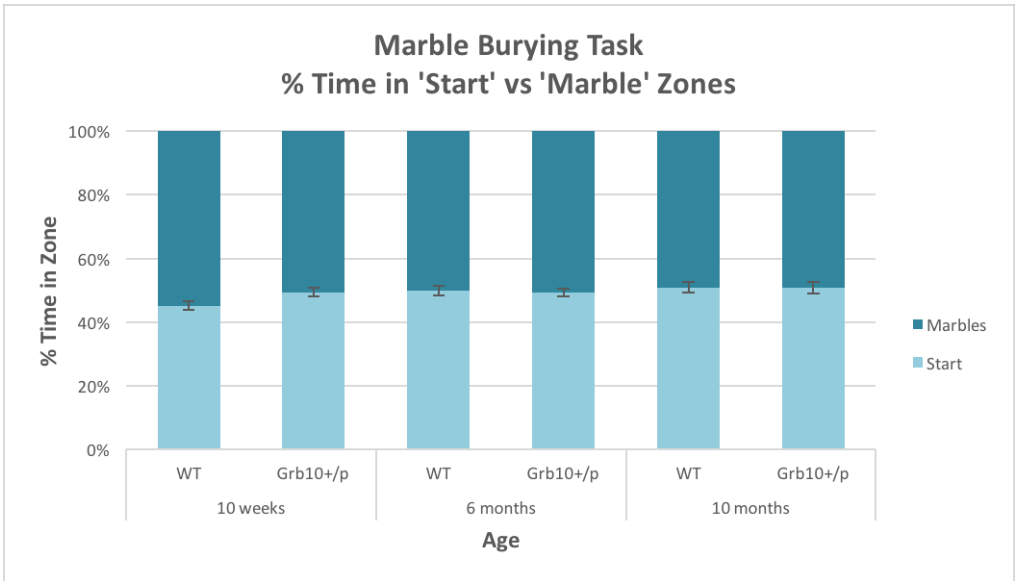

Figure 6.4 Marble Burying-% Time in "Start" vs "Marble" Zones

"Transitions"

There was no statistically significant interaction between GENOTYPE and AGE for 'transitions' between zones of the marble burying task, $F(2,138) = 1.535$, $p = 0.219$, partial $\eta^2 = 0.022$. Therefore, we performed main effects analyses. There was no significant main effect of GENOTYPE, $F(1,138) = 3.606$, $p = 0.060$, partial $\eta^2 = 0.025$. There was also no significant main effect of AGE, $F(2,138) = 2.517$, $p = 0.084$, partial $\eta^2 = 0.035$.

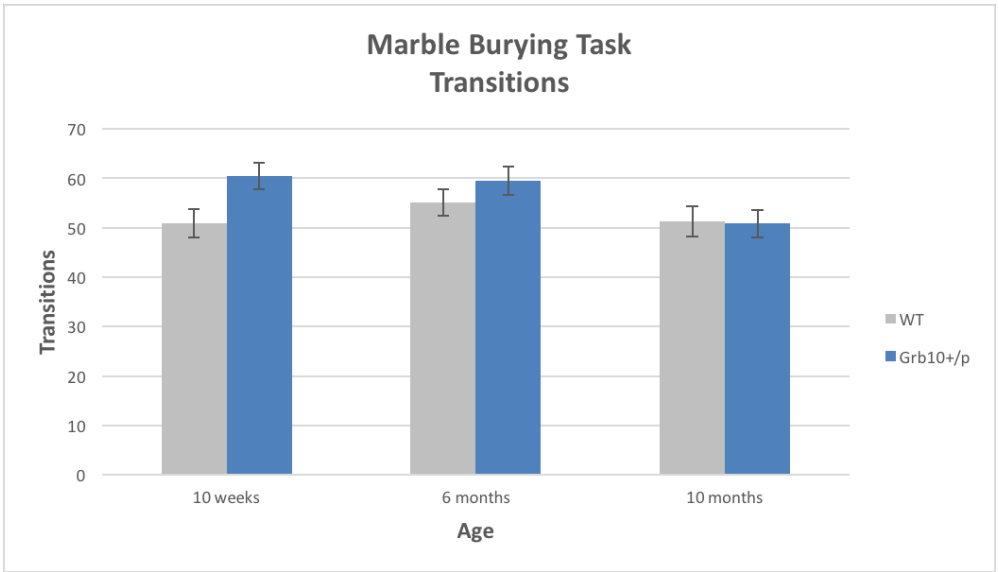

Figure 6.5 Marble Burying–Transitions

6.3.2 Marbles Buried, Half-buried, and Displaced–Males 8-10 weeks

"*Marbles Buried*"

Summary

There was no significant interaction between GENOTYPE and TIME for marbles buried, nor was there a significant main effect of GENOTYPE. There was a significant main effect of TIME. Marbles buried significantly increased from 5, 10, and 15 minutes to all later time points, but was not significantly different in pairwise comparisons between 20 and 30 minutes. Removal of the identified outliers across the marble burying task did not change the outcome of the analysis for marbles buried by mice 8-10 weeks of age.

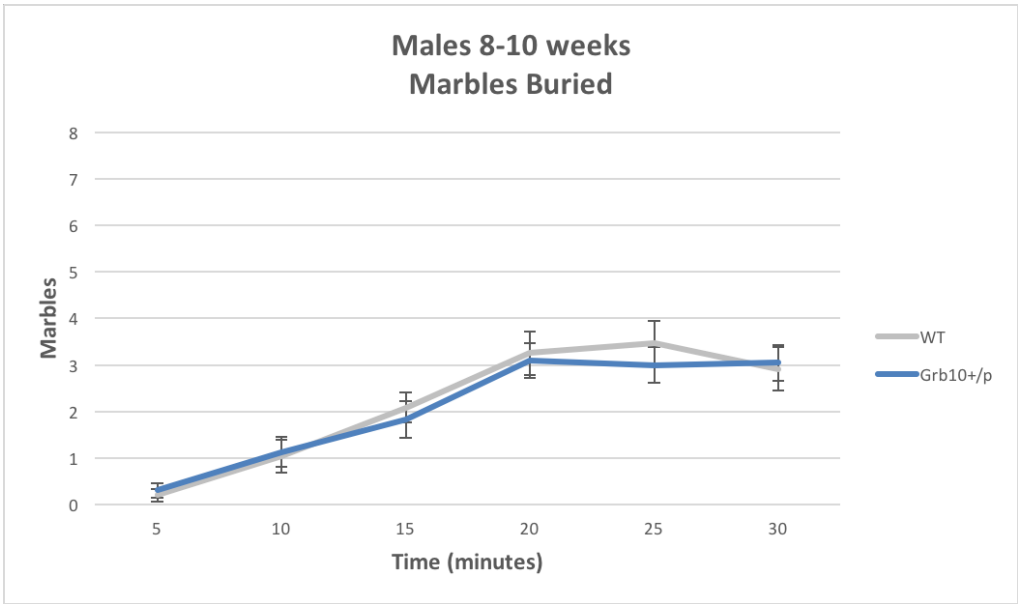

Figure 6.6 Males 8-10 wks Marbles Buried

Report

Marbles buried over the course of 30 minutes was assessed using a two-way mixed ANOVA, with "genotype" as the between-subjects factor with two groups, and "time" as the within-subjects factor with 6 levels. The aim was primarily to determine whether there was an interaction between genotype and time for marbles buried and secondarily to determine the contributions of each factor.

Three outliers were identified using studentized residuals: D22 P and D18 P were genuinely unusual data points at the 5-minute level, and D22 P and D7 P were genuinely unusual data points at the 10-minute level. These outliers were left in the analysis. The final trials included were WT (n = 24), *Grb10*$^{+/p}$ (n = 23).

Normality was assessed using Shapiro-Wilk's test of normality for the raw data and Q-Q plots of the studentized residuals. Shapiro-Wilk's test indicated the data were distributed normally for time points 20, 25, and 30 minutes. Data were distributed normally for WT samples at 15 minutes but not for *Grb10*$^{+/p}$ samples. Data were not normal for time points 5 and 10 minutes. Q-Q plots for studentized residuals at 20, 25, and 30 minutes were normal, at 15 minutes were less normal, and showed moderate positive skew at 5 and 10 minutes.-Transformation of data in all bins for moderate positive skew did not improve normality, and ANOVA is robust to violations of normality, so the data were left untransformed for the remaining analysis.

There was homogeneity of variances ($p > 0.05$) and co-variance ($p = 0.824$), as assessed by Levene's test for homogeneity of variances and Box's M test, respectively. Mauchly's test of sphericity indicated the assumption of sphericity was violated for the two-way interaction, $\chi^2(14) = 36.822$, $p = 0.001$. Epsilon (ε) was 0.708, calculated using Greenhouse-Geisser method, and was used to correct the mixed measures ANOVA.

There was no statistically significant interaction between TIME and GENOTYPE on marbles buried, $F(3.538, 159.216) = 0.507$, $p = 0.708$, partial $\eta^2 = 0.011$, $\varepsilon = 0.708$. The main effect of GENOTYPE showed there was not a statistically significant difference between *Grb10*$^{+/p}$ and WT groups, $F(1,45) = 0.050$, $p = 0.823$, partial $\eta^2 = 0.001$.

The main effect of TIME showed a statistically significant difference in marbles buried at different time points, $F(3.538, 159.216) = 54.826$, $p < 0.001$,

partial η^2 = 0.549, ε = 0.708. Data for the following time points are estimated mean $\pm$ standard error. Marbles buried changed significantly over time, with 0.256 ± 0.099 at 5 minutes, 1.086 ± 0.240 at 10 minutes, 1.955 ± 0.253 at 15 minutes, 3.168 ± 0.297 at 20 minutes, 3.229 ± 0.306 at 25 minutes, and 2.980 ± 0.304 marbles at 30 minutes.

Post hoc analysis with the Bonferroni adjustment was carried out for all pairwise comparisons. Data are presented as mean difference with the 95% confidence interval. Marbles buried statistically significantly increased from 5 to 10 minutes (0.830 (95% CI 0.232 to 1.428) marbles, p = 0.001), from 10 to 15 minutes (0.869 (95% CI 0.237 to 1.501) marbles, p = 0.002), and from 15 to 20 minutes (1.214 (95% CI 0.501 to 1.927), p < 0.001), but not from 20 to 25 minutes (0.061 (95% CI -0.494 to 0.616), p = 1.000) or from 25 to 30 minutes (-0.249 (95% CI -0.792 to 0.294), p = 1.000) .

Additionally, marbles buried statistically significantly increased from 5 to 15 minutes (1.698 (95% CI 0.965 to 2.432), p < 0.001), from 5 to 20 minutes (2.912 (95% CI 2.079 to 3.746), p < 0.001), from 5 to 25 minutes (2.973 (95% CI 2.111 to 3.835), p < 0.001), and from 5 to 30 minutes (2.724 (95% CI 1.851 to 3.596), p < 0.001). Marbles buried statistically significantly increased from 10 to 20 minutes, (2.082 (95% CI 1.294 to 2.871), p < 0.001), from 10 to 25 minutes (2.143 (95% CI 1.305 to 2.981), p < 0.001), and from 10 to 30 minutes (1.894 (95% CI 1.130 to 2.658), p < 0.001). Marbles buried statistically significantly increased from 15 to 25 minutes (1.274 (95% CI 0.515 to 2.034), p < 0.001), and from 15 to 30 minutes (1.025 (95% CI 0.302 to 1.749), p = 0.001).

Marbles buried were not statistically significantly different between 20 and 30 minutes (-0.188 (95% CI -0.836 to 0.459), p = 1.000).

"Marbles Half Buried"

Summary

There was no significant interaction between GENOTYPE and TIME for marbles half-buried, nor was there a significant main effect of GENOTYPE. The main effect of TIME was significant. Marbles half-buried increased from 5 to 10, 15, 20, and 30 minutes, and decreased from 15 to 20 and 25 minutes. The removal of outliers with SRE more extreme than ± 3SD resulted in no significant change from 5 to 20 minutes, but otherwise did not change the outcome of the 2-way mixed ANOVA for marbles half-buried by male mice 8-10 weeks of age.

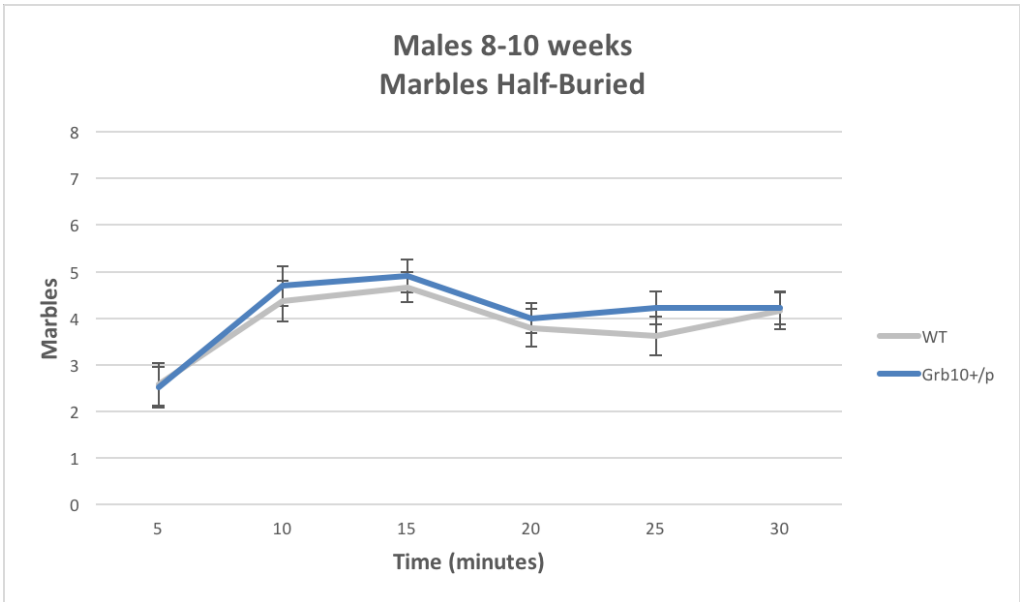

Figure 6.7 Males 8-10 wks Marbles Half-Buried

Report

Marbles half-buried over the course of 30 minutes was assessed using a two-way mixed ANOVA, with "genotype" as the between-subjects factor with two groups, and "time" as the within-subjects factor with 6 levels. The aim was primarily to determine whether there was an interaction between genotype and time for marbles displaced and secondarily to determine the contributions of each factor. There were no outliers with studentized residuals (SREs) more extreme than $\pm$ 3 SD. The final trials included were WT (n = 24) and *Grb10*$^{+/p}$ (n = 23).

Shapiro-Wilk's test indicated the data were normally distributed for both WT and *Grb10*$^{+/p}$ trials at 10 and 30 minutes, for WT but not *Grb10*$^{+/p}$ trials at 15, 20, and 25 minutes, and for neither genotype group at 5 minutes. Histogram distributions of the raw data show slight positive skew for both genotype groups at 5 minutes and for *Grb10*$^{+/p}$ trials at 20 minutes. *Grb10*$^{+/p}$ trials at 15 minutes showed slight negative skew, and at 25 minutes showed bimodal distribution. Q-Q plots of the studentized residuals (SREs) were visually inspected and determined to be normal for all time points. Transformations were not appropriate for this data and were not applied.

There was homogeneity of variances for all time points (Levene's test $p > 0.05$) and homogeneity of covariance (Box's Test $p = 0.910$). Mauchly's test of sphericity indicated the assumption of sphericity was violated for the two-way interaction, $\chi^2(14) = 96.162$, $p < 0.001$. Epsilon (ε) was 0.503, as calculated by Greenhouse-Geisser, and was used to correct the mixed measures ANOVA.

There was no statistically significant interaction between TIME and GENOTYPE, F(2.517, 113.272) = 0.239, p = 0.836, partial η^2 = 0.005, ε = 0.503. The main effect of GENOTYPE was not statistically significant, F(1,45) = 0.401, p = 0.530, partial η^2 = 0.009.

The main effect of TIME showed a statistically significant difference in marbles half-buried at different time points, F(2.517, 113.272) = 11.345, p < 0.001, partial η^2 = 0.201, ε = 0.503. Data for the following time points are estimated marginal mean $\pm$ standard error. Marbles half-buried changed significantly over time, with 2.553 ± 0.313 at 5 minutes, 4.535 ± 0.303 at 10 minutes, 4.790 ± 0.239 at 15 minutes, 3.896 ± 0.259 at 20 minutes, 3.921 ± 0.275 at 25 minutes, and 4.192 ± 0.266 marbles at 30 minutes.

Post hoc analysis with the Bonferroni adjustment was carried out for all pairwise comparisons. Data are presented as mean difference with the 95% confidence interval. Marbles half-buried statistically significantly increased from 5 to 10 minutes (1.983 (95%CI 0.975 to 2.990) marbles, p < 0.001), 5 to 15 minutes (2.237 (95%CI 0.981 to 3.494) marbles, p < 0.001), 5 to 20 minutes (1.343 (95%CI 0.006 to 2.681) marbles, p = 0.048), and from 5 to 30 minutes (1.639 (95%CI 0.297 to 2.982) marbles, p = 0.007), but not from 5 to 25 minutes (1.369 (95%CI -0.016 to 2.753) marbles, p = 0.055).

Marbles half-buried was not statistically significantly different from 10 to 15 minutes (0.255 (95%CI -0.738 to 1.247) marbles, p = 1.000), 10 to 20 minutes (-0.639 (95%CI -1.724 to 0.445) marbles, p = 1.000), 10 to 25 minutes (-0.614 (95%CI -1.821 to 0.592) marbles, p = 1.000), or 10 to 30 minutes (-0.343 (95%CI -1.413 to 0.726) marbles, p = 1.000). Marbles half-buried statistically

significantly decreased from 15 to 20 minutes (-0.894 (95%CI -1.603 to -0.185) marbles, p = 0.005), and from 15 to 25 minutes (-0.869 (95%CI -1.737 to 0.000) marbles, p = 0.050), but was not statistically different between 15 and 30 minutes (-0.598 (95%CI -1.308 to 0.112) marbles, p = 0.184).

Marbles half-buried was not statistically significantly different between 20 and 25 minutes (0.025 (95%CI -0.494 to 0.544) marbles, p = 1.000), or from 20 to 30 minutes (0.296 (95%CI -0.266 to 0.858) marbles, p = 1.000). Marbles half-buried was not statistically significantly different between 25 and 30 minutes (0.271 (95%CI -0.301 to 0.843) marbles, p = 1.000). When the identified outliers were removed, marbles half-buried were not significantly different from 5 to 20 minutes (1.441 (95%CI -0.013 to 2.895) marbles, p = 0.054).

"Marbles Displaced"

Summary

There was no significant interaction between GENOTYPE and TIME for marbles displaced, nor was there a significant main effect of GENOTYPE. The main effect of TIME was significant, with marbles displaced increasing rapidly and reaching the ceiling value (8 marbles) by ~25 to 30 minutes.

When the outliers were removed, Levene's test could not be computed because all absolute deviations were constant within each cell. Box's test of equality of covariance matrices could not be computed because there were fewer than two nonsingular cell covariance matrices. Mauchly's test of sphericity could not be calculated. Therefore, we did not continue the analysis.

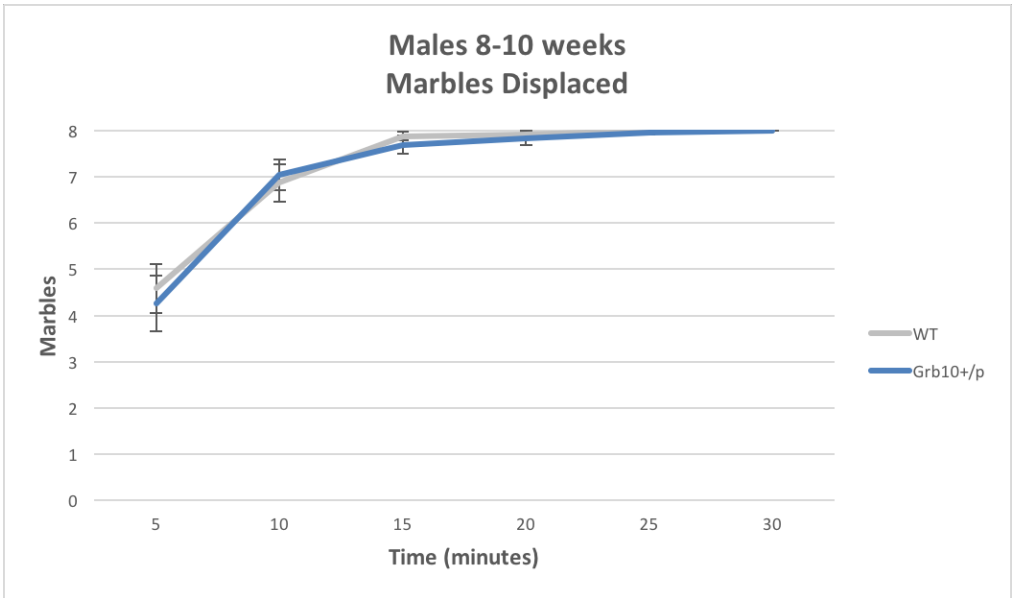

Figure 6.8 Males 8-10 wks Marbles Displaced

Report

Marbles displaced over the course of 30 minutes was assessed using a two-way mixed ANOVA, with "genotype" as the between-subjects factor with two groups, and "time" as the within-subjects factor with 6 levels. The aim was primarily to determine whether there was an interaction between genotype and time for marbles displaced and secondarily to determine the contributions of each factor.

There were three outliers with SRE more extreme than ± 3 SD. D21 P was a genuinely unusual data point at 15 minutes (SRE = -5.23), 20 minutes (SRE = -5.35), and 25 minutes (SRE = -6.71). D42 P was a genuinely unusual data point at 20 minutes (SRE = -3.62). These outliers were left in the analysis. The final trials included were WT (n = 24), *Grb10*$^{+/p}$ (n = 23).

Shapiro-Wilk's test indicated the data were only normally distributed for wildtype mice at 5 minutes. "Marbles displaced" was a constant value for both genotypes at thirty minutes, and for wildtypes at twenty-five minutes. For all other time points for both genotypes, the data were negatively skewed. Q-Q plots of the SREs were negatively skewed. The data were left untransformed for analysis.

Levene's test of equality of error variances showed the assumption of homogeneity of variances was met for all time points ($p > 0.05$), except twenty-five ($p = 0.038$) and thirty minutes, which could not be calculated, as it was a constant. Mixed ANOVA is not robust to violations of this assumption, so we first interpreted the 2-way MIXED ANOVA including all time bins, then removed the 25 and 30 min bins from the analysis and ran the 2-way ANOVA again for comparison. Removal of these time bins did not change the outcome of the analysis, so data for 25 and 30 minutes was left in the mixed ANOVA. When all time bins were included, Mauchly's test of sphericity indicated the assumption of sphericity was violated for the two-way interaction, $\chi^2(14) = 440.813$, $p < 0.001$. Epsilon (ε) was 0.315, as calculated by the Greenhouse-Geisser method, and was used to correct the mixed measures ANOVA.

Box's Test for equality of covariance matrices could not be computed because there were fewer than two nonsingular cell covariance matrices. When the 25 and 30 min bins were removed from the mixed ANOVA, Box's M was significant ($p = 0.004$). The interaction term between TIME and GENOTYPE should not be interpreted in our conclusions. However, we report the interaction term to help justify the interpretation of main effects analyses for

TIME and GENOTYPE below. There was no statistically significant interaction between TIME and GENOTYPE on marbles displaced, F(1.575, 70.884) = 0.213, p = 0.756, partial η^2 = 0.005, ε = 0.315.

The main effect of GENOTYPE showed there was not a statistically significant difference between *Grb10*$^{+/p}$ and WT groups, F(1,45) = 0.111, p = 0.741, partial η^2 = 0.002. The main effect of TIME shows a statistically significant difference in marbles displaced at different time points, F(1.575, 70.884) = 60.386, p < 0.001, partial η^2 = 0.573. Data for the following time points are estimated marginal mean $\pm$ standard error. Marbles displaced changed significantly over time, with 4.422 ± 0.398 at 5 minutes, 6.959 ± 0.262 at 10 minutes, 7.785 ± 0.105 at 15 minutes, 7.871 ± 0.079 at 20 minutes, 7.978 ± 0.021 at 25 minutes, and 8 ± 0.000 marbles at 30 minutes.

Post hoc analysis with the Bonferroni adjustment was carried out for all pairwise comparisons. Data are presented as mean difference with the 95% confidence interval. Marbles displaced statistically significantly increased from 5 to 10 minutes (2.537 (95% CI 1.582 to 3.493) marbles, p < 0.001), 5 to 15 minutes (3.363 (95% CI 2.194 to 4.532) marbles, p < 0.001), 5 to 20 minutes (3.449 (95% CI 2.241 to 4.657) marbles, p < 0.001), 5 to 25 minutes (3.556 (95% CI 2.330 to 4.782) marbles, p < 0.001), and from 5 to 30 minutes (3.587 (95% CI 2.345 to 4.811) marbles, p < 0.001). Marbles displaced statistically significantly increased from 10 to 15 minutes (0.826 (95% CI 0.155 to 1.498) marbles, p = 0.006), 10 to 20 minutes (0.912 (95% CI 0.177 to 1.647) marbles, p = 0.006), 10 to 25 minutes (1.019 (95% CI 0.220 to 1.818) marbles, p = 0.004), and from 10 to 30 minutes (1.041 (95% CI 0.227 to 1.853) marbles, p = 0.004).

Marbles displaced was not statistically significantly different from 15 to 20 minutes (0.086 (95% CI -0.073 to 0.245) marbles, p = 1.000), 15 to 25 minutes (0.193 (95% CI -0.086 to 0.471) marbles, p = 0.557), or from 15 to 30 minutes (0.215 (95%CI -0.112 to 0.541) marbles, p = 0.714. Marbles displaced was not statistically significantly different from 20 to 25 minutes (0.107 (95% CI -0.089 to 0.303) marbles, p = 1.000), or from 20 to 30 minutes (0.129 (95%CI -0.116 to 0.373) marbles, p = 1.000). Marbles displaced was not statistically significantly different between 25 and 30 minutes (0.022 (95% CI -0.044 to 0.088) marbles, p = 1.000).

6.3.3 Marbles Buried, Half-buried, and Displaced–Males 6 months

"Marbles Buried"

Summary

The five-minute bin violated the assumption of homogeneity of variances. Removal of this time bin from the two-way ANOVA did not change the significance outcomes of the analysis, so the 5 minute time bin was left in the final analysis.

Box's M was significant, so we did not interpret the interaction term of the two-way ANOVA analysis of marbles buried by male mice 6 months of age. The main effect of GENOTYPE was not significant. The main effect of TIME was significant. Marbles buried by male mice 6 months of age increased from 5, 10, and 15 minutes to all later time points, but was not significantly different in pairwise comparisons between 20, 25, and 30 minutes.

When the eight outliers were removed, the five minute time bin satisfied the assumption of homogeneity of error variance and was included in the analysis. Box's M still could not be calculated, so we could not interpret the interaction term for the two-way mixed ANOVA. The removal of the eight outliers did not change outcome of the 2-way mixed ANOVA for main effects or post hoc pairwise comparisons for TIME.

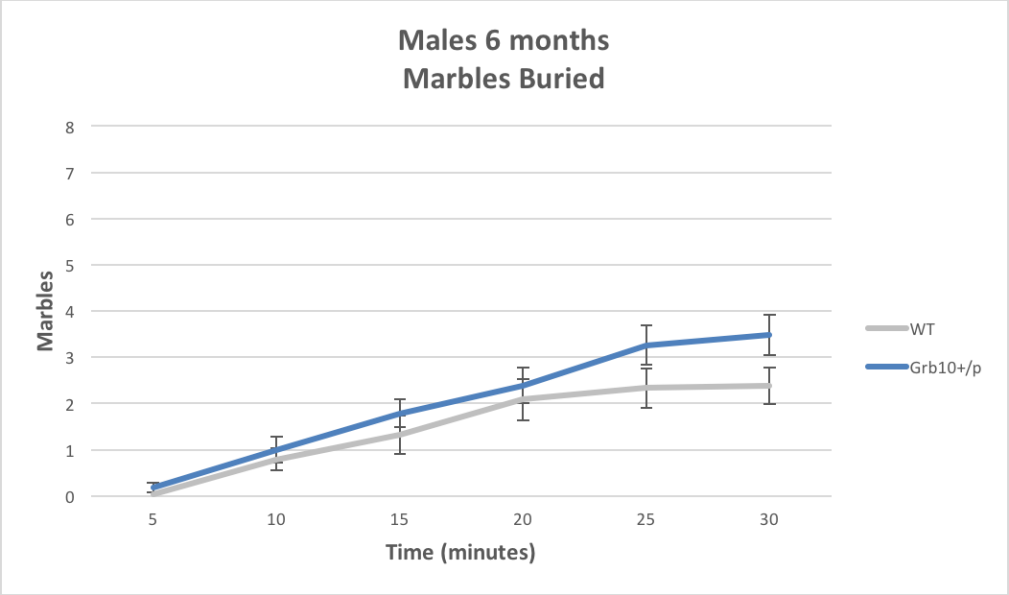

Figure 6.9 Males 6 months Marbles Buried

Report

The Shapiro-Wilk's test indicated none of the data was normally distributed except *Grb10*$^{+/p}$ trials for 25 and 30 minutes. Histograms of the raw data show positive skew for both genotype groups at 5, 10, and 15 minutes. At 20 minutes, the histogram for wildtypes shows positive skew, and the histogram for *Grb10*$^{+/p}$ shows a bimodal distribution. At 25 and 30 minutes, the WT histograms are bimodal. Visual inspection of the Q-Q plots of the SREs

indicates SREs for 20, 25, and 30 minutes are normally distributed. The Q-Q plots of the SREs for 5, 10, and 15 minutes are not normal.

Levene's test indicated there was homogeneity of variance for all time bins ($p > 0.05$) except 5 minutes ($p = 0.014$). There are no appropriate transformations for this data and there are no mixed ANOVA methods robust to the violation of the assumption of homogeneity. Therefore, the two-way ANOVA was first including the 5-minute bin, and then again excluding the 5-minute bin for comparison. Mauchly's test was significant, indicating the assumption of sphericity was violated, $\chi^2(14) = 57.631$, $p < 0.001$. A Greenhouse-Geisser correction was applied to the 2-way mixed ANOVA, $\varepsilon = 0.643$.

With the 5-minute bin included, Box's M was significant, indicating the assumption of homogeneity of covariances was violated, $p < 0.001$. Therefore, we will not interpret the interaction between TIME and GENOTYPE, though it is reported to help justify the main effects analysis. The interaction between TIME and GENOTYPE was reported as not significant, $F(3.213,144.601) = 1.367$, $p = 0.254$, partial $\eta^2 = 0.029$.

The main effect of GENOTYPE was not significant, $F(1,45) = 1.870$, $p = 0.178$, partial $\eta^2 = 0.040$. The main effect of TIME was statistically significant, $F(3.213,144.601) = 42.050$, $p < 0.001$, partial $\eta^2 = 0.483$. Data for the following time points are estimated marginal mean ± standard error, unless otherwise stated. Marbles buried changed significantly over time with 0.108 ± 0.054 at 5 minutes, 0.896 ± 0.182 at 10 minutes, 1.558 ± 0.258 at 15 minutes, 2.237 ±

0.291 at 20 minutes, 2.797 ± 0.303 at 25 minutes, and 2.927 ± 0.293 marbles at 30 minutes.

Post hoc analysis with the Bonferroni adjustment was carried out for all pairwise comparisons. Data are presented as mean difference in marbles with the 95% confidence interval. Marbles buried increased significantly from 5 to 10 minutes (0.788 (95%CI 0.275 to 1.301) marbles, $p < 0.001$), 5 to 15 minutes (1.450 (95%CI 0.692 to 2.208) marbles, $p < 0.001$), 5 to 20 minutes (2.130 (95%CI 1.253 to 3.006) marbles, $p < 0.001$), 5 to 25 minutes (2.689 (95%CI 1.773 to 3.606) marbles, $p < 0.001$), and 5 to 30 minutes (2.819 (95%CI 1.934 to 3.704) marbles, $p < 0.001$). There was a significant difference from 10 to 15 minutes (0.662 (95%CI 0.030 to 1.294) marbles, $p = 0.033$, 10 to 20 minutes (1.341 (95%CI 0.571 to 2.112) marbles, $p < 0.001$), 10 to 25 minutes (1.901 (95%CI 1.058 to 2.744) marbles, $p < 0.001$), and 10 to 30 minutes (2.031 (95%CI 1.217 to 2.844) marbles, $p < 0.001$). There was a significant difference from 15 to 20 minutes (0.679 (95%CI 0.033 to 1.326) marbles, $p = 0.032$), 15 to 25 minutes (1.239 (95%CI 0.425 to 2.053) marbles, $p < 0.001$), and 15 to 30 minutes (1.369 (95%CI 0.612 to 2.125), $p < 0.001$).

There was no significant difference from 20 to 25 minutes (0.560 (95%CI -0.157 to 1.277) marbles, $p = 0.294$), or from 20 to 30 minutes (0.689 (95%CI -0.033 to 1.412) marbles, $p = 0.074$). There was no significant difference in marbles buried by male mice 6 months of age from 25 to 30 minutes (0.130 (95%CI -0.312 to 0.571) marbles, $p = 1.000$).

"Marbles Half-Buried"

Summary

There was no significant interaction between GENOTYPE and TIME on marbles half-buried, nor was there a significant main effect of GENOTYPE. There was a significant main effect of TIME, with marbles half-buried increasing from 5 minutes to 10 and 15 minutes, but leveling out between all other pairwise comparisons. The removal of the eight identified outliers did not change the outcome of the analysis.

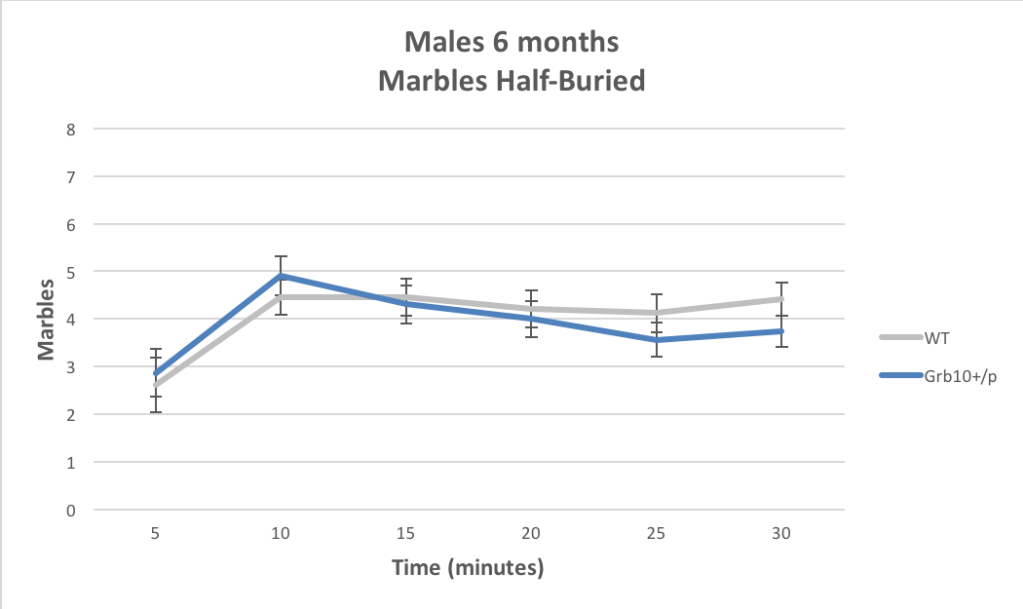

Figure 6.10 Males 6 months Marbles Half-Buried

Report

The Shapiro-Wilk's test indicated the assumption of normality was met for data sets at all time points except 5 minutes, where both wildtype and *Grb10*$^{+/p}$ trials were non-normally distributed. Histograms of the raw data show wildtype data at 5 minutes were bimodally distributed and *Grb10*$^{+/p}$ data were positively skewed. The Q-Q plots of the studentized residuals show

normality for 10, 15, 20, 25, and 30 minutes, with some deviations from normality for 5 minutes. No transformations were applied. There was homogeneity of variance and covariance, as assessed by Levene's test ($p > 0.05$) and Box's M ($p = 0.702$) respectively. Mauchly's Test was significant, indicating a violation of the assumption of sphericity, $\chi^2(14) = 58.600$, $p < 0.001$. A Greenhouse-Geisser correction was applied to the 2-way mixed ANOVA, $\varepsilon = 0.598$.

The interaction between TIME and GENOTYPE was not statistically significant, $F(2.992, 134.646) = 0.693$, $p = 0.558$, partial $\eta^2 = 0.015$, $\varepsilon = 0.598$. The main effect of GENOTYPE was also not statistically significant, $F(1,45) = 0.223$, $p = 0.639$, partial $\eta^2 = 0.005$.

There was a statistically significant main effect of TIME on marbles half-buried, $F(2.992,134.646) = 6.339$, $p < 0.001$, partial $\eta^2 = 0.123$, $\varepsilon = 0.598$. Data for the following time points are estimated marginal mean $\pm$ standard error. The number of marbles half buried changed over time, with 2.747 ± 0.379 at 5 minutes, 4.686 ± 0.271 at 10 minutes, 4.381 ± 0.281 at 15 minutes, 4.104 ± 0.272 at 20 minutes, 3.845 ± 0.268 at 25 minutes, and 4.078 ± 0.244 marbles at 30 minutes.

Post hoc analysis with the Bonferroni adjustment was carried out for all pairwise comparisons. Data are presented as mean difference in marbles with the 95% confidence interval. The number of marbles half-buried increased significantly from 5 to 10 minutes (1.938 (95%CI 0.876 to 3.001) marbles, $p < 0.001$) and from 5 to 15 minutes (1.634 (95%CI 0.328 to 2.940) marbles, $p = 0.005$, but not from 5 to 20 minutes (1.357 (95%CI -0.148 to 2.862)

marbles, p = 0.114), 5 to 25 minutes (1.098 (95%CI -0.417 to 2.613) marbles, p = 0.444), or 5 to 30 minutes (1.331 (95%CI -0.205 to 2.866) marbles, p = 0.151).

The number of marbles half-buried was not statistically different from 10 to 15 minutes (-0.304 (95%CI -1.339 to 0.790) marbles, p = 1.000), 10 to 20 minutes (-0.582 (-1.777 to 0.614) marbles, p = 1.000), 10 to 25 minutes (-0.841 (-2.040 to 0.359) marbles, p = 0.527), or from 10 to 30 minutes (-0.608 (95%CI -1.859 to 0.643) marbles, p = 1.000). Marbles half-buried was not statistically different from 15 to 20 minutes (-0.277 (95%CI -1.170 to 0.616) marbles, p = 1.000), 15 to 25 minutes (-0.536 (95%CI -1.450 to 0.378) marbles, p = 1.000), or 15 to 30 minutes (-0.303 (95%CI -1.341 to 0.734) marbles, p = 1.000). Marbles half-buried was not statistically different from 20 to 25 minutes (-0.259 (95%CI -1.067 to 0.549) marbles, p = 1.000), or from 20 to 30 minutes (-0.026 (95%CI -1.018 to 0.966) marbles, p = 1.000). Marbles half-buried did not statistically differ between 25 and 30 minutes (0.233 (95%CI -0.462 to 0.929) marbles, p = 1.000).

"Marbles Displaced"

Summary

The interaction between GENOTYPE and TIME could not be interpreted because Box's M was significant. Main effects analysis was carried out. There was no significant main effect of GENOTYPE on marbles displaced by mice 6 months of age, but there was a significant main effect of TIME. Marbles displaced increased significantly in pairwise comparisons from 5 or 10 minutes to all other time points, but not between any other time points.

When the eight identified outliers were removed, none of the cells except *Grb10*$^{+/p}$ data at 5 minutes were normally distributed, and *Grb10*$^{+/p}$ data at 25 and 30 minutes became constant values. There was homogeneity of error variance for all time bins except 10 minutes, which was removed from the subsequent analysis. Box's M and Mauchly's test could not be calculated. When the analysis was run without time points 25 and 30 minutes, Mauchly's test was calculated and was found to be significant. Therefore, we did not interpret the interaction term of the two-way mixed ANOVA and applied a Greenhouse-Geisser correction to the main effect of TIME. The main effect of TIME, but not of GENOTYPE, was significant. Marbles displaced increased from 5 minutes to 15, 20, 25, and 30 minutes. No other pairwise comparisons were significant.

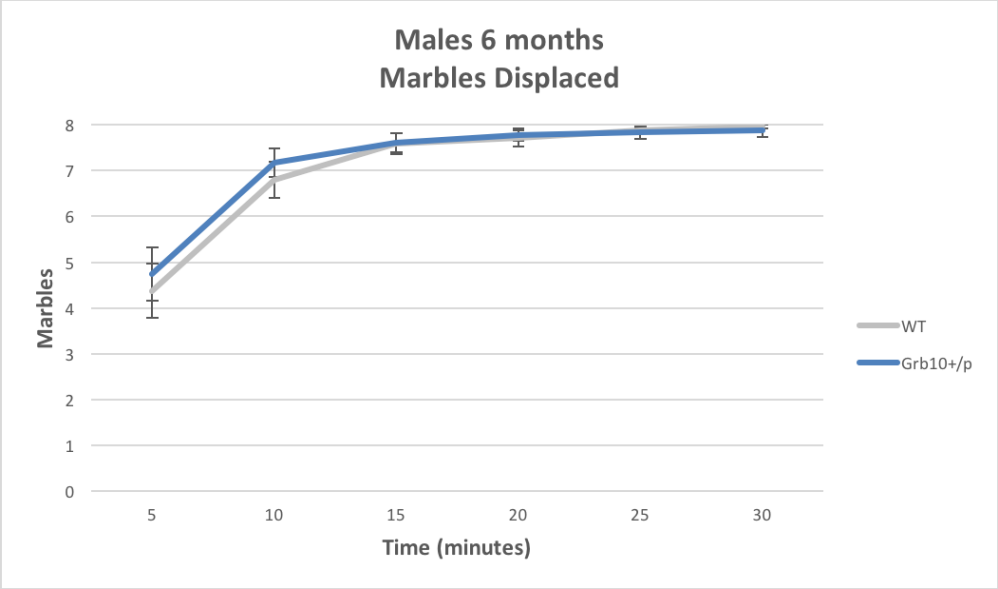

Figure 6.11 Males 6 months Marbles Displaced

Report

The Shapiro-Wilks test indicated the assumption of normality was violated for all data sets in marbles displaced. Histograms of the raw data show negative skew for 5, 10, 15, 20, 25, and 30 minutes. Visual analysis of the Q-Q plots for studentized residuals (SREs) shows non-normal distributions for all time points except 5 minutes. Transformations were not appropriate and not applied. There was homogeneity of error variances ($p > 0.05$) for all time bins, as calculated by Levene's test. Mauchly's test of sphericity was significant, indicating the assumption of sphericity was violated, $\chi^2(14) = 350.918$, $p < 0.001$. We applied the Greenhouse-Geisser correction to the 2-way mixed ANOVA ($\varepsilon = 0.320$).

Box's M indicated the assumption of equality of covariances was violated ($p < 0.001$). Therefore, the interaction between TIME and GENOTYPE is not interpreted in our conclusions, but it is reported to help justify the subsequent interpretation of main effects analyses below: the interaction between TIME and GENOTYPE was calculated to be nonsignificant, $F(1.602,72.107) = 0.339$, $p = 0.666$, partial $\eta^2 = 0.007$.

The main effect of GENOTYPE was not significant, $F(1,45) = 0.167$, $p = 0.685$, partial $\eta^2 = 0.004$. There was a significant main effect of TIME on marbles displaced, $F(1.602, 72.107) = 53.635$, $p < 0.001$, partial $\eta^2 = 0.544$. Data for the following time points are estimated marginal mean $\pm$ standard error. The number of marbles displaced increased significantly over time, with 4.557 ± 0.413 at 5 minutes, 6.983 ± 0.253 at 10 minutes, 7.596 ± 0.156 at 15 minutes,

7.745 ± 0.113 at 20 minutes, 7.851 ± 0.075 at 25 minutes, and 7.914 ± 0.067 at 30 minutes.

Post hoc analysis with the Bonferroni adjustment was carried out for all pairwise comparisons. Data are presented as mean difference in marbles with the 95% confidence interval. Marbles displaced statistically significantly increased from 5 to 10 minutes (2.426 (95%CI 1.427 to 3.425) marbles, $p < 0.001$), 5 to 15 minutes (3.039 (95%CI 1.894 to 4.184) marbles, $p < 0.001$), 5 to 20 minutes (3.188 (95%CI 2.001 to 4.376) marbles, $p < 0.001$), 5 to 25 minutes (3.293 (95%CI 2.076 to 4.511) marbles, $p < 0.001$), and 5 to 30 minutes (3.357 (95%CI 2.098 to 4.615) marbles, $p < 0.001$). Marbles displaced statistically significantly increased from 10 to 15 minutes (0.613 (95%CI 0.110 to 1.116) marbles, $p = 0.007$), 10 to 20 minutes (0.763 (95%CI 0.147 to 1.378) marbles, $p = 0.006$), 10 to 25 minutes (0.868 (95%CI 0.177 to 1.559) marbles, $p = 0.005$), and 10 to 30 minutes (0.931 (95%CI 0.180 to 1.683) marbles, $p = 0.006$).

Marbles displaced was not statistically different between 15 and 20 minutes (0.149 (95%CI -0.102 to 0.401) marbles, $p = 1.000$), 15 to 25 minutes (0.255 (95%CI -0.108 to 0.617) marbles, $p = 0.520$), or 15 to 30 minutes (0.318 (95%CI -0.130 to 0.765) marbles, $p = 0.492$). Marbles displaced was not statistically different between 20 and 25 minutes (0.105 (95%CI -0.111 to 0.321) marbles, $p = 1.000$), or between 20 and 30 minutes (0.168 (95%CI -0.120 to 0.457) marbles, $p = 1.000$. Marbles displaced was not statistically different between 25 and 30 minutes (0.063 (95%CI -0.049 to 0.176) marbles, $p = 1.000$).

6.3.4 Marbles Buried, Half-Buried, and Displaced–Males 10 mo

"Marbles Buried"

Summary

All "marbles buried" data were non-normally distributed except *Grb10*$^{+/p}$ data at 30 minutes. The assumption of homogeneity of covariance was violated, so we did not interpret the interaction between TIME and GENOTYPE. The main effect of GENOTYPE was not significant, but there was a significant main effect of TIME. Marbles buried by male mice 10 months of age increased from 5, 10, and 15 minutes to all later time points and leveled out between 20 and 30 minutes.

Removing the six outliers resulted in the normalization of some, but not all, data sets for marbles buried. Box's M could be computed, allowing interpretation of the interaction term for the two-way mixed ANOVA. Data at 10 minutes violated the assumption of homogeneity of error variance. When the 10 minute time bin was included, the removal of the six outliers did not change the outcome of the 2-way ANOVA.

However, when the 10 minute time bin was removed as well as the six outliers, the interaction between TIME and GENOTYPE was statistically significant ($F(2.426, 101.882) = 2.965$, $p = 0.046$, partial $\eta^2 = 0.066$), as was the simple main effect of TIME (Wildtype trials $F(2.364,59.109) = 27.805$, $p < 0.001$, partial $\eta^2 = 0.527$; *Grb10*$^{+/p}$ $F(2.088, 35.489) = 17.862$, $p < 0.001$, partial $\eta^2 = 0.512$). The simple main effect of GENOTYPE was significant only at 15 minutes, $F(1,42) = 5.275$, $p = 0.027$, partial $\eta^2 = 0.112$. For wildtype trials, the number of marbles buried increased statistically significantly in all pairwise comparisons

except from 20 to 30 and 25 to 30 minutes. For *Grb10*$^{+/p}$ trials, the number of marbles buried increased between 5 minutes and all other time bins, but not between any other pairwise comparisons.

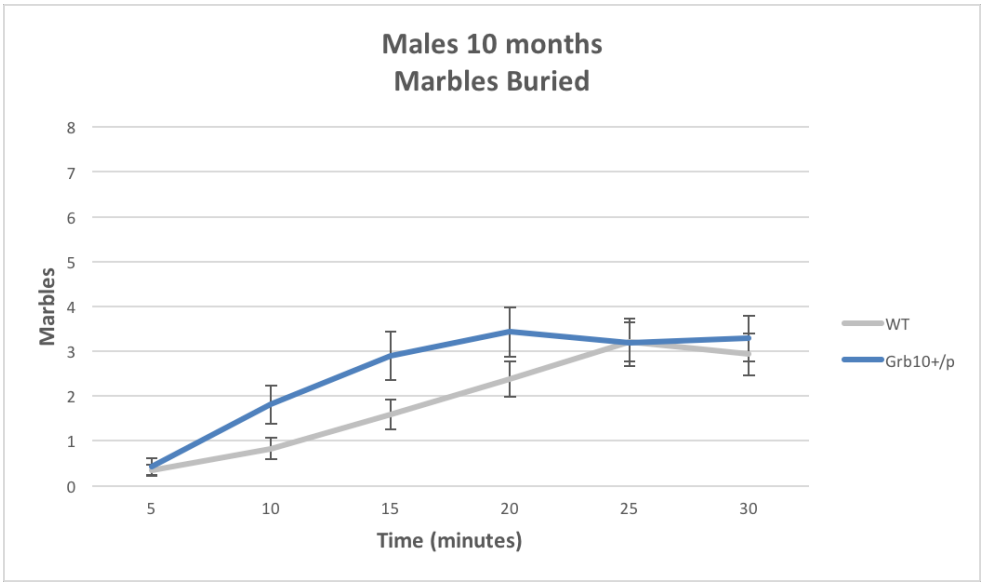

Figure 6.12 Males 10 months Marbles Buried

Report

The Shapiro-Wilk's test indicated the data all were non-normally distributed except for *Grb10*$^{+/p}$ data at 30 minutes. Histograms of the raw data show positive skew for data at 5 and 10 minutes (both genotypes). There is also positive skew for WT data at 20 and 30 minutes and *Grb10*$^{+/p}$ data at 25 minutes. The histogram for *Grb10*$^{+/p}$ data at 15 and 20 minutes and for WT data at 25 minutes is approximately bimodal. The histogram of *Grb10*$^{+/p}$ data at 30 minutes is leptokurtotic. Transformations were not appropriate to this data set and were not applied. Q-Q plots of the studentized residuals (SREs) showed normal distributions at 15, 20, 25, and 30 minutes. The Q-Q plots at 5 and 10 minutes showed some negative skew. At 5 minutes, there were two

outliers with SRE more extreme than ±3 SD: A53 P, SRE = 3.44; A69 P SRE = 3.35.

There was homogeneity of error variances for all time bins, as assessed by Levene's Test ($p > 0.05$). Mauchly's test was significant, indicating the assumption of sphericity was violated, $\chi^2(14) = 86.388$, $p < 0.001$. A Greenhouse-Geisser correction was applied to the two-way mixed measures ANOVA, $\varepsilon = 0.522$. The assumption of homogeneity of covariances was violated, as Box's M was significant ($p = 0.027$). Therefore, we do not interpret the interaction term between TIME and GENOTYPE in our conclusions, but it is reported to help justify the use of main effects analyses below. The interaction between TIME and GENOTYPE was reported as not significant, $F(2.611, 125.351) = 2.672$, $p = 0.058$, partial $\eta^2 = 0.053$.

The main effect of GENOTYPE on marbles buried was not significant, $F(1,48) = 1.692$, $p = 0.200$, partial $\eta^2 = 0.034$. There was a significant main effect of TIME on marbles buried, $F(2.611, 125.351) = 43.586$, $p < 0.001$, partial $\eta^2 = 0.476$. Data for the following time points are estimated marginal mean ± standard error, unless otherwise stated. Marbles buried changed significantly over TIME, with 0.387 ± 0.113 at 5 minutes, 1.319 ± 0.228 at 10 minutes, 2.245 ± 0.300 at 15 minutes, 2.904 ± 0.323 at 20 minutes, 3.199 ± 0.344 at 25 minutes, and 3.108 ± 0.346 marbles at 30 minutes.

Post hoc analysis with the Bonferroni adjustment was carried out for all pairwise comparisons. Data are presented as mean difference in marbles with the 95% confidence interval. Marbles buried increased significantly from 5 to 10 minutes (0.932 (95%CI 0.404 to 1.459) marbles, $p < 0.001$), from 5 to

15 minutes (1.859 (95%CI 1.029 to 2.688) marbles, p < 0.001), from 5 to 20 minutes (2.517 (95%CI 1.616 to 3.418) marbles, p < 0.001), from 5 to 25 minutes (2.812 (95%CI 1.845 to 3.779) marbles, p < 0.001), and from 5 to 30 minutes (2.722 (95%CI 1.712 to 3.731) marbles, p < 0.001). Marbles buried increased significantly from 10 to 15 minutes (0.927 (95%CI 0.260 to 1.594) marbles, p = 0.001), from 10 to 20 minutes (1.585 (95%CI 0.808 to 2.363) marbles, p < 0.001), from 10 to 25 minutes (1.880 (95%CI 1.000 to 2.760) marbles, p < 0.001), and from 10 to 30 minutes (1.790 (95%CI 0.909 to 2.670) marbles, p < 0.001). Marbles buried significantly increased from 15 to 20 minutes (0.658 (95%CI 0.198 to 1.119) marbles, p = 0.001), from 15 to 25 minutes (0.953 (95%CI 0.337 to 1.570), p < 0.001), and from 15 to 30 minutes (0.863 (95%CI 0.170 to 1.555) marbles, p = 0.005).

Marbles buried was not statistically different from 20 to 25 minutes (0.295 (95%CI -0.255 to 0.844) marbles, p = 1.000), or from 20 to 30 minutes (0.204 (95%CI -0.459 to 0.868) marbles, p = 1.000). Marbles buried was not statistically different from 25 to 30 minutes (-0.090 (95%CI -0.583 to 0.403) marbles, p = 1.000).

"Marbles Half-Buried"

Summary

Data for time bin 10 minutes violated the assumption of homogeneity of error variances. Removal of this time bin from the two-way ANOVA did not change the significance outcomes of the analysis, so the 10 minute time bin was left in the final analysis.

There was no significant interaction between TIME and GENOTYPE, nor was the main effect of GENOTYPE significant. There was a significant main effect of TIME; marbles half-buried by male mice 10 months of age increased from 5 to 10 and 15 minutes, but not for any other pairwise comparisons.

Removing the six outliers restored the normality of data at 30 minutes, acquired a non-normal distribution of data at 15 minutes, and maintained non-normal distributions at 5 and 20 minutes. There was homogeneity of variance for all time bins, including 10 minutes, which was left in the analysis of the data. The outcome of the analysis of marbles half-buried did not change when the six original outliers were removed.

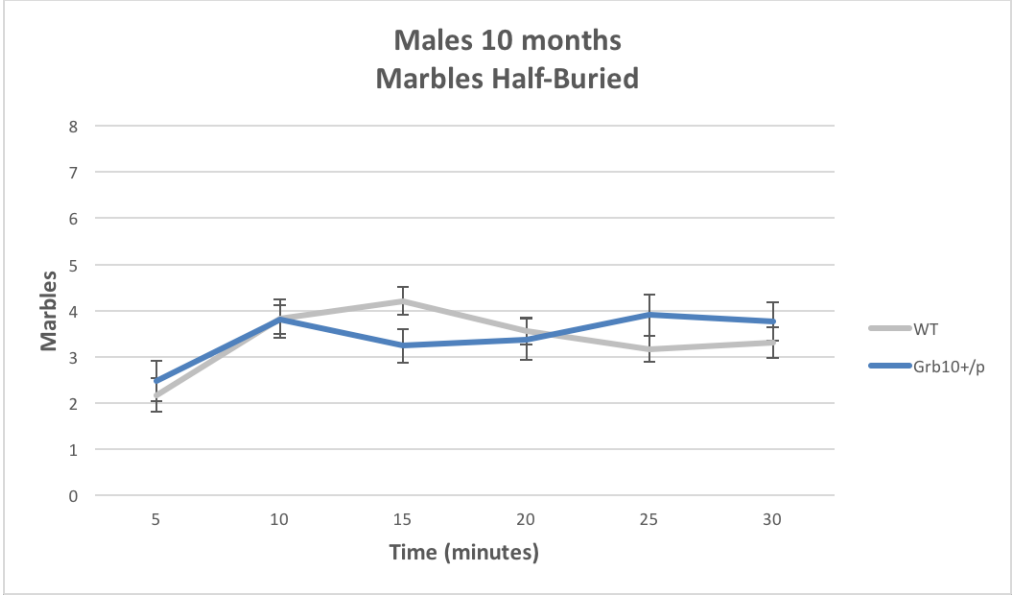

Figure 6.13 Males 10 months Marbles Half-Buried

Report

Shapiro-Wilk's test indicated the data were normally distributed for all genotypes and time bins ($p > 0.05$) except wildtype data at 5 ($p = 0.002$), 20 (p

= 0.001), and 30 minutes (p = 0.034). Histograms of the raw data show positive skew for wildtype data at 5, 20, and 30 minutes. Wildtype data at 30 minutes were also platykurtic at lower values. Transformations were not appropriate for this data and were not applied. ANOVA is robust to deviations from normality. There were no outliers with studentized residuals (SREs) more extreme than $\pm$ 3 SD. Q-Q plots of the SREs showed normal distributions for all time bins.

There was homogeneity of error variances for all time bins (p > 0.05) except 10 minutes (p = 0.039). As there are no methods for mixed ANOVA robust to this violation, we first interpreted the 2-way mixed ANOVA including the 10 minutes time bin, and then removed the 10 minute time bin from the analysis and ran the 2-way mixed ANOVA again for comparison. Including the 10 minute time bin, there was homogeneity of covariances, as assessed by Box's M (p = 0.477). Mauchly's test was significant, indicating the assumption of sphericity was violatd, $\chi^2(14) = 95.023$, p < 0.001. A Greenhouse-Geisser correction was applied to the 2-way mixed ANOVA, $\varepsilon = 0.503$.

There was no significant interaction between TIME and GENOTYPE for marbles half-buried, F(2.514, 120.678) = 1.662, p = 0.186, partial $\eta^2 = 0.033$. The main effect of GENOTYPE was not significant, F(1,48) = 0.032, p = 0.860, partial $\eta^2 = 0.001$. There was a statistically significant main effect of TIME on marbles half-buried by male mice 10 months of age, F(2.514, 120.678) = 5.514, p = 0.03, partial $\eta^2 = 0.103$. Data for the following time points are estimated marginal mean ± standard error, unless otherwise stated. Marbles half-buried changed significantly over time, with 2.324 ± 0.283 marbles at 5 minutes, 3.819

± 0.280 at 10 minutes, 3.722 ± 0.236 at 15 minutes, 3.466 ± 0.253 at 20 minutes, 3.539 ± 0.253 at 25 minutes, and 3.536 ± 0.263 marbles at 30 minutes.

Post hoc analysis with the Bonferroni adjustment was carried out for all pairwise comparisons. Data are reported as mean difference with 95% confidence intervals. Marbles half-buried increased significantly from 5 to 10 minutes (1.494 (95%CI 0.498 to 2.491) marbles, $p < 0.001$) and 5 to 15 minutes (1.398 (95%CI 0.171 to 2.625) marbles, $p = 0.014$), but not from 5 to 20 minutes (1.142 (95%CI -0.190 to 2.474) marbles, $p = 0.163$), 5 to 25 marbles (1.214 (95%CI -0.158 to 2.586) marbles, $p = 0.131$), or from 5 to 30 marbles (1.212 (95%CI -0.170 to 2.593) marbles, $p = 0.140$).

Marbles half-buried did not statistically differ from 10 to 15 minutes (-0.096 (95%CI -0.948 to 0.756) marbles, $p = 1.000$), 10 to 20 minutes (-0.352 (95%CI -1.521 to 0.817) marbles, $p = 1.000$), 10 to 25 minutes (-0.280 (95%CI -1.402 to 0.842) marbles, $p = 1.000$), or from 10 to 30 minutes (-0.282 (95%CI -1.371 to 0.806) marbles, $p = 1.000$). There was no significant difference from 15 to 20 minutes (-0.256 (95%CI -1.026 to 0.513) marbles, $p = 1.000$), 15 to 25 minutes (-0.184 (95%CI -0.922 to 0.555) marbles, $p = 1.000$), or 15 to 30 minutes (-0.186 (95%CI -0.892 to 0.519) marbles, $p = 1.000$). There was no significant difference from 20 to 25 minutes (0.072 (95%CI -0.560 to 0.705) marbles, $p = 1.000$), or from 20 to 30 minutes (0.070 (95%CI -0.589 to 0.728) marbles, $p = 1.000$). There was no significant difference from 25 to 30 minutes (-0.002 (95%CI -0.537 to 0.532) marbles, $p = 1.000$).

In a secondary comparative analysis, the 10 minute time bin was removed due to its violation of the assumption of homogeneity of error variances. This did not change the outcome of the 2-way ANOVA, so the 10 minute time bin was left in the final analysis.

"Marbles Displaced"

Summary

Data at 15 minutes violated the assumption of homogeneity of error variances. Removal of this time bin from the 2-way ANOVA did not change the significance outcomes of the analysis, so the 15 minute time bin was left in the final analysis.

Box's M could not be computed and therefore the interaction between TIME and GENOTYPE was not interpreted. Mauchly's test was also not computed. When time points 25 and 30 minutes (which have identical data) were removed from the analysis, Mauchly's test was significant. Therefore, a Greenhouse-Geisser correction was applied to the two-way mixed ANOVA including all time bins. The main effect of GENOTYPE was not significant. There was a significant main effect of TIME on marbles displaced by male mice 10 months of age. Marbles displaced increased from 5 and 10 minutes to all other time bins, but not between any other pairwise comparisons.

Outliers were separately removed from the analysis to check for their potential impact on the significance outcome. Levene's F statistics could not be computed for this 2-way mixed ANOVA because all absolute deviations are

constant within each cell. There are no robust mixed ANOVA methods to deal with this violation. Therefore, we did not continue to interpret the analysis.

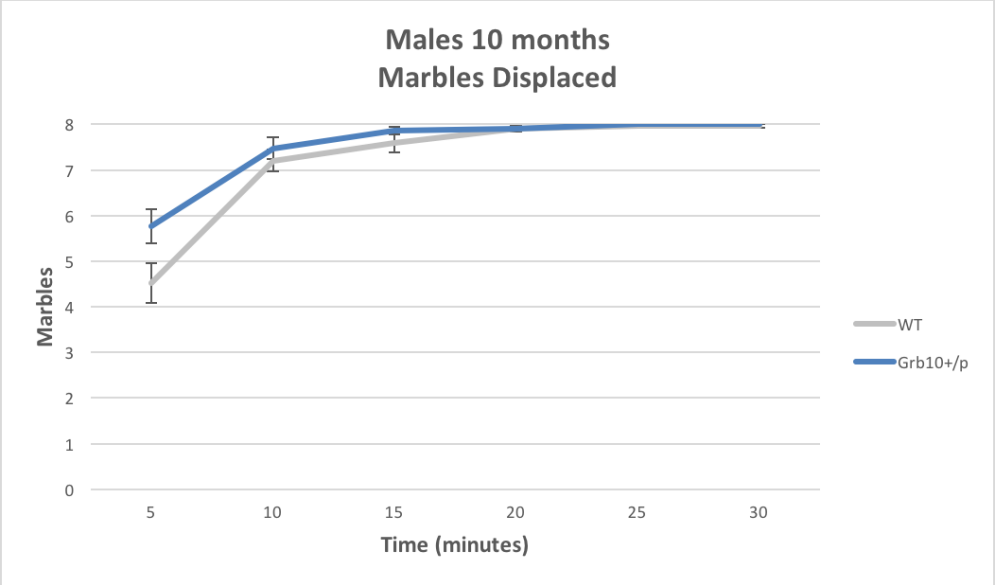

Figure 6.14 Males 10 months Marbles Displaced

Report

Shapiro-Wilk's test indicated none of the data were normally distributed except for *Grb10*$^{+/p}$ data at 5 minutes (p = 0.083). Data for *Grb10*$^{+/p}$ trials at 25 and 30 minutes were constant values. Histograms of the data show a platykurtotic distribution for WT data at 5 minutes. There is negative skew for data at 10, 15, 20, and WT data at 25 and 30 minutes. WT data at 25 and 30 minutes are kept from being constant values by the outlier A66 P, SRE = -6.93 at 25 and 30 minutes.

Q-Q plots of the studentized residuals (SREs) show a normal distribution at 5 minutes, with right-skewed SREs at 10 and 15 minutes. Q-Q plots of the SREs at 20, 25, and 30 minutes are far from normal, due to the

near-constant values at these time bins. There were four outliers with SREs more extreme than $\pm$ 3SD: A18 P SRE = -3.50 at 10 minutes, SRE = -5.42 at 15 minutes; A66 P SRE = -3.06 at 15 minutes, SRE = -6.93 at 25 and 30 minutes; A15 P SRE = -3.03 at 20 minutes; A25 P SRE = -3.03 at 20 minutes. These genuinely unusual data points were left in the analysis. Transformations were not appropriate to the data and were not applied.

Levene's test indicated there was homogeneity of error variances for all time bins ($p > 0.05$) except 15 minutes ($p = 0.038$). Mixed ANOVA is not robust to violations of this assumption, so we first interpreted the 2-way mixed ANOVA including the 15 minutes time bin, and then removed the 15 minute time bin from the analysis and ran the 2-way mixed ANOVA again for comparison. Mauchly's test was not computed. When time points 25 and 30 minutes (which have identical data) were removed from the analysis, Mauchly's test was significant, $\chi^2(5) = 72.823$, $p < 0.001$. A Greenhouse-Geisser correction was applied to the two-way mixed ANOVA including time points 25 and 30 min, $\varepsilon = 0.320$.

Box's M could not be computed because there are fewer than two nonsingular cell covariance matrices. Therefore, the interaction term between TIME and GENOTYPE is not interpreted in our conclusions. The failure of the Box's M calculation suggests the data are very similar, especially at 25 and 30 minutes where the outlier A66 P keeps them from being constant values. We report the interaction term to help justify the interpretation of main effects analyses for TIME and GENOTYPE below: the interaction between TIME and

GENOTYPE was calculated to be F(1.598,76.696) = 3.217, p = 0.056, partial η^2 = 0.063.

The main effect of GENOTYPE on marbles displaced by male mice 10 months of age was not significant, F(1,48) = 2.734, p = 0.105, partial η^2 = 0.054. There was a significant main effect of TIME, F(1.598,76.696) = 70.418, p < 0.001, partial η^2 = 0.595. Data for the following time points are estimated marginal mean ± standard error, unless otherwise stated. Marbles displaced by male mice 10 months of age significantly increased over time with 5.140 ± 0.302 marbles at 5 minutes, 7.342 ± 0.175 at 10 minutes, 7.722 ± 0.123 at 15 minutes, 7.901 ± 0.044 marbles at 20 minutes, and 7.983 ± 0.020 marbles at both 25 and 30 minutes.

Post hoc analysis with the Bonferroni adjustment was carried out for all pairwise comparisons. Data are presented as mean difference with the 95% confidence interval. Marbles displaced increased significantly from 5 to 10 minutes (2.202 (95%CI 1.5112 to 2.891) marbles, p < 0.001), 5 to 15 minutes (2.582 (95%CI 1.755 to 3.409) marbles, p < 0.001), 5 to 20 minutes (2.761 (95%CI 1.868 to 3.654) marbles, p < 0.001), 5 to 25 minutes (2.843 (95%CI 1.924 to 3.762) marbles, p < 0.001), and 5 to 30 minutes (2.843 (95%CI 1.924 to 3.762) marbles, p < 0.001). There was a significant increase from 10 to 15 minutes (0.380 (95%CI 0.020 to 0.740) marbles, p = 0.031), 10 to 20 minutes (0.559 (95%CI 0.067 to 1.051) marbles, p = 0.015), 10 to 25 minutes (0.641 (95%CI 0.112 to 1.170) marbles, p = 0.007), and 10 to 30 minutes (0.641 (95%CI 0.112 to 1.170) marbles, p = 0.007).

There was no significant difference in marbles displaced from 15 to 20 minutes (0.179 (95%CI -0.166 to 0.524) marbles, p = 1.000), 15 to 25 minutes (0.261 (95%CI -0.097 to 0.619) marbles, p = 0.433), or 15 to 30 minutes (0.261 (95%CI -0.097 to 0.619) marbles, p = 0.433). There was no significant difference from 20 to 25 or 30 minutes (for both: 0.082 (95%CI -0.040 to 0.205) marbles, p = 0.655). There were no differences in the data for 25 and 30 minutes.

6.3.5 False Discovery Rate Corrections–Marble Burying

The Benjamini-Liu (BL) procedure was used to correct for false discovery rate (FDR) of 5% over the entirety of measures in the marble burying analysis (Yoav Benjamini et al., 2001). Out of 172 tests, 83 were originally found to be significant. After FDR correction, 56 tests remained significant. Of these 56 tests, 9 were significant main effects: 8 were significant main effects of TIME, and 1 was a significant main effect of AGE. There were no significant main effects of GENOTYPE for any measures of the marble burying test after FDR corrections.

Table 6.2 Abridged FDR Corrections–Marble Burying

Finding	P value	Rank (m=172)	BL = (min 0.05, 0.05*m/(m+1-i)^2	(BL) – P value
Cohort D Marbles Buried–Greenhouse-Geisser main effect TIME	5.71E-27	1	2.91E-04	2.91E-04
Cohort C Marbles Buried–Greenhouse-Geisser main effect TIME	1.88E-20	2	2.94E-04	2.94E-04

Cohort A Marbles Buried–Greenhouse-Geisser main effect TIME	8.24E-18	3	2.98E-04	2.98E-04
Cohort A Marbles Displaced–Greenhouse-Geisser main effect of TIME	4.16E-16	4	3.01E-04	3.01E-04
Cohort D Marbles Displaced—Greenhouse-Geisser main effect TIME	3.55E-14	5	3.05E-04	3.05E-04
Cohort C Marbles Displaced—Greenhouse-Geisser main effect TIME	2.44E-13	6	3.08E-04	3.08E-04
Cohort D Marbles Buried –5 to 20 minutes Bonferroni adjusted	6.06E-13	7	3.12E-04	3.12E-04
Cohort D Marbles Buried –5 to 25 minutes Bonferroni adjusted	9.14E-13	8	3.16E-04	3.16E-04
Cohort A Marbles Displaced–5 to 10 minutes Bonferroni adjusted	5.90E-12	9	3.20E-04	3.20E-04
Cohort C Marbles Buried –5 to 30 minutes Bonferroni adjusted	1.15E-11	10	3.24E-04	3.24E-04
Cohort A Marbles Displaced–5 to 15 minutes Bonferroni adjusted	1.23E-11	11	3.28E-04	3.28E-04
Cohort A Marbles Displaced–5 to 25 minutes Bonferroni adjusted	1.64E-11	12	3.32E-04	3.32E-04
Cohort A Marbles Displaced–5 to 30 minutes Bonferroni adjusted	1.64E-11	13	3.36E-04	3.36E-04
Cohort A Marbles Displaced–5 to 20 minutes Bonferroni adjusted	1.67E-11	14	3.40E-04	3.40E-04
Cohort D Marbles Buried –5 to 30 minutes Bonferroni adjusted	2.14E-11	15	3.44E-04	3.44E-04
Cohort A Marbles Buried –5 to 25 minutes Bonferroni adjusted	1.13E-10	16	3.49E-04	3.49E-04
Cohort C Marbles Buried –5 to 25 minutes Bonferroni adjusted	1.39E-10	17	3.53E-04	3.53E-04

Cohort D Marbles Displaced–5 to 30 minutes Bonferroni adjusted	1.91E-10	18	3.58E-04	3.58E-04
Cohort D Marbles Displaced –5 to 25 minutes Bonferroni adjusted	1.96E-10	19	3.63E-04	3.63E-04
Cohort D Marbles Displaced –5 to 15 minutes Bonferroni adjusted	2.48E-10	20	3.67E-04	3.67E-04
Cohort D Marbles Displaced –5 to 20 minutes Bonferroni adjusted	3.08E-10	21	3.72E-04	3.72E-04
Cohort A Marbles Buried –5 to 20 minutes Bonferroni adjusted	3.75E-10	22	3.77E-04	3.77E-04
Cohort A Marbles Buried –5 to 30 minutes Bonferroni adjusted	1.05E-09	23	3.82E-04	3.82E-04
Cohort C Marbles Displaced –5 to 25 minutes Bonferroni adjusted	1.41E-09	24	3.87E-04	3.87E-04
Cohort C Marbles Displaced –5 to 20 minutes Bonferroni adjusted	1.76E-09	25	3.93E-04	3.93E-04
Cohort C Marbles Displaced–5 to 30 minutes Bonferroni adjusted	2.11E-09	26	3.98E-04	3.98E-04
Cohort D Marbles Displaced –5 to 10 minutes Bonferroni adjusted	2.39E-09	27	4.03E-04	4.03E-04
Cohort C Marbles Displaced –5 to 15 minutes Bonferroni adjusted	2.44E-09	28	4.09E-04	4.09E-04
Cohort D Marbles Buried –10 to 20 minutes Bonferroni adjusted	2.81E-09	29	4.15E-04	4.15E-04
Cohort D Marbles Buried –10 to 25 minutes Bonferroni adjusted	6.56E-09	30	4.21E-04	4.21E-04
Cohort C Marbles Buried –10 to 30 minutes Bonferroni adjusted	1.24E-08	31	4.27E-04	4.26E-04
Cohort D Marbles Buried –10 to 30 minutes Bonferroni adjusted	1.50E-08	32	4.33E-04	4.33E-04

Cohort C Marbles Buried –5 to 20 minutes Bonferroni adjusted	2.48E-08	33	4.39E-04	4.39E-04
Cohort C Marbles Displaced –5 to 10 minutes Bonferroni adjusted	2.53E-08	34	4.45E-04	4.45E-04
Cohort D Marbles Buried –5 to 15 minutes Bonferroni adjusted	8.34E-08	35	4.52E-04	4.52E-04
Cohort A Marbles Buried –5 to 15 minutes Bonferroni adjusted	1.44E-07	36	4.58E-04	4.58E-04
Cohort C Marbles Buried –10 to 25 minutes Bonferroni adjusted	1.58E-07	37	4.65E-04	4.65E-04
Cohort A Marbles Buried –10 to 25 minutes Bonferroni adjusted	4.53E-07	38	4.72E-04	4.71E-04
Cohort A Marbles Buried –10 to 20 minutes Bonferroni adjusted	1.00E-06	39	4.79E-04	4.78E-04
Cohort A Marbles Buried –10 to 30 minutes Bonferroni adjusted	1.00E-06	40	4.86E-04	4.85E-04
Cohort D Marbles Half-Buried –5 to 10 minutes Bonferroni adjusted	3.00E-06	41	4.94E-04	4.91E-04
Cohort C Marbles Buried –5 to 15 minutes Bonferroni adjusted	6.00E-06	42	5.01E-04	4.95E-04
Cohort D Marbles Half-Buried—Greenhouse-Geisser main effect TIME	6.00E-06	43	5.09E-04	5.03E-04
Cohort C Marbles Half-Buried –5 to 10 minutes Bonferroni adjusted	1.50E-05	44	5.17E-04	5.02E-04
Time Digging–main effect AGE	1.80E-05	45	5.25E-04	5.07E-04
Cohort C Marbles Buried –15 to 30 minutes Bonferroni adjusted	1.80E-05	46	5.33E-04	5.15E-04
Cohort D Marbles Half-Buried –5 to 15 minutes Bonferroni adjusted	2.40E-05	47	5.42E-04	5.18E-04
Cohort A Marbles Buried –5 to 10 minutes Bonferroni adjusted	2.50E-05	48	5.50E-04	5.25E-04

Cohort C Marbles Buried – 10 to 20 minutes Bonferroni adjusted	3.60E-05	49	5.59E-04	5.23E-04
Cohort D Marbles Buried – 15 to 20 minutes Bonferroni adjusted	5.40E-05	50	5.68E-04	5.14E-04
Cohort D Marbles Buried – 15 to 25 minutes Bonferroni adjusted	7.00E-05	51	5.78E-04	5.08E-04
Cohort A Marbles Buried – 15 to 25 minutes Bonferroni adjusted	2.57E-04	52	5.87E-04	3.30E-04
Cohort C Marbles Buried –5 to 10 minutes Bonferroni adjusted	3.00E-04	53	5.97E-04	2.97E-04
Cohort C Marbles Buried – 15 to 25 minutes Bonferroni adjusted	3.49E-04	54	6.07E-04	2.58E-04
Cohort A Marbles Half-Buried–5 to 10 minutes Bonferroni adjusted	4.16E-04	55	6.18E-04	2.02E-04
Cohort C Marbles Half-Buried—Greenhouse-Geisser main effect TIME	4.77E-04	56	6.28E-04	1.51E-04
Cohort A Marbles Buried – 15 to 20 minutes Bonferroni adjusted	8.55E-04	57	6.39E-04	-2.16E-04

6.3.6 EPM Males

Data Screening

Table 6.3 EPM Cases Summary

Genotype	Age	N
WT	10 weeks	23
	6 months	22
	10 months	22
***Grb10*$^{+/p}$**	10 weeks	23
	6 months	20
	10 months	21

A two-way ANOVA was conducted to determine the effects of GENOTYPE and AGE on ethovision measures during the elevated plus maze,

including: “all entries to zones of the EPM”, “total open arm entries”, “total closed arm entries”, “total middle zone entries”, “lactency to first open arm entry”, “time per open arm entry”, “time per closed arm entry”, “time per middle zone entry”, “velocity”, “percent time in the open arms”, “percent time in the closed arms”, “percent time in the middle zone”, “percent time in open vs closed arms (excluding the middle zone)”, “head dip duration”, “stretch-attend duration”, and “grooming duration”.

Shapiro-Wilk’s test was used with the residuals (RES) to calculate normality for each cell for each measure. Non-normal results were investigated with Q-Q plots. Outliers were identified using the studentized residuals (SRE). “All entries” was normally distributed and had one outlier with an SRE more extreme than ±3 SD: A17 P (SRE = 3.26). “Total open arm entries” were normally distributed except for *Grb10*$^{+/p}$ RES at 6 months (p = 0.004) and 10 months (p = 0.008). The Q-Q plots for these cells were positively skewed. There was one outlier with an SRE more extreme than ±3 SD: A17 P (SRE = 4.61). “Total closed arm entries” were normally distributed except for WT RES at 10 weeks (p = 0.003) and *Grb10*$^{+/p}$ RES at 6 months (p = 0.030). The WT RES Q-Q plot was positively skewed, and the *Grb10*$^{+/p}$ RES Q-Q plot deviated from normality somewhat at lower values. There was one outlier with an SRE more extreme than ±3 SD: D24 P (SRE = 3.83). “Total middle entries” was normally distributed, but the SREs identified one outlier: A17 P (SRE = 3.20). “Latency to first open arm entry” RES were not normally distributed for any cell of the design (Shapiro-Wilks, $p < 0.001$ for all cells). The RES Q-Q plots were all

positively skewed. There were two SREs more extreme than ±3 SD: C45 P (SRE = 7.95), A66 P (SRE = 5.09).

"Time per open arm entry" RES were normally distributed except *Grb10*$^{+/p}$ data at 6 months (Shapiro-Wilk's $p < 0.001$). The RES Q-Q plot for this cell showed a positively skewed distribution with a strong outlier. The SREs identified one extreme outlier: C52 P SRE = 8.22. "Time per closed arm entry" RES were normally distributed as assessed by Shapiro-Wilk's test ($p > 0.05$) except WT data at 10 months ($p < 0.001$) and 6 months ($p = 0.002$), and *Grb10*$^{+/p}$ data at 10 weeks ($p < 0.001$). The RES Q-Q plots for these non-normal cells were positively skewed. There were three outliers with SRE more extreme than ±3 SD: A3 P (SRE = 5.15), C19 P (SRE = 3.97), D51 P (SRE = 3.86). "Time per middle zone entry" data were normally distributed (Shapiro-Wilk's $p > 0.05$) except for WT RES at 10 weeks ($p = 0.022$). The RES Q-Q plot showed positive skew for this cell. There were no SREs more extreme than ±3 SD. "Velocity" RES were normally distributed for all cells, as assessed by Shapiro-Wilk's test ($p > 0.05$). There was one outlier with an SRE more extreme than ±3SD: A17 P (SRE = 3.73).

The RES for "percent time in open arm" were normally distributed for all cells (Shapiro-Wilk's $p > 0.05$), except for *Grb10*$^{+/p}$ data at 10 months ($p = 0.026$) and 6 months ($p < 0.001$). The RES Q-Q plots show mild positive skew for *Grb10*$^{+/p}$ RES at 10 months, and stronger positive skew at 6 months. There were two SREs more extreme than ±3 SD: C52 P (SRE = 5.38) and A17 P (SRE = 3.18). The RES for "percent time in closed arm" were normally distributed for all cells (Shapiro-Wilk's $p > 0.05$), except for WT at 6 months ($p = 0.025$) and

Grb10$^{+/p}$ at 6 months (p = 0.015). The RES Q-Q plot for WT data at 6 months was bimodal and the plot for *Grb10*$^{+/p}$ data at 6 months was skewed at lower values. There were no SREs more extreme than ±3 SD. The RES for "percent time in middle zone" were normally distributed for all cells and there were no outliers with SRE more extreme than ±3 SD. "Percent time in open vs closed" RES were normally distributed for all cells (Shapiro-Wilk's p > 0.05), except for *Grb10*$^{+/p}$ at 6 months (p < 0.001). The RES Q-Q plot was positively skewed for this cell. There were two outliers with SRE more extreme than ±3 SD: C52 P (SRE = 4.09), A17 P (SRE = 3.14).

The RES for "head dip duration" were normally distributed (Shapiro-Wilk's p > 0.05) except for *Grb10*$^{+/p}$ data at 10 months (p = 0.026), and 6 months (p < 0.000). The RES Q-Q plot for *Grb10*$^{+/p}$ data at 10 months and 6 months were positively skewed. There was one outlier with an SRE more extreme than ±3 SD: C52 P (SRE = 5.19). "Stretch attend duration" RES were normally distributed for all cells (Shapiro-Wilk's p > 0.05). There was one outlier with an SRE more extreme than ±3 SD: C52 P (SRE = 3.44). "Grooming duration" RES were not normally distributed for any cells except *Grb10*$^{+/p}$ data at 6 months (Shapiro-Wilk's p = 0.090): Wildtype RES at 10 months (p < 0.001), 6 months (p = 0.004), 10 weeks (p = 0.046), *Grb10*$^{+/p}$ RES at 10 months (p = 0.016), 10 weeks (p < 0.001). The RES Q-Q plots for all non-normal cells were positively skewed. There were three outliers identified by SREs more extreme than ±3 SD: D100 P (SRE = 4.45), D51 P (SRE = 4.20), D49 P (SRE = 3.11). The total outliers in the data set with SRE more extreme than ±3 SD were: D24 P, D51 P, D100 P, C19 P, C45 P, C52 P, A3 P, A17 P, A49 P, A66 P. All outliers were

kept in the two-way ANOVAs, and the outcomes were compared to a two-way ANOVA in which the outliers in any one measure were removed across all measures.

The assumption of homogeneity of variance was met for all measures (Levene's test $p > 0.05$) except: "open entries" ($p = 0.010$), "latency to first open entry" ($p = 0.004$), "time per closed arm entry" ($p = 0.002$), "time per middle zone entry" ($p = 0.003$), "percent time in closed arm" ($p = 0.007$), "percent time in middle zone" ($p = 0.033$), "percent time in open vs closed" ($p = 0.035$), and "grooming duration" ($p = 0.002$). The ratio of the largest group variance to smallest group variance for each of these measures was greater than 3, so the two-way ANOVA was insufficiently robust. Therefore, these measures were analyzed with one-way ANOVAs for each age group separately.

The data reported in the text and graphs are unweighted estimated marginal means ± standard error, unless otherwise specified. All pairwise comparisons run are reported with mean difference, 95% confidence intervals, and Bonferroni adjusted p values.

Summary

The interaction between GENOTYPE and AGE was not statistically significant for any measures analyzed, except for "closed arm entries" once outliers were removed. The following summaries refer to the main effects or the outcomes of one-way ANOVAs. Removal of outliers did not change the significance outcomes of the analyses unless specifically stated. In this cross-sectional study, each age group refers to a different cohort.

Grb10$^{+/p}$ mice made more open arm entries than wildtypes at 6 months but not 10 weeks or 10 months. When outliers were removed, the data could be analyzed by two-way ANOVA. *Grb10*$^{+/p}$ mice overall made more open arm entries than wildtypes. Mice 10 weeks of age made more open arm entries than mice at 6 or 10 months, and there was no difference in open arm entries made between 6 and 10 months.

Total entries, closed arm entries, and middle zone entries were analyzed to determine if the above effect was specific to the open arm. Overall, *Grb10*$^{+/p}$ mice made more total entries than wildtypes. Mice 10 weeks of age made more total entries than mice at 6 or 10 months, and there was no difference in total entries made between 6 and 10 months. Over all cohorts, *Grb10*$^{+/p}$ mice made more closed arm entries than wildtypes. There was no significant effect of AGE on closed arm entries. When outliers were removed, there was a statistically significant interaction between GENOTYPE and AGE for "total closed arm entries". Again, at every age group *Grb10*$^{+/p}$ mice made more closed arm entries than wildtypes. Additionally, there was a significant simple main effect of AGE on *Grb10*$^{+/p}$, but not wildtype mice. There were significantly more *Grb10*$^{+/p}$ closed arm entries at 10 weeks of age compared to 10 months, but the difference from 10 weeks to 6 months and 6 to 10 months was not significantly different. Over all cohorts, *Grb10*$^{+/p}$ mice made more entries to the middle zone than wildtype mice. Mice at 10 weeks made more entries to the middle zone than mice 6 or 10 months of age, and there was no difference in entries between 6 or 10 months.

Next, we examined the division of time between zones of the EPM. Over all cohorts, *Grb10*$^{+/p}$ spent a greater percentage of their time on the open arm than wildtypes. Mice 10 weeks of age spent more time on the open arms than mice 10 months of age, but there was no difference between mice 10 weeks and 6 months of age, or 6 months and 10 months of age. When outliers were removed, mice 10 weeks of age also spent more time on the open arms than mice 6 months of age. *Grb10*$^{+/p}$ mice spent a lower percentage of their time on the closed arm than wildtypes at 6 months of age but not at 10 weeks or 10 months of age. *Grb10*$^{+/p}$ mice spent a greater percent of their time in the middle zone than wildtypes at 6 months, but not at 10 weeks or 10 months of age. At 6 months of age, *Grb10*$^{+/p}$ mice spend more time than wildtypes in the open arm compared to total time on open and closed arms, excluding time in the middle zone. There was no difference at 10 weeks or 10 months.

We examined time per entry and velocity to determine the quality of entries to zones in the EPM. There was no significant difference overall between *Grb10*$^{+/p}$ and wildtype mice in time per open entry, nor was there a difference between mice 10 weeks, 6 months, and 10 months of age. When outliers were removed, there was a significant main effect of AGE but not GENOTYPE on “time per open entry”. Mice 10 weeks of age spent more time per entry than mice 10 months of age, but there was no difference from 10 weeks to 6 months or from 6 to 10 months. At 6 months, *Grb10*$^{+/p}$ mice spent less time per closed arm entry than wildtypes. There was no significant difference in time per closed arm entry between *Grb10*$^{+/p}$ and wildtype mice at 10 weeks or 10 months of age. When outliers were removed, *Grb10*$^{+/p}$ mice

spent less time per closed arm entry than wildtypes at 10 weeks and 6 months of age, but not at 10 months. *Grb10*$^{+/p}$ mice spent less time per entry to the middle zone than wildtypes at 10 weeks, but not at 6 or 10 months of age. *Grb10*$^{+/p}$ mice moved at a higher velocity overall than wildtypes. Mice 10 months of age were faster than mice 6 and 10 months of age, and there was no statistically significant difference in velocity between mice 6 and 10 months of age.

We then turned to latency to first open arm entry. There was no statistically significant difference in latency to first open arm entry between *Grb10*$^{+/p}$ and wildtype mice at 10 weeks, 6 months, or 10 months of age. When outliers were removed, "latency to first open arm entry" could be analyzed with a two-way ANOVA. There was a significant main effect of GENOTYPE but not AGE. *Grb10*$^{+/p}$ mice had a lower latency overall to first open arm entry compared to wildtypes.

Over all cohorts, *Grb10*$^{+/p}$ mice spent more time in head dip behaviour than wildtypes. There was no significant effect of AGE on total head dip duration. When outliers were removed, "head dip duration" data necessitated analysis by one-way ANOVA. *Grb10*$^{+/p}$ mice spent more time in head dip behaviour than wildtypes at 6 months of age, but not at 10 weeks or 10 months. *Grb10*$^{+/p}$ mice over all cohorts spent more time in stretch-attend behaviour than wildtypes. Mice 10 weeks of age spent less time in stretch-attend behaviour than mice 10 months of age, but there was no difference between mice 10 weeks and 6 months, or 6 months and 10 months of age. When outliers were removed, genotype had no significant main effect on

stretch-attend behaviour. There was no statistically significant difference in total grooming duration between *Grb10*$^{+/p}$ and wildtype mice in any age group.

Reports

Entries to EPM Zones

"Open Entries"– ONE WAY ANOVAS

The first measure of anxiety we examined was total entries to the open arms of the EPM. Data for one way ANOVAs are reported as mean ± standard deviation. The graph depicts mean ± standard error of the mean.

At 10 weeks, total "open arm entries" was not statistically significantly different between *Grb10*$^{+/p}$ (19.478 ± 6.626 entries) and wildtype (16.783 ± 7.722 entries) mice, $F(1,44) = 1.614$, $p = 0.211$, partial $\eta^2 = 0.035$. At 6 months, "open arm entries" were statistically different between *Grb10*$^{+/p}$ (15.700 ± 6.182 entries) and wildtype (9.955 ± 6.484) trials $F(1,40) = 8.596$, $p = 0.006$, partial $\eta^2 = 0.177$. This did not survive FDR correction. At 10 months, the assumption of homogeneity of variance was violated (Levene's test $p = 0.019$). Therefore, we interpreted Welch's ANOVA. There was no statistically significant difference in "open arm entries" between *Grb10*$^{+/p}$ (16.286 ± 12.546 entries) and wildtype (11.000 ± 6.347 entries) trials, Welch's $F(1,29.300) = 2.995$, $p = 0.094$.

When outliers were removed, data for "total open arm entries" could be analyzed by two-way ANOVA. Data for main effects in two-way ANOVAs are presented as estimated mean ± standard error of the mean. There was no statistically significant interaction between GENOTYPE and AGE for "open arm

entries", F(2,115) = 0.212, p = 0.809, partial η^2 = 0.004. Therefore, analyses for main effects were performed. There was a statistically significant main effect of GENOTYPE on entries to the open arms, F(1,115) = 8.694, p = 0.004, partial η^2 = 0.070. *Grb10*$^{+/p}$ mice made significantly more entries to the open arms (16.812 ± 0.934 entries) than wildtypes (12.933 ± 0.927 entries), mean difference 3.879 (95%CI 1.273 to 6.485) entries, p = 0.004.

There was also a significant main effect of AGE on "open arm entries" when outliers were removed, F(2,115) = 6.648, p = 0.002, partial η^2 = 0.104. Mice 10 weeks of age made 18.207 ± 1.102 open arm entries, 6 months of age made 13.346 ± 1.157 entries, and 10 months of age made 13.066 ± 1.157 entries. Mice 10 weeks of age made statistically more entries than mice at 6 months (4.861 (95%CI 0.977 to 8.744) entries, p = 0.009), and 10 months of age (5.141 (95%CI 1.258 to 9.024) entries, p = 0.005). There was no statistically significant difference between mice 6 and 10 months of age (0.280 (95%CI -3.697 to 4.257) entries, p = 1.000).

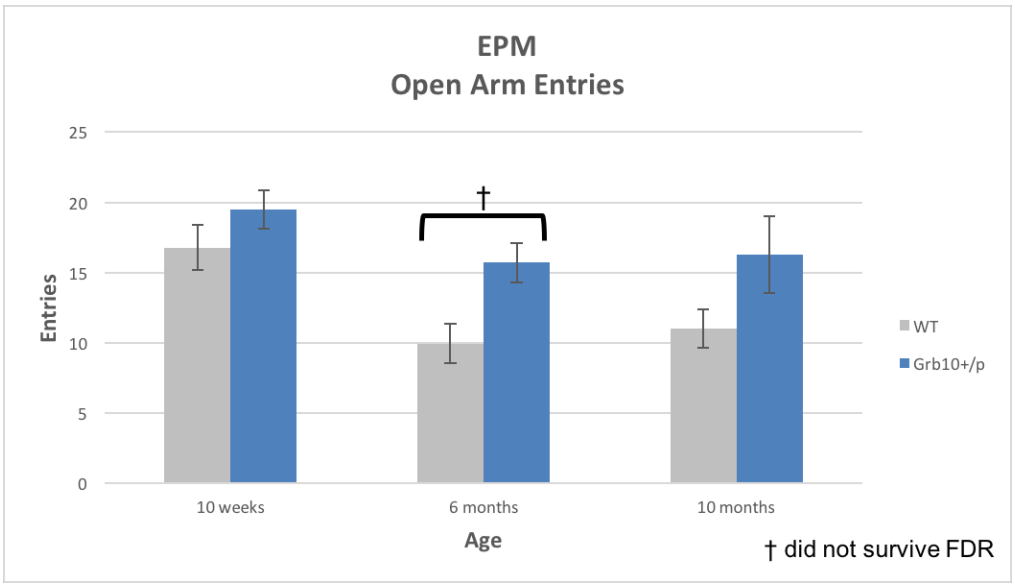

Figure 6.15 EPM Open Arm Entries

“All Entries”

As there was a significant genotype difference in total open arm entries at 6 months of age (pre-FDR correction), we also examined total entries to all zones of the EPM to determine if this effect was specific to the open arm.

The interaction between GENOTYPE and AGE was not statistically significant for “all entries”, $F(2,125) = 0.631$, $p = 0.534$, partial $\eta^2 = 0.010$. Therefore, analyses for main effects were performed. There was a statistically significant main effect of GENOTYPE for “all entries”, $F(1,125) = 17.909$, $p < 0.001$, partial $\eta^2 = 0.125$. This survived FDR correction, and the main effects graph may be found in the FDR–EPM section. *Grb10*$^{+/p}$ mice made more entries to EPM zones (82.834 ± 2.898 entries) than wildtype mice (65.698 ± 2.828 entries), mean difference 17.137 (95%CI 9.122 to 25.151) entries, $p < 0.001$.

There was a statistically significant main effect of AGE on “all entries”, $F(2,125) = 6.709$, $p = 0.002$, partial $\eta^2 = 0.097$. Mice at 10 weeks made the most entries (84.565 ± 3.413 entries), while mice at 6 months (68.155 ± 3.575 entries) and 10 months (70.078 ± 3.531 entries) made fewer. Mice 10 weeks of age made significantly more entries than mice at 6 months, mean difference 16.411 (95% CI 4.417 to 28.404) entries, $p = 0.004$. Mice 10 weeks of age also made 14.487 (95%CI 2.572 to 26.402) entries than mice at 10 months, $p = 0.011$. There was no statistically significant difference between “all entries” made by mice at 6 months and 10 months, mean difference -1.923 (95%CI -14.117 to 10.270) entries, $p = 1.000$. The main effect of AGE and the pairwise comparisons did not survive FDR correction.

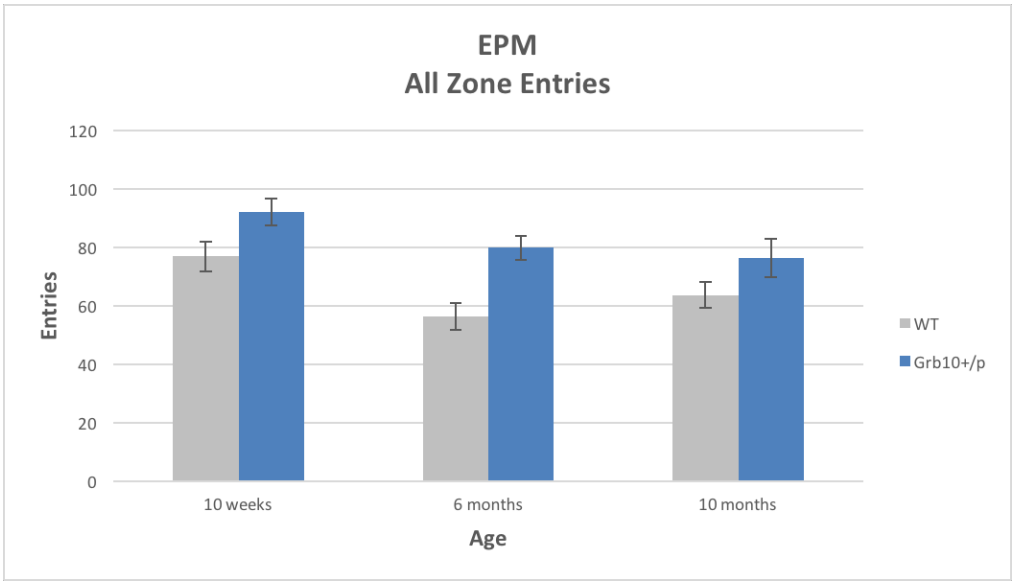

Figure 6.16 EPM All Entries

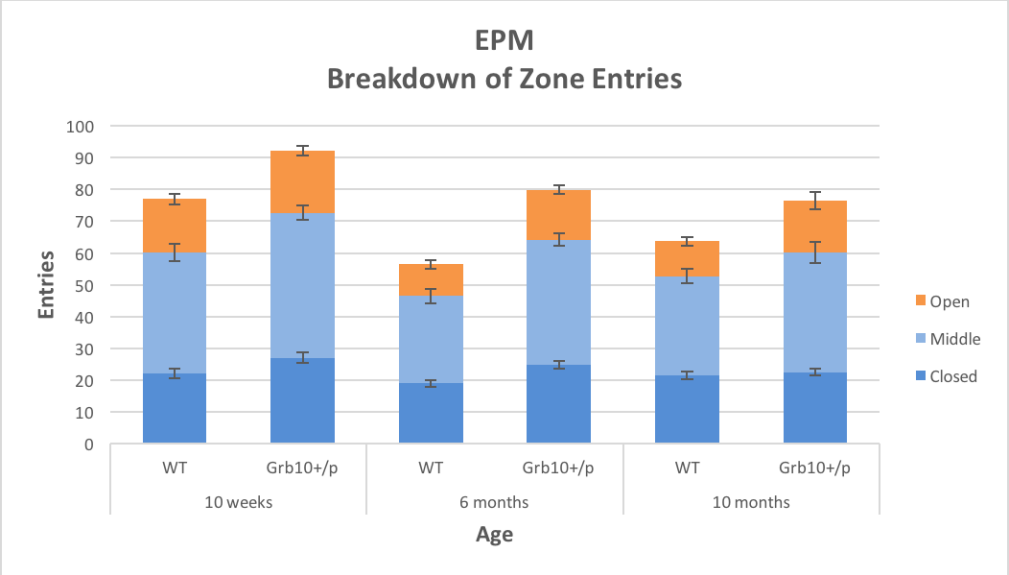

Figure 6.17 EPM Breakdown of Zone Entries

There was a significant genotype difference in "all entries" made to zones of the EPM, indicating increased entries by *Grb10*$^{+/p}$ mice at 6 months was not specific to the open arm. We therefore also examined closed arm and middle zone entries individually.

“Closed Entries”

There was no statistically significant interaction between GENOTYPE and AGE for “closed entries”, F(2,125) = 1.836, p = 0.164, partial η^2 = 0.029. Therefore, analyses for main effects were performed. There was no statistically significant main effect of AGE on “closed entries”, F(2,125) = 2.898, p = 0.059, partial η^2 = 0.044.

The main effect of GENOTYPE on “closed entries” was statistically significant, F(1,125) = 13.301, p < 0.001, partial η^2 = 0.096. This survived FDR correction, and the graph of the main effect may be found in the FDR–EPM section. *Grb10*$^{+/p}$ mice made significantly more closed arm entries (24.741 ± 0.764 entries) than wildtype mice (20.847 ± 0.746 entries), mean difference 3.894 (95%CI 1.781 to 6.007) entries, p < 0.001.

When outliers were removed, there was a statistically significant interaction between GENOTYPE and AGE for “total closed arm entries”, F(2,115) = 4.851, p = 0.009, partial η^2 = 0.078. Therefore, we ran simple main effects analyses and pairwise comparisons with a Bonferroni adjustment. Data are mean ± standard deviation for the following reports.

At 10 weeks with outliers removed, mean “closed arm entries” for *Grb10*$^{+/p}$ mice was 28.191 ± 6.765 entries and for wildtypes was 21.091 ± 5.051 entries, a statistically significant mean difference of 7.100 (95%CI 4.026 to 10.173) entries, F(1,115) = 20.935, p < 0.001, partial η^2 = 0.154. At 6 months, mean “closed arm entries” for *Grb10*$^{+/p}$ mice was 25.632 ± 3.933 entries and for wildtypes was 19.900 ± 4.424 entries, a statistically significant mean difference of 5.732 (95%CI 2.504 to 8.959) entries, F(1,115) = 12.374, p = 0.001,

partial η^2 = 0.097. At 10 months, mean "closed arm entries" for *Grb10*$^{+/p}$ mice was 22.350 ± 5.081 entries and for wildtypes was 21.947 ± 4.612 entries, a mean difference of 4.03 (95%CI -2.825 to 3.630) entries, F(1,115) = 0.061, p = 0.805, partial η^2 = 0.001, which was not statistically significant.

AGE did not have a statistically significant simple main effect on "total closed arm entries" for wildtype mice when outliers were removed, F(2,115) = 0.800, p = 0.452, partial η^2 = 0.014. However, there was a statistically significant simple main effect of AGE on *Grb10*$^{+/p}$ "total closed arm entries", F(2,115) = 6.775, p = 0.002, partial η^2 = 0.105. *Grb10*$^{+/p}$ mean closed arm entries at 10 weeks (28.191 ± 6.765 entries) was not significantly higher than at 6 months (25.632 ± 3.933 entries), mean difference 2.559 (95%CI -1.353 to 6.471) entries, p = 0.344. *Grb10*$^{+/p}$ mean closed arm entries at 10 weeks was significantly higher than at 10 months (22.350 ± 5.081 entries), mean difference 5.840 (95%CI 1.980 to 9.701) entries, p = 0.001. There was no significant difference between *Grb10*$^{+/p}$ mean closed arm entries at 6 and 10 months, mean difference 3.282 (95%CI -0.677 to 7.240) entries, p = 0.139.

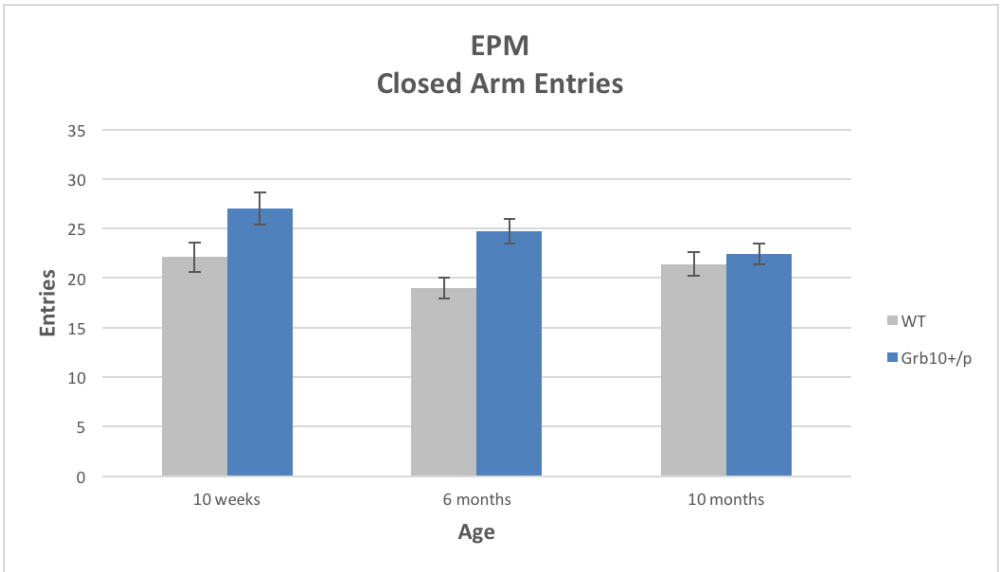

Figure 6.18 EPM Closed Arm Entries

"Middle Entries"

There was no statistically significant interaction between GENOTYPE and AGE for "middle entries", $F(2,125) = 0.682$, $p = 0.507$, partial $\eta^2 = 0.011$. Therefore, analyses for main effects were performed. There was a statistically significant effect of GENOTYPE on "middle entries", $F(1,125) = 18.166$, $p < 0.001$, partial $\eta^2 = 0.127$. This survived FDR correction, and the main effects graph may be found in the FDR–EPM section. *Grb10*$^{+/p}$ mice made significantly more entries to the middle zone (40.939 ± 1.455 entries) than wildtype mice (32.272 ± 1.420 entries), mean difference 8.667 (95%CI 4.642 to 12.691) entries, $p < 0.001$.

The main effect of AGE on "middle entries" was statistically significant, $F(2,125) = 6.905$, $p = 0.001$, partial $\eta^2 = 0.099$. Mice 10 weeks of age made 41.848 ± 1.714 entries, 6 months of age made 33.452 ± 1.795 entries, and 10 months of age made 34.516 ± 1.773 entries. Mice at 10 weeks of age made significantly more entries compared to mice at 6 months (8.396 (95%CI 2.373

to 14.418) entries, p = 0.003) and 10 months (7.332 (95%CI 1.348 to 13.315) entries, p = 0.011). There was no significant difference between entries made at 6 months and 10 months (-1.064 (95%CI -7.187 to 5.059) entries, p = 1.000). Overall, *Grb10*$^{+/p}$ mice moved at a higher velocity than wildtypes. Mice at 10 weeks of age were faster than mice at 6 and 10 months of age, and there was no difference in velocity between 6 and 10 months of age. The main effect of AGE and the pairwise comparisons did not survive FDR correction.

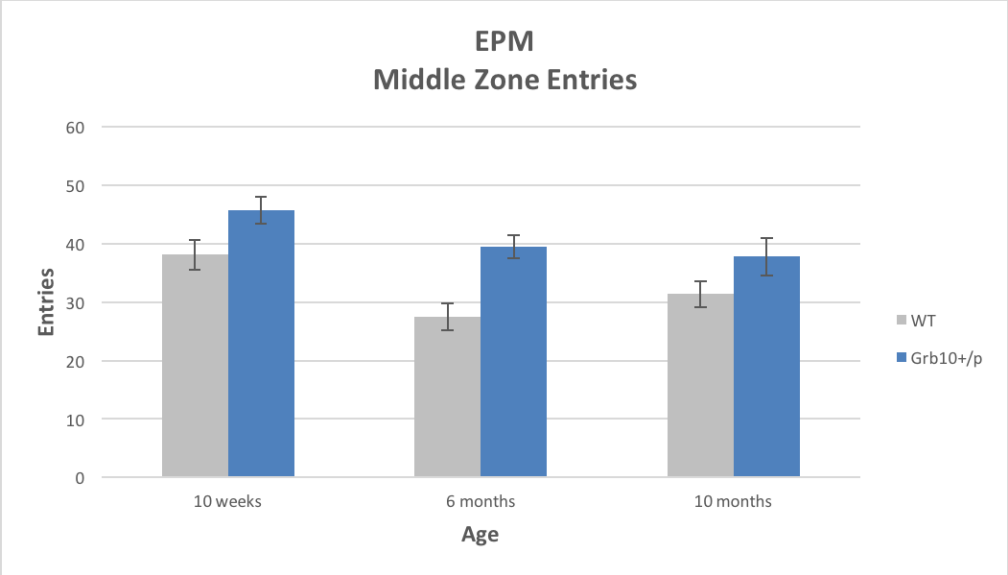

Figure 6.19 EPM Middle Zone Entries

Division of Time between EPM Zones

We next examined whether the total percent time spent per EPM zone differed by GENOTYPE and AGE. The analyses below account for open arm, closed arm, and middle zone time. An analysis of open vs closed arm time, excluding time spent in the middle zone, can be found in Appendix III.

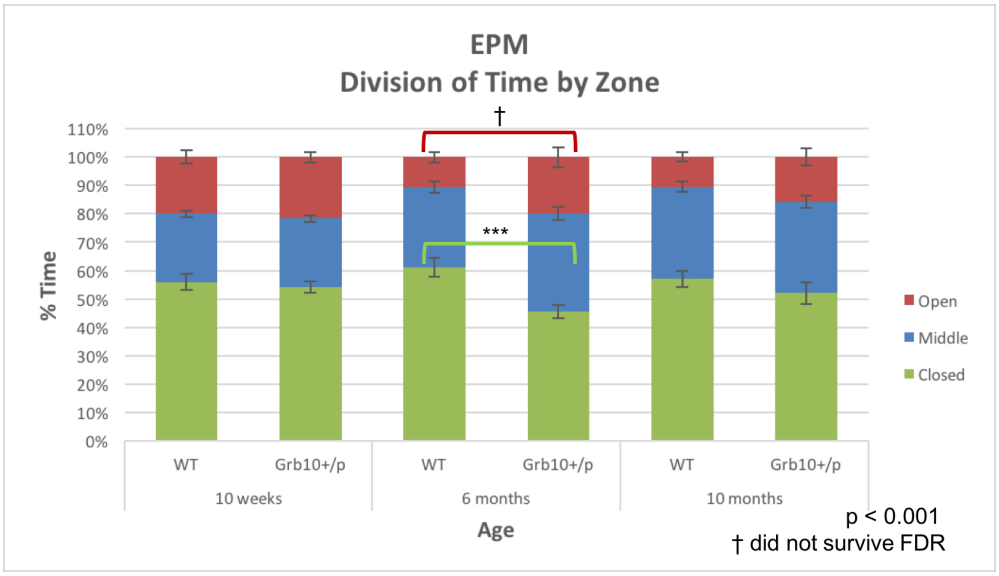

Figure 6.20 EPM Division of Time By Zone

"Percent time in open arms"

There was no statistically significant interaction between GENOTYPE and AGE for "percent time in open arms", F(2,125) = 1.226, p = 0.297, partial η^2 = 0.019. Therefore, analyses for main effects were performed. There was a statistically significant main effect of GENOTYPE on "percent time in open arms", F(1,125) = 7.727, p = 0.006, partial η^2 = 0.058. *Grb10*$^{+/p}$ mice spent significantly more time on the open arm (19.094 ± 1.390%) than wildtypes (13.697 ± 1.356%), mean difference 5.398 (95%CI 1.555 to 9.241) %, p = 0.006. This effect of GENOTYPE did not survive FDR correction.

There was a statistically significant main effect of AGE on "percent time in open arms", F(2,125) = 5.786, p = 0.004, partial η^2 = 0.085. Mice 10 weeks of age spent 20.823 ± 1.636%, 6 months of age spent 15.289 ± 1.715%, and 10 months of age spent 13.074 ± 1.693% of the total time on open arms. Time at 10 weeks was statistically higher than at 10 months (7.749 (95%CI 2.035 to 13.462) %, p = 0.004, but not than at 6 months (5.534 (95%CI -0.217 to 11.285)

%, p = 0.063. There was no significant difference between percent time spent on open arms at 6 months and 10 months (2.214 (95%CI -3.633 to 8.062) %, p = 1.000. Neither the main effect of AGE, nor the pairwise comparisons survived FDR correction.

When outliers were removed, mice 10 weeks of age also spent more time on the open arm than mice 10 months of age (12.541 ± 1.499%), mean difference 8.453 (95%CI 3.422 to 13.483) %, p < 0.001.

"Percent time in closed arms" –ONE WAY ANOVAS

"Percent time in closed arms" was analyzed using separate one-way ANOVAs for each cohort. Data are presented as mean ± standard deviation.

At 10 weeks, there was no statistically significant difference between *Grb10*$^{+/p}$ (54.277% $\pm$ 9.945) and wildtype (56.017% $\pm$ 13.152) trials in percent time in the closed arms, F(1,44) = 0.256, p = 0.615, partial η^2 = 0.006. At 6 months, the assumption of homogeneity of variances was violated (Levene's test p = 0.011). Therefore, we interpreted Welch's ANOVA. "Percent time in the closed arm" was statistically different between *Grb10*$^{+/p}$ (45.610 $\pm$ 10.962%) and wildtype (61.296 $\pm$ 15.725%) trials, Welch's F(1,37.583) = 14.265, p = 0.001. This survived FDR correction. At 10 months, there was no statistically significant difference in "percent time in closed arm" between *Grb10*$^{+/p}$ (52.100 $\pm$ 17.441%) and wildtype (57.050 $\pm$ 12.904%) trials, F(1,41) = 1.127, p = 0.295, partial η^2 = 0.027.

“Percent time in middle zone”–ONE WAY ANOVAS

“Percent time in middle zone” was analyzed using separate one-way ANOVAs for each cohort. Data are presented as mean ± standard deviation. There was homogeneity of variance for each cohort individually, as assessed by Levene’s test ($p > 0.05$).

At 10 weeks, there was no statistically significant difference between *Grb10*$^{+/p}$ ($24.031 \pm 6.040\%$) and wildtype ($24.028 \pm 5.424\%$) trials in percent time spent in the middle zone, $F(1,44) = 0.000$, $p = 0.999$, partial $\eta^2 < 0.001$. At 6 months, “percent time in the middle zone” was statistically different between *Grb10*$^{+/p}$ ($34.523 \pm 10.601\%$) and wildtype ($27.997 \pm 9.368\%$) trials, $F(1,40) = 4.485$, $p = 0.040$, partial $\eta^2 = 0.101$. This did not survive FDR correction. At 10 months, there was no statistically significant difference in “percent time in middle zone” between *Grb10*$^{+/p}$ ($32.178 \pm 9.854\%$) and wildtype ($32.523 \pm 8.263\%$) trials, $F(1,41) = 0.015$, $p = 0.902$, partial $\eta^2 < 0.001$.

Quality of Entries

As *Grb10*$^{+/p}$ mice made more entries to the open arm (and overall) and spent more time on the open arm prior to FDR correction, we wanted to examine the quality of entries by analyzing time spent per open and closed arm entries.

“Time per open entry”

There was no statistically significant interaction between GENOTYPE and AGE for “time per open entry”, $F(2,125) = 2.138$, $p = 0.122$, partial $\eta^2 =$

0.033. Therefore, analyses for main effects were performed. There was no statistically significant effect of GENOTYPE on “time per open entry”, F(1,125) = 1.197, p = 0.276, partial η^2 = 0.009. There was no significant difference between *Grb10*$^{+/p}$ mice (3.308 ± 0.220 s) and wildtypes (2.972 ± 0.215 s) per open arm entry. There was also no significant effect of AGE, F(2,125) = 2.972, p = 0.055, partial η^2 = 0.045. There was no significant difference between time per open entry at 10 weeks (3.470 ± 0.259 s), 6 months (3.334 ± 0.271 s), and 10 months (2.617 ± 0.268 s).

When outliers were removed, there was no statistically significant interaction between GENOTYPE and AGE for “time per open arm entry”, F(2,115) = 0.453, p = 0.637, partial η^2 = 0.008. Therefore, we ran main effects analyses. There was no statistically significant main effect of GENOTYPE on “time per open arm entry”, F(1,115) = 0.007, p = 0.933, partial η^2 = 0.000. There was a statistically significant main effect of AGE on “time per open arm entry” when outliers were removed, F(2,115) = 5.346, p = 0.006, partial η^2 = 0.085. Mice at 10 weeks (3.467 ± 0.181 s) were not statistically different from mice at 6 months (3.080 ± 0.190 s), mean difference 0.387 (95%CI -0.251 to 1.026) s, p = 0.430. Mice at 10 weeks spent significantly more time per open arm entry than mice at 10 months (2.608 ± 0.190 s), mean difference 0.859 (95%CI 0.220 to 1.497) s, p = 0.004. There was no statistical difference in “time spent per open arm entry” between mice 6 and 10 months of age, mean difference 0.472 (95%CI -0.182 to 1.126) s, p = 0.247.

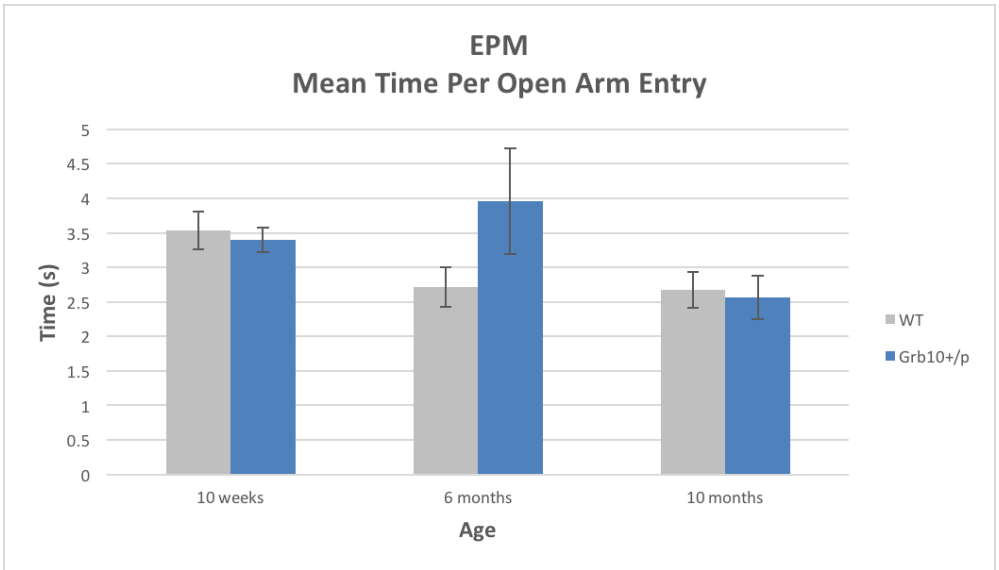

Figure 6.21 EPM Time Per Open Arm Entry

"Time per closed"

"Time per closed arm entry" was analyzed using separate one-way ANOVAs for each cohort. Data are presented as mean ± standard deviation.

At 10 weeks, there was no statistically significant difference between *Grb10*$^{+/p}$ (6.856 ± 4.175 s) and wildtype (8.257 ± 3.088 s) trials in time spent per closed arm entry, $F(1,44) = 1.698$, $p = 0.199$, partial $\eta^2 = 0.037$. When outliers were removed, there was a statistically significant difference between *Grb10*$^{+/p}$ (5.959 ± 1.820 s) and wildtype (8.4861 ± 2.954 s) trials in time spent per closed arm entry, $F(1,41) = 11.281$, $p = 0.002$, partial $\eta^2 = 0.216$. At 6 months, the assumption of homogeneity of variance was violated (Levene's test $p < 0.001$). Therefore, we interpreted Welch's ANOVA. "Time per closed arm entry" was statistically different between *Grb10*$^{+/p}$ (5.648 ± 1.510 s) and wildtype (11.064 ± 6.333 s) trials, Welch's $F(1,23.605) = 15.143$, $p = 0.001$. When all outliers were removed, there was a statistically significant difference in "time per closed arm entry" between *Grb10*$^{+/p}$ (5.728 ± 1.506 s) and wildtype

(9.580 ± 4.236 s) trials, Welch's F(1,23.942) = 14.591, p = 0.001. This survived FDR correction. At 10 months, there was no statistically significant difference in "time per closed arm entry" between *Grb10*$^{+/p}$ (7.608 ± 3.905 s) and wildtype (9.354 ± 6.324 s) trials, F(1,41) = 1.173, p = 0.285, partial η^2 = 0.028.

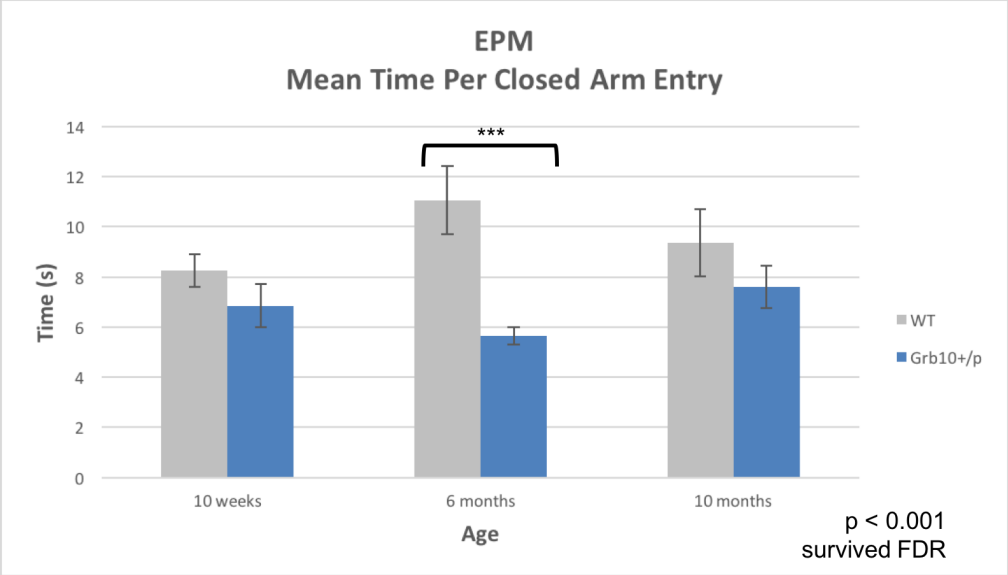

Figure 6.22 EPM Time Per Closed Arm Entry

We do not report time per middle zone entries here, as the results did not survive FDR correction. However, this analysis can be found in Appendix III.

"Velocity"

As *Grb10*$^{+/p}$ mice made more total entries, closed entries, and middle zone entries, and spent less time per closed arm entry than wildtypes (after FDR correction), we investigated their velocity on the EPM. There was no statistically significant interaction between GENOTYPE and AGE for "velocity", F(2,125) = 0.410, p = 0.665, partial η^2 = 0.007. Therefore, analyses for main

effects were performed. There was a statistically significant main effect of GENOTYPE on "velocity", $F(1,125) = 14.186$, $p < 0.001$, partial $\eta^2 = 0.102$. *Grb10*$^{+/p}$ mice moved at a significantly higher velocity (4.442 ± 0.128 cm/s) than wildtypes (3.767 ± 0.125 cm/s), mean difference 0.675 (95%CI 0.320 to 1.030) cm/s, $p < 0.001$. This survived FDR correction, and the main effects graph can be found in the FDR–EPM section.

There was also a statistically significant main effect of AGE on "velocity", $F(2,125) = 6.458$, $p = 0.002$, partial $\eta^2 = 0.094$. Velocity for mice at 10 weeks of age was 4.553 ± 0.151 cm/s, 6 months of age was 3.864 ± 0.158 cm/s, and 10 months of age was 3.895 ± 0.156 cm/s. Mice at 10 weeks of age were significantly faster than mice at 6 months (0.689 (95%CI 0.158 to 1.220) cm/s, $p = 0.006$) and 10 months (0.658 (95%CI 0.131 to 1.186) cm/s, $p = 0.009$). There was no significant difference between mice at 6 months and 10 months of age (-0.031 (95%CI -0.570 to 0.509) cm/s, $p = 1.000$). Neither the main effect of AGE nor the pairwise corrections survived FDR correction.

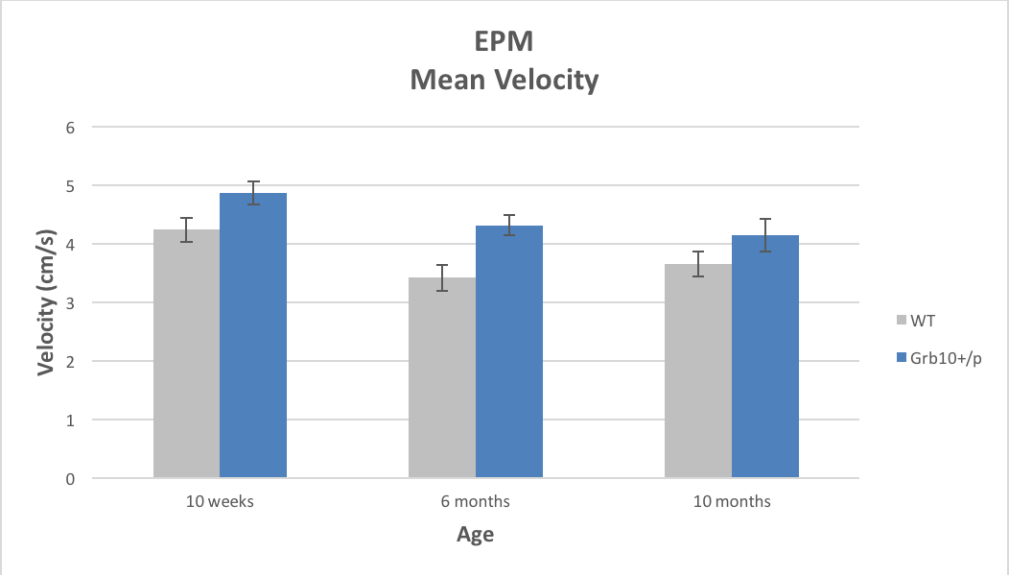

Figure 6.23 EPM Mean Velocity

“Latency to first open arm entry”–ONE WAY ANOVAS

Our next most important indicator of anxiety behaviour was “latency to first open arm entry”. This was analyzed using separate one way ANOVAs for each cohort. Data are presented as mean ± standard deviation.

At 10 weeks, there was no statistically significant difference between *Grb10*$^{+/p}$ (16.414 $\pm$ 14.295 s) and wildtype (23.713 $\pm$ 18.927 s) trials in latency to first open arm entry, F(1,44) = 2.178, p = 0.147, partial η^2 = 0.047. At 6 months, the assumption of homogeneity of variances was violated (Levene’s test p = 0.018). Therefore, we interpreted Welch’s ANOVA. Latency to first open arm entry was not statistically different between *Grb10*$^{+/p}$ (11.874 $\pm$ 7.799 s) and wildtype (37.406 $\pm$ 60.531 s) trials, Welch’s F(1,21.766) = 3.844, p = 0.063. At 10 months, there was no statistically significant difference in “latency to first open arm entry” between *Grb10*$^{+/p}$ (16.939 $\pm$ 15.609 s) and wildtype (31.718 $\pm$ 42.091 s) trials, F(1,41) = 2.287, p = 0.138, partial η^2 = 0.053.

When outliers were removed, the data no longer violated the assumption of homogeneity of variance, and we could use two-way ANOVA analysis. There was no statistically significant interaction between GENOTYPE and AGE for “latency to first open arm entry”, F(2,115) = 0.106, p = 0.889, partial η^2 = 0.002. Therefore, we ran main effects analyses. There was no statistically significant main effect of AGE on “latency to first open arm entry”, F(2,115) = 0.355, p = 0.702, partial η^2 = 0.006. There was a statistically significant main effect of GENOTYPE on “latency to first open arm entry” when outliers were removed, F(1,115) = 10.714, p = 0.001, partial η^2 = 0.085. Data

are presented as mean ± standard error. *Grb10*$^{+/p}$ mice were significantly quicker to first open arm entry (14.444 ± 2.202 s) than wildtypes (24.600 ± 2.186 s), mean difference -10.156 (95%CI -16.301 to -4.010) s, p = 0.001.

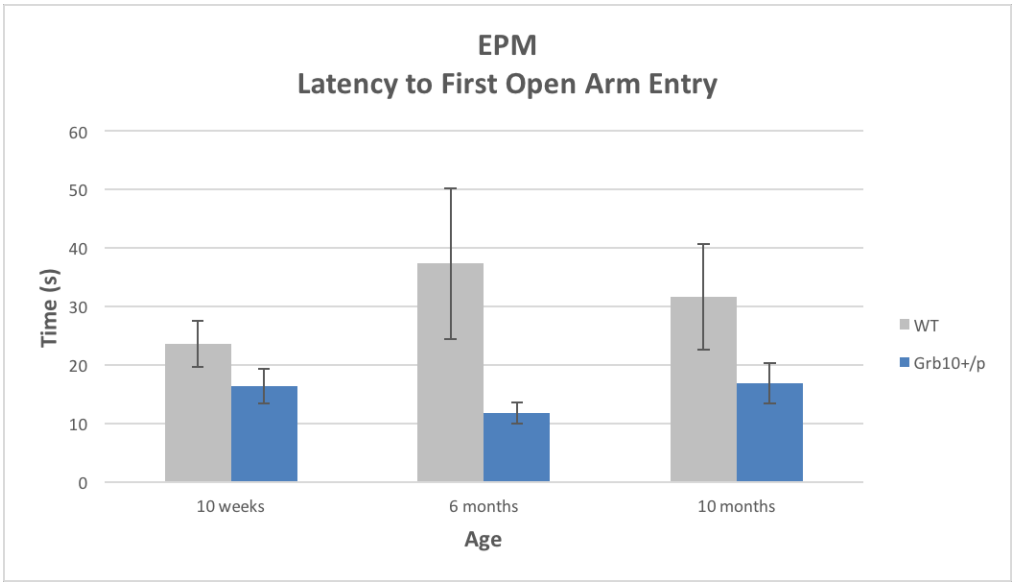

Figure 6.24 EPM Latency to First Open Arm Entry

Additional EPM Measures

We also analyzed head-dip duration, stretch-attend duration, and grooming duration during the EPM trials. Head-dip duration results survived FDR correction and is reported here, while stretch-attend duration and grooming duration results are reported in Appendix III.

"Head dip duration"

There was no statistically significant interaction between GENOTYPE and AGE for "head dip duration", $F(2,125) = 2.181$, $p = 0.117$, partial $\eta^2 = 0.034$. Therefore, analyses for main effects were performed. There was no

statistically significant main effect of AGE, F(2,125) = 0.113, p = 0.875, partial η^2 = 0.002.

There was a significant main effect of GENOTYPE on "head dip duration", F(1,125) = 14.540, p < 0.001, partial η^2 = 0.002. *Grb10*$^{+/p}$ mice spent significantly more time (48.203 ± 2.555 s) than wildtypes (34.588 ± 2.494 s) in head dip behaviours, mean difference 13.615 (95%CI 6.549 to 20.682) s, p < 0.001. This survived FDR correction.

When outliers were removed, the data necessitated analysis by one-way ANOVA. The mean duration data is presented as mean ± standard deviation. At 10 weeks with outliers removed, total head dip duration was not statistically different between *Grb10*$^{+/p}$ (45.250 ± 18.547 s) and wildtype (37.876 ± 18.002 s) trials, F(1,40) = 1.709, p = 0.199, partial η^2 = 0.041. At 6 months with outliers removed, there was a significant difference in "head dip duration" between *Grb10*$^{+/p}$ (46.903 ± 14.372 s) and wildtype (30.028 ± 11.870 s) trials, F(1,37) = 16.053, p < 0.001, partial η^2 = 0.303. At 10 months with outliers removed, there was no significant difference in "head dip duration" between *Grb10*$^{+/p}$ (45.680 ± 25.803 s) and wildtypes (39.430 ± 14.392 s), Welch's F(1,30.077) = 0.884, p = 0.355.

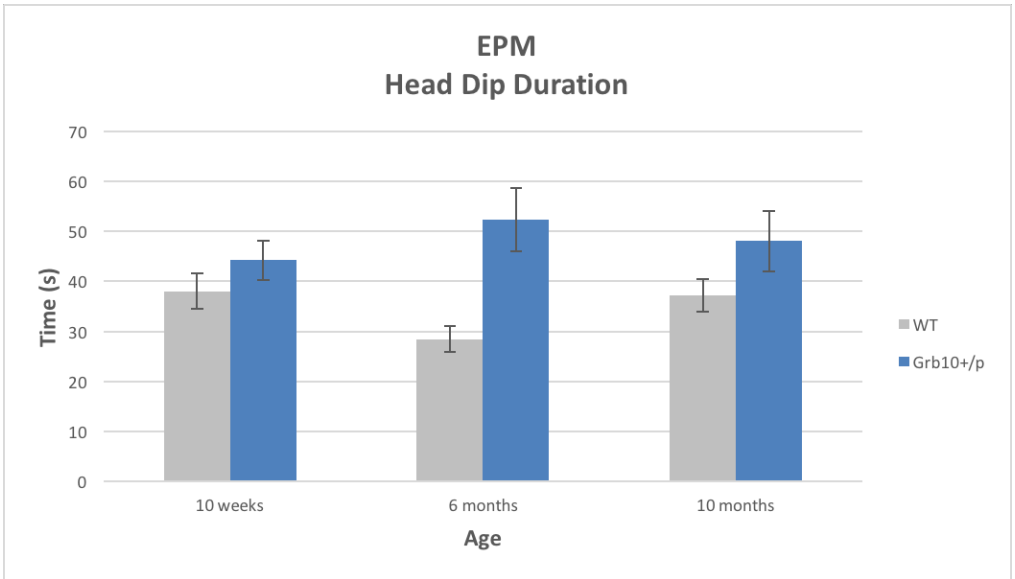

Figure 6.25 EPM Head Dip Duration

6.3.7 False Discovery Rate Corrections–EPM

The Benjamini-Liu (BL) procedure was used to correct for false discovery rate (FDR) of 5% over the entirety of measures in the EPM analysis (Yoav Benjamini et al., 2001). Nineteen findings with raw p values < 0.05 became insignificant after the FDR correction. Seven findings with p < 0.05 remained significant. Five of these significant findings were main effects of GENOTYPE across all cohorts and two are significant differences between genotype groups within a single cohort. Graphs of the main effects of GENOTYPE are presented in this section as the estimated marginal means collapsed across AGE. 'Percent time in closed arms–6 months (Welch)' and 'Time per closed entry–6 months (Welch)' are depicted in the EPM results section.

Table 6.4 Abridged FDR Corrections–EPM

Finding	P value	Rank m = 63	(min 0.05, 0.05*m/(m+1-i)^2	(BL) – P value
Middle Entries–main effect GENOTYPE	4.00E-05	1	7.94E-04	7.54E-04
All Entries–main effect GENOTYPE	4.40E-05	2	8.19E-04	7.75E-04
Head dip duration–main effect GENOTYPE	2.14E-04	3	8.47E-04	6.33E-04
Velocity–main effect GENOTYPE	2.54E-04	4	8.75E-04	6.21E-04
Closed Entries–main effect GENOTYPE	3.88E-04	5	9.05E-04	5.17E-04
Percent time in closed arms–6 months (Welch)	5.50E-04	6	9.36E-04	3.86E-04
Time per closed entry–6 months (Welch)	7.09E-04	7	9.70E-04	2.61E-04
Middle Entries–main effect AGE	0.001	8	0.0010	-4.26E-04

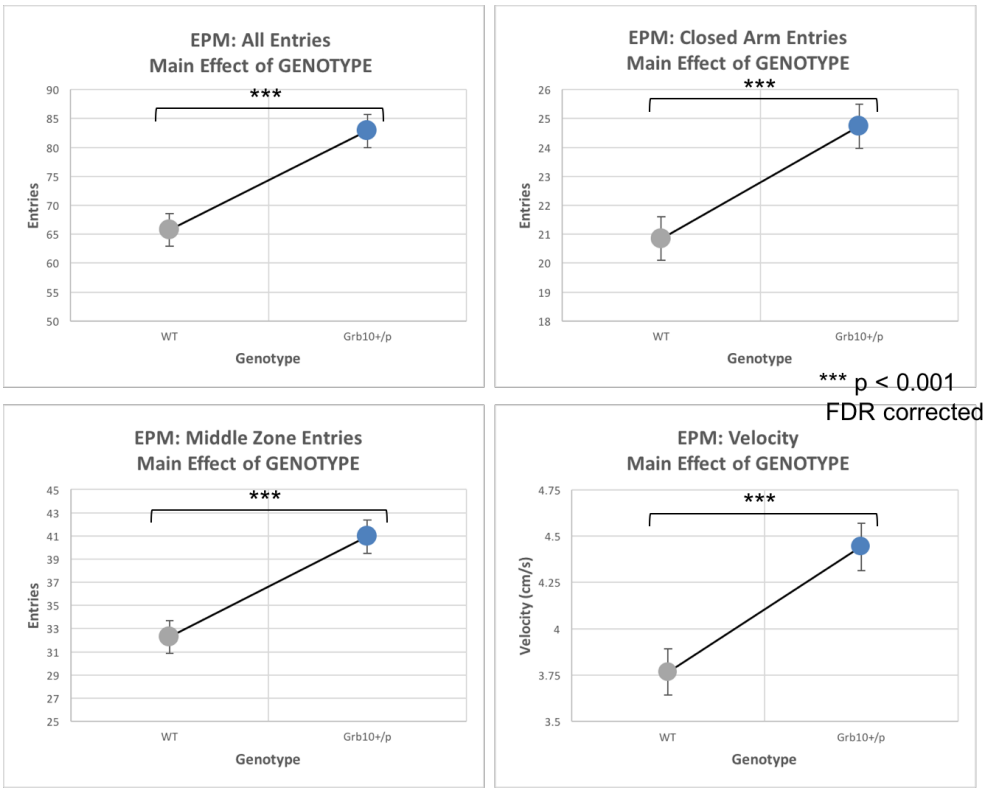

Figure 6.26 EPM Entries and Velocity–Significant Main Effects of GENOTYPE

The significant main effects of GENOTYPE across all cohorts for “All Entries”, “Closed Arm Entries”, “Middle Zone Entries”, and “Velocity” survived FDR corrections. *Grb10*$^{+/p}$ mice made more total entries, more closed arm entries, and more middle zone entries than wildtypes. *Grb10*$^{+/p}$ mice moved faster on the EPM than wildtypes.

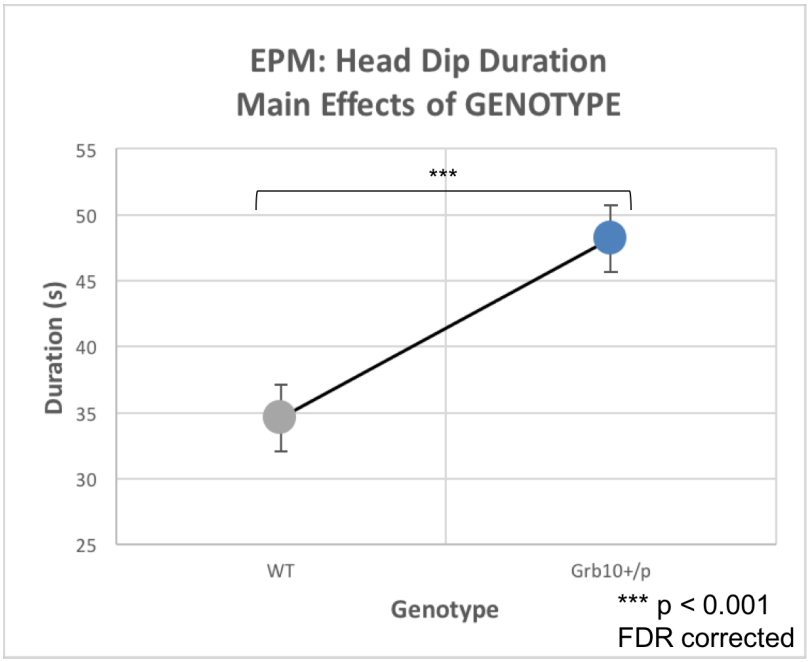

Figure 6.27 EPM Head Dip Duration–Significant Main Effect of GENOTYPE

The main effect of GENOTYPE over all cohorts for “Head Dip Duration” survived FDR corrections. *Grb10*$^{+/p}$ mice spent longer in head dip behaviour on the EPM than wildtypes.

6.4 Discussion

This chapter investigated compulsive behaviour and anxiety in *Grb10*$^{+/p}$ mice. Although previously Garfield et al. presented whisker barbering in *Grb10*$^{+/p}$ as an indicator of social dominance, it might alternatively be explained as a compulsive trichotillomania-like behaviour (Curley, 2011). This was of particular concern because serotonergic and dopaminergic neurotransmitter systems both are implicated in the pathophysiology of obsessive compulsive disorder (OCD) and are sites of high paternal *Grb10* expression (Albelda & Joel, 2012; Garfield et al., 2011). We assessed compulsive behaviour in *Grb10*$^{+/p}$ mice using the marble burying task, and anxiety using the EPM. We found *Grb10*$^{+/p}$ are no different to wildtypes on the main measures of compulsivity and anxiety. However, we did find differences in auxiliary measures that could suggest Grb10+/p mice are more excitable and/or engage in more risk-taking behaviours.

There were no significant main effects of GENOTYPE, nor any interactions between GENOTYPE and TIME or GENOTYPE and AGE for any of the measures in the marble burying test. There was a significant main effect of TIME for marbles buried, half-buried, and displaced in all three cohorts, indicating mice of both genotypes tended to bury, half-bury, and displace more marbles over time. The main effect of AGE for time spent digging survived FDR correction, indicating mice 10 months of age (both genotypes) spent less time digging than mice 6 months or 10 weeks of age. Overall, there was no indication in any measure that *Grb10*$^{+/p}$ mice show different compulsivity behaviours than wildtypes over the course of the 30–minute marble burying task. Additionally,

long term isolation of barbered *Grb10*$^{+/p}$ and wildtype mice from the mixed genotype cages in both Garfield's colony and our own resulted in whisker regrowth (Garfield, 2007; Garfield et al., 2011). We conclude the whisker barbering phenotype is unlikely to result from trichotillomania-like behaviours.

The lack of correlation of the whisker barbering with our other social dominance tests, and the difference in barber genotype between Garfield's study (*Grb10*$^{+/p}$ barbers) and our own (wildtype barbers), still begs explanation. Garfield originally interpreted the whisker barbering as an indication of enhanced dominance in *Grb10*$^{+/p}$ mice. Alternatively, we suggest the barbering in these colonies may better indicate an unstable dominance hierarchy. Curley argued barbering occurs among groups of mice that have yet to conclusively determine their dominance status (Curley, 2011; Long, 1972). *Grb10*$^{+/p}$ mice may fail to develop full social competence in social dominance interactions, prolonging or preventing the settlement of stable hierarchies. Human children and Rhesus macaques acquire these kinds of essential social skills for adult behaviour through peer interactions during development. These early social interactions have also been reported as characteristic features of rodents, but there are fewer direct investigations of their consequences for adult behavior (Branchi, D'Andrea, Santarelli, Bonsignore, & Alleva, 2011). As discussed in the last chapter, knockouts and wildtypes can modify each other's behaviour in mixed-genotype housing (Kalbassi et al., 2017). Again, this stresses the need for experimental designs using single-genotype housing, and perhaps single-genotype rearing, of *Grb10*$^{+/p}$ and their wildtype siblings.

Anxiety phenotypes impact both the results of the marble burying task and social dominance competitions. *Grb10*$^{+/p}$ anxiety at 10-12 months of age has already been assessed using the open field and light/dark box paradigms and was found to be no different from wildtypes (Garfield, 2007; Garfield et al., 2011). We used the elevated plus maze (EPM) as a standard for comparison across all three cohorts (10 weeks, 6 months, 10 months) in our cross-sectional study.

The results of the EPM analysis were consistent with the findings from open field and light/dark box testing from Garfield 2007. There were no significant differences after FDR corrections between *Grb10*$^{+/p}$ and wildtype mice across the three cohorts in the main measures of anxiety behaviour, specifically 'open arm entries', 'percent time spent on the open arm', 'time per open arm entry', and 'latency to first open arm entry'. We conclude anxiety in *Grb10*$^{+/p}$ mice in all three cohorts is no different to wildtype controls.

However, five other EPM measures survived FDR corrections with significant main effects of GENOTYPE. *Grb10*$^{+/p}$ mice moved at a higher velocity and made more closed arm, middle zone, and overall entries to EPM zones than wildtypes. *Grb10*$^{+/p}$ mice also spent more time in head dipping behaviours. Two possible explanations of the *Grb10*$^{+/p}$ increased velocity and transitions on the EPM during the five-minute test are (1) more exploratory behaviour, or (2) higher general activity levels. In Garfield 2007, *Grb10*$^{+/p}$ mice were assessed for exploration and habituation. In this test, they were introduced to an environment fitted with infra-red beams for 1 hour on three consecutive nights. There were no general reactivity differences to the novel

environment on the first night, though *Grb10*$^{+/p}$ mice habituated more slowly, spending more time exploring than wildtypes on the second and third nights. Based on this evidence, we may not expect general reactivity differences during a 5-minute exposure to a novel environment. However, the results of the exploration and habituation study summed activity over the duration of the 1 hour exposure. In our 30-minute marble burying task, the main effect of GENOTYPE on transitions and velocity were not significant, even before FDR corrections. Acute differences between *Grb10*$^{+/p}$ and wildtype mice in exploratory behaviour may appear in shorter time frames. Novelty reactivity and exploration was tested more acutely in Dent 2014. *Grb10*$^{+/p}$ mice were no different to wildtypes in breaks and runs analyzed in 5 minute bins over a 120 minute locomotor activity test conducted in a novel environment (Dent, 2014). *Grb10*$^{+/p}$ and wildtypes also displayed equivalent habituation to this novel environment over three days. Furthermore, *Grb10*$^{+/p}$ mice were also tested for novel exploration more specifically using the Novelty Place Preference task. There was no significant difference between *Grb10*$^{+/p}$ mice and wildtype controls in number of entries to the novel arena or time spent in the novel arena (Dent, 2014). These tests suggest *Grb10*$^{+/p}$ mice have normal levels of novelty reactivity and exploration.

Garfield 2007 also assessed individually housed *Grb10*$^{+/p}$ mice for general activity levels in a familiar environment. In this task, mice were acclimated over 1 week to test cages containing three horizontal infrared beams across their width. Animals were assessed for 10 hours per day or night on three consecutive days. *Grb10*$^{+/p}$ mice did not demonstrate significantly different

total locomotor activity compared to wildtypes during either the day or night. This evidence suggests the difference in velocity and transitions on the EPM are not due to environment–indiscriminate differences in total locomotor activity in *Grb10*$^{+/p}$ mice.

In both Bath and Cardiff, staff and experimenters independently note highly excitable behaviour in *Grb10*$^{+/p}$/wildtype cages of young mice (Garfield, 2007). This consists of rapid circling of the cage, escape attempts, and tail rattling when the cage lid is removed. We noted these behaviours became less pronounced with age. Some element of excitability in the presence of researchers may contribute to the observations in the short-duration EPM, which even out over longer duration testing.

Grb10$^{+/p}$ mice also spent more total time in head dipping behaviours than wildtypes, though time on the open arm is not statistically different. Head dipping is a risk-taking behaviour on the EPM. *Grb10*$^{+/p}$ mice also display risk-taking choice during the delay-reinforcement task. The choice of a delayed but larger reward in considered more risky (and less impulsive) than an immediate but small reward (Xu, Das, Hueske, & Tonegawa, 2017). Delay adds an element of uncertainty to receipt of the reward and/or the value-to-delay ratio (Schonberg, Fox, & Poldrack, 2011). *Grb10*$^{+/p}$ mice are more tolerant of an increased delay to the larger reward in the delayed-reinforcement task (Dent et al., 2018). Increased head dipping on the EPM may also be an indicator of disposition to riskier choice.

This chapter found no differences in compulsivity or anxiety in *Grb10*$^{+/p}$ mice, but did highlight potential differences in excitability and risk taking

behaviours. Further investigations of whisker barbering behaviours in *Grb10*$^{+/p}$/wildtype colonies should account for mixed-genotype rearing and housing. Investigations of excitability should examine acute effects of interaction with researchers which may persist despite handling habituation protocols. Increased head dipping behaviour on the EPM supports the risky and less impulsive choice phenotype identified in Dent et al. 2018 through the delayed-reinforcement task.

7 dCas9-TET2(CD)

7.1 Introduction

Conventional methods of investigating imprinting architecture rely upon methods which provide only indirect or associative evidence of the function of epigenetic marks, and/or may disrupt the DNA itself. These techniques have nevertheless helped researchers deduce much of the *Grb10* regulatory architecture. However, new targeted epigenetic editing tools provide improvements on the specificity of experimental changes in genomic space and in developmental time, while leaving the DNA sequence of imprinting regulatory regions intact. These improvements will help confirm and expand our mechanistic understanding of *Grb10* regulation. The objective of this chapter was to create an epigenetic editor for targeted demethylation (dCas9-TET2(CD), detailed later in this introduction) to confirm previous findings about *Grb10* regulatory architecture while (a) avoiding sequence changes to the *Grb10* ICR, (b) improving on the specificity of the epigenetic experimental manipulation, and (c) expanding our experimental capacity for targeting later developmental stages.

To begin, I will discuss elements of *Grb10* regulation revealed by conventional techniques, and point out the weaknesses associated with these experimental manipulations. I will then summarize these weaknesses in our understanding of *Grb10* regulation, and distill the three technical goals (a, b, and c above) which we may achieve using targeted epigenetic editors. After discussing these editing systems, I will expand upon the specific system, dCas9-

TET2(CD), I created and tested in this chapter intending to resolve some of the experimental issues accrued by conventional techniques. Finally, I will detail in retrospect several changes which would have improved the experimental goals and execution described in this chapter.

7.1.1 Current knowledge of *Grb10* regulation from conventional methods

Loss of imprinting (LOI) KO models reveal functional effects of imprinting regulation by interrupting or deleting the imprinting control region (ICR). Precise placement of these interruptions and deletions defines the boundaries and function of discrete regulatory sequences. For example, paternal deletion of murine Grb10 CGI2 germline DMR maternalizes the expression pattern of the paternal allele (Shiura et al., 2009). Consequently, these +/-DMR mice have growth abnormalities similar to mice with maternal duplication of proximal Chromosome 11, containing Grb10 (Cattanach, Beechey, Rasberry, Jones, & Papworth, 1996; Cattanach et al., 1998; Cattanach & Kirk, 1985; Shiura et al., 2009). Limiting the knockout model to the paternal DMR (and not both parental alleles) refined the association between this DNA-based element of imprinting architecture and the functional phenotypic consequences observed in the mouse disomy model (Shiura et al., 2009). Specifically, this ICR is required for silencing of the maternal transcripts. However, deletion of the CGI2 DMR also deleted exon 1b, from which paternally expressed transcripts originate. This loss confounds some conclusions of causality which otherwise might be drawn– does transcription from exon 1b have a role in silencing the major upstream transcripts, or is that

function solely attributable to the DMR at this site? Additionally, this deletion fails to illuminate the role of the paternal ICR in regulating paternal specific transcripts.

Several strategies circumvent the issues created by DNA deletions by disrupting the endogenous epigenetic marks or imprinting mechanisms. Some of these strategies delete essential endogenous effectors, such as those in the DNA methyltransferase family, to prevent the establishment or maintenance of the imprinting mark. Mouse embryos with *Dnmt3L*$^{-/-}$ knockout mothers aided analysis of germline imprinting at Grb10 (Arnaud et al., 2006). Dnmt3L (not imprinted) belongs to the Dnmt3 methyltransferase family but lacks a functional methyltransferase domain (U Aapola et al., 2000; Ulla Aapola, Liiv, & Peterson, 2002). Regardless, this protein enhances Dnmt3a and Dnmt3b (neither imprinted) de novo methyltransferase activity and is essential for proper establishment of maternal methylation at germline DMRs (Bourc'his, Xu, Lin, Bollman, & Bestor, 2001; Chedin, Lieber, & Hsieh, 2002; Hata, Okano, Lei, & Li, 2002; Suetake, Shinozaki, Miyagawa, Takeshima, & Tajima, 2004). In the maternal *Dnmt3L*$^{-/-}$ model, the Grb10 CGI2 DMR became biallelically hypomethylated and the major-type Grb10 transcript was not expressed. This result suggested a functional link between the methylation status of the DMR and the major transcript expression phenotype. However, the global loss of Dnmt3L methylation complicates interpretation of this data–did dysregulation elsewhere contribute to change of expression?

Other factors at the *Grb10* DMR suggested it is loss of methylation at CGI2, rather than indirect effects from elsewhere, that cause the silencing of

the major-type transcript in pups born to *Dnmt3L*$^{-/-}$ mothers. CCCTC-binding factor (CTCF), a multifunctional transcription factor recruited in a methylation-sensitive manner, is bound to the unmethylated paternal ICR at murine *Grb10* CGI2 in all tissues (Ohlsson, Renkawitz, & Lobanenkov, 2001; Shiura et al., 2009). Depletion of CTCF in mESCs using shRNA resulted in a significant up-regulation of the major Grb10 isoform expressed from the major promoter at CGI1 (Plasschaert & Bartolomei, 2015). Normal imprinted expression of the neuron-specific isoform was unaffected. This suggests a repressive regulatory relationship, where CTCF recruited to the unmethylated paternal ICR suppresses the major promoter on the cis allele. However, again possible indirect effects allowed by global CTCF depletion create a possible caveat to causal interpretations of this relationship. Additionally, human *GRB10* lacks the CTCF binding sites found in murine *Grb10* (Hikichi, Kohda, Kaneko-Ishino, & Ishino, 2003). This may be one reason why human *GRB10* is expressed biallelically in almost all tissues (notably excepting the placental trophoblast and brain.

A third assessment disrupting Grb10 imprinting via endogenous effectors targeted the Polycomb group (PcG) gene Eed (embryonic ectoderm development) (Mager, Montgomery, de Villena, & Magnuson, 2003). The Eed/Ezh2 PcG complex contains histone methyltransferase (HMT) activity for histone 3 lysine 27 and interacts with histone deacetylases, creating a repressive effect at targeted sites (Cao et al., 2002; Müller et al., 2002; van der Vlag & Otte, 1999). Eed$^{-/-}$ embryos expressed the major-type Grb10 transcript expression biallelically rather than from the maternal allele alone (Mager et

al., 2003). Despite disruption of normal imprinting, there was no major alteration of allele-specific DNA methylation at CGI2 (Mager et al., 2003). H3K27 methylation precipitates from Grb10 CGI1 but not CGI2 in cultured cortical neurons and fibroblasts from F1 hybrid wild type mice, and is specific to the paternal chromosome in fibroblasts (Yamasaki-Ishizaki et al., 2007). This suggests the major-type transcript originating at CGI1 was paternally repressed in fibroblasts by the Eed PcG complex (Yamasaki-Ishizaki et al., 2007). Yamasaki-Ishizaki et al proposed the functional consequence of chromatin remodelling by PcG proteins during cell differentiation was tissue-specific imprinting in embryonic tissues, like that demonstrated by Grb10.

7.1.2 Summary of *Grb10* regulatory knowledge and limitations

The evidence suggests major-type *Grb10* transcripts are paternally repressed through a combination of CTCF binding to the unmethylated CGI2 ICR and the addition of paternal-specific H3K27 methylation. Unfortunately, while *Dnmt3L*$^{-/-}$ mother and *Eed*$^{-/-}$ models provide some insight into the expression of the major-type Grb10 transcript, neither can cast light on the relationship between the imprinting architecture on Grb10 and the neuron-specific expression patterns observed later in development. *Eed*$^{-/-}$ embyros and embryos with *Dnmt3L*$^{-/-}$ mothers are lethal by E8.5 and E10.5 respectively– just prior to neurogenesis (Bourc'his et al., 2001; Faust, Schumacher, Holdener, & Magnuson, 1995; Hata et al., 2002; Yamasaki-Ishizaki et al., 2007). They therefore cannot provide a mechanism for disrupting DNA methylation or histone modifications in the imprinting architecture past this stage. What we do know of neuron- and paternal-specific transcript expression comes from

ChIP analysis by Sanz et al (Sanz et al., 2008). *Grb10* neuron-specific transcripts rely on the resolution of the monoallelic bivalent chromatin domain present at unmethylated paternal CGI2. Repressive H3K27me3 is lost upon neural stem cell commitment (probably in both glial and neuronal cells). Subsequently, unspecified 'neuronal factors' may recruit histone acetylases to CGI2 through H3K4me2 (an activating mark) or a putative neuron-specific enhancer (Sanz et al., 2008). This neuron-specific mechanism is unknown. Though incredibly useful, the ChIP data is associative, and lacks the power of experimental manipulation to demonstrate mechanism, again calling for the further development of targeted epigenetic editing tools.

In addition to early embryonic lethality problems, approaches such as *Dnmt3* maternal knockout, *Eed* knockout, and CTCF depletion are unspecific to the locus of interest. They may create widespread changes across the genome, dysregulating many genes and obscuring the resulting LOI phenotype (John, 2010). Studies referenced above using the *Dnmt3L* and *Eed* deletion models specifically showed disruption of other imprinted genes besides Grb10 (Arnaud et al., 2006; Mager et al., 2003). For example, depletion of CTCF using shRNA most likely prevented its activity at a range of sites besides Grb10, including the H19/Igf2 imprinted locus, where CTCF acts as an enhancer blocker (Hark et al., 2000; Plasschaert & Bartolomei, 2015). Equally, pharmacological removal of a mark using an agent such as 5-azacytidine (inducing global demethylation) has widespread rather than specific effects (Christman, 2002; Heerboth et al., 2014). Global effects on imprinted genes may also mask the regulatory relationship between the *Grb10* ICR and

neighbouring imprinted *Ddc*. While association, knockout, and pharmacological studies are very helpful for discerning the broad impacts of imprinting on biological systems, these strategies fall short of the high resolution needed to probe the function of imprinting marks independent of the genetic sequence beneath them and to make a broader range of temporally-specific manipulations.

7.1.3 Tools for Targeted Epigenetic Editing

In future experiments, we want to avoid sequence changes that disrupt exons around the ICR. Thus, our techniques must only make **epigenetic** changes. This requires our modifications to survive mitotic divisions. We also need greater **specificity** of manipulation; we wish to avoid the indirect effects accrued by global changes. This requires precise targeting of our epigenetic changes. Finally, we require greater flexibility in when we make the targeted change. This feature is particularly important when imprinting architecture varies between tissues and developmental stages, resulting in differing transcript expression patterns. For *Grb10* regulation, we wanted our tool to create a targeted epigenetic change that could last through later developmental stages such as neurogenesis (E10.5 and on) or be made during these later time points.

There are several systems for targeted epigenetic editing that fulfill the above requirements. The basic structure of a targeted epigenetic editing tool, which we will refer to as an EpiEffector, is a programmable DNA binding domain (DBD) or other targeting mechanism coupled to an epigenetic effector domain (Laufer & Singh, 2015). Some binding domains include zinc finger

nucleotides (ZFNs), transcription activator-like effector nucleases (TALENs), and the clustered regularly interspaced short palindromic repeats/nuclease deficient-Cas9 (CRISPR/dCas9) system (Laufer & Singh, 2015; Rienecker, Hill, & Isles, 2016). Some example epigenetic editors (EpiEffectors) are summarized in Table 7.1. CRISPR based tools afford an advantage over ZFNs and TALENs because they are easy to clone, transfect, integrate into cell lines, and retarget by editing the sgRNAs. The CRISPR/dCas9 system is targeted by single guide RNA (sgRNA, aka synthetic guide RNA). sgRNAs are composed of a fused crRNA or guide RNA, which binds a complimentary DNA target, and a tracrRNA, which associates with dCas9. “gRNAs” refer to all CRISPR guide RNA formats, while “sgRNAs” refer to the combined crRNA and tracrRNA elements in a single guide molecule. Because sgRNAs are ~23 bp in length, they can be easily synthesized for re-targeting, or multiplexed at a genomic site by creating a variety of sgRNAs spanning a local area larger than any one sgRNA target. sgRNAs are designed through various guide design tools (here we used the CRISPR guide design tool from the Zhang Lab, since shut down). These require an input target genomic region, and look for unique sequences of ~20 bp starting with a 3 bp protospacer adjacent motif (PAM) sequence– 5’-NGG-3’.

Table 7.1 Example EpiEffectors

EpiEffector	*Description*	*Reference*
dCas9-TET2(CD)	*Potentially demethylates DNA by directing the Ten Eleven Translocation 2 (TET2) catalytic domain dioxygenase activity*	*Subject of this chapter (2015-2016)*
dCas9-DNMT3A	*Adds DNA methylation to CpG sites at the target by directing DNA methyltransferase 3A (DNMT3A) activity*	(Vojta et al., 2016)
dCas9-TET1	*Demethylates DNA by directing the Ten Eleven Translocation 1 (TET1) activity*	(Liu et al., 2016)
dCas9-p300(core)	*Acetylates H3K27 and activates transcription by targeting human E1A-associated protein p300 acetyltransferase activity*	*(Hilton et al., 2015)*
dCas9-VP64	*Activates transcription by recruiting a transcription complex to the target*	*(Perez-Pinera et al., 2013)*
CD54-TET2(CD)/-TET1(CD)/TET3(CD)	*Zinc Finger DBD directed; Demethylates the ICAM1 locus by directing the activity of a TET protein family catalytic domain*	(Chen et al., 2014)
pMX-CD54-TET2(CD)	*GFP tagged and Zinc Finger DBD directed; Demethylates the ICAM1 locus by directing the TET2 catalytic domain*	(Chen et al., 2014)
ZF_B-TET2(CD)	*Zinc Finger DBD directed; Demethylates EpCAM locus by directing the TET2 catalytic domain*	(Chen et al., 2014)

The nuclease-inactivated deactivated Cas9 (dCas9) domain itself is ideal for targeted epigenetic editing, because it maintains its localization capabilities while inactivating the nuclease function of Cas9. Thus, the dCas9 domain of an EpiEffector can localize a fused or associated epigenetic reader,

writer, or eraser enzyme domain to the DNA locus specified by the sgRNA sequence, without cutting the targeted site (Rienecker et al., 2016). The same dCas9-epigenetic editor construct may be retargeted to another locus by introducing a different, easily synthesized sgRNA (Vojta et al., 2016). The dCas9 construct may even be continuously expressed in a cell line, awaiting the introduction of a targeting sgRNA. By contrast, ZFNs and TALENs DNA binding domains must be redesigned for each target in a cumbersome process (Laufer & Singh, 2015).

An elegant example of a CRISPR/dCas9 of EpiEffector may be found in Vojta 2016, and is included in this thesis as Figure 7.1 (Vojta et al., 2016). This tool uses the catalytic domain of DNA methyltransferase DNMT3A to add repressive DNA methylation marks. Vojta et al (2016) achieved targeted CpG methylation over a region of ~35bp using this tool, and expanded this by multiplexing sgRNAs (Vojta et al., 2016). Among the tested targets, IL6ST, a gene relevant for N-glycosylation of immunoglobulin G (IgG) and associated with some autoimmune diseases, showed more than 2-fold decrease in transcript level, providing proof of concept for targeted dosage control by epigenome editing (Lauc et al., 2013; Ling et al., 2004). Moreover, changes in methylation were heritable across mitotic divisions up to 42 days after transfection. Long-term maintenance of imprinting marks is an important element qualifying imprinting architecture as epigenetic rather than simply regulatory. Epigenetic editing tools need to effect similarly stable changes to be useful for functional research. While EpiEffectors enable causal experiments investigating the function of specific regulatory marks, tools must

still be chosen carefully, as the context of marks within imprinting control regions is complex (Surani, 2001). Some imprinting architectures, such as the bivalent chromatin domain at *Grb10,* may require simultaneous changes to multiple marks to alter transcription (Sanz et al., 2008). We also need to be confident our regulatory tools are capable of changes to proximal marks without accumulating non-specific changes off-target. One way to accomplish this is to cross-link the construct to the DNA and precipitate these sites by digestion and ChiP. Any off-target binding sites should be examined for off-target editing, in addition to the region of interest (Liu et al., 2016).

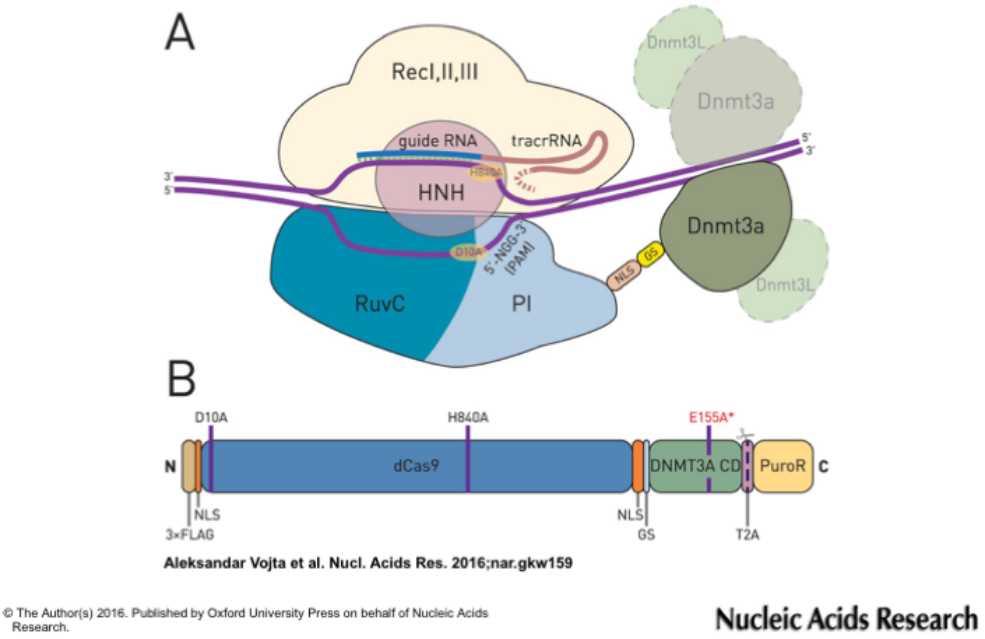

Figure 7.1 Anatomy of Example CRISPR-based EpiEffector: dCas9-DNMT3A (Adapted from Vojta et al 2016)

Figure 7.1 Legend:

(A) The dCas9-DNMT3A fusion protein complexes with the sgRNA (composed of the fused crRNA or guide RNA and tracrRNA) to target the DNMT3A effector domain to the target region. The dCas9 segment is composed of a recognition lobe (Rec I, II, and III) and an inactivated nuclease lobe (HNH, RuvC, and PI domains). The DNMT3A effector is fused to the PAM-interacting (PI) domain on the nuclease lobe by a nuclear localization signal (NLS) and a Gly_4Ser (GS) peptide linker. The DNMT3A catalytic domain recruits partners for dimerization to carry out targeted methylation.

(B) Linear order of domains on the dCas9-DNMT3A fusion protein. The N-terminal begins with the 3x FLAG epitome tag and the nuclear localization signal (NLS), followed by the nuclease-inactivated deactivated Cas9 (dCas9) domain (inactivating mutations D10A and H840A ARE INDICATED). dCas9 is

followed by a second NLS, and a GS peptide linker which fuse it to the catalytic domain of human de novo DNA methyltransferase 3A (DNMT3A CD). In this domain, E155A indicates the DNMT3A inactivating mutation used as a negative control. The mRNA for this fusion protein also contains a puromycin resistance gene transcript (protein domain–PuroR) or EGFP gene (not shown) for selection of successfully transfected cells. During translation, this selector separates from the EpiEffector when the T2A self-cleaving peptide detaches the fusion protein's C terminal end.

7.1.4 Creating a dCas9-TET2(CD) construct

In this chapter, we construct a CRISPR/dCas9 targeted demethylator to circumvent the issues of global methylation disruption and early lethality within the maternal *Dnmt3L*$^{-/-}$ model (Arnaud et al., 2006). Targeted demethylation of the maternal DMR could replicate the silencing of the major transcript on the major allele observed in pups born to *Dnmt3L*$^{-/-}$ mothers. We hypothesized a dCas9 targeted tool with a TET2 catalytic domain could induce targeted demethylation of the *GRB10/Grb10* ICR. We aimed to (1) measure demethylation at the targeted locus, the DMR at *GRB10* CGI-2, in a HEK cell model (2) measure expression of maternal-specific transcripts, and (3) measure expression of paternal- or neuron-specific transcripts. We did not anticipate any change in paternal- or neuronal-specific expression in our HEK cell model, as further modifications to the chromatin are likely required to achieve paternal expression patterns. This construct was designed for a proof of concept in a workhorse cell system, HEK 293T, with the intention of employing the verified tool in further *in vitro* neuronal differentiation experiments (not carried out in this thesis). The same tool proved in HEK 293T cells could be transferred to a new *in vitro* model (human or mouse) by redesigning the sgRNAs.

We chose the catalytic domain (CD) of the dioxygenase Ten Eleven Translocation 2 (TET2) as the effector domain component of our construct. TET2 and other members of the TET family initiate 5-mC oxidation as part of active demethylation, catalyzing the conversion of 5-methyl cytosine to 5-hydroxymethyl cytosine (Ito et al., 2011; Ko et al., 2010; Tahiliani et al., 2009).

Possible mechanisms concluding the demethylation process involve further modification of 5-hmC, repair by base excision repair machinery, and incorporation of an unmethylated cytosine (Guo et al., 2011; He et al., 2011; Ito et al., 2011). At the right target, such demethylation can facilitate the reactivation of gene or alternative transcript expression (Christman, 2002; De Smet, Lurquin, Lethé, Martelange, & Boon, 1999; Liu et al., 2016). Here, we were hoping to remove the methylation at maternal CGI-2, the ICR of *GRB10*. TET2 (CD) is a good candidate for fusion into the enzymatically inactive CRISPR/dCas9 system because this effector domain was successfully used in a designer system with DNA binding zinc fingers (Chen et al., 2014). The Zinc Finger based EpiEffector CD54-TET2CD was targeted to *ICAM-1* in A2780 cells (a human ovarian cancer line) and induced a small but significant increase in expression not seen in similar constructs using -TET1CD, -TET3CD, or a mutated -TET2CD. Sorted A2780 cells expressing GFP after pMX-CD54-TET2CD transduction showed significant demethylation through pyrosequencing analysis for four CpG sites located in the effector domain target region. In the same region, a construct using –TET1CD displayed only two and a construct using –TET3CD displayed no significantly demethylated sites (Chen et al., 2014).

As part of a CRISPR/dCas9 based system, demethylation induced by TET2CD could be much more easily retargeted with a new guide RNA, avoiding the difficulty of designing a new ZFN DNA binding domain for every target. This targeting system also allows for greater multiplexing capacity, as the same dCas9-TET2(CD) construct may be simultaneously used for multiple targets at

once, rather than requiring expression of multiple DBD-effector domain fusions. A dCas9-TET(CD) construct might additionally be incorporated into a stable cell line for diverse inquiries requiring targeted demethylation.

We targeted our sgRNAs to the differentially methylated region (DMR) at CpG Island 2 (CGI-2), which overlaps with paternal-transcript specific exon UN2. The details of our sgRNA design are in Methods section 7.2.2. Our dCas9-TET2(CD) fusion construct, guided by these sgRNAs, was expected to demethylate this locus on the maternal allele to match the unmethylated paternal allele. Previous CRISPR-guided constructs have tested the efficacy of sgRNA at a range of distances from the target site. Vojta et al found the highest CpG methylation activity of their dCas9-DNMT3A construct centered at 27 bp downstream of the sgRNA PAM sequence (Vojta et al., 2016). Multiplexing, or tiling, a region with multiple sgRNAs has also improved the efficacy of dCas9 systems (Laufer & Singh, 2015). Our pyrosequencing target, taken from Woodfine 2011, was in the middle of our tiled region (Woodfine, Huddleston, & Murrell, 2011). We expected sgRNA A9, or a combination of all sgRNAs (simultaneous transfection), to be most effective at demethylating the pyrosequenced region.

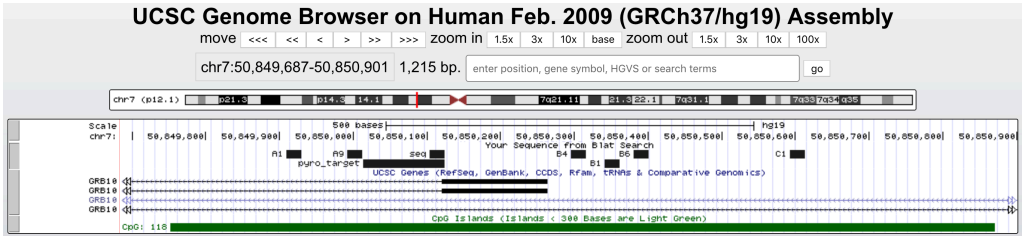

Figure 7.2 sgRNAs tiled across GRB10 CGI-2 in relationship to the pyrosequencing target

Figure 7.2 Legend: A1, A9, B1, B4, B6, and C1 represent sgRNA targets. "seq" represents the sequencing primer genomic equivalent site (pre-bisulfite conversion), and "pyro_target" represents the pyrosequencing read (pre-bisulfite conversion).

Most human tissues including the placenta express GRB10 biallelically, but the brain and placental trophoblast are monoallelic, expressing the paternal and maternal alleles respectively (Monk et al., 2009). Transcripts originating at human exon UN2 in HEK 293T cells are expressed only from the paternal allele and only in the brain (Monk et al., 2009). We therefore also monitored parent-of-origin and tissue-specific transcripts for change in expression during our experimental manipulations. However, our main chapter was to create and test a tool to directly disrupt normal imprinted methylation at the *GRB10* ICR.

7.1.5 Experimental design in retrospect

In retrospect, we should not have used HEK 293T cells to test our construct at *GRB10*. While HEK cells are a common workhorse culture for expressing cloned plasmids, we had two major design problems. First, we were unable to pyrosequence the human *GRB10* locus using the Woodfine primers or newly designed primers (Woodfine et al., 2011). Efforts to identify and solve

the problem are detailed in the results and discussion sections below. This was the crucial measure of the efficacy of our construct. Only after spending time troubleshooting this pyrosequencing problem did we finally generate mouse embryonic stem cells (mESCs) from our colony and confirm our ability to pyrosequence the murine *Grb10* CGI2 locus (we did not progress to transfections with the construct in mESCs). Secondly, human *GRB10* CGI-2 lacks the CTCF binding sites found at murine *Grb10* CGI2. Therefore, HEK 293T cells were useful *only* in demonstrating the expression of the mRNA and protein for the construct (and theoretically but not practically for measuring the effect on methylation) and were not useful in determining whether demethylation of the ICR would replicate the upregulation of the major transcript observed in murine pups born to *Dnmt3L*$^{-/-}$ dams. This construct would have been better tested in murine cells from the start.

7.2 Materials & Methods

7.2.1 dCas9-TET2 cloning

The catalytic domain of TET2 was amplified from FH-Tet2-pEF plasmid (Addgene # 41710) using primers designed from the coding domain indicated by primers in Supplementary Table 1 of Chen 2014 (H. Chen et al., 2014). Recognition sequences for Asc1 and Pme1 were added to the ends of these primers, with AscI on the forward primer, on the 5' end of the gene, and Pme1 on the reverse primer, at the 3' end of the gene, for ligation into the pcDNA dCas9-p300 Core plasmid (Addgene #61357). TET2 PCR amplification product was purified with the QIAquick PCR Purification Kit. Vector plasmid was digested with Asc1 and Pme1 and FastAP for dephosphorylation of the vector and the cut p300 insert. TET2(CD) PCR product was digested with both enzymes but without FastAP, leaving the ends phosphorylated. Both digestions were incubated at 37ºC for 30 minutes and inactivated by incubation at 75º for 15 minutes. Vector and insert were ligated at a 1:3 and 1:6 ratio, with 50 ng of vector in each and 41.85 ng and 83.7 ng of insert respectively. Ligation was performed with Quickligase for 10 minutes at room temperature. Transformation was carried out by heat shock. 1.5 ul ligation was mixed with 30 ul of high efficiency 5-alpha competent E. coli from NEB by flicking and incubated on ice for 30 minutes. Bacteria were incubated for 45 seconds in a 42ºC water bath and returned to ice. Once the sample had cooled for several minutes, 300 ul SOC Outgrowth medium was added and the sample was incubated in a 37ºC waterbath for 1 hour. Bacteria were plated on LB agar + Amp (1 µM) and incubated at 37ºC overnight. Selected colonies were tested

for the TET2(CD) insert within the dCas9 vector and grown in larger liquid LB cultures for plasmid mini-prep.

7.2.2 *GRB10* targets to DMR for sgRNA

GRB10 synthetic guide RNA targets were designed to the DMR described in CpG island 2 in Monk 2009, covering chr7:50849753-50850871 in the February 2009 alignment. The DMR was identified via the "EMBOSS CpG plot" as spanning chr7:50,850,205-50,850,454. This section was broken into three parts for adequate CRISPR coverage and targets for each were selected from those identified by the CRISPR Design tool by the Zhang Lab. See Figure 7.2 in the introduction for sgRNA targets on CGI2.

7.2.3 sgRNA cloning

sgRNA target sequences were amplified by PCR from complementary primers with sequences matching the pSp gRNA vector (Addgene #47108) overhang generated by Bbs1 digestion. sgRNAs were cloned into the vector using the Target Sequence Cloning Protocol in the CRISPR Genome Engineering ToolBox. Neither gel purification nor PlasmidSafe exonucleases were used. Restriction enzymes digesting the vector plasmid were inactivated by incubation at 65ºC for 20 minutes. Transformations by heat shock were carried out as described above, using 1 ul of ligation and 20 ul NEB 5-alpha competent E. coli

7.2.4 Plasmid Isolation from E. coli

Plasmids were initially isolated from E. coli cultures using the PureYield Plamid MiniPrep System. Cultures of 2-3 ml were spun down and resuspended in 600 µl double deionized water for lysis. dCas9-p300 plasmid required 6 ml for adequate plasmid production. Larger quantities of the dCas9-TET2(CD) plasmid were isolated using the Qiagen Midiprep kit. Cultures of ~100ml were spun down for lysis and extraction per directions.

7.2.5 HEK culture

HEK 293T cells were cultured in DMEM media with FBS and Glutamate. Media was made up with 445 ml DMEM, 50 ml FBS, and 5 ml Glutamate.

7.2.6 Aza treatment

On the first day of the treatment, HEK 293T cells at confluency were mechanically separated and split at 1:20 into a T25. 5 µl of 25 mM 5-aza in DMSO stock was added to 5 ml fresh DMEM + FBS + Glu media for a final concentration of 25 µM 5-aza on the cells each day for 72 hours. 5 µl DMSO was added to a parallel culture as a control. Cells were harvested by spinning down in old media, washing in 1.5 ml PBS (for T25) or 500 µl PBS (for 1 well of a 24 well plate), and freezing down in a -80ºC freezer.

7.2.7 Transfection

HEK 293T cells were plated in 24 well plates at 100,000-150,000 cells per well (counted by haemocytometer) for 24 hours or more before transfection. 750 ng dCas9 plasmid and 250 ng total of guide RNA plasmids were mixed in blank DMEM media to a total volume of 25 µl per transfection

well. All transfection batches included a transfection carrying dCas9 plasmid only, without guide RNA, as a negative control. Each 25 µl of plasmids was mixed with 23 µl blank DMEM + 2 µl Lipofectamine 2000 mix. The final solution was added slowly to the side of the well and left on the HEK cells for at least 4 hours before the media was changed for fresh DMEM + FBS + Glu.

7.2.8 Protein Extraction

Cells were plated at 400,000 cells/well of a 6 well plate and transfected with dCas9_TET2(CD) plasmid using Lipofectamine, as described in the Transfection protocol. No guide RNA plasmids were introduced. One well of the plate was transfected with GFP and transfection rates were compared with those of the 24 well transfections to ensure consistency. Transfected cells were grown to confluency for 48 hours and harvested using Lysis Buffer containing final concentrations of 75 mM Tris, 3.8% SDS, 4M Urea, 20% glycerol. Three hundred microliters of lysis buffer were added to each well of the 6 well plate and left for several minutes before scooping off into a 1.5 ml Eppendorf tube and freezing at -80˚C.

7.2.9 BCA Protein Assay

Samples were sonicated for 2-4 s to reduce viscosity. The sonicator tip was cleaned between samples. A portion of the unknown protein samples to be quantified was diluted 1:20 with Millipore ultra-pure water for measurement. A ‘blank’ reading was made up by diluting Lysis buffer without a protein sample 1:20 in Millipore ultra-pure water. 25 µl of each known

standard or unknown sample was mixed with 200 µl of a 50:1 reagent A: reagent B mixture (WR) in a well of a 96 well plate. The plate was incubated at 37 °C for 30 minutes and absorbance was read at 562 nm. A protein standard was calculated from the known standards and fit with a 3rd order polynomial. Absorbance readings from the 1:20 lysis buffer dilution (the 'blank) was subtracted from the absorbance readings of the unknown samples. The adjusted readings for the unknown samples and the 3rd order polynomial were used to calculated the concentration of the 1:20 sample dilutions. Stock concentrations were calculated from the 1:20 dilution.

7.2.10 Western Blot

Samples were prepared for western blot by defrosting on ice and diluting a portion of the sample to 0.5 mg/ml using lysis buffer (under Protein Extraction). 20 µl (or 10 µg) of the sample was mixed with 20 µl of 2x Loading Buffer (0.125M Tris HCL pH 6.8, 20% glycerol, 4% (W/v) SDS, 0.004% bromophenol blue in Tris pH 8.0, 10% 2-mercaptoethanol). The sample-loading buffer mix had a final concentration of 0.002% bromophenol blue and 5% 2-mercaptoethanol. Samples in loading buffer were heated for 5 minutes in a 95˚ heat block prior to loading on the gel. An identical volume and concentration of samples were loaded in each well to ensure even running of the gel.

Proteins were visualized on a Novex™ WedgeWell™ 4-12% Tris-Glycine Mini Gel (ThermoFisher) run at 200V for 41 minutes using 1x NuPAGE MES SDS Running Buffer (Life Technologies). Samples were run against the Spectra

Multicolor High Range Protein Ladder (ThermoFisher). After electrophoresis, samples were transferred to a nitrocellulose membrane (pore size 0.45µm, Life Tech) using the BioRad transfer system. The transfer was run in transfer buffer at 75V for 1 hour. An ice pack was placed in the tank with a magnetic stir bar at the bottom to keep the transfer cool.

When a sufficient size difference between the protein of interest and the housekeeping protein existed, the membrane was midway between the expected sizes for separate incubation in the 1˚ antibodies. The two halves of the membrane were blocked and washed together where possible to maintain identical treatment. After the transfer, the membrane was blocked in 5% milk in TBST (1% Tween-40) for 1 hour. The membrane was washed 3x10 min in TBST before incubating in the 1˚ antibody in 5% milk in TBST overnight at 4˚C with mild agitation. The membrane was washed 4x10 min in TBST prior to 2˚ antibody incubation in 5% milk in TBST at room temperature for 1 hour with agitation. The membranes were washed 4x10 min in TBST and 1x in PBS prior to imaging on the LiCor Imager.

Table 7.2– Antibodies Used

Antibody	Immunogen	Biological source	Specificity	Western Blot Dilution	Origin
Monoclonal ANTI-FLAG M2 antibody	FLAG epitope tag	Mouse	FLAG epitope tag	1:2000	Sigma
Monoclonal Anti-β-Actin antibody	Modified β-cytoplasmic actin N-terminal peptide	Mouse	β-actin, canine, guinea pig, *Hirudo medicinalis*, feline, pig, mouse, carp, chicken, sheep, rabbit, rat, human, bovine	1:3000	Sigma
Odyssey donkey anti-mouse (800)	Mouse IgG	Donkey	Mouse IgG	1:3000	LiCor

7.2.11 qRTPCR

7.2.11.1 RNA isolation and cDNA synthesis

RNA was isolated from HEK cells using the RNeasy Mini Kit and DNaseI digestion and was stored in a -80ºC freezer. cDNA for optimization was synthesized using RNA to cDNA EcoDry Double Primed Premix strips.

7.2.11.2 q RT PCR

GRB10 primers were designed based on tissue-specific alternative promoter transcripts outlined in Arnaud 2009. Primers were designed to cover general *GRB10*, brain-specific, and placenta-specific transcripts. Reactions were assembled by robot using SybrGreen no-rox mix. Each reaction was

performed in triplicate. Primer pairs were optimized on the Corbett Rotor-Gene Q qRT PCR machine in comparison to no-template controls.

7.2.11.3 GRB10 transcript primer targets for q RT PCR

Primers targeting general, paternal- and maternal-specific transcripts were designed using tissue specific transcript information found in Monk 2009 (Monk et al., 2009). Maternal-specific expression was detected through amplification of transcripts containing exons UN3-3.2, which are placenta-specific. Paternal-specific expression was detected through amplification of transcripts containing exon UN2, which is brain-specific. General transcript was detected using a common exon downstream.

Table 7.3 Human GRB10 qRT PCR Primers

Primer Name	Target	Species	Sequence	Q RT PCR final concentration
GRB10_F	General GRB10 transcript	Human	CCAGTGCTGTGTCCTGTGAA	300 nM
GRB10_R	General GRB10 transcript	Human	CTCCCTGCTGGCAATGGATT	300 nM
UN3-3.2_F	Placenta-specific GRB10 Transcript	Human	TTGGCATGAAGGGGTGAGAG	300 nM
UN3-3.2_R	Placenta-specific GRB10-transcript	Human	AGGTGGTTCAGAGGTCACAC	300 nM
UN2_alt1_F	Paternal and neuron-specific transcript	Human	AGACTTGGGAGGCTGCATT	300 nM
UN2_R	Paternal and neuron-specific transcript	Human	GGTGGTCAGAGGTCACACC	300 nM

7.2.12 Sanger Sequencing

Genomic DNA (gDNA), 2.5 hour BS converted DNA, and 12 hour BS converted DNA samples were amplified using primers targeted to the DMR region. The gDNA product was 308 bp long and the BS converted product was 139 bp long. Amplified samples were purified with the Promega Wizard PCR

purification system. All Sanger Sequencing samples were diluted to specifications and sent to Source Biosciences for processing.

Table 7.4–Sanger Sequencing Primers for genomic and BS converted GRB10 DNA

Primer Name	Direction	Sequence	Notes
GRB10 gDNA 2F	Forward	GGGTTTCCGTGGGTACAGTT	
GRB10 gDNA 2R	Reverse	CGCTCTCCAGGTACTCAGGT	
BS gDMR F	Forward	CTCTCCAAATACTCAAATAAACTC	Woodfine 2011 primer
BS gDMR R	Reverse	CGCCAGGGTTTTCCCAGTCACG ACGGTCGGGGTTTTTGTAGTTTG	Woodfine 2011 primer + common recognition sequence

Plasmid DNA was sequenced using primers spanning the dCas9 and TET2 (CD) fusion site and the length of the TET2 coding domain. The dCas9-TET2(CD) plasmid was 12,226 bp, and sequencing reads were spaced for coverage and some overlap. Separate sequencing reactions began from five primers (Found in Table 7.5) along the murine TET2(CD) sequence and the dCas9 sequence within the plasmid. Four primers ran forwards along the sequence and one ran in reverse, spanning the dCas9-TET2(CD) junction and AscI RE site. Sequence reads were aligned to the expected sequence using the Clustal Omega Multiple Sequence Alignment tool from the European Bioinformatics Institute.

Table 7.5 dCas9-TET2(CD) Sanger Sequencing Primers

Primer Name	Orientation	Sequence (5'-3')	Sequencing Notes
Plasmid_F	Forward	CCATCAATCCATCACTGGTCT	Covers dCas9-TET2(CD) fusion junction and the AscI restriction enzyme site
Int_F	Forward	GCCAGAAGCAAGAAACCAAG	Internal forward primer complementary to TET2(CD)
Int_R	Reverse	CCTTCCTTCAGACCCAAACA	Internal reverse primer complementary to antisense strand of TET2(CD)
Mid_F	Forward	CAACACTCCAGAGGCACCTT	Internal forward primer complementary mid-way into the TET2(CD) sequence
Late_F	Forward	TGCCTCCAGATCACCATACA	Internal forward primer complementary late into the TET2(CD) sequence

7.2.13 Pyrosequencing

7.2.13.1 Phenol-Chloroform DNA isolation

DNA for bisulfite conversion and pyrosequencing was isolated using phenol chloroform. Cells were lysed with Tris lysis buffer and digested overnight with proteinase K. An equal volume of phenol was added, vortexed for 5 seconds, left for 5 minutes, and vortexed again for 5 seconds before a 10-minute centrifuge. The aqueous phase was removed to a fresh tube and an

equal volume of chloroform was added and vortexed for 5 seconds before centrifuging for 10 minutes. The aqueous phase was removed to a fresh tube again and 1/30th volume of 3 M NaOAc was added with one volume ethanol and mixed to precipitate. DNA was scooped out with a tip and transferred to a clean eppendorf before rinsing in 70% ethanol, draining, and leaving to dry before resuspending in elution buffer. Isolated DNA was stored in a -20ºC freezer.

7.2.13.2 BS conversion

DNA was bisulfite converted using the EZ DNA Methylation-Gold Kit from Zymo Research Corp. 500 ng of DNA in a total volume of 20 µl was added to 130 µl of CT conversion reagent. The reaction was placed in a thermal cycler at 98ºC for 10 minutes and 64ºC for 2.5 hours. Bisulfite converted sample was loaded into a IC spin column containing M-binding buffer, mixed by inverting, and centrifuged at 13,000xg. The column was washed in 100 µl of M-Wash Buffer by centrifuge and incubated for 15 minutes with 200 µl of M-Desulfonation Buffer. M-Desulfonation buffer was pulled through the column by centrifugation and the column was washed twice more with M-Wash Buffer. Bisulfite converted DNA was eluted with 10 µl of M-Elution Buffer and stored at -20ºC.

7.2.13.3 Post- BS conversion PCR–Human GRB10

Bisulfite converted HEK DNA was amplified with primers targeting the GRB10 germline DMR (maternally methylated) outlined in Woodfine 2011. This 2-step PCR reaction used a common biotinylated primer: B-

CGCCAGGGTTTTCCCAGTCACGAC 3'. Germline DMR primers were optimized to 55ºC using a gradient set from 55-60ºC. The hot start period was set at 98ºC for 2 minutes and the reaction was carried out for 39 cycles with denaturation at 98ºC for 45 s, annealing at 55-60ºC for 45 seconds, and elongation at 72ºC for 30 s. PCR products were check on a 1% agarose gel with Ethidium Bromide staining.

Table 7.6 Human GRB10 pyrosequencing primers

Primer Name	Direction	Sequence	Product Size	Annealing Temp	Notes
BS gDMR F	Forward	CTCTCCAAATACTCAAATAAACTC	139 bp	55˚C	Human; Woodfine 2011 germline primer
BS gDMR R	Reverse	CGCCAGGGTTTTCCCAGTCACGACGGTCGGGGTTTTTGTAGTTTG		55˚C	Human; Woodfine 2011 germline primer + common Btn primer recognition sequence
BS gDMR seq	sequencing	CCAAATACTCAAATAAACTCC			Human; Woodfine 2011
Common Btn primer	Common Biotinylated primer	btnCGCCAGGGTTTTCCCAGT			

7.2.13.4 Post- BS conversion PCR–Murine Grb10

Murine *Grb10* primers were designed to the second (81bp) CpG island on *Grb10*. These primers required a 2-step PCR reaction to amplify the bisulfite

converted region and add the common biotinylated primer. Primers were optimized to ~56.7˚C on a temperature gradient. PCR products were checked against a 100bp HyperLadder from Bioline on a 1.5% agarose gel with Ethidium Bromide staining.

Table 7.7 Murine Grb10 pyrosequencing primers

Primer Name	Direction	Sequence	Product Size	Annealing	Notes
mGrb10_D1A_F	Forward	ATTGTAGATTTAGGGAGGTGAATTTT	343 bp	56.7˚C	Murine
mGrb10_D1A_R	Reverse	CGCCAGGGTTTTCCCAGTCACGACCTAAACTCCAAAACCCTTTTTCT		56.7˚C	Murine
mGrb10_D1A_Seq	Sequencing	AGTTTATTTGAGTATTTGGAGA			

7.2.13.5 Pyrosequencing

Screened samples were prepared with Pyromark Gold Q96 Reagents according to Qiagen manufacturing instructions on the Pyromark Q96 IQ. At least 15-18 µl of final PCR product was bound to streptavidin-sepharose high performance beads (GE healthcare, Lot #10215436) and prepared using the pyromark vacuum tool and buffers (Qiagen). Sequencing results were analyzed using the Pyromark Q96 software.

7.2.14 Statistics

7.2.14.1 Q RT PCR

Results were analyzed using the ΔΔCt method and normalized to the housekeeping gene B-actin. Individual ΔCt values were calculated from the difference between individual raw Ct values and the sample's respective

housekeeper Ct value. Delta Ct (ΔCt) values were used to calculate an average ΔCt for each experimental condition (ex. ALL, A1, etc). The raw ΔCt values were also used to calculate standard error of the mean. The ΔΔCt value was calculated using the calibrator condition 'N', the dCas9_TET2(CD) transfection without any synthetic guide RNA. Fold change in expression relative to the calibrator sample was calculated with 2^(-ΔΔCt). Upper and lower bounds were calculated by 2^(ΔΔCt ± SEM). Fold Change was normalized to the control condition at 0 by subtracting 1. Results in histograms are presented as "Fold Change -1" to show change away from the baseline at the axis.

For analysis using the Student t-test, individual ΔCt values were transformed by 2^(-ΔCt). Each set of samples per condition was compared to the control sample for the same primer set. Results shown for conditions 'ALL' and 'A1' had n=7, 'B6' and 'N' had n=6, 'A9', 'C1', and 'IL1RN' had n=4, and the remainder had n=3.

7.2.14.2 Methylation Data Analysis

Every biological replicate was measured in technical triplicate on the pyrosequencer. During analysis, we averaged the three technical replicates for each individual CpG site to generate the percent methylation of the site for the individual biological replicate sample. We then used 2-tailed independent t-tests in SPSS to compare average methylation at individual CpG sites between treatment conditions and to generate confidence intervals of the difference.

7.3 Results

7.3.1 dCas9-p300(Core) Transfection Positive Control: IL1RN Upregulation

We first confirmed the activity of the established dCas9-p300 construct by using gRNA targeting IL1RN. In one trial, this transfection successfully upregulated IL1RN mRNA production 814-fold from baseline expression levels when calibrated using the housekeeping gene beta-actin and the ΔΔCt method. Thus, we validated the capacity of EpiEffectors to upregulate gene expression in our hands.

7.3.2 dCas9_TET2(CD) Construct Sequence Confirmation

Once successfully cloned, the expected dCas9-TET2(CD) sequence was confirmed by Sanger sequencing of key sections of the plasmid as described in Materials & Methods. Sanger sequencing results were aligned to the expected sequence using the Clustal Omega Multiple Sequence Alignment tool, confirming successful cloning of TET2(CD) into the dCas9 plasmid using AscI and replacing the p300(core) sequence.

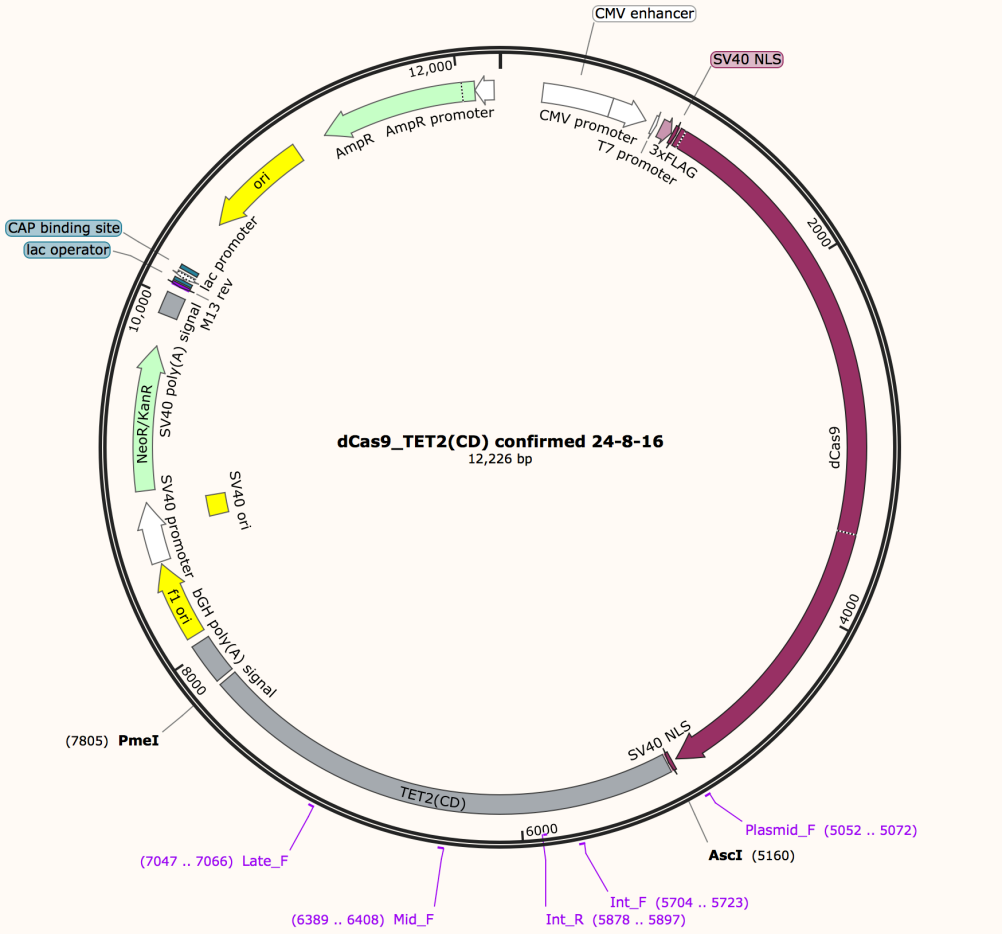

Figure 7.3 dCas9-TET2 Sequence Confirmed Plasmid Map

7.3.3 RNA Expression from the dCas9-TET2(CD) Construct

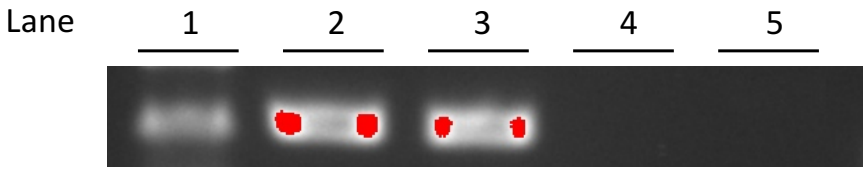

Figure 7.4 Internal mouse TET2 amplification in HEK cDNA samples

Figure 7.4: Lane 1–Ladder, 150 bp band; Lane 2–dCas9-TET2(CD) HEK transfection targeting A1; Lane 3–dCas9-TET2(CD) HEK transfection targeting B6; Lane 4–Water control; Lane5–dCas9-p300 (core) transfection targeting IL1RN.

We tested cDNA samples from HEK transfections targeting A1 and B6 for a mouse TET2 PCR amplification product only present in transfected cells successfully expressing mRNA from our construct plasmid. We found this product in A1 and B6 and not in a water control or a dCas9-p300(core) transfected HEK sample targeted at IL1RN. BLAT identified no matches to the TET2 CD internal primers in the human genome in the February 2009 assembly but did match these primers to the mouse December 2011 assembly. We concluded the transfected construct dCas9-TET2(CD) was successfully transcribed in transfected HEK cultures.

7.3.4 Protein Expression from the dCas9-TET2(CD) Construct

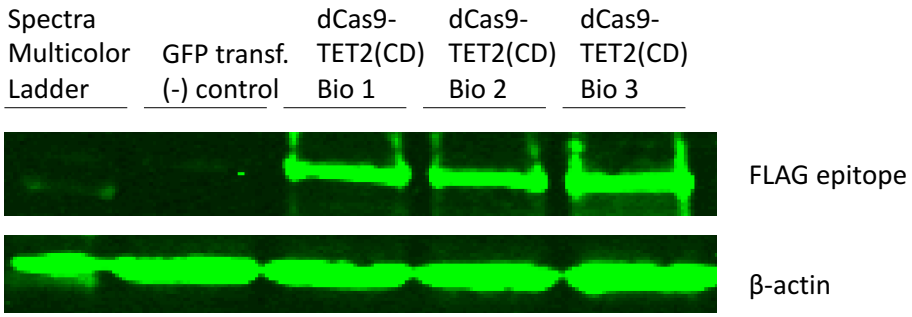

Figure 7.5–Western Blot Anti-FLAG to dCas9-TET2(CD) 'N' transfection in HEK293T

Figure 7.5: *Lane 1–Spectra Multicolor High Range Protein Ladder; Lane 2– GFP transfection, (-) control; Lane 3-5: Biological replicates of dCas9-TET2(CD) transfection with no guide RNA*

Three biological replicates were separately transfected with dCas9-TET2(CD) plasmid and no guide RNA and lysed 48 hrs later. The extracted

protein samples were run on a 4-12% Tris-Glycine Mini Gel next to a control sample transfected with pMax GFP plasmid. We detected strong signal from the FLAG epitope at the expected size of the construct's protein product, 262 kDa. This signal was not present in the control. We concluded the dCas9-TET2(CD) transcript was successfully translated into protein.

7.3.5 dCas9-TET2(CD) Transfection: GRB10 General Transcript Expression

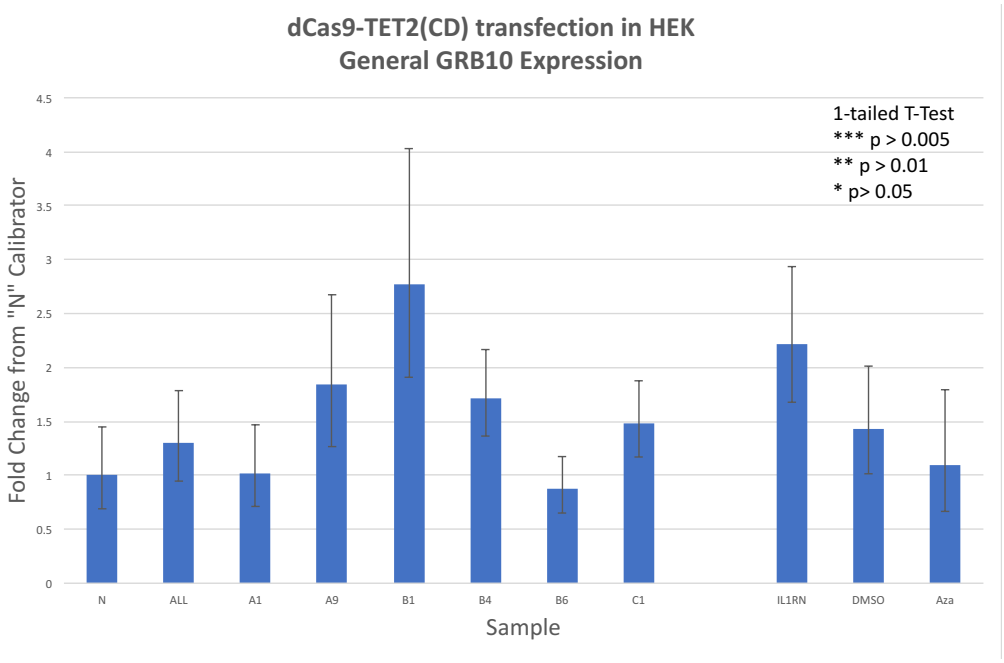

Figure 7.6 dCas9_TET2(CD) transfection, General GRB10 Transcript Expression in HEK

Figure 7.6: Change in GRB10 general transcript expression following dCas9-TET2 (CD) transfection targeted at the DMR in CGI2 compared to dCas9-TET2 (CD) transfection with no synthetic guide RNA ('N'). This figure also includes the conditions 'IL1RN' (dCas9_TET2(CD) targeted to the IL1RN locus), 'DMSO' (HEK

culture treated with DMSO, and 'Aza' (HEK culture treated with 5-Aza). Bars indicate mean ±SEM.

We next determined whether successful expression of our construct altered transcript expression from *GRB10*. We used q RT PCR primers complimentary to a common downstream exon junction to represent a general *GRB10* transcript without tissue- or parent-of-origin-specificity. $2^{-\Delta Ct}$ values for each transfection condition were compared to the "N", or "no sgRNA", condition using the independent samples t-test. Data were normally distributed, as assessed by the Shapiro-Wilk's test ($p > 0.05$), and there was homogeneity of variance, as assessed by Levene's test ($p > 0.05$). N= 7 for transfection conditions targeting "All" gRNA sites and the "A1" site; N= 6 for "B6" and "N"; N=4 for "A9", "C1", and "IL1RN"; N=3 for "B1 and "B4. N=3 for the "DMSO" and "5-Aza" treatments. We found no significant difference in *GRB10* general transcript expression following dCas9-TET2 (CD) transfection targeted at the DMR in CGI2 compared to the "N" condition. We also found no significant change following treatment with 5-azacytidine or its solvent DMSO. Statistics are summarized in the table below (Table 7.8).

Table 7.8 General GRB10 transcript qRT PCR Independent T-test Statistics

Transfection Condition	Mean of test group (2^(-ΔCt))	Levene's test	t	df	Sig
ALL vs N	0.035	0.575	0.461	11	0.654
A1 vs N	0.030	0.58	0.147	11	0.886
A9 vs N	0.046	0.485	0.918	8	0.386
B1 vs N	0.065	0.276	1.623	7	0.149
B4 vs N	0.037	0.666	0.508	7	0.627
B6 vs N	0.022	0.617	-0.505	10	0.624
C1 vs N	0.032	0.649	0.293	8	0.777
IL1RN vs N	0.051	0.557	1.228	8	0.254
DMSO vs N	0.033	0.915	0.252	7	0.808
Aza vs N	0.029	0.761	0.03	7	0.977

7.3.6 dCas9-TET2(CD) Transfection: GRB10 Tissue and Parent-of-origin Specific Expression

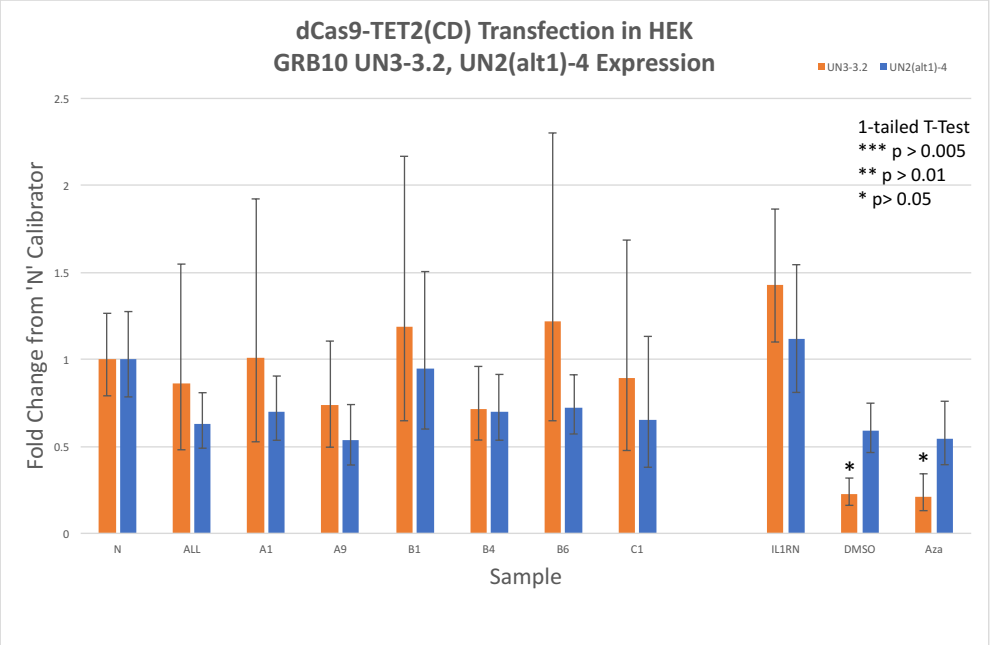

Figure 7.7 dCas9_TET2(CD) transfection, UN3-3.2 & UN2(alt1-4) Expression in HEK

Figure 7.7: Change in GRB10 expression of transcripts containing placenta-specific exons UN3-3.2 and paternal expression-specific exon UN2 in dCas9-

*TET2 (CD) transfections targeting the DMR in CGI2 compared to dCas9-TET2 (CD) transfections with no synthetic guide RNA ('N'). *significant, p<0.05. Bars indicate mean ±SEM*

We used q RT PCR primers targeting exon junction UN3-3.2 to detect the placenta-specific *GRB10* transcript. $2^{-\Delta Ct}$ values for each transfection condition were compared to the control condition "N", for "no sgRNA" using the independent samples t-test. The data were normally distributed except for transfection conditions "All", "A1", "A9", and "B6". These four data sets were compared to "N" using the nonparametric Mann-Whitney U test. There was homogeneity of variance for the remaining conditions tested with the independent t-test, except "C1", which violated Levene's test (p = 0.004). "C1" was compared to "N" using Welch's ANOVA.

We also used primers (UN2alt1_F and UN4_R) targeting exon junction UN2-4 to detect the paternal- and neuron-specific *GRB10* transcript. $2^{-\Delta Ct}$ values for each transfection condition were compared to the control condition "N", for "no sgRNA" using the independent samples t-test. The data were normally distributed for all transfection conditions and treatments except "ALL", which violated Shapiro-Wilk's Test (p = 0.043). "ALL" was compared to "N" using the nonparametric Mann-Whitney U Test. There was homogeneity of variances for all of the remaining conditions analyzed with the independent samples t-test (Levene's test p > 0.05). N= 7 for transfections targeting "All" gRNA sites and the "A1" gRNA site; N=6 for "B6" and "N"; N= 4 for "A9", "C1", and "IL1RN"; N=3 for "B1" and "B4".

We found no significant changes in *GRB10* expression of either tissue-specific transcript in dCas9-TET2 (CD) transfections with gRNAs targeting any sites on the *GRB10* germline DMR. Statistics are summarized in the tables below. UN3-3.2 transcript levels did show significant decrease in the DMSO and 5-Aza treated conditions compared to the dCas9_TET2 transfection with no guide RNA ('N'). "DMSO" ($2^{-\Delta Ct}$ = 6.670E-04) was significantly lower than "None" ($2^{-\Delta Ct}$ = 2.945E-03), mean difference -2.278E-03 (95%CI -4.335E-03 to -2.215E-04), t(7) = -2.619, p = 0.034. "5-Aza" ($2^{-\Delta Ct}$ = 6.930E-04) was also significantly lower than "None", mean difference -2.252E-03 (95%CI -4.336E-03 to -1.68E-04), t(7) = -2.555, p = 0.038. DMSO and 5-Aza did not show a significant difference in expression of general GRB10 (5-Aza N=3, DMSO N=3) or UN2(alt1)-4 (5-Aza N=4, 5-Aza N=3) transcripts compared to dCas9_TET2(CD) transfection with no guide RNA.

Table 7.9 UN3-3.2 GRB10 transcript qRT PCR 2^(-ΔCt) Independent T-test Statistics

Transfection Condition	Mean of test group (2^(-ΔCt))	Levene's test	df	t	Sig
B1 vs N	4.122E-03	0.177	7	0.837	0.43
B4 vs N	2.043E-03	0.875	7	-0.958	0.37
C1 vs N	3.897E-03	0.004	3.637	0.251[a]	0.645
IL1RN vs N	4.178E-03	0.327	8	1.038	0.33
DMSO vs N	6.670E-04	0.406	7	-2.619	0.034*
Aza vs N	6.930E-04	0.496	7	-2.555	0.038*

[a]Welch's Test; *p > 0.05

Table 7.10 UN3-3.2 GRB10 transcript qRT PCR 2^(-ΔCt) Mann-Whitney Statistics

Transfection Condition	Median of test group (2^(-ΔCt))	Mean Rank	U	z	Sig
ALL vs N	1.145E-03	–	24	0.429	0.731
A1 vs N	9.900E-04	–	23	0.286	0.836
A9 vs N	–	A9 = 4.475, N = 6.00	15	0.64	0.61
B6 vs N	1.879E-03	–	20.5	0.401	0.699

Table 7.11 UN2(alt1)-4 GRB10 transcript qRT PCR 2^(-ΔCt) Independent T-test Statistics

Transfection Condition	Mean of test group (2^(-ΔCt))	Levene's test	df	t	Sig
A1 vs N	4.246E-03	0.774	11	-0.958	0.359
A9 vs N	3.202E-03	0.634	8	-1.481	0.177
B1 vs N	5.666E-03	0.728	7	-0.017	0.987
B4 vs N	3.765E-03	0.316	7	-1.096	0.31
B6 vs N	4.091E-03	0.462	10	-1.164	0.272
C1 vs N	5.132E-03	0.238	8	-0.22	0.831
IL1RN vs N	6.385E-03	0.854	8	0.366	0.724
DMSO vs N	3.213E-03	0.224	8	-1.638	0.14
Aza vs N	3.070E-03	0.392	7	-1.474	0.184

Table 7.12 UN2(alt1)-4 GRB10 transcript qRT PCR 2^(-ΔCt) Mann Whitney Statistics

Transfection Condition	Median of test group (2^(-ΔCt))	Mean Rank	U	z	Sig
ALL vs N	—	ALL = 5.79, N = 8.42	29.5	1.216	0.234

7.3.7 False Discovery Rate Corrections– General, UN3-3.2, UN2(alt1)-4 qRT PCR $2^{-\Delta Ct}$

The Benjamini-Liu (BL) procedure was used to correct for false discovery rate (FDR) of 5% over the entirety of statistical comparisons of $2^{-\Delta Ct}$ values for

each transcript. Neither of the two original significant findings–DMSO and 5-Aza comparisons to "N" for UN3-3.2 transcripts– survived FDR correction.

Table 7.13 General GRB10 transcript qRT PCR $2^{-\Delta Ct}$ FDR

Variable	P value	Rank (m=10)	BL = (min 0.05, 0.05*m/(m+1-i)^2	(BL) – P value
B1 vs N	0.149	1	5.000E-03	-1.440E-01
IL1RN vs N	0.254	2	6.173E-03	-2.478E-01
A9 vs N	0.386	3	7.813E-03	-3.782E-01
B6 vs N	0.624	4	1.020E-02	-6.138E-01
B4 vs N	0.627	5	1.389E-02	-6.131E-01
ALL vs N	0.654	6	2.000E-02	-6.340E-01
C1 vs N	0.777	7	3.125E-02	-7.458E-01
DMSO vs N	0.808	8	5.000E-02	-7.580E-01
A1 vs N	0.886	9	5.000E-02	-8.360E-01
Aza vs N	0.977	10	5.000E-02	-9.270E-01

Table 7.14 UN3-3.2 GRB10 transcript qRT PCR $2^{-\Delta Ct}$ FDR

Variable	P value	Rank (m=10)	BL = (min 0.05, 0.05*m/(m+1-i)^2	(BL) – P value
DMSO vs N	0.034	1	5.000E-03	-2.900E-02
Aza vs N	0.038	2	6.173E-03	-3.183E-02
IL1RN vs N	0.33	3	7.813E-03	-3.222E-01
B4 vs N	0.37	4	1.020E-02	-3.598E-01
B1 vs N	0.43	5	1.389E-02	-4.161E-01
A9 vs N	0.61	6	2.000E-02	-5.900E-01
C1 vs N	0.645	7	3.125E-02	-6.138E-01
B6 vs N	0.699	8	5.000E-02	-6.490E-01
ALL vs N	0.731	9	5.000E-02	-6.810E-01
A1 vs N	0.836	10	5.000E-02	-7.860E-01

Table 7.15 UN2(alt1)-4 GRB10 transcript qRT PCR 2-ΔCt FDR

Variable	P value	Rank (m=10)	BL = (min 0.05, 0.05*m/(m+1-i)^2	(BL) – P value
DMSO vs N	0.140	1	5.000E-03	-1.350E-01
A9 vs N	0.177	2	6.173E-03	-1.708E-01
Aza vs N	0.184	3	7.813E-03	-1.762E-01
ALL vs N	0.234	4	1.020E-02	-2.238E-01
B6 vs N	0.272	5	1.389E-02	-2.581E-01
B4 vs N	0.31	6	2.000E-02	-2.900E-01
A1 vs N	0.359	7	3.125E-02	-3.278E-01
IL1RN vs N	0.724	8	5.000E-02	-6.740E-01
C1 vs N	0.831	9	5.000E-02	-7.810E-01
B1 vs N	0.987	10	5.000E-02	-9.370E-01

7.3.8 *GRB10* DMR Methylation

We failed to measure DNA methylation at the *GRB10* DMR using pyrosequencing or several other techniques. These are discussed in depth in the discussion. We used *PEG3* DMR methylation to validate our pyrosequencing techniques under similar treatment conditions.

7.3.9 *PEG3* DMR Methylation under DMSO and 5-Azacytidine Treatment

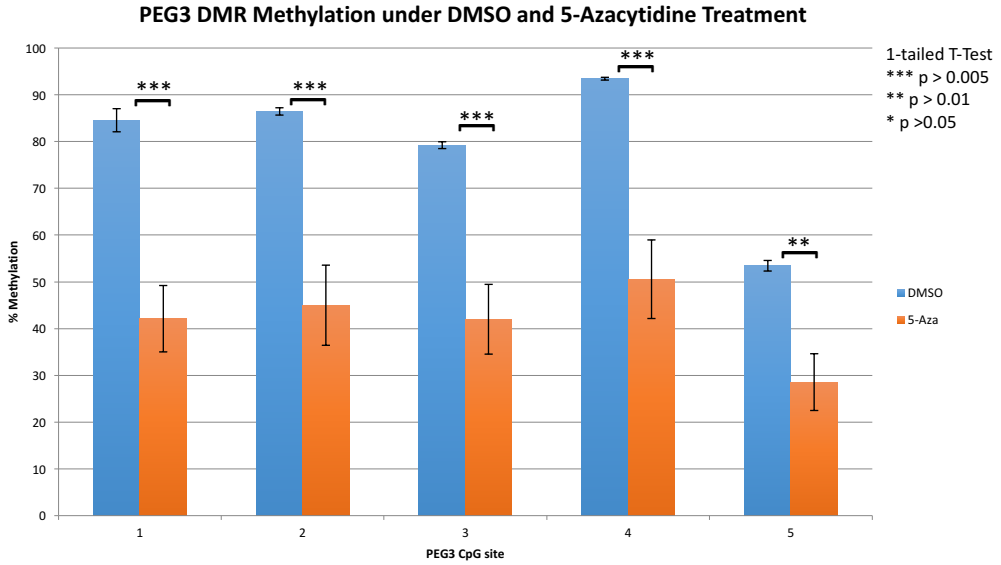

Figure 7.8 PEG3 DMR Methylation under DMSO and 5-Azacytidine Treatment

Figure 7.8: Change in methylation at five CpG sites in the PEG3 CpG island. All sites showed a significant difference between the DMSO control and 5-Aza test conditions when compared with the Independent Samples T-test. One tail is used because 5-Aza is known to be a global demethylator. Site 1 p = 0.0024, Site 2 p= 0.0043, Site 3 p= 0.0038, Site 4 p = 0.0035, Site 5 p = 0.0079. Bars indicate mean ± SEM. N=3 biological replicates for each condition.

We analyzed PEG3 DMR methylation as a control site demonstrating successful 5-Azacytidine (5-Aza) treatment. Methylation of 5-Aza samples were compared to samples treated only with its solvent, DMSO. We found a significant difference in % methylation between the DMSO solvent treatment and the 5-Azacytidine (5-Aza) treatment at all 5 PEG3 DMR CpG sites measured. We used a 1-tailed Student's T-test because 5-Azacitidine is a known demethylator. All 5 sites passed Levene's Test for equality of variance and had DF= 4. Treatment with 5-Azacytidine significantly reduced methylation across the sites measured on the DMR. FDR was not carried out because only 5 sites were measured. The lowest mean difference between the sites was Site 5 with a 24.89% reduction in methylation between DMSO and 5-Aza and the highest was Site 4 with a 42.89% reduction in methylation.

Table 7.16 PEG3 DMR CpG Site Methylation Under DMSO and 5-Azacytidine Treatment

Site	Sig (1-tailed)	Mean Difference between conditions	95% CI of the difference
CpG1	0.0024	42.44	[21.57, 63.32]
CpG2	0.0043	41.44	[17.55, 65.34]
CpG3	0.0038	37.22	[16.42, 58.02]
CpG4	0.0035	42.89	[19.55, 66.23]
CpG5	0.0078	24.89	[7.75, 42.03]

7.4 Discussion

Our objective in this chapter was to construct a flexible and specific tool for a causal investigation of the functional role of *Grb10* imprinting architecture in the brain. We designed the dCas9-TET2(CD) EpiEffector for targeted (and re-targetable) demethylation of the DMR at CGI2, a key feature distinguishing the *Grb10* parental alleles. We opted to test our dCas9-TET2(CD) construct on *GRB10* in human embryonic kidney (HEK). Not only does *GRB10* serve as a model for features of imprinting under epigenome editing, its tissue- and parent-specific alternative transcripts provided a useful method for monitoring the functional consequences of site-specific demethylation. Our target site, the CpG island 2 (CGI2) DMR, distinguishes *GRB10* alleles by parent of origin, founding the differential regulation which generates parental allele- and tissue-specific alternative transcripts (Arnaud et al., 2003; Monk et al., 2009). A successful dCas9-TET2(CD) construct targeting this locus would allow us to attribute any observed effects to the intended epigenetic change and determine whether this mark retained functional purpose in our culture

model, or whether other features of the imprinting architecture made it redundant at this point.

We first validated the capacity of EpiEffectors to change transcript expression at a targeted locus. The dCas9-p300(core) construct induces acetylation at histone H3, lysine 27 (Hilton et al., 2015). This tool permits the targeted addition of the activating histone 3, lysine 27 acetylation (H3K27ac) mark. H3K27ac is used here as a relative measurement of broad p300 acetyltransferase activity and a widely-documented indicator of enhancer activity. Targeting this construct to a positive control locus, *IL1RN*, successfully upregulated expression and revalidated the concept of CRISPR/Cas9 directed epigenome editing.

Next, we successfully constructed, transfected, and expressed the dCas9-TET2(CD) construct in the HEK cell model. However, qRT-PCR data indicates targeting this construct to the DMR in CGI2 of *GRB10* did not change the expression of any of the *GRB10* transcripts we investigated. Our targets included transcripts containing general downstream exons common to all protein encoding isoforms of *GRB10* and transcripts containing the placental-specific and biallelically expressed exon UN3-3.2 and the brain- and paternal allele-specific exon UN2 (Monk et al., 2009). These transcripts served as measurement proxies for the effect of our construct on separate maternal and paternal allele specific transcriptional regulation. We compared our CRISPR/dCas9 targeted EpiEffector to a 'conventional' method manipulating DNA methylation by using the global demethylator 5-azacytidine (Christman, 2002; Heerboth et al., 2014). This pharmacological agent was intended to

induce strong demethylation at imprinted DMRs for confirmation of our pyrosequencing and serve as a comparison condition for expression analyses detected by q RT PCR. There were no significant effects of 5-azacytidine administration on any of our *GRB10* transcripts after FDR correction. Therefore, we do not expect successful demethylation of CGI2 by our dCas9-TET2(CD) construct should induce any change in expression of these transcripts. One concern is that our *GRB10* transcripts may not be very highly expressed naturally in HEK cells. The average raw Ct value was ~24 for the general transcript, ~27 for the placental UN3-3.2 transcript, and ~27 for the neuronal UN2(alt1)-4 transcript. Thus, a floor effect might prevent us from detecting downregulation of the general or placental transcripts if successful demethylation of the DMR activated the neuronal transcript and suppressed the general and/or placental transcripts. Regardless, we cannot use transcript expression to determine whether our construct successfully demethylated the targeted locus.

7.4.1 Redundant architecture

To contextualize the application of epigenetic modifying tools and their lack of effect on *GRB10* expression, we describe human *GRB10* imprinting architecture below. DNA methylation at CGI2 on *GRB10* is an imprinting mark distinguishing the methylated maternal allele from the unmethylated paternal allele. As this mark exhibits no variation by tissue, tissue-specific differences in alternative transcript expression from *GRB10* must result from higher regulatory structures built upon the distinguished alleles (Monk et al., 2009).

Normal *GRB10* tissue- and parent-specific expression in human cells is characterized by bialleleic general transcript expression from the UN1 and UN1A major promoter in most tissues, and parent-specific expression in imprinted tissues such as the placenta, CNS, and brain (Monk et al., 2009). Untransfected HEK cells have likely already established normal parent-specific regulatory architecture based on the methylated maternal DMR, and should express general *GRB10* transcripts originating from the UN1 and UN1A exons biallelically. Placenta-specific transcripts originating from both alleles, detected by the transcription of the UN3-3.2 exon section, should be absent. Likewise, the neuron-specific paternal UN2 transcripts should remain suppressed by a monoallelic bivalent chromatin domain over CGI2 (Sanz et al., 2008). Normal imprinting on the maternal DMR at CGI2 is accompanied by the repressive histone mark H4K20me3, which prevents transcription initiating from UN2 in all tissues (Monk et al., 2009). The paternal allele expresses transcripts from UN2 only when the bivalent chromatin domain over CGI2 is resolved in brain tissue (Monk et al., 2009). Therefore, both parent- and tissue-specific transcripts should be silent in untransfected HEK.

As our dCas9-TET2(CD) construct theoretically acts only to initiate 5-mC oxidation and induce active demethylation, any resulting expression changes would have resulted from demethylation of the maternal allele. The absence of an expression change could be due either to ineffective editing by the construct or to more complex regulatory architecture which makes the DMR redundant in HEK cells. The simple degradation of this maternal mark is not a complete transition to the paternal allele-specific regulatory mechanism

which typically promotes expression from the UN2 exon, and may not in of itself be able to initiate UN2 transcript expression from the maternal copy (Sanz et al., 2008). We cannot assess the effectiveness of the construct by expression data from our *GRB10* target.

Preliminary data (not shown here) also suggested upregulation of general exon, UN3-3.2, or UN2 containing transcripts failed in dCas9-p300(core) transfected samples. The construct's acetylation at H3K27 could be blocked by endogenous H3K27me3 at the bivalent chromatin domain at the paternal ICR within CGI2 (Hilton et al., 2015; Sanz et al., 2008). Furthermore, upregulation of the paternal allele specific transcript containing UN2 is achieved through resolution of the bivalent chromatin marks, removal of the repressive H3K27me3, and addition of the activating H3K9ac (Monk et al., 2009; Sanz et al., 2008). The acetylating construct may have more success in upregulating *GRB10* transcripts if targeted to the major promoter region near CGI1, where H3K27ac is most abundant.

7.4.2 Pyrosequencing and Sanger Sequencing

Methylation at the targeted region is the most important test of our construct's efficacy. Initially, we tried to use pyrosequencing to examine the methylation at the DMR after transfection with dCas9-TET2(CD) compared both to untransfected or untargeted samples and to the general chemical demethylator 5-azacytidine. We attempted to assess methylation at CGI2 in our samples using the *GRB10* pyrosequencing primers noted in Woodfine 2011 (Woodfine, Huddleston, & Murrell, 2011). While we could amplify a 139 bp

PCR product from our bisulfite converted DNA, this was accompanied by a smaller product. We attempted to optimize our PCR and remove the smaller product by means of temperature gradients, varying concentrations of primers, and the addition of DMSO to our PCR reaction for stability. We were unable to remove the second product. Pyrosequencing of these amplified samples failed due to 'failed surrounding reference sequence'.

We also attempted to sequence the genomic DNA and bisulfite converted PCR product by Sanger sequencing to investigate the possibility of a deviant reference sequence. We amplified a 308 bp product from the genomic DNA around the *GRB10* germline DMR using AccuPrime GC-rich DNA polymerase from Thermo Fisher. Sanger sequencing confirmed the sequence matched the reference sequence on Genome Browser, our basis for our pyrosequencing reference sequence. The bisulfite converted PCR product was gel and PCR-purified using the Promega Wizard gel and PCR purification system prior to Sanger Sequencing. All samples attempted yielded no readable Sanger Sequencing results.

We further attempted to assess methylation at the DMR by redesigning the pyrosequencing primers. The best predicted primer set generated by the pyrosequencing primer design tool, aside from the Woodfine sequences, failed to generate a product in a temperature gradient PCR. One of the main issues with the pyrosequencing target is the 82% GC content at the genomic DMR for *GRB10*. We investigated the possibility of incomplete bisulfite conversion by varying the conversion protocol. We attempted conversion protocols with 2.5, 12, and 16-hour incubation periods and using 250 ng and 500 ng of genomic

DNA. The 16-hour incubation period degraded the DNA too much to generate a clean PCR product. The remaining conditions still failed pyrosequencing and sanger sequencing efforts.

We confirmed our pyrosequencing technique and materials by sequencing another imprinted gene, PEG3, using DMSO and 5-Aza samples. This attempt generated viable data, indicating our reagents, machines, and technique are functional.

7.4.3 Southern Blotting

We also tried methylation sensitive restriction enzyme digestion and southern blotting as another approach to measuring methylation at the GRB10 CGI2 DMR. The advantage to a fluorescent southern blot was the possibility of (1) covering the whole CGI2 region and (2) comparing relative fluorescence levels as a proxy for % methylation. We digested each test sample under two control conditions and one test condition: HindIII (to break up genomic DNA) alone served as a 100% methylated control, HindIII + MspI (methylation insensitive) served as a 0% methylated control, and HindIII + HspII (methylation sensitive) served as the test condition. DNA digestion in the test condition should fall somewhere between the two controls, with relative fluorescence as a proxy of % methylation across the locus. The six 6-FAM labeled probes failed to bind the DNA under 35˚C incubation for 3 hours in PerfectHyb–Plus hybridization buffer and we detected no signal under the ChemiDoc MP system's Fluorescein setting.

7.4.4 COBRA

Combined Bisulfite Restriction Analysis (COBRA) is another way of measuring methylation. BS conversion, PCR amplification, and digestion with the restriction enzyme Bsh1263I inform us of the cytosine methylation status at its CG cutting site. A methylated cytosine protects the Bsh1263I site during BS conversion, so it is still digestible after BS conversion. In contrast, an unmethylated cytosine is converted to uracil and PCR amplified as thymine, altering the site and preventing digestion. There are two Bsh1263I targets within the Woodfine primer-defined pyrosequencing target at GRB10 CGI2. However, we did not pursue COBRA as we had concerns about the efficiency of the BS conversion at the GRB10 CGI2 locus. Our concerns arise from the difficulty we had Sanger sequencing the BS converted product, the 'failed surrounding reference sequence' in the pyrosequencing, and the 82% GC content of the locus. The efficiency of the BS conversion is critical because any unconverted unmethylated cytosines would yield false positives for methylation. This could mask the effect of the demethylation construct dCas9-TET2(CD).

7.4.5 Quantitative DNA methylation Analysis using methylation-sensitive RE and qPCR

Analysis by methylation-sensitive restriction enzyme digestion and qPCR circumvents some of the problems with COBRA. In this technique, the genomic DNA is digested under four conditions: without restriction enzymes (REs), with methylation-sensitive REs, with methylation-insensitive REs, and with methylation-dependent REs. These samples are then amplified under

qPCR conditions targeting the locus of interest. Differences in the Ct values for each sample digestion condition indicate the levels of remaining uncleaved DNA. The more intact DNA left after digestion, the lower the Ct value. Comparison of the different conditions can determine the methylation status of the locus. This strategy is a possibility for our locus, but the spread of our sgRNA targets across the region would require several PCR targets amplifying a smaller (~200 bp) region to assess methylation across the whole locus. Additionally, the dense GC content makes primer design in this region more difficult, as the primers have higher risk of self-complementarity.

7.4.6 Murine *Grb10*

Rather than continue to pursue methylation measurements at the human *GRB10* locus, we planned to target the murine *Grb10* CGI2 locus. We successfully pyrosequenced a portion of this region and planned to redesign our sgRNAs to target the locus in neuroblastoma N2a cells or mESCs. This easy shift from a human to a mouse target is one of the advantages of a CRISPR/sgRNA targeted epigenetic editing system. We can use the same plasmid construct with new sgRNA oligos to transfect a different cell line. While our transfection into HEK cells demonstrate successful expression of the dCas9-TET2(CD) transcript and protein production, future studies transfecting into mouse cells will allow us to address the essential question of whether the construct is an effective tool for targeted demethylation.

8 Discussion

8.1 Thesis Aims

The overarching purpose of this thesis was to correlate features of convergent social dominance behaviours in the *Grb10*$^{+/p}$ mouse with multiple measures of brain allometry in adult life. Isolated *Grb10*$^{+/p}$ male mice 10 months of age were reported to win Taylor tube test encounters with unfamiliar wildtype more frequently and were responsible for increased whisker barbering in home cages (Garfield et al., 2011). *Grb10*$^{+/p}$ brains were also reported to be heavier than wildtypes at 3 and 10 months, and continued to gain weight between these time points where wildtypes did not. Brain weight at P0 indicated no difference between *Grb10*$^{+/p}$ and wildtype brains at birth, suggesting *Grb10*$^{+/p}$ brains show different postnatal allometry. Whole and subcortical areas, but not cortical areas, were larger in *Grb10*$^{+/p}$ Nissl stained brain slices (Garfield, 2007). Thus, we expected to find a region-specific effect on brain growth which reflected the paternal *Grb10* expression profile. We investigated brain allometry using a cross sectional study in which we used histology and IHC to describe brain area and cell densities. We complimented this with a longitudinal MRI study which described within-subjects volumetric change over time. We hypothesized social dominance features of *Grb10*$^{+/p}$ behaviour would emerge or become more distinct in adult life as the brain overgrowth phenotype became more pronounced.

We chose to measure social dominance features using the Lindzey tube test (stranger encounter and within-cage encounters), the urine marking test,

and whisker barbering profiling. Group housing was an important to our design, as mice in group housing form transitive hierarchies, while this feature is absent under social isolation. Multiple tests of social dominance and within-cage rank contributed to more robust behavioural evidence. The tube test, urine marking test, and barbering profiles are expected to correlate, and also rule out factors unrelated to dominance (such as sensorimotor capacity, persistence, learning etc) which might interfere with any one test alone (F. Wang et al., 2011). To address previous criticisms which propose trichotillomania as an alternative explanation of the whisker barbering phenotype, we also conducted the marble burying test to screen for compulsivity in our *Grb10*$^{+/p}$ mice (Curley, 2011). We accompanied this with the elevated plus maze to test for anxiety behaviour, as marble burying alone does not distinguish between anxiety and compulsivity.

A secondary aim of this thesis was to develop an epigenetic editing tool, or EpiEffector, with which we could manipulate the *GRB10/Grb10* DMR in cell culture, with an eye to manipulating the *Grb10* DMR *in vivo* in the future. Causal investigations of the function of specific components of imprinting architectures, such as the DMR or bivalent chromatin domain on paternal *Grb10*, require targetable tools capable of making mitotically heritable modifications (Rienecker et al., 2016). We aimed to create the dCas9-TET2(CD) construct to demethylate the *GRB10* DMR at CGI2, and to validate this using pyrosequencing in human embryonic kidney cells.

The experimental aims of this thesis were as follows:

1. I aimed to characterize brain overgrowth in *Grb10*$^{+/p}$ mice over time.
2. I aimed to assess social dominance behaviours in a cross sectional study of *Grb10*$^{+/p}$ mice at 2, 6, and 10 months of age and correlate any changes with brain growth.
3. I aimed to construct and test a CRISPR/dCas9 targeted epigenome editor capable of manipulating the DMR at *GRB10/Grb10.*

8.2 Results Summary

We used brain weight data collected from our behavioural cohorts and supporting colony, Nissl-stained brain sections, and longitudinal MRI volume data to describe the allometry of *Grb10*$^{+/p}$ brains. Our analysis of whole brain weights across our colony and behavioural cohorts indicated *Grb10*$^{+/p}$ brain allometry was significantly different from wildtype and *Grb10*$^{+/m}$ brains. After FDR correction, *Grb10*$^{+/p}$ brains were ~6.6% heavier than wildtype brains at 75-95 days, ~8.5% heavier than wildtypes at 305-325 days, and ~15.8% heavier than *Grb10*$^{+/m}$ brains at 305-325 days. *Grb10*$^{+/p}$ brains continued to increase in weight between 185-205 days and 205-325 days though this increase did not survive FDR. In contrast, wildtypes and *Grb10*$^{+/m}$ brain weight decreased during this period, a change that did survive FDR. In Nissl-stained brain slices (Bregma 0.74 mm) at 2, 6, and 10 months, we found no significant differences in whole brain, cortical, subcortical, caudate putamen, or ventricle area for males or females, with one exception. Caudate putamen area in female brain slices increased significantly between 2 months (10 weeks) and 6 or 10 months, but there was no difference by genotype. There were no significant

genotype differences in neuronal or total cell counts in the caudate putamen. Our longitudinal MRI study of *Grb10*$^{+/p}$ and wildtype mice determined there was no interaction between age and genotype for whole brain volume. We concluded brain volume allometry across 2, 6, and 10 months was no different between wildtypes and *Grb10*$^{+/p}$ brains, though *Grb10*$^{+/p}$ whole brain volume was consistently ~7% larger. At 10 months, *Grb10*$^{+/p}$ brains also had significantly larger cortical and subcortical volumes than wildtypes.

Overall, *Grb10*$^{+/p}$ brains have consistently larger whole brain weight and volumes, with whole weight being maintained between 2, 6, and 10 months, while wild wildtype and *Grb10*$^{+/m}$ mice have smaller whole brain volumes and decrease in weight between 6 and 10 months. At 10 months, both cortical and subcortical *Grb10*$^{+/p}$ volumes are significantly larger than wildtypes, but there was no significant difference between cortical or subcortical areas of *Grb10*$^{+/p}$, *Grb10*$^{+/m}$, and wildtype Nissl-stained brain slices at Bregma 0.74 mm for any age measured.

Table 8.1 Interpretable Significant Results–Weight, Area, and Volume

Result	BL corrected p-value	Interpretation	Note
Whole Wet Brain Weight AGE*GENOTYPE	0.014	*Grb10*$^{+/p}$ maintained weight, while WT and *Grb10*$^{+/m}$ brains increased from 75-95 days to 185-205 days and decreased from 185-205 to 305-325 days.	Allometric Brain Growth
Caudate putamen–main effect AGE	2.083E-03	Caudate Putamen area in female slices at Bregma 0.74 mm (all genotypes) increased significantly with age	Female Nissl Staining
Caudate putamen 10 weeks to 6 months	2.268E-03	Caudate Putamen area in female slices at Bregma 0.74 mm increased between 10 weeks and 6 months of age	Female Nissl Staining
Caudate putamen 10 weeks to 10 months	2.479E-03	Caudate putamen area in female slices at Bregma 0.74 mm increased between 10 weeks and 10 months of age	Female Nissl Staining
Whole Brain Main Effect of GENOTYPE	0.044	Whole brain volume was greater in *Grb10*$^{+/p}$ brains than WT	MRI
Whole Brain Main Effect of AGE	6.250E-03	Whole brain volume increased with age, irrespective of genotype	MRI
Subcortical Volume Effect of GENOTYPE	0.025	Subcortical volume at 10 mo was greater in *Grb10*$^{+/p}$ brains than WT	MRI
Cortical Volume Effect of GENOTYPE	0.050 (significant post FDR value)	Cortical Volume at 10 mo was greater in *Grb10*$^{+/p}$ brains than WT	MRI

After determining *Grb10*$^{+/p}$ brains are larger, we wanted to examine whether this was due to an accumulation of excess tissue of the same cell and neuronal density. This increase in weight and volume could alternatively be due to an increase in non-neuronal cell counts or a change in connectivity due to increased white matter or neuronal arborization. The former alternative might be indicated by comparable total cell density with reduced neuronal density, while the latter alternative would be indicated by reduced total and neuronal cell densities. The brain slices used for total (DAPI) and neuronal (NeuN) stereological counts were parallel to the slices used for Nissl-stained area measures. We found no difference in absolute cell counts for total or neuronal staining. However, the discrepancy between our Nissl-stained area findings and Garfield's cast doubt on our interpretation of cell density in the caudate putamen. We attempted to resolve this by using MRI volume as a more sensitive measure of morphology. *Grb10*$^{+/p}$ brains were 7% larger than wildtypes, which paralleled their ~6.5% increase in weight at 75-95 days and ~8.5% increase in weight at 305-325 days. This data suggests increased weight and volume in *Grb10*$^{+/p}$ brains is likely the result of excess tissue of the same cellular density and composition. Nevertheless, further calculations of cell density in brain slices are required and should use greater power.

If *Grb10*$^{+/p}$ brains possess the same neuronal and total cell density, *Grb10*$^{+/p}$ brain overgrowth may be the result of extended or enhanced total cellular proliferation, rather than reduced synaptic pruning, increased connectivity, or an increased number of non-neuronal cells. However, further studies are required to assess how paternal *Grb10*, with purported neuron-

specific expression, impacts total cellular proliferation in the brain, and why subcortical *Grb10* expression might induce larger cortical volumes as well as subcortical volume.

Table 8.2 Interpretable NS Results–Histology

Result	**p-value**	**Interpretation**	**Note**
DAPI main effect of GENOTYPE	0.863	DAPI cell counts were no different between *Grb10*$^{+/p}$ and WT caudate putamen	Stereology
DAPI main effect of SEX	0.857	DAPI cell counts were no different between male and female brains	Stereology
NeuN (males) main effect of GENOTYPE	0.923	NeuN cell counts in male brains were no different between *Grb10*$^{+/p}$ and WT caudate putamen	Stereology
NeuN (females) main effect of GENOTYPE	0.900	NeuN cell counts in female brains were no different between *Grb10*$^{+/p}$ and WT caudate putamen	Stereology
Ratio NeuN:DAPI interaction GENOTYPE*SEX	0.954	NeuN:DAPI cell ratios did not have a significant interaction between GENOTYPE and SEX	Stereology
Ratio NeuN:DAPI main effect GENOTYPE	0.747	NeuN:DAPI cell ratios were no different between *Grb10*$^{+/p}$ and WT caudate putamen	Stereology
Ratio NeuN:DAPI main effect SEX	0.354	NeuN:DAPI cell ratios were no different between male and female brains	Stereology

We next turned to behavioural testing to determine whether the development of the social dominance phenotype described in Garfield 2011 correlated with our description of *Grb10*$^{+/p}$ brain growth (Garfield et al., 2011).

Socially housed *Grb10*$^{+/p}$ mice of both sexes were no more likely to win the stranger-encounter tube test, social-encounter tube test, or urine marking test at 2, 6, or 10 months. The number of *Grb10*$^{+/p}$ barbers in cages with clear 1:3 unbarbered to barbered ratios was also not significantly different from chance, and in fact, a greater absolute number of the barbers in our cohorts were wildtypes. Thus, we decided to test whether social isolation stress enhanced a social dominance phenotype that was sub-threshold in group housing. Under social isolation, we found male *Grb10*$^{+/p}$ mice were in fact *less* likely to win the stranger encounter tube test, female *Grb10*$^{+/p}$ mice were *more* likely to win, and when both sexes were considered together, *Grb10*$^{+/p}$ mice were no more likely to win or lose than chance. We then considered whether *Grb10*$^{+/p}$ mice contribute to unstable social hierarchies, as with *Cdkn1c*^{BACx1} mice (McNamara et al., 2018). There was no correlation between the social tube test, urine test, or whisker barbering cage ranks for our mixed *Grb10*$^{+/p}$ and wildtype cages. This lack of correlation between tests suggests instability in cage hierarchy, and we recommend further experiments specifically examine this feature.

There was no difference between *Grb10*$^{+/p}$ and wildtype mice in the marble burying test. We concluded the whisker barbering feature reported in Garfield 2011 is not due to compulsivity, and as all whiskers grew back in social isolation, this is not a trichotillomania-like phenotype. We also did not detect any differences in anxiety using the EPM, consistent with previous results from the light-dark box and the open field assessments (Garfield et al., 2011). However, we did note five accessory measurements from the EPM survived

FDR correction: *Grb10*$^{+/p}$ mice made more total, closed, and middle zone entries than wildtypes, moved at a higher velocity, and spent more time in head dip behaviours when on the open arm, though no more time on the open arm itself.

Table 8.3 Interpretable Significant Behaviour Results

Result	**BL corrected p-value**	**Interpretation**	**Note**
Isolated Males–Stranger Encounter Days 1-3	8.33E-03	Isolated *Grb10*$^{+/p}$ males were less likely to win against unfamiliar mice	Isolation
Isolated Females–Stranger Encounter Days 1-3	0.012	Isolated *Grb10*$^{+/p}$ females were more likely to win against unfamiliar mice	Isolation
All Entries–main effect GENOTYPE	8.19E-04	*Grb10*$^{+/p}$ mice made more total entries to EPM zones	EPM (males)
Closed Entries–main effect GENOTYPE	9.05E-04	*Grb10*$^{+/p}$ mice made more closed arm entries	EPM (males)
Middle Entries–main effect GENOTYPE	7.94E-04	*Grb10*$^{+/p}$ mice made more entries to the middle zone	EPM (males)
Velocity–main effect GENOTYPE	8.75E-04	*Grb10*$^{+/p}$ mice moved faster than wildtypes	EPM (males)
Head dip duration–main effect GENOTYPE	8.47E-04	*Grb10*$^{+/p}$ mice spent a longer total duration in head dip behaviours	EPM (males)

Finally, we successfully constructed and expressed the dCas9-TET2(CD) construct in HEK, confirming the presence of the protein product with Western blot. However, various efforts to assess methylation at the targeted locus

failed. There were no significant changes in *Grb10* expression under treatment with the targeted construct, as assessed by qRT-PCR, but this does not indicate whether the DMR was successfully demethylated.

8.3 Brain Overgrowth Mechanisms

A key question in our analyses of brain weight, volume, and area was whether there was an interaction between GENOTYPE and AGE, which would indicate *Grb10*$^{+/p}$ had a different growth allometry compared to *Grb10*$^{+/m}$, and wildtype brains. *Grb10*$^{+/p}$ brains might grow at a different rate postnatally than controls, or might be consistently larger but grow at the same rate. Garfield's whole wet brain weight data suggested the *Grb10*$^{+/p}$ overgrowth phenotype is absent at P0 and becomes more extreme with age. Student t-tests revealed *Grb10*$^{+/p}$ brain weight increased significantly between D84 and D308, while wildtype brain weights were not significantly different over the same period (Garfield, 2007). In our analysis, there was a significant interaction between GENOTYPE and AGE for whole wet brain weight, supporting the conclusion that adult *Grb10*$^{+/p}$ brains maintain or gain weight when controls do not. In contrast, volume data from our longitudinal study did not identify a significant interaction between GENOTYPE and AGE–*Grb10*$^{+/p}$ brains were consistently larger than wildtypes. Area measures from Nissl-stained brain sections in our cross-sectional study of ages 10 weeks, 6 months, and 10 months also did not corroborate an interaction between GENOTYPE and AGE. However, there were no significant differences in area by GENOTYPE or AGE in our samples, except

for caudate putamen area, which increased in area with AGE, irrespective of genotype.

Based on these data, we question whether the *Grb10*$^{+/p}$ brain overgrowth phenotype truly emerges in adult mice, with no difference in neonatal animals, or if some difference arises in embryonic development and early neuronal differentiation, and then matures with postnatal development. An alternative genetic model of *Grb10* disruption, *Grb10Δ2-4*, provides some supporting evidence for the former scenario. On day of birth, brain weight as a percentage of body weight is no different between wildtypes, *Grb10Δ2-4*$^{m/+}$, and *Grb10Δ2-4*$^{+/p}$ mice (Charalambous et al., 2003). However, the *Grb10Δ2-4*$^{+/p}$ model has limited utility for discerning the function of paternal *Grb10*, as the model fails to replicate the full paternal expression pattern found in the brain, instead showing limited *LacZ* reporter staining in the hypothalamus (Cowley et al., 2014; F. M. Smith et al., 2007). One possible explanation for the different growth descriptions from wet weight and volume in our experiments is that brain density also changes with AGE. If neonatal brains show the same trends as adult brains from 8 weeks to 10 months, *Grb10*$^{+/p}$ brains at birth may be less dense than controls.

The mechanism of brain overgrowth may also help distinguish between a phenotype which emerges only in adulthood and one which begins with embryonic development and matures with age. Possible means of overgrowth include increased cellular proliferation, altered cellular dimensions, alteration or acceleration of cell cycle stages, and altered apoptosis. Again, we will use the *Grb10Δ2-4* model as a comparison for *Grb10*$^{+/p}$ overgrowth, but this time

we will focus on *Grb10Δ2-4*$^{m/+}$ body overgrowth (sparing the brain) (Charalambous et al., 2003). Both maternal and paternal transcripts are predicted to encode the same protein, which initiates from the translational start in exon 3 (Arnaud et al., 2003). In conjunction with complementary overgrowth phenotypes, this gives us reason to hypothesize paternally expressed Grb10 acts on the same or similar signaling pathways as the maternal, though in the context of the brain.

8.3.1 Proliferation, apoptosis, cell morphology, and cell-cycle suppression mechanisms

In our samples, neuronal and total cell densities in the caudate putamen at 10 months of age were identical between all three genotypes. In combination with weight and volume comparisons, this suggested *Grb10*$^{+/p}$ brains were larger because they accumulated more tissue of the same cellular density. However, paternal *Grb10* expression is putatively neuron-specific. It is therefore interesting we did not see a differential effect between neuronal and total cell counts. For comparison, in *Grb10Δ2-4*$^{m/+}$ placentas, the 50% increase labyrinthine volume was cell autonomous, and there was no difference in volume fraction of the spongiotrophoblast, glycogen cells, and giant cells, where maternal *Grb10* is not expressed (Charalambous et al., 2010).

Based on comparison to the *Grb10*$^{+/m}$ overgrowth phenotypes, cellular hyper-proliferation is a possible cause of the overgrowth in *Grb10*$^{+/p}$ brains. *In vitro* studies of *Grb10*$^{+/m}$ mouse embryonic fibroblasts (MEFs) indicated embryonic overgrowth in *Grb10*$^{+/m}$ mice was a consequence of cellular hyper-proliferation, and not reduced apoptotic sensitivity or an autonomous increase

in cell size (Garfield, 2007). Supporting this finding, overexpression of *Grb10* in MEFs inhibits IGF1- but not insulin-mediated cellular proliferation, and macroscopically, androgenetic MEFs (lacking the maternal genome) are hyper-proliferative (Hernandez, Kozlov, Piras, & Stewart, 2003; Morrione et al., 1997). Garfield proposed a possible role for maternal Grb10 in MEFs in progression through the later phases of the cell cycle, as more cells accumulated in the G2/M phases and were depleted in the S phase in the *in vitro* model (Garfield, 2007). However, in a converse model, overexpression of the major transcript mGrb10α caused a delay in the S and G2 phases of the cell cycle (Morrione et al., 1997). A variety of experimental design factors could influence these potentially conflicting outcomes, and Garfield recommended a more detailed study.

An important consideration when assessing the relevance of the *Grb10*$^{+/m}$ MEF data to our interest in the mechanism of *Grb10*$^{+/p}$ overgrowth is variability between models of *Grb10* disruption. Unlike the *Grb10*$^{+/m}$ model, *Grb10Δ2-4*$^{m/p}$ MEF cell lines were hypo-proliferative (Garfield, 2007). The *Grb10Δ2-4* deletion of 36 kb is much larger than the 12 bp deletion of the *Grb10KO* model, and displayed divergent paternal reporter expression (Cowley et al., 2014). The hypo-proliferative phenotype in *Grb10Δ2-4*$^{m/p}$ MEFs is more indicative of an anti-apoptotic phenotype, and is consistent with reports from Kebache 2007. This study demonstrated the interaction of Grb10 with Raf-1 is required for PI3K/Akt and MAPK pathways which modulate the phosphorylation and inactivation of the proapoptotic protein Bad. Thus, MEFs depleted of *Grb10* by small interfering RNAs (siRNA) exhibited enhanced

sensitivity to Bad induced apoptosis (Kebache et al., 2007). Thus, MEF cultures of *Grb10*$^{+/m}$, the complement of our *Grb10*$^{+/p}$ model, implicate hyper-proliferation as a mechanism of overgrowth, while MEF cultures of more biallelic disruption, such as *Grb10Δ2-4*$^{m/p}$ and siRNA depletion, implicate anti-apoptotic activity.

8.3.2 Insulin/IGF signaling pathways in overgrowth phenotypes

Grb10 is well known as a pseudosubstrate inhibitor of the receptor tyrosine kinases insulin receptor (IR) and type 1 insulin-like growth factor receptor (IGF1R) (Holt & Siddle, 2005). These signaling pathways have well-known effects on growth, including embryonic and placental growth (Baker, Liu, Robertson, & Efstratiadis, 1993; Bowman, Streck, & Chapin, 2010). In the brain, insulin is known to impact neuronal survival, translation & gene expression, neuronal activity, and cognition. Insulin-like growth factors 1 (IGF1) has roles in neurogenesis, amyloid clearance, and protection against cellular injury, while IGF2 plays a role in memory enhancement (Werner & LeRoith, 2014). Another way to investigate mechanisms of *Grb10* regulation of brain growth is to compare it to models disrupting insulin/IGF signaling cascades alone and in epistatic models with disrupted *Grb10*. *Grb10Δ2-4*$^{m/+}$ and *Grb10Δ2-4*$^{m/p}$ mouse models implicate insulin signaling as a mechanism of their general overgrowth, increased lean muscle mass, reduced adiposity, and improved whole-body glucose tolerance (F. M. Smith et al., 2007). Grb10 normally protects Insr from activation loop dephosphorylation in muscle and white adipose tissue (WAT), indirectly disrupting the association of IRS-1 with

Insr, required for IRS-1 phosphorylation and signal transduction (F. M. Smith et al., 2007). The related protein Grb14 inhibits insulin signaling using similar mechanisms, but with different tissue-specificity, acting in muscle and liver (Depetris et al., 2005). Likewise, given maternal and paternally expressed *Grb10* transcripts are predicted to encode the same protein, reciprocal imprinting could prescribe tissue-specificity differences on comparable mechanisms (Arnaud et al., 2003). Several studies have investigated specific IR/IGF signaling cascades in relationship to the growth effects of maternal *Grb10KO*. These studies reveal mechanisms which may be held in common with paternal *Grb10* and in some cases, show phenotypes directly relevant to the regulation of brain growth. However, downstream deletion models of insulin signaling do not necessarily result in brain overgrowth, though insulin signaling knockout models can be associated with altered sensitivity to insulin and glucose homeostasis, reminiscent of maternal *Grb10* knockout models (Bruning et al., 2000; F. M. Smith et al., 2007).

Table 8.4 Insulin/IGF signaling comparisons to Grb10 knockout models

Pathway component	Evidence	Comparison to *Grb10*$^{+/m}$ and/or *Grb10Δ2-4*$^{m/+}$	Comparison to *Grb10*$^{+/p}$	Conclusion
IGF2	(Charalambous et al., 2003)	*Grb10Δ2-4*$^{m/+}$::Igf2Δ$^{+/p}$ display an intermediate phenotype		Unlikely to mediate overgrowth in paternal or maternal models
IGF2R	Clearance receptor for IGF2; potential function of IGF2-IGF2R signaling in regulating placental labyrinthine volume (Baker et al., 1993; Harris, Crocker, Baker, Aplin, & Westwood, 2011; Sferruzzi-Perri, Owens, Standen, & Roberts, 2008)	*Grb10Δ2-4*$^{m/+}$ mice show overgrowth of placental labyrinthine volume; *Grb10Δ2-4*$^{m/+}$::Igf2Δ$^{+/p}$ display an intermediate phenotype	IGF2R expressed in dentate gyrus, the choroid plexus, the brain stem, & spinal cord–choroid plexus more associated with maternal *Grb10* expression than paternal (Russo, Gluckman, Feldman, & Werther, 2005)	Signaling through IGF2R unlikely to mediate overgrowth in paternal or maternal models
IGF1	*Igf1* overexpression causes brain overgrowth; *Igf1* ablation reduces brain; IGF1 promotes survival and neurite outgrowth in cultured monoaminergic neurons; *Igf1* brain phenotypes attributed to white matter; striatal cell density increased in *Igf*$^{-/-}$ mice (Beck, Powell-Braxtont, Widmer, Valverde, &		No difference in striatal cell density between *Grb10*$^{+/p}$ & wildtypes; DTI data yet to be analyzed for potential white matter effects	Unlikely to mediate *Grb10*$^{+/p}$ brain overgrowth

	Hefti, 1995; Carson, Behringer, Brinster, & McMorris, 1993)			
IGF1R	High expression in midbrain; *Igf1r*$^{-/-}$ reduced *in utero* growth and increased cell density in brainstem and spinal cord (Russo et al., 2005)	Embryonic & placental growth overgrowth in maternal *Grb10* disruption models (Charalambous et al., 2003)	No difference in striatal cell density between *Grb10*$^{+/p}$ and wildtypes	Unlikely to mediate *Grb10*$^{+/p}$ brain overgrowth
Insulin	Grb10 is known to interact with Insulin Receptor (IR), which has effects on growth and neuronal survival (Baker et al., 1993; Holt & Siddle, 2005; Werner & LeRoith, 2014); overexpression of mGrb10α in cell culture did not inhibit insulin stimulation of cell proliferation (Morrione et al., 1997)	Embryonic & placental growth overgrowth in maternal *Grb10* disruption models (Charalambous et al., 2003)		Maternal overgrowth likely not mediated by Insulin/ IR stimulated cell proliferation; *Grb10*$^{+/p}$ overgrowth a possibility through Insulin-IR-IRS2 signaling?
IRS1	*Irs1*$^{-/-}$ bodies are 50% smaller, but brains are relatively spared (Schubert et al., 2003)	*Grb10Δ2-4*$^{m/+}$ mice overgrow; brain is spared (Charalambous et al., 2003)		Further work warranted
IRS2	*Irs2*$^{-/-}$ mice have reduced brain size, with sparing of the body; brain reduction is proportionate and cortical density is normal (Schubert et al., 2003) IRS2 modulates neuronal proliferation		*Grb10*$^{+/p}$ brains are overgrown, with sparing of body size; caudate putamen density is normal	Neuronal proliferation mediated by IRS2 is a possible explanation of *Grb10*$^{+/p}$ brain overgrowth

8.4 Social Dominance

The most surprising result of our social dominance testing was the absence of a clear social dominance phenotype in our *Grb10*$^{+/p}$ mice. We originally designed our cross-sectional behavioural study to determine whether the emergence or significance of the social dominance phenotype identified in Garfield 2011 correlated with brain overgrowth allometry described in Chapters 3 and 4 of this thesis. There was no significant difference between *Grb10*$^{+/p}$ and wildtype cage mates in our social dominance test results for socially housed males or females at any age after FDR correction. Thus, we did not pursue a correlation between social rank measures and brain weight or volume. In isolated cohort of both genders, there was a significantly different likelihood of winning the stranger encounter tube test. However, males were less likely to win–opposite to the findings reported in Garfield 2011–while females were more likely to win. The source of this disparity is unclear. There may be a real sex difference, or the result may be attributed to low power (although the 'n' for each of our male and female cohorts were larger than Garfield's published male cohort). When male and female mice were combined (oestrus status was determined not to predict likelihood of winning), results of the stranger encounter tube test performed by isolated mice were no longer significantly different between genotypes.

8.4.1 Social Instability rather than Social Dominance?

There was a lack of correlation between combinations of tube test social rank, urine marking social rank, and barbering rank in our data, suggesting further experimentation may reveal an unstable hierarchy within mixed

genotype cages containing *Grb10*$^{+/p}$ mice. A comparable phenotype, interpreted as social instability, is present in the *Cdkn1c*^{BACx1} mouse model, which overexpresses imprinted cyclin dependent kinase inhibitor 1c (*Cdkn1c*) (McNamara et al., 2018). Like *Grb10*$^{+/p}$ mice, initial reports concluded *Cdkn1c*^{BACx1} mice displayed enhanced social dominance in the tube test (McNamara et al., 2017). This was revised when further experimentation determined *Cdkn1c*^{BACx1} mice do not occupy more dominant ranks than their wildtype cage-mates on any individual measure of within-cage social hierarchy. However, in the *Cdkn1c*^{BACx1} experiments, an individual's rank in one dominance measure did not correlate with its rank in another. Within individual measures of social dominance, clear transitive hierarchies were apparent, indicating hierarchies could form, but were unstable. The rank of *Cdkn1c*^{BACx1} mice varied more frequently than wildtype cage mates when odor cues were removed via a cage bedding change. When odor cues remained constant, there was no greater change in rank between *Cdkn1c*^{BACx1} and wildtype cage-mates across repeated testing. In the urine marking test, *Cdkn1c*^{BACx1} animals and wild-type cage mates increased scent marking compared to control cages by 30%, although this failed to reach significance ($p = 0.07$). The accumulated evidence suggested, but did not conclusively demonstrate, a greater propensity for *Cdkn1c*^{BACx1} animals to challenge the established hierarchy in the absence of odor cues. The authors suggested a role for imprinted *Cdkn1c* in maintenance of a cohesive social unit (McNamara et al., 2018). It is possible *Grb10* fulfills a similar role, and even that isolation stress enhances this social instability (perhaps differently in males and

females). However, a different experimental set up is required to determine the stability of within-cage rank over time for social groups with *Grb10*$^{+/p}$ animals. Our cross-sectional study suggests if a social instability phenotype exists, it is not likely to vary with age or brain weight/volume, though this is best tested directly. Additionally, future experimental designs aiming to test social instability over time should account for mixed genotype cages as a possible confounding variable. This was highlighted by recent work showing that both male *Nlgn3*$^{y/-}$ and female *Nlgn3*$^{-/-}$ mice modified the behaviour of control littermates/cage-mates. Of particular relevance here, tube test ranking and courtship behaviours correlated in single genotype housing of *Nlgn3*$^{y/-}$ or wildtype male mice, but not in mixed genotype housing (Kalbassi et al., 2017). Tests of social hierarchy stability in *Grb10*$^{+/p}$ cohorts should test the stability of rank across multiple testing both in single and mixed genotype housing.

8.4.2 Converging functions in social stability for paternal *Grb10* and maternal *Cdkn1c*

The possibility of convergent roles in social stability for *Grb10* and *Cdkn1c* is intriguing because these genes are oppositely imprinted in the brain (with paternal *Grb10* and maternal *Cdkn1c* expression), and have coincident presence in monoaminergic regions. The significance of monoaminergic signaling to social dominance hierarchies is discussed in Chapter 5. The functional convergence between *Cdkn1c* and *Grb10* was first pointed out in McNamara 2017, but was revised when *Cdkn1c*^{BACx1} animals were found to differ in social rank stability rather than social rank per say. In this thesis, we suggest this convergence may be restored, subject to direct testing of social

rank stability in *Grb10*$^{+/p}$ colonies, because we found no difference in likelihood of winning or social rank for *Grb10*$^{+/p}$ mice and found lack of correlation between different measures of social rank. We describe the phenotypes of *Cdkn1c* models below to aid our assessment of the likelihood of functional convergence of *Cdkn1c* and *Grb10* on social stability and the monoaminergic system.

Cdkn1c (encoding CDKN1C aka p57^{Kip2}) is a maternally expressed imprinted gene located on the *Kcnq1* imprinting locus on mouse distal chromosome 7 (human chromosome 11q15). Expression of this gene peaks at E13.5, and has restricted postnatal and adult expression (Furutachi, Matsumoto, Nakayama, & Gotoh, 2013; Furutachi et al., 2015; Westbury, Watkins, Ferguson-Smith, & Smith, 2001). *Cdkn1c* plays a role in neurogenesis, migration, morphology, and regulation of the cell cycle. In the midbrain, *Cdkn1c* interaction with *Nurr1* promotes proliferation and differentiation of dopaminergic neurons (Joseph et al., 2003). *Cdkn1c* also maintains quiescence of adult neural stem cells and regulates G1/S phase transition (Borges, Arboleda, & Vilain, 2015; Furutachi et al., 2013, 2015). We note evidence in Garfield 2007 and Morrione 1997 that *Grb10* may have a role in the G2, S, and M phases, though the evidence is contradictory and unclear (Garfield, 2007; Morrione et al., 1997).

Loss of function of maternally inherited *Cdkn1c* reduces Nurr1- and Th-positive cells in the ventral midbrain at E18.5, and conversely overexpression in the *Cdkn1c*^{BACx1} model results in significantly more Th-positive cells in the ventral tegmental area (VTA) compared to wildtypes (Joseph et al., 2003; McNamara et al., 2017). This increase in *Cdkn1c*^{BACx1} brains did not extend to

the substantia nigra pars compacta (SNc), nor total neuronal (NeuN stained) cell number in the striatum or surrounding cortex (McNamara et al., 2017). Cell proliferation, in contrast to Th-positive cell count, was unaltered at several developmental stages in *Cdkn1c* ($p57^{Kip2}$) knockout embryos. Thus, while *Cdkn1c* may have a (redundant) role in proliferation, it may also play a role in cell cycle exit and differentiation of dopaminergic neurons after they have exited the cell cycle (Joseph et al., 2003; Tury, Mairet-Coello, & Dicicco-Bloom, 2011). In $Grb10^{+/p}$ brains, we did not find a difference between neuronal (NeuN) or total cell number in the striatum compared to wildtypes. However, $Grb10^{+/p}$ whole brain, cortical, and subcortical MRI volumes were larger, and whole and subcortical area in Nissl stained sections were larger than wildtypes in Garfield 2007 (though not in our sampled brains parallel to the stereological cell counts) (Garfield, 2007). We concluded neuronal and total cell density in the striatum was no different between $Grb10^{+/p}$ and wildtype brains, but $Grb10^{+/p}$ brains accumulate more tissue. We did not count cells within the VTA or SNc, and therefore cannot compare $Grb10^{+/p}$ to $Cdkn1c^{BACx1}$ models in the ventral midbrain. No difference in total brain size has been reported in *Cdkn1c* disruption or overexpression models.

Crude indicators of dopaminergic signaling activity also differ between $Cdkn1c^{BACx1}$ and $Grb10^{+/p}$ models. HPLC analysis of postmortem $Cdkn1c^{BACx1}$ tissue indicated a 20% increase of dopamine in the dorsal striatum, without change in the metabolite DOPAC or in turnover. Concurrently, there was a nine-fold increase in dopamine transporter (*Dat*) mRNA in the dorsal striatum (McNamara et al., 2017). In contrast, HPLC analysis of the $Grb10^{+p}$ brain

detected no significant changes in neurotransmitter levels (including dopamine, noradrenalin, acetylcholine, serotonin, and associated metabolites) in any region (Garfield et al., 2011; Supplementary Figure 6). While some of the phenotypes of the *Cdkn1c*^{BACx1} model, such as increased motivation to obtain sucrose reward, have clearer links to dopaminergic signaling, phenotypes such as social instability also could arise from early developmental dysregulation not limited to the dopaminergic system (McNamara et al., 2017). Based on evidence thus far, we hypothesize *Grb10*$^{+/p}$ and *Cdkn1c* functional impacts on social stability converge through distinct effects on total and monoaminergic proliferation (or differentiation) and consequent indirect effects on signaling.

8.5 Compulsivity, Anxiety, and Impulsivity

8.5.1 Whisker Barbering and Trichotillomania

We did not find *Grb10*$^{+/p}$ mice to be any different from wildtype controls in measures of compulsivity in the marble burying task. The lack of evidence of compulsive behaviour and complete whisker recovery during social isolation in both Garfield's report and our own should allay concerns that the presentation of whisker barbering in *Grb10*$^{+/p}$ is a trichotillomania-like phenotype (Curley, 2011; Garfield et al., 2011). We do note that within our cohort, a greater total number of the primary barbers were wildtypes, though there was no statistically significant difference in the proportion of *Grb10*$^{+/p}$ and wildtype barbers in male or female cages that presented a clear barber. In three *Grb10*$^{+/p}$/wildtype balanced cages containing male mice 10 months of

age, all four mice were barbered. These patterns may be related to social instability, as discussed in comparison to *Cdkn1c* above, but further testing is required to make this connection. We also noted *Grb10*$^{+/m}$ cages presented barbering, though the total cage numbers were low, and we had no other B6CBA/F1 control colonies for comparison to the *Grb10*$^{+/p}$ cages.

8.5.2 Anxiety and Social Dominance

We undertook anxiety testing using the EPM to account for possible confounds of the marble burying test, which does not distinguish between compulsivity and anxiety. In addition to interfering with the marble burying test, anxiety impacts social competitions and dominance behaviour. Anxious individuals adopt less competitive behaviour and a subordinate status. In high anxious rats, this is mediated by lower mitochondrial respiratory activity in the nucleus accumbens (NAc) (Hollis et al., 2015). Administration of diazepam to these rats facilitates social competitive behaviour by disinhibiting VTA dopaminergic neurons. This leads to the release of dopamine into the NAc and the activation of D1 receptor signaling which facilitates mitochondrial function (van der Kooij et al., 2018). Paternal *Grb10* is highly expressed in the VTA and the NAc, as reported by *LacZ* staining in *Grb10*$^{+/p}$ mice (Garfield, 2007; Garfield et al., 2011). Thus, anxiety modulates competitive confidence and dominance behaviour particularly via regions which also show high paternal *Grb10* expression. As with open field and light/dark box testing in Garfield 2011, we found no difference in EPM anxiety measures between *Grb10*$^{+/p}$ and wildtype mice (Garfield et al., 2011). We conclude anxiety is not interfering with the

results of our social dominance tests. We also note all three anxiety tests were performed on mice from mixed genotype housing, and mutant and wildtype mice may modify each other's behaviour (Kalbassi et al., 2017). However, values in our EPM results were superficially comparable to expected values, and we believe a masking effect due to mixed genotype housing to be unlikely in this instance.

8.5.3 Risk Behaviours

Auxiliary measures on the EPM reveal a possible 'risk taking' phenotype. *Grb10*$^{+/p}$ mice spent a longer total duration in head dipping behaviours, though there was no significant difference compared to wildtypes in entries onto or time spent on the open arm. This 'risk taking' behaviour on the EPM may have some relationship to the previously identified delay discounting phenotype (Dent et al., 2018). This is discussed in Chapter 6. The relationship between monoaminergic brain regions with paternal *Grb10* expression and impulsive behaviour is discussed in Dent et al 2018. *Grb10*$^{+/p}$ mice were directly assessed for risk taking behaviour using the Predator Odour Risk Taking (PORT) task, in which mice must cross a central chamber with a predator odour (fox) to collect a food reward (Dent, Isles, & Humby, 2014). There was no difference in risk-taking behaviour in this task between *Grb10*$^{+/p}$ mice and their wildtype littermate controls (Dent, 2014). Risk behaviour in delay discounting and PORT tasks may recruit different neurological systems. Notably, the delay discounting task is an ethologically artificial environment whereas the PORT is an 'ethologically plausible semi-naturalistic' environment (Dent, 2014). Thus,

the PORT task may rely on fear and recruitment of the amygdala where delay discounting does not (Choi & Kim, 2010). It may also be of interest to test *Grb10*$^{+/p}$ mice for impulsive choice in a more naturalistic model of delay discounting, which incorporates elements such as perceived competition and group training (Amita, Kawamori, & Matsushima, 2010).

8.5.4 Impulsive Choice, Social Dominance, and Aggression

If *Grb10*$^{+/p}$ mice are demonstrating a social instability phenotype comparable to the *Cdkn1c*^{BACx1} model, the question remains of what behaviour or interaction mediates this instability. McNamara et al suggest *Cdkn1c*^{BACx1} social instability arises from increased challenges to the social hierarchy when a bedding change removes odor cues (McNamara et al., 2018). Dominance challenges represent a risk taking behaviour, where winning increases access to food, territory, and courtship opportunities, but loss comes with a cost of effort and potentially health (Hillman, 2013; F. Wang et al., 2014). This cost-benefit analysis depends on accurate self- and peer-assessment as well as transitive reasoning about status (Cummins, 2000). Impulsivity may also moderate likelihood of risk taking in social contexts. In humans and rodents, reactive or offensive aggression (respectively) is associated with impulsive choice (M. C. Cervantes & Delville, 2007; Stanford et al., 2003). In humans, reactive aggression is characterized as impulsive aggression with high emotional reactivity, as opposed to proactive aggression, which is characterized as premeditative aggression with low emotional reactivity (Stanford et al., 2003). In animal models, offensive aggression is compared

with reactive aggression (M. C. Cervantes & Delville, 2007). There is also evidence for a role in serotonin signaling in moderating offensive aggression and impulsivity in humans and rodents (Audero et al., 2013; M. Catalina Cervantes, Biggs, & Delville, 2010; Cherek, Lane, Pietras, & Steinberg, 2002). Increased challenges to the social hierarchy, such as those proposed in McNamara 2018, might result from enhanced offensive aggression through disrupted monoaminergic signaling.

If social instability is present in *Grb10*$^{+/p}$ colonies, it is not very likely to be mediated by impulsive choice and offensive aggression. First, *Grb10*$^{+/p}$ mice prefer larger but delayed reward in the delay discounting task (Dent et al., 2018). In the delay discounting task, smaller but more immediate rewards are characterized as a lower risk, more impulsive choice compared to larger but delayed rewards (Xu et al., 2017). Longer delays increase risk of being interrupted and losing the reward, known as the 'collection risk' hypothesis (Amita et al., 2010; Benson & Stephens, 1996). Thus, *Grb10*$^{+/p}$ mice make less impulsive, but perhaps riskier, choices. Secondly, *Grb10*$^{+/p}$ displayed no increased aggression during a resident-intruder test (Garfield, 2007). In this test, individually housed resident animals were challenged with weight matched socially housed wildtype intruders. The number of *Grb10*$^{+/p}$ animals engaged in aggressive confrontations with intruders was not significantly greater than expected by chance. Of those that did fight, there was no significant difference in latency to first fight, total time spent fighting, or total non-aggressive interaction time (Garfield, 2007).

However, these measures of impulsive choice and aggression may fail to incorporate the social context requisite for a social instability phenotype, or distinguish between different behavioural strategies for social risk. Impulsive choice was trained and tested individually, without elements such as perceived competition which might modify the 'risk' of the delayed reward. Likewise, the resident-intruder paradigm relied upon a social isolation paradigm. Under isolation or low-population density conditions, social strategies such as territorialism and aggressive confrontation are optimal, whereas under high-population density conditions, group-housed animals benefit from a stable social hierarchy which reduces costly conflicts (Singleton & Krebs, 2007; F. Wang et al., 2014). Multiple cages, in both Garfield's colony and our own, were separated for fighting within cage, though we note this occurrence dissipated with the age of the colony. We also noted frequent fighting within the mixed-genotype home cage when mice were returned after participating in behavioural tasks. Aggressive confrontations within the resident-intruder paradigm may not differ, but no detailed report exists of group-housed confrontation strategies for *Grb10*$^{+/p}$ mice in mixed- or single-genotype cages. Information about social confrontations strategies within the home cage could reveal whether potential social instability results from increased challenges precipitated by reactive aggression (impulsive and high emotional reactivity) or proactive aggression (premeditative and low emotional reactivity) strategies.

8.6 Strain differences in behaviour

Model choice is significant in behavioural studies because mouse strains with different genetic backgrounds also have phenotypic variability. Comparisons between studies must account for genetic variation that may be unrelated to the target gene. In these studies, our *Grb10*$^{+/p-}$mice were maintained on a C57BL/6:CBA mixed genetic background (aka B6CBAF1/J, Charles River). Because we maintain on a mixed (F1) background and our experimental group is on an F2 background, the various "B6" and "CBA" genes are segregating. Previous studies have examined C57BL/6 and CBA mice individually for strain differences with respect to social interaction, dominance, and anxiety behaviours. CBA mice have shown elevated visceral pain responses and anxiety, as well as lower basal corticosterone levels in comparison to other strains (Moloney, Dinan, & Cryan, 2015). Interestingly, rearing conditions (group/isolation, handling/non-handled) and dominance status also impacted plasma corticosterone and blood pressure (Watson, Henry, & Haltmeyer, 1974). C57BL/6 mice, on the other hand, lack the described increase in hypertension shown in CBA animals (Lockwood & Turney, 1981). They also display low or negligible levels of aggressive dominance behaviours such as tail wounding and territory patrol, even after social isolation (Gaskill et al., 2017). Low aggression does not indicate an absence of hierarchy formation or dominance systems. C57BL/6 mice in a social interaction task following 3 weeks of social isolation have increased following behaviours and ultrasonic vocalizations (USVs) compared to three other strains (Faure et al., 2017). Following has been associated with an array

of dominance behaviours and is distinct from aggressiveness (Coura et al., 2013).

While these strain difference studies have relied strongly on social isolation to induce social stress or interactions, they inform our consideration of whether strain-specific features may explain our behavioural results. As we are using mice derived from the same colony used in Garfield et al 2011, we can directly compare our results. Additionally, as our colony is maintained on a comparable mixed genetic background (B6CBAF1/crl mice from Charles River) with segregating "B6" and "CBA" genes, we conclude the differences between our social dominance results is not due to strain differences (Garfield et al., 2011).

We also wish to consider whether mouse strain has impacted our lack of correlation between dominance tests. We know both C57BL/6 and CBA mice individually appear to form stable hierarchies (though C57BL/6 may rely on fewer aggressive behaviours) after social isolation conditions (Faure et al., 2017; Watson et al., 1974). Additionally, Wang et al 2011 found robust correlation between dominance tests using socially housed male C57BL/6 mice (Wang et al., 2011). We are aware of no previous investigation of correlation between dominance tests specifically on a mixed C57BL/6:CBA background. Additionally, our experimental design did not afford a control cage comparable to *Cdkn1c*^{BACxLacZ} and wildtype cages in McNamara et al 2018, nor a separate colony of a different inbred mouse strain or cross, which would separately investigate the dominance test correlations in wildtype mixed C57BL/6:CBA background cages (McNamara, John, & Isles, 2018). Regardless, there is reason

to expect stable dominance hierarchies with agreement between different dominance tests in our B6CBAF1/J (aka C57BL/6:CBA F1) colony in the absence of the intervention of the paternal *Grb10* knockout.

There are no other detailed studies of social dominance, compulsivity, or of brain weight and volume in *Grb10* paternal knockout mice, aside from the work presented here and in Garfield 2007. Thus, there are also no results from other strains for comparison to our findings. However, many of the analyses I have made here rely on internal wildtype vs $Grb10^{+/p}$ comparisons on the same mixed genetic background, and display a strong effect of genotype. Any inquiries into whether these effects are enhanced or hidden by mouse strain-specific differences would require further experimentation.

8.7 Caveats to the *Grb10*$^{+/p}$ *LacZ* cassette model

The *Grb10*$^{+/p}$ model was derived by inserting a *LacZ:neomycin*^{r} cassette into *Grb10* exon 7 using the XC302 gene-trap ES cell line (Garfield et al., 2011). However, *LacZ* expressing models have behavioural effects attributed to the accumulation of β-galactosidase (Reichel et al., 2016). The bacterial β-galactosidase product is an analog of the mammalian senescence-associated β-galactosidase, which is also a molecular marker for aging (Dimri et al., 1995). In Reichel et al, the mouse model R26R:Nex-Cre^{+} expresses *LacZ* in glutamatergic neurons throughout the cortical layers, the hippocampus, and the basolateral amygdala (Reichel et al., 2016). R26R:Nex-Cre^{+} mice (glutamatergic *LacZ* expression) aged 4 months display increased locomotor activity in the open field, decreased anxiety related behaviour in the light/dark box, and impaired contextual hippocampus-dependent memory. Additionally, hippocampal volume was reduced and there was decreased dendritic arborization following *LacZ* expression. Transfection of N2A cells with a *LacZ* expressing plasmid decreased cell viability.

An additional model, the R26R:Dlx5/6-Cre^{+} mouse, expressed *LacZ* in GABAergic forebrain neurons, with strong staining in the striatum and ventral tegmental area, both regions of *Grb10* expression. Like R26R:Nex-Cre^{+} mice, R26R:Dlx5/6-Cre^{+} mice displayed increased locomotor activity in the open field, and decreased anxiety in the light/dark box. GABAergic *LacZ* expression also led to decreased acoustic startle response and slightly impaired hippocampus-dependent spatial learning, but left contextual fear memory unaffected. In contrast to the glutamatergic *LacZ* expression model,

R26R:Dlx5/6-Cre^{+} mice showed no alterations in hippocampal volume, suggesting the impact of *LacZ* expression on the brain and behaviour depends on the targeted neuronal population (Reichel et al., 2016). Several control experiments for these models indicated these effects were due to *LacZ* expression, rather than the specific *LacZ* expression mechanism (Cre, AAV, etc) (Reichel et al., 2016).

Grb10$^{+/p}$ *LacZ* staining overlaps with some areas in the Reichel models, raising concerns that some *Grb10*$^{+/p}$ phenotypes may be attributable to *LacZ* accumulation. *Grb10*$^{+/p}$ *LacZ* staining was strong in the striatum (caudate putamen) and the ventral tegmental area, overlapping with the GABAergic R26R:Dlx5/6-Cre^{+} *LacZ* expression. Additionally, the intensity of *Grb10*$^{+/p}$ *LacZ* staining in the nucleus accumbens (NAc) is not explained by cholinergic neurons alone, and is possibly also due to GABAergic neurons (Garfield, 2007). These concerns may be allayed somewhat as *Grb10*$^{+/p}$ mice demonstrated no baseline locomotor activity differences over 24 hours, nor any anxiety differences in the light/dark box, open field, or EPM (Garfield, 2007). We do not see *LacZ* expression in the cortex or hippocampus of *Grb10*$^{+/p}$ mice, and therefore are not concerned about volume reductions or impaired hippocampal function due to *LacZ* accumulation. If *LacZ* accumulation in the midbrain and other areas of high *Grb10* expression are contributing to decreased neuronal survival, the *Grb10*$^{+/p}$ overgrowth phenotype certainly outweighs this effect, as we have measured consistently heavier brains with larger volumes compared to wildtype controls.

8.8 Epigenetic editing tools for probing the functional consequences of *Grb10* imprinting

Identification of the mechanisms by which paternal *Grb10* expression regulates brain growth will benefit from a better understanding of the functional consequence of its tissue-specificity and developmental timing. This regulatory pattern depends upon an epigenetic distinction between the maternal and paternal chromosomes which has defined functional consequences. Many conventional methods determining the functional consequence of epigenetic imprinting marks are unspecific to the locus of interest or involve direct manipulation of the DNA, which may also disrupt chromatin interactions or regulatory and coding sequences. Newly developing EpiEffectors allow us to make targeted changes to the imprinting architecture itself. Targeted epigenetic editing will be instrumental in resolving many of the regulatory questions currently informed only by correlative and associative data. Conventional and emerging methods of manipulating imprinting architectures are described in detail in (Rienecker et al., 2016).

8.8.1 Future applications of EpiEffectors to *Grb10*

In Chapter 7, we aimed to design an EpiEffector capable of targeted demethylation of the *GRB10* DMR at CGI2. We successfully cloned and expressed the dCas9-TET2(CD) construct in human embryonic kidney (HEK) cells. However, we were unable to obtain methylation data about the targeted locus in HEK cells, though we confirmed demethylation of another imprinting target under 5-azacytidine treatment. To overcome this difficulty in future experiments, we generated murine embryonic stem cell cultures (mESCs) from

our colony to improve our ability to successfully pyrosequence the *GRB10* CGI2 locus and to more directly compare cell culture results to mouse model phenotypes. One application of validated EpiEffectors in this system would be to investigate a causal relationship between elements of the paternal regulatory architecture at *Grb10* and the downstream mechanisms responsible for brain overgrowth in the murine *Grb10*$^{+/p}$ model. Targeted editing might be used to determine if resolution of the paternal *Grb10* bivalent chromatin domain is sufficient to induce ectopic expression and perhaps restrict growth in cortical cultures. Combination of this manipulation with FACS and RNA sequencing might reveal downstream pathways responsible for mediating growth phenotypes. If resolution of the bivalent domain failed to reactivate paternal expression, we might determine that the bivalent domain is not the causal regulatory change initiating paternal expression but rather perhaps a response to or reinforcement of the regulatory change. Alternatively, EpiEffectors might be used to define critical periods of paternal *Grb10* expression by delaying or reverting the switch from maternal to paternal expression during neuronal differentiation programs (Plasschaert & Bartolomei, 2015). This would reveal whether paternal *Grb10* expression is required for a limited decision stage in differentiation (such as regulating proliferation) or if it has a persistent role in mature neurons (such as preventing apoptosis). As more effective EpiEffectors emerge in this field, more precise manipulations of imprinting architectures will be possible.

8.9 Paternal *Grb10* within Imprinting Theory

The contribution of *Grb10* maternal expression to imprinting theory is fairly robust, as detailed by numerous papers describing its roles in parental conflict in the placenta and maternal-offspring coordination of postnatal nutrients (Charalambous et al., 2010, 2003; Cowley et al., 2014). In contrast, the place of *Grb10* paternal expression within imprinting theory is more opaque, both because detailed descriptions of its function are still developing and because the predictions of imprinted regulation of adult social behaviours are not yet strong enough for clear experimental challenge. However, here we suggest two main themes which may contextualize the results of this thesis within imprinting theory. First, brain overgrowth in the $Grb10^{+/p}$ model makes a clear contribution to our understanding of androgenetic/parthenogenetic contributions to chimera brain development. These early experiments showed differential contribution of maternal and paternal genomes to brain tissues, with the paternal contribution favoring hypothalamic, septal and preoptic areas and functions in restricting brain growth (Davies et al., 2008; Keverne, 1997; Keverne et al., 1996). Paternal *Grb10* expression matches this profile, with midbrain and hypothalamic expression and demonstrating in this thesis a function in restricting brain growth (Garfield, 2007; Garfield et al., 2011).

The second theme we suspect is a role for paternal *Grb10* in regulating social stability. We found no significant difference in likelihood of winning social dominance matches between $Grb10^{+/p}$ and wildtype controls, but did identify an unexpected lack of correlation between any of our social hierarchy rankings at any age. Thus, $Grb10^{+/p}$ mice show some compelling similarities to

the unstable social hierarchies of *Cdkn1c*^{BACx1} mice, in addition to overlapping expression in dopaminergic regions. It is possible paternally expressed *Grb10* and maternally expressed *Cdkn1c* have convergent functional roles in social hierarchies, which may disrupt hierarchical stability when experimentally manipulated. While a new experimental set up is required to directly explore social stability in *Grb10*$^{+/p}$ mice, social stability is an intriguing substrate for imprinting evolutionary theory. Unstable social environments have consequences for the fitness of all group members, as instability induces anxiety, stress, and a reduced overall breeding rate (Lardy et al., 2015; Saavedra-Rodríguez & Feig, 2013). However, characteristics such as breeding strategies, group size, group composition (by sex, relative dominance, and relatedness) affect male and female fitness differently (Ebensperger et al., 2016; Lardy et al., 2015). Thus, group stability achieved by a balance of these characteristics enhances fitness of all members of the group, but this balance is determined by competing maternal and paternal optimums. Thus, social behaviours are a potential substrate for genomic imprinting (Haig, 2006; McNamara & Isles, 2014).

The relationship between group living and brain size in mammals may also help connect the social behaviour and brain overgrowth phenotypes in our *Grb10*$^{+/p}$ mice. More complex and gregarious group living, expanded neocortical neuron numbers, and increased connectivity are associated with eutherian mammals compared to monotremes and marsupials (Cheung et al., 2010; Krubitzer, 1998; A. E. Müller & Thalmann, 2000). Notably, while in general larger brains are associated with larger and/or more complex social

groups, the group members considered significant to this association differ somewhat between primates and other mammals (Dunbar, 2009; Sandel et al., 2016). Genomic imprinting may have a relationship to phylogenetic change in brain regions with a parental contribution bias (Keverne et al., 1996). While maternally expressed *Cdkn1c* is implicated in neocortical development and cortical function, paternally expressed *Grb10* may operate in subcortical regions where it is highly expressed to restrict growth. Region-specific functions may have competing impacts on behaviours which influence social stability and group characteristics. *Grb10* supports multiple evolutionary theories of imprinting, but these possible origins are not mutually exclusive. In fact, the reciprocal imprinting of *Grb10* maternal and paternal alleles suggests once genomic imprinting was established at this locus, other tissues (or the other parental genome) adopted this regulatory strategy and adapted it to new functions (Wilkins, 2013).

8.10 Summary

In this thesis, the data demonstrate *Grb10*$^{+/p}$ brains are overgrown in adult life, both in weight and volume, and that in some dimensions, their allometry differs from both wildtype and *Grb10*$^{+/m}$ controls. This overgrowth results from excess tissue of the same total and neuronal cell density, potentially implicating differential or extended proliferation early in development, which impacts postnatal allometry. Contrary to previous report using the stranger encounter tube test and isolated male *Grb10*$^{+/p}$ mice 10 months of age, we found no evidence of a social dominance phenotype in

group housed mice at 2, 6, or 10 months of age, or of isolated mice when both sexes were considered together. There were no correlations between three measures of within-cage rank, suggesting *Grb10*$^{+/p}$ mice may contribute to instability in social hierarchies. This is strongly reminiscent of findings for *Cdkn1c*^{BACx1} mice. The opposite imprinting profiles of *Grb10* (paternal) and *Cdkn1c* (maternal) expression in the brain suggest these genes may have convergent and competing functions in regulating adult social relationships. Finally, while we successfully constructed the dCas9-TET2(CD) EpiEffector, we were unable to test its efficacy in demethylating *GRB10* in HEK cells. We recommend the use of mESCs for future epigenetic engineering experiments attempting to investigate the functional consequences of *Grb10* imprinting architecture on cellular proliferation and neuronal differentiation in culture.

9 Bibliography

Aapola, U., Kawasaki, K., Scott, H. S., Ollila, J., Vihinen, M., Heino, M., … Peterson, P. (2000). Isolation and initial characterization of a novel zinc finger gene, DNMT3L, on 21q22.3, related to the cytosine-5-methyltransferase 3 gene family. *Genomics*, *65*(3), 293–298.

Aapola, U., Liiv, I., & Peterson, P. (2002). Imprinting regulator DNMT3L is a transcriptional repressor associated with histone deacetylase activity. *Nucleic Acids Research*, *30*(16), 3602–3608. https://doi.org/https://doi.org/10.1093/nar/gkf474

Al Adhami, H., Evano, B., Le Digarcher, A., Gueydan, C., Dubois, E., Parrinello, H., … Journot, L. (2015). A systems-level approach to parental genomic imprinting: The imprinted gene network includes extracellular matrix genes and regulates cell cycle exit and differentiation. *Genome Research*, *25*(3), 353–367. https://doi.org/10.1101/gr.175919.114

Albelda, N., & Joel, D. (2012). Current animal models of obsessive compulsive disorder: An update. *Neuroscience*, *211*, 83–106. https://doi.org/10.1016/j.neuroscience.2011.08.070

Amita, H., Kawamori, A., & Matsushima, T. (2010). Social influences of competition on impulsive choices in domestic chicks. *Biology Letters*, *6*(2), 183–186. https://doi.org/10.1098/rsbl.2009.0748

Angoa-Pérez, M., Kane, M. J., Briggs, D. I., Francescutti, D. M., & Kuhn, D. M. (2013). Marble Burying and Nestlet Shredding as Tests of Repetitive, Compulsive-like Behaviors in Mice. *Journal of Visualized Experiments*, (82), e50978. https://doi.org/10.3791/50978

Angulo, J. A., Printz, D., Ledoux, M., & McEwen, B. S. (1991). Isolation stress increases tyrosine hydroxylase mRNA in the locus coeruleus and midbrain and decreases proenkephalin mRNA in the striatum and nucleus accumbens. *Molecular Brain Research*, *11*(3–4), 301–308. https://doi.org/10.1016/0169-328X(91)90039-Z

Anvar, Z., Cammisa, M., Riso, V., Baglivo, I., Kukreja, H., Sparago, A., … Riccio, A. (2016). ZFP57 recognizes multiple and closely spaced sequence motif variants to maintain repressive epigenetic marks in mouse embryonic stem cells. *Nucleic Acids Research*, *44*(3), 1118–1132. https://doi.org/10.1093/nar/gkv1059

Arnaud, P. (2010). Genomic imprinting in germ cells: Imprints are under control. *Reproduction*, *140*(3), 411–423. https://doi.org/10.1530/REP-10-0173

Arnaud, P., Hata, K., Kaneda, M., Li, E., Sasaki, H., Feil, R., & Kelsey, G. (2006). Stochastic imprinting in the progeny of Dnmt3L-/- females. *Human Molecular Genetics*, *15*(4), 589–598.

Arnaud, P., Monk, D., Hitchins, M., Gordon, E., Dean, W., Beechey, C. V., … Kelsey, G. (2003). Conserved methylation imprints in the human and mouse GRB10 genes with divergent allelic expression suggests differential reading of the same mark. *Human Molecular Genetics*. https://doi.org/10.1093/hmg/ddg110

Audero, E., Mlinar, B., Baccini, G., Skachokova, Z. K., Corradetti, R., & Gross,

C. (2013). Suppression of Serotonin Neuron Firing Increases Aggression in Mice. *Journal of Neuroscience*, *33*(20), 8678–8688. https://doi.org/10.1523/JNEUROSCI.2067-12.2013

Baker, J., Liu, J. P., Robertson, E. J., & Efstratiadis, a. (1993). Role of insulin-like growth factors in embryonic and postnatal growth. *Cell*, *75*(1), 73–82. https://doi.org/10.1016/0092-8674(93)90680-O

Barlow, D. P. (2011). Genomic Imprinting: A Mammalian Epigenetic Discovery Model. *Annual Review of Genetics*, *45*, 379–403. https://doi.org/10.1146/annurev-genet-110410-132459

Bartolomei, M. S., & Ferguson-Smith, A. C. (2011). Mammalian genomic imprinting. *Cold Spring Harbor Perspectives in Biology*, *3*(7), a002592. https://doi.org/10.1101/cshperspect.a002592

Barton, S. C., Surani, M. a, & Norris, M. L. (1984). Role of paternal and maternal genomes in mouse development. *Nature*, *311*, 374–376. https://doi.org/10.1038/311374a0

Beck, K. D., Powell-Braxtont, L., Widmer, H. R., Valverde, J., & Hefti, F. (1995). Igf1 gene disruption results in reduced brain size, CNS hypomyelination, and loss of hippocampal granule and striatal parvalbumin-containing neurons. *Neuron*, *14*(4), 717–730. https://doi.org/10.1016/0896-6273(95)90216-3

Benjamini, Y., Drai, D., Elmer, G., Kafkafi, N., & Golani, I. (2001). Controlling the false discovery rate in behavior genetics research. *Behavioural Brain Research*, *125*(1–2), 279–284. https://doi.org/10.1016/S0166-4328(01)00297-2

Benjamini, Y., & Liu, W. (1999). A distribution-free multiple test procedure that controls the false discovery rate. *Tel Aviv University Department of Statistics and O.R*, *RP-SOR-99-3*.

Benson, K. E., & Stephens, D. W. (1996). Interruptions, tradeoffs, and temporal discounting. *American Zoologist*, *36*(4), 506–517. https://doi.org/10.1093/icb/36.4.506

Blagitko, N., Mergenthaler, S., Schulz, U., Wollmann, H. a, Craigen, W., Eggermann, T., … Kalscheuer, V. M. (2000). Human GRB10 is imprinted and expressed from the paternal and maternal allele in a highly tissue- and isoform-specific fashion. *Human Molecular Genetics*, *9*(11), 1587–1595. https://doi.org/10.1093/hmg/9.11.1587

Borges, K. S., Arboleda, V. A., & Vilain, E. (2015). Mutations in the PCNA-binding site of CDKN1C inhibit cell proliferation by impairing the entry into S phase. *Cell Division*, *10*(2). https://doi.org/10.1186/s13008-015-0008-8

Børglum, A. D., Kirov, G., Craddock, N., Mors, O., Muir, W., Murray, V., … Kruse, T. A. (2003). Possible parent-of-origin effect of Dopa decarboxylase in susceptibility to bipolar affective disorder. *American Journal of Medical Genetics Part B: Neuropsychiatric Genetics*. https://doi.org/10.1002/ajmg.b.10030

Bourc'his, D., Xu, G. L., Lin, C. S., Bollman, B., & Bestor, T. H. (2001). Dnmt3L and the establishment of maternal genomic imprints. *Science (New York, N.Y.)*, *294*(5551), 2536–2539.

Bowman, C. J., Streck, R. D., & Chapin, R. E. (2010). Maternal-placental insulin-like growth factor (IGF) signaling and its importance to normal embryo-fetal development. *Birth Defects Research Part B - Developmental and Reproductive Toxicology*, *89*(4), 339–349. https://doi.org/10.1002/bdrb.20249

Branchi, I., D'Andrea, I., Santarelli, S., Bonsignore, L. T., & Alleva, E. (2011). The richness of social stimuli shapes developmental trajectories: Are laboratory mouse pups impoverished? *Progress in Neuro-Psychopharmacology and Biological Psychiatry*, *35*(6), 1452–1460. https://doi.org/10.1016/j.pnpbp.2011.01.002

Bruning, J. C., Gautam, D., Burks, D. J., Gillette, J., Schubert, M., Orban, P. C., … Kahn, C. R. (2000). Role of brain insulin receptor in control of body weight and reproduction. *Science*, *289*(5487), 2122–2125. https://doi.org/10.1126/science.289.5487.2122

Cao, R., Wang, L., Wang, H., Xia, L., Erdjument-Bromage, H., Tempst, P., … Zhang, Y. (2002). Role of histone H3 lysine 27 methylation in Polycomb-group silencing. *Science*, *298*(5595), 1039–1043. https://doi.org/10.1126/science.1076997

Carson, M. J., Behringer, R. R., Brinster, R. L., & McMorris, F. A. (1993). Insulin-like growth factor I increases brain growth and central nervous system myelination in transgenic mice. *Neuron*, *10*(4), 729–740. https://doi.org/10.1016/0896-6273(93)90173-O

Cattanach, B. M., Beechey, C. V, Rasberry, C., Jones, J., & Papworth, D. (1996). Time of initiation and site of action of the mouse chromosome 11 imprinting effects. *Genetical Research*, *68*(1), 35–44. https://doi.org/10.1017/S0016672300033863

Cattanach, B. M., & Kirk, M. (1985). Differential activity of maternally and paternally derived chromosome regions in mice. *Nature*, *315*(6019), 496–498. Retrieved from http://www.nature.com/nature/journal/v315/n6019/pdf/315496a0.pdf

Cattanach, B. M., Shibata, H., Hayashizaki, Y., Townsend, K. M. S., Ball, S., & Beechey, C. V. (1998). Association of a redefined proximal mouse chromosome 11 imprinting region and U2afbp-rs/U2af1-rs1 expression. *Cytogenetics and Cell Genetics*, *80*(1–4), 41–47. https://doi.org/10.1159/000014955

Cervantes, M. C., Biggs, E. A., & Delville, Y. (2010). Differential responses to serotonin receptor ligands in an impulsive-aggressive phenotype. *Behavioral Neuroscience*, *124*(4), 455–469. https://doi.org/10.1037/a0020171

Cervantes, M. C., & Delville, Y. (2007). Individual differences in offensive aggression in golden hamsters: A model of reactive and impulsive aggression? *Neuroscience*, *150*(3), 511–521. https://doi.org/10.1016/j.neuroscience.2007.09.034

Charalambous, M., Cowley, M., Geoghegan, F., Smith, F. M., Radford, E. J., Marlow, B. P., … Ward, A. (2010). Maternally-inherited Grb10 reduces placental size and efficiency. *Developmental Biology*, *337*(1), 1–8. https://doi.org/10.1016/j.ydbio.2009.10.011

Charalambous, M., da Rocha, S. T., & Ferguson-Smith, A. C. (2007). Genomic imprinting, growth control and the allocation of nutritional resources: consequences for postnatal life. *Current Opinion in Endocrinology, Diabetes, and Obesity*, *14*(1), 3–12. https://doi.org/10.1097/MED.0b013e328013daa2

Charalambous, M., Smith, F. M., Bennett, W. R., Crew, T. E., Mackenzie, F., & Ward, A. (2003). Disruption of the imprinted Grb10 gene leads to disproportionate overgrowth by an Igf2-independent mechanism. *Proceedings of the National Academy of Sciences*, *100*(14), 8292–8297. https://doi.org/10.1073/pnas.1532175100

Chedin, F., Lieber, M. R., & Hsieh, C.-L. (2002). The DNA methyltransferase-like protein DNMT3L stimulates de novo methylation by Dnmt3a. *Proceedings of the National Academy of Sciences of the United States of America*, *99*(26), 16916–16921. https://doi.org/10.1073/pnas.262443999

Chen, H., Kazemier, H. G., De Groote, M. L., Ruiters, M. H. J., Xu, G. L., & Rots, M. G. (2014). Induced DNA demethylation by targeting Ten-Eleven Translocation 2 to the human ICAM-1 promoter. *Nucleic Acids Research*, *42*(3), 1563–1574.

Chen, J., Liu, R., Yang, Y., Li, J., Zhang, X., Li, J., … Ma, J. (2011). The simulated microgravity enhances the differentiation of mesenchymal stem cells into neurons. *Neurosci Lett*, *505*(2), 171–175. https://doi.org/10.1016/j.neulet.2011.10.014

Cherek, D. R., Lane, S. D., Pietras, C. J., & Steinberg, J. L. (2002). Effects of chronic paroxetine administration on measures of aggressive and impulsive responses of adult males with a history of conduct disorder. *Psychopharmacology*, *159*(3), 266–274. https://doi.org/10.1007/s002130100915

Cheung, A. F. P., Kondo, S., Abdel-Mannan, O., Chodroff, R. A., Sirey, T. M., Bluy, L. E., … Molnár, Z. (2010). The subventricular zone is the developmental milestone of a 6-layered neocortex: Comparisons in metatherian and eutherian mammals. *Cerebral Cortex*, *20*(5), 1071–1081. https://doi.org/10.1093/cercor/bhp168

Choi, J.-S., & Kim, J. J. (2010). Amygdala regulates risk of predation in rats foraging in a dynamic fear environment. *Proceedings of the National Academy of Sciences*, *107*(50), 21773–21777. https://doi.org/10.1073/pnas.1010079108

Chotalia, M., Smallwood, S. A., Ruf, N., Dawson, C., Lucifero, D., Frontera, M., … Kelsey, G. (2009). Transcription is required for establishment of germline methylation marks at imprinted genes. *Genes and Development*, *23*(1), 105–117. https://doi.org/10.1101/gad.495809

Christenson, J. G. (1972). On the Identity of DOPA Decarboxylase and 5-hydroxytryptophan Decarboxylase. *Proceedings of the National Academy of Sciences*. https://doi.org/10.1073/pnas.69.2.343

Christman, J. (2002). 5-Azacytidine and 5-aza-2'-deoxycytidine as inhibitors of DNA methylation: mechanistic studies and their implications for cancer therapy. *Oncogene*, *21*(35), 5483–5495.

https://doi.org/10.1038/sj.onc.1205699
Coura, R. S., Cressant, A., Xia, J., De Chaumont, F., Olivo-Marin, J. C., Pelloux, Y., … Granon, S. (2013). Nonaggressive and adapted social cognition is controlled by the interplay between noradrenergic and nicotinic receptor mechanisms in the prefrontal cortex. *FASEB Journal*. https://doi.org/10.1096/fj.13-231084
Cowley, M., Garfield, A. S., Madon-Simon, M., Charalambous, M., Clarkson, R. W., Smalley, M. J., … Ward, A. (2014). Developmental programming mediated by complementary roles of imprinted Grb10 in mother and pup. *PLoS Biology*, *12*(2), e1001799. https://doi.org/10.1371/journal.pbio.1001799
Creeth, H. D. J., McNamara, G. I., Tunster, S. J., Boque-Sastre, R., Allen, B., Sumption, L., … John, R. M. (2018). Maternal care boosted by paternal imprinting in mammals. *PLoS Biology*, *16*(7), e2006599. https://doi.org/10.1371/journal.pbio.2006599
Cummins, D. D. (2000). How the social environment shaped the evolution of mind. *Synthese*, *122*(1–2), 3–28. https://doi.org/10.1023/A:1005263825428
Curley, J. P. (2011). Is there a genomically imprinted social brain? *BioEssays*, *33*(9), 662–668. https://doi.org/10.1002/bies.201100060
Davies, W., Isles, A. R., Humby, T., & Wilkinson, L. S. (2008). What are imprinted genes doing in the brain? *Advances in Experimental Medicine and Biology*, *626*, 62–70. https://doi.org/10.4161/epi.2.4.5379
Davies, W., Isles, A. R., & Wilkinson, L. S. (2005). Imprinted gene expression in the brain. *Neuroscience & Biobehavioral Reviews*, *29*(3), 421–430. https://doi.org/10.1016/j.neubiorev.2004.11.007
Dawkins, R. (1999). *The Extended Phenotype: The Long Reach of the Gene* (Revised Impression). Oxford: Oxford University Press.
De Smet, C., Lurquin, C., Lethé, B., Martelange, V., & Boon, T. (1999). DNA Methylation Is the Primary Silencing Mechanism for a Set of Germ Line- and Tumor-Specific Genes with a CpG-Rich Promoter. *Molecular and Cellular Biology*, *19*(11), 7327–7335. Retrieved from http://mcb.asm.org/lookup/doi/10.1128/MCB.19.11.7327
Dent, C. L. (2014). *Imprinted genes, Impulsivity and Risk-Taking*. Cardiff University School of Medicine.
Dent, C. L., Humby, T., Lewis, K., Ward, A., Fischer-Colbrie, R., Wilkinson, L. S., … Isles, A. R. (2018). Impulsive choice in mice lacking paternal expression of Grb10 suggests intragenomic conflict in behavior. *Genetics*, *209*(1), 233–239. https://doi.org/10.1534/genetics.118.300898
Dent, C. L., & Isles, A. R. (2014). Brain-expressed imprinted genes and adult behaviour: The example of Nesp and Grb10. *Mammalian Genome*, *25*(1–2), 87–93.
Dent, C. L., Isles, A. R., & Humby, T. (2014). Measuring risk-taking in mice: Balancing the risk between seeking reward and danger. *European Journal of Neuroscience*, *39*(4), 520–530. https://doi.org/10.1111/ejn.12430
Depetris, R. S., Hu, J., Gimpelevich, I., Holt, L. J., Daly, R. J., & Hubbard, S. R.

(2005). Structural basis for inhibition of the insulin receptor by the adaptor protein Grb14. *Molecular Cell*, *20*(2), 325–333. https://doi.org/10.1016/j.molcel.2005.09.001

Depetris, R. S., Wu, J., & Hubbard, S. R. (2009). Structural and functional studies of the Ras-associating and pleckstrin-homology domains of Grb10 and Grb14. *Nature Structural & Molecular Biology*, *16*(8), 833–839. https://doi.org/10.1038/nsmb.1642

Desbuquois, B., Carré, N., & Burnol, A. F. (2013). Regulation of insulin and type 1 insulin-like growth factor signaling and action by the Grb10/14 and SH2B1/B2 adaptor proteins. *FEBS J.*, *280*(3), 794–816. https://doi.org/10.1111/febs.12080

Desjardins, C., Maruniak, J. A., & Bronson, F. H. (1973). Social rank in house mice: Differentiation revealed by ultraviolet visualization of urinary marking patterns. *Science*, *182*(4115), 939–941. https://doi.org/10.1126/science.182.4115.939

Dimri, G. P., Lee, X., Basile, G., Acosta, M., Scott, G., Roskelley, C., … Pereira-Smith, O. (1995). A biomarker that identifies senescent human cells in culture and in aging skin in vivo. *Proceedings of the National Academy of Sciences of the United States of America*, *92*(20), 9363–9367. https://doi.org/DOI 10.1073/pnas.92.20.9363

Dunbar, R. I. M. (2009). The social brain hypothesis and its implications for social evolution. *Annals of Human Biology*, *36*(5), 562–572. https://doi.org/10.1080/03014460902960289

Ebensperger, L. A., Correa, L. A., León, C., Ramírez-Estrada, J., Abades, S., Villegas, Á., & Hayes, L. D. (2016). The modulating role of group stability on fitness effects of group size is different in females and males of a communally rearing rodent. *Journal of Animal Ecology*, *85*(6), 1502–1515. https://doi.org/10.1111/1365-2656.12566

Eggermann, T., Schönherr, N., Jäger, S., Spaich, C., Ranke, M. B., Wollmann, H. A., & Binder, G. (2008). Segmental maternal UPD(7q) in Silver-Russell syndrome. *Clinical Genetics*, *74*(5), 486–489. https://doi.org/10.1111/j.1399-0004.2008.01057.x

Engel, N., Thorvaldsen, J. L., & Bartolomei, M. S. (2006). CTCF binding sites promote transcription initiation and prevent DNA methylation on the maternal allele at the imprinted H19/Igf2 locus. *Human Molecular Genetics*, *15*(19), 2945–2954. https://doi.org/10.1093/hmg/ddl237

Faure, A., Pittaras, E., Nosjean, A., Chabout, J., Cressant, A., & Granon, S. (2017). Social behaviors and acoustic vocalizations in different strains of mice. *Behavioural Brain Research*. https://doi.org/10.1016/j.bbr.2016.11.003

Faust, C., Schumacher, A., Holdener, B., & Magnuson, T. (1995). The eed mutation disrupts anterior mesoderm production in mice. *Development*, *121*(2), 273–285.

Ferguson-Smith, A. C. (2011). Genomic imprinting: the emergence of an epigenetic paradigm. *Nature Reviews. Genetics*, *12*(8), 565–575. https://doi.org/10.1038/nrg3032

Franklin, K., & Paxinos, G. (2007). *The Mouse Brain in Stereotaxic Coordinates*

Third Edition (Third). Elsevier.
Frye, C. A., Petralia, S. M., & Rhodes, M. E. (2000). Estrous cycle and sex differences in performance on anxiety tasks coincide with increases in hippocampal progesterone and 3α,5α-THP. *Pharmacology Biochemistry and Behavior*, *67*(3), 587–596. https://doi.org/10.1016/S0091-3057(00)00392-0
Furutachi, S., Matsumoto, A., Nakayama, K. I., & Gotoh, Y. (2013). P57 controls adult neural stem cell quiescence and modulates the pace of lifelong neurogenesis. *EMBO Journal*, *32*(7), 970–981. https://doi.org/10.1038/emboj.2013.50
Furutachi, S., Miya, H., Watanabe, T., Kawai, H., Yamasaki, N., Harada, Y., … Gotoh, Y. (2015). Slowly dividing neural progenitors are an embryonic origin of adult neural stem cells. *Nat Neurosci*, *18*(5), 657–665. https://doi.org/10.1038/nn.3989
Garfield, A. S. (2007). *Investigating the roles of mouse Grb10 in the regulation of growth and behaviour*. University of Bath. Retrieved from https://europepmc.org/abstract/eth/442877
Garfield, A. S., Cowley, M., Smith, F. M., Moorwood, K., Stewart-Cox, J. E., Gilroy, K., … Ward, A. (2011). Distinct physiological and behavioural functions for parental alleles of imprinted Grb10. *Nature*, *469*(7331), 534–538. https://doi.org/10.1038/nature09651
Garner, J. P., Dufour, B., Gregg, L. E., Weisker, S. M., & Mench, J. A. (2004). Social and husbandry factors affecting the prevalence and severity of barbering ("whisker trimming") by laboratory mice. *Applied Animal Behaviour Science*, *89*(3–4), 263–282. https://doi.org/10.1016/j.applanim.2004.07.004
Gaskill, B. N., Stottler, A. M., Garner, J. P., Winnicker, C. W., Mulder, G. B., & Pritchett-Corning, K. R. (2017). The effect of early life experience, environment, and genetic factors on spontaneous home-cage aggression-related wounding in male C57BL/6 mice. *Lab Animal*. https://doi.org/10.1038/laban.1225
Guibert, S., Forné, T., & Weber, M. (2012). Global profiling of DNA methylation erasure in mouse primordial germ cells. *Genome Research*, *22*(4), 633–641. https://doi.org/10.1101/gr.130997.111
Guo, J. U., Su, Y., Zhong, C., Ming, G., Song, H., Baker, D., … Zhu, J. K. (2011). Hydroxylation of 5-methylcytosine by TET1 promotes active DNA demethylation in the adult brain. *Cell*, *145*(3), 423–434. https://doi.org/10.1016/j.cell.2011.03.022
Hager, R., & Johnstone, R. A. (2003). The genetic basis of family conflict resolution in mice. *Nature*, *421*(6922), 533–535. https://doi.org/10.1038/nature01239
Haig, D. (2006). Genomic Imprinting, Sex-Biased Dispersal, and Social Behavior. *Annals of the New York Academy of Sciences*, *907*(1), 149–163. https://doi.org/10.1111/j.1749-6632.2000.tb06621.x
Haig, D. (2014). Coadaptation and conflict, misconception and muddle, in the evolution of genomic imprinting. *Heredity (Edinb)*, *113*(2), 96–103. https://doi.org/10.1038/hdy.2013.97

Haig, D., & Úbeda, F. (2011). Genomic imprinting: An obsession with depilatory mice. *Current Biology*, *21*(7), R257-9. https://doi.org/10.1016/j.cub.2011.02.027

Han, D. C., Shen, T. L., & Guan, J. L. (2001). The Grb7 family proteins: structure, interactions with other signaling molecules and potential cellular functions. *Oncogene*, *20*(44), 6315–6321. https://doi.org/10.1038/sj.onc.1204775

Handley, S. L., & Mithani, S. (1984). Effects of alpha-adrenoceptor agonists and antagonists in a maze-exploration model of 'fear'-motivated behaviour. *Naunyn-Schmiedeberg's Archives of Pharmacology*, *327*(1), 1–5. https://doi.org/10.1007/BF00504983

Hark, A. T., Schoenherr, C. J., Katz, D. J., Ingram, R. S., Levorse, J. M., & Tilghman, S. M. (2000). CTCF mediates methylation-sensitive enhancer-blocking activity at the H19/Igf2 locus. *Nature*, *405*(6785), 486–489. https://doi.org/10.1038/35013106

Harris, L. K., Crocker, I. P., Baker, P. N., Aplin, J. D., & Westwood, M. (2011). IGF2 Actions on Trophoblast in Human Placenta Are Regulated by the Insulin-Like Growth Factor 2 Receptor, Which Can Function as Both a Signaling and Clearance Receptor1. *Biology of Reproduction*, *84*(3), 440–446. https://doi.org/10.1095/biolreprod.110.088195

Hata, K., Okano, M., Lei, H., & Li, E. (2002). Dnmt3L cooperates with the Dnmt3 family of de novo DNA methyltransferases to establish maternal imprints in mice. *Development (Cambridge, England)*, *129*(8), 1983–1993.

He, Y.-F., Li, B.-Z., Li, Z., Liu, P., Wang, Y., Tang, Q., … Xu, G.-L. (2011). Tet-Mediated Formation of 5-Carboxylcytosine and Its Excision by TDG in Mammalian DNA. *Science*, *333*(6047), 1303–1307. https://doi.org/10.1126/science.1210944

Heerboth, S., Lapinska, K., Snyder, N., Leary, M., Rollinson, S., & Sarkar, S. (2014). Use of epigenetic drugs in disease: An overview. *Genetics and Epigenetics*, *1*(6), 9–19. https://doi.org/10.4137/GEG.S12270

Henckel, A., Chebli, K., Kota, S. K., Arnaud, P., & Feil, R. (2012). Transcription and histone methylation changes correlate with imprint acquisition in male germ cells. *EMBO Journal*, *31*(3), 606–615. https://doi.org/10.1038/emboj.2011.425

Henckel, A., Nakabayashi, K., Sanz, L. A., Feil, R., Hata, K., & Arnaud, P. (2009). Histone methylation is mechanistically linked to DNA methylation at imprinting control regions in mammals. *Human Molecular Genetics*, *18*(18), 3375–3383. https://doi.org/10.1093/hmg/ddp277

Hernandez, L., Kozlov, S., Piras, G., & Stewart, C. L. (2003). Paternal and maternal genomes confer opposite effects on proliferation, cell-cycle length, senescence, and tumor formation. *Proceedings of the National Academy of Sciences of the United States of America*, *100*(23), 13344–13349. https://doi.org/10.1073/pnas.2234026100

Hikichi, T., Kohda, T., Kaneko-Ishino, T., & Ishino, F. (2003). Imprinting regulation of the murine Meg1/Grb10 and human GRB10 genes; roles of brain-specific promoters and mouse-specific CTCF-binding sites. *Nucleic*

Acids Research, *31*(5), 1398–1406. https://doi.org/10.1093/nar/gkg232
Hillman, K. L. (2013). Cost-benefit analysis: The first real rule of fight club? *Frontiers in Neuroscience*, *7*(248). https://doi.org/10.3389/fnins.2013.00248
Hilton, I. B., D'Ippolito, A. M., Vockley, C. M., Thakore, P. I., Crawford, G. E., Reddy, T. E., & Gersbach, C. A. (2015). Epigenome editing by a CRISPR-Cas9 based acetyltransferase activates genes from promoters and enhancers. *Nature Biotechnology*, *33*(5), 510–519. https://doi.org/10.1038/nbt.3199
Hitchins, M., Bentley, L., Monk, D., Beechey, C., Peters, J., Kelsey, G., … Moore, G. E. (2002). DDC and COBL, flanking the imprinted GRB10 gene on 7p12, are biallelically expressed. *Mammalian Genome*. https://doi.org/10.1007/s00335-002-3028-z
Hitchins, M., Monk, D., Bell, G. M., Ali, Z., Preece, M., Stanier, P., & Moore, G. E. (2001). Maternal repression of the human GRB10 gene in the developing central nervous system; evaluation of the role for GRB10 in Silver-Russell syndrome. *European Journal of Human Genetics : EJHG*, *9*(2), 82–90. https://doi.org/10.1038/sj.ejhg.5200583
Hollis, F., van der Kooij, M. A., Zanoletti, O., Lozano, L., Cantó, C., & Sandi, C. (2015). Mitochondrial function in the brain links anxiety with social subordination. *Proceedings of the National Academy of Sciences*, *112*(50), 15486–15491. https://doi.org/10.1073/pnas.1512653112
Holt, L. J., Lyons, R. J., Ryan, A. S., Beale, S. M., Ward, A., Cooney, G. J., & Daly, R. J. (2009). Dual ablation of Grb10 and Grb14 in mice reveals their combined role in regulation of insulin signaling and glucose homeostasis. *Molecular Endocrinology (Baltimore, Md.)*, *23*(9), 1406–1414. https://doi.org/10.1210/me.2008-0386
Holt, L. J., & Siddle, K. (2005). Grb10 and Grb14: enigmatic regulators of insulin action – and more? *Biochemical Journal*, *388*(Pt 2), 393–406. https://doi.org/10.1042/BJ20050216
Hsu, P. P., Kang, S. A., Rameseder, J., Zhang, Y., Ottina, K. A., Lim, D., … Sabatini, D. M. (2011). The mTOR-regulated phosphoproteome reveals a mechanism of mTORC1-mediated inhibition of growth factor signaling. *Science*, *332*(6035), 1317–1322. https://doi.org/10.1126/science.1199498
Ichimaru, Y., Egawa, T., & Sawa, a. (1995). 5-HT1A-receptor subtype mediates the effect of fluvoxamine, a selective serotonin reuptake inhibitor, on marble-burying behavior in mice. *Japanese Journal of Pharmacology*, *68*(1), 65–70. https://doi.org/10.1254/jjp.68.65
Ichinose, H., Ohye, T., Fujita, K., Nagatsu, T., Sumi-Ichinose, C., & Hagino, Y. (1992). Tissue-Specific Alternative Splicing of the First Exon Generates Two Types of mRNAs in Human Aromatic L-Amino Acid Decarboxylase. *Biochemistry*. https://doi.org/10.1021/bi00161a036
Ichinose, H., Ohye, T., Fujita, K., Pantucek, F., Lange, K., Riederer, P., & Nagatsu, T. (1994). Quantification of mRNA of tyrosine hydroxylase and aromatic L-amino acid decarboxylase in the substantia nigra in Parkinson's disease and schizophrenia. *Journal of Neural Transmission -*

Parkinsons Disease and Dementia Section. https://doi.org/10.1109/CCDC.2011.5968205

Ideraabdullah, F. Y., Vigneau, S., & Bartolomei, M. S. (2008). Genomic imprinting mechanisms in mammals. *Mutation Research - Fundamental and Molecular Mechanisms of Mutagenesis*, *647*(1–2), 77–85. https://doi.org/10.1016/j.mrfmmm.2008.08.008

Isles, A. R., Davies, W., & Wilkinson, L. S. (2006). Genomic Imprinting and the Social Brain. *Philosophical Transactions of the Royal Society B: Biological Sciences*, *361*(1476), 2229–2237. https://doi.org/10.1098/rstb.2006.1942

Ito, S., Shen, L., Dai, Q., Wu, S. C., Collins, L. B., Swenberg, J. A., … Zhang, Y. (2011). Tet proteins can convert 5-methylcytosine to 5-formylcytosine and 5-carboxylcytosine. *Science*, *333*(6047), 1300–1303. https://doi.org/10.1126/science.1210597

Jacobs, F. M. J., van der Linden, A. J. A., Wang, Y., von Oerthel, L., Sul, H. S., Burbach, J. P. H., & Smidt, M. P. (2009). Identification of Dlk1, Ptpru and Klhl1 as novel Nurr1 target genes in meso-diencephalic dopamine neurons. *Development*, *136*(14), 2363–2373. https://doi.org/10.1242/dev.037556

Jahn, T., Seipel, P., Urschel, S., Peschel, C., & Duyster, J. (2002). Role for the Adaptor Protein Grb10 in the Activation of Akt. *Molecular and Cellular Biology*, *22*(4), 979–991. https://doi.org/10.1128/MCB.22.4.979-991.2002

John, R. M. (2010). Engineering mouse models to investigate the function of imprinting. *Briefings in Functional Genomics and Proteomics*, *9*(4), 294–303. https://doi.org/10.1093/bfgp/elq010

John, R. M., & Lefebvre, L. (2011). Developmental regulation of somatic imprints. *Differentiation*, *81*(5), 270–280. https://doi.org/10.1016/j.diff.2011.01.007

Joseph, B., Wallen-Mackenzie, A., Benoit, G., Murata, T., Joodmardi, E., Okret, S., & Perlmann, T. (2003). p57Kip2 cooperates with Nurr1 in developing dopamine cells. *Proceedings of the National Academy of Sciences*, *100*(26), 15619–15624. https://doi.org/10.1073/pnas.2635658100

Kabir, N. N., & Kazi, J. U. (2014). Grb10 is a dual regulator of receptor tyrosine kinase signaling. *Molecular Biology Reports*, *41*(4), 1985–1992. https://doi.org/10.1007/s11033-014-3046-4

Kalbassi, S., Bachmann, S. O., Cross, E., Roberton, V. H., & Baudouin, S. J. (2017). Male and Female Mice Lacking Neuroligin -3 Modify the Behavior of their wild-type littermates. *ENeuro*, *4*(4). https://doi.org/10.1523/ENEURO.0145-17.2017

Kaneda, M., Okano, M., Hata, K., Sado, T., Tsujimoto, H., Li, E., & Sasaki, H. (2004). Essential role for de novo DNA methyltransferase Dnmt3a in paternal and maternal imprinting. *Nature*, *429*(6994), 900–903. https://doi.org/10.1038/nature02633

Kebache, S., Ash, J., Annis, M. G., Hagan, J., Huber, M., Hassard, J., … Nantel, A. (2007). Grb10 and active Raf-1 kinase promote bad-dependent cell survival. *Journal of Biological Chemistry*, *282*(30), 21873–21883.

https://doi.org/10.1074/jbc.M611066200
Kelsey, G., & Feil, R. (2013). New insights into establishment and maintenance of DNA methylation imprints in mammals. *Philosophical Transactions of the Royal Society B: Biological Sciences*, *368*(1609), 20110336. https://doi.org/10.1098/rstb.2011.0336
Keverne, E. B. (1997). Genomic imprinting in the brain. *Current Opinion in Neurobiology*, *7*(4), 463–468.
Keverne, E. B., Fundele, R., Narasimha, M., Barton, S. C., & Surani, M. A. (1996). Genomic imprinting and the differential roles of parental genomes in brain development. *Developmental Brain Research*, *92*(1), 91–100. https://doi.org/10.1016/0165-3806(95)00209-X
Kirley, A., Hawi, Z., Daly, G., McCarron, M., Mullins, C., Millar, N., … Gill, M. (2002). Dopaminergic system genes in ADHD: Toward a biological hypothesis. *Neuropsychopharmacology*. https://doi.org/10.1016/S0893-133X(02)00315-9
Ko, M., Huang, Y., Jankowska, A. M., Pape, U. J., Tahiliani, M., Bandukwala, H. S., … Rao, A. (2010). Impaired hydroxylation of 5-methylcytosine in myeloid cancers with mutant TET2. *Nature*, *468*(7325), 839–843. https://doi.org/10.1038/nature09586
Kotzot, D., & Utermann, G. (2005). Uniparental disomy (UPD) other than 15: Phenotypes and bibliography updated. *American Journal of Medical Genetics*, *136*(3), 287–305. https://doi.org/10.1002/ajmg.a.30483
Krubitzer, L. (1998). What can monotremes tell us about brain evolution? *Philosophical Transactions of the Royal Society B: Biological Sciences*, *353*(1372), 1127–1146. https://doi.org/10.1098/rstb.1998.0271
Kurien, B. T., Gross, T., & Scofield, R. H. (2005). Barbering in mice: A model for trichotillomania. *British Medical Journal*, *331*(7531), 1503–1505. https://doi.org/10.1136/bmj.331.7531.1503
Langlais, P., Dong, L. Q., Ramos, F. J., Hu, D., Li, Y., Quon, M. J., & Liu, F. (2004). Negative regulation of insulin- stimulated mitogen-activated protein kinase signaling by Grb10. *Molecular Endocrinology*, *18*(2), 350–358. https://doi.org/10.1210/me.2003-0117
Lardy, S., Allainé, D., Bonenfant, C., & Cohas, A. (2015). Sex-specific determinants of fitness in a social mammal. *Ecology*, *96*(11), 2947–2959. https://doi.org/10.1890/15-0425.1
Latos, P. A., Stricker, S. H., Steenpass, L., Pauler, F. M., Huang, R., Senergin, B. H., … Barlow, D. P. (2009). An in vitro ES cell imprinting model shows that imprinted expression of the Igf2r gene arises from an allele-specific expression bias. *Development*, *136*(3), 437–448. https://doi.org/10.1242/dev.032060
Lauc, G., Huffman, J. E., Pučić, M., Zgaga, L., Adamczyk, B., Muini, A., … Rudan, I. (2013). Loci Associated with N-Glycosylation of Human Immunoglobulin G Show Pleiotropy with Autoimmune Diseases and Haematological Cancers. *PLoS Genetics*, *9*(1), e1003225. https://doi.org/10.1371/journal.pgen.1003225
Laviola, L., Giorgino, F., Chow, J. C., Baquero, J. A., Hansen, H., Ooi, J., … Smith, R. J. (1997). The adapter protein Grb10 associates preferentially

with the insulin receptor as compared with the IGF-I receptor in mouse fibroblasts. *Journal of Clinical Investigation*, *99*(5), 830–837. https://doi.org/10.1172/JCI119246

Le Van Thai, A., Coste, E., Allen, J. M., Palmiter, R. D., & Weber, M. J. (1993). Identification of a neuron-specific promoter of human aromatic l-amino acid decarboxylase gene. *Molecular Brain Research*. https://doi.org/10.1016/0169-328X(93)90006-B

Lee, J. T., & Bartolomei, M. S. (2013). X-inactivation, imprinting, and long noncoding RNAs in health and disease. *Cell*, *152*(6), 1308–1323. https://doi.org/10.1016/j.cell.2013.02.016

Li, X., Ito, M., Zhou, F., Youngson, N., Zuo, X., Leder, P., & Ferguson-Smith, A. C. (2008). A Maternal-Zygotic Effect Gene, Zfp57, Maintains Both Maternal and Paternal Imprints. *Developmental Cell*, *15*(4), 547–557. https://doi.org/10.1016/j.devcel.2008.08.014

Lim, Mei, A. (2004). Grb10: more than a simple adaptor protein. *Frontiers in Bioscience*, *9*, 387–403. https://doi.org/10.2741/1226

Lindzey, G., Winston, H., & Manosevitz, M. (1961). Social dominance in inbred mouse strains. *Nature*, *191*, 474–476. https://doi.org/10.1038/191474a0

Ling, J., Ainol, L., Zhang, L., Yu, X., Pi, W., & Tuan, D. (2004). HS2 enhancer function is blocked by a transcriptional terminator inserted between the enhancer and the promoter. *Journal of Biological Chemistry*, *279*(49), 51704–51713. https://doi.org/10.1074/jbc.M404039200

Liu, M., Bai, J., He, S., Villarreal, R., Hu, D., Zhang, C., … Liu, F. (2014). Grb10 promotes lipolysis and thermogenesis by phosphorylation-dependent feedback inhibition of mTORC1. *Cell Metabolism*, *19*(6), 967–980. https://doi.org/10.1016/j.cmet.2014.03.018

Liu, X. S., Wu, H., Ji, X., Stelzer, Y., Wu, X., Czauderna, S., … Jaenisch, R. (2016). Editing DNA Methylation in the Mammalian Genome. *Cell*, *167*(1), 233–247. https://doi.org/10.1016/j.cell.2016.08.056

Lockwood, J. A., & Turney, T. H. (1981). Social Dominance and Stress-Induced Hypertension: Strain Differences in Inbred Mice. *Physiology & Behaviour*, *26*(3), 547–549.

Long, S. Y. (1972). Hair-nibbling and whisker-trimming as indicators of social hierarchy in mice. *Animal Behaviour*, *20*(1), 10–12. https://doi.org/10.1016/S0003-3472(72)80167-2

Mager, J., Montgomery, N. D., de Villena, F. P.-M., & Magnuson, T. (2003). Genome imprinting regulated by the mouse Polycomb group protein Eed. *Nature Genetics*, *33*(4), 502–507. https://doi.org/10.1038/ng1125

Matthews, G. A., Nieh, E. H., Vander Weele, C. M., Halbert, S. A., Pradhan, R. V., Yosafat, A. S., … Tye, K. M. (2016). Dorsal Raphe Dopamine Neurons Represent the Experience of Social Isolation. *Cell*, *164*(4), 617–631. https://doi.org/10.1016/j.cell.2015.12.040

McGrath, J., & Solter, D. (1984). Completion of mouse embryogenesis requires both the maternal and paternal genomes. *Cell*, *37*(1), 179–183. https://doi.org/10.1016/0092-8674(84)90313-1

McNamara, G. I., Davis, B. A., Browne, M., Humby, T., Dalley, J. W., Xia, J., …

Isles, A. R. (2017). Dopaminergic and behavioural changes in a loss-of-imprinting model of Cdkn1c. *Genes, Brain and Behavior*, *17*(2), 149–157. https://doi.org/10.1111/gbb.12422

McNamara, G. I., & Isles, A. R. (2013). Dosage-sensitivity of imprinted genes expressed in the brain: 15q11–q13 and neuropsychiatric illness. *Biochemical Society Transactions*, *41*(3), 721–726. https://doi.org/10.1042/BST20130008

McNamara, G. I., & Isles, A. R. (2014). Influencing the social group: The role of imprinted genes. *Advances in Genetics*, *86*, 107–134. https://doi.org/10.1016/B978-0-12-800222-3.00006-1

McNamara, G. I., John, R. M., & Isles, A. R. (2018). Territorial Behavior and Social Stability in the Mouse Require Correct Expression of Imprinted Cdkn1c. *Frontiers in Behavioral Neuroscience*, *12*(28). https://doi.org/10.3389/fnbeh.2018.00028

Menheniott, T. R., Woodfine, K., Schulz, R., Wood, A. J., Monk, D., Giraud, A. S., … Oakey, R. J. (2008). Genomic Imprinting of Dopa decarboxylase in Heart and Reciprocal Allelic Expression with Neighboring Grb10. *Molecular and Cellular Biology*. https://doi.org/10.1128/MCB.00862-07

Miyoshi, N., Kuroiwa, Y., Kohda, T., Shitara, H., Yonekawa, H., Kawabe, T., … Ishino, F. (1998). Identification of the Meg1/Grb10 imprinted gene on mouse proximal chromosome 11, a candidate for the Silver-Russell syndrome gene. *Proceedings of the National Academy of Sciences of the United States of America*, *95*(3), 1102–1107. Retrieved from http://www.pnas.org/content/95/3/1102

Moloney, R. D., Dinan, T. G., & Cryan, J. F. (2015). Strain-dependent variations in visceral sensitivity: Relationship to stress, anxiety and spinal glutamate transporter expression. *Genes, Brain and Behavior*. https://doi.org/10.1111/gbb.12216

Monk, D., Arnaud, P., Frost, J., Hills, F. A., Stanier, P., Feil, R., & Moore, G. E. (2009). Reciprocal imprinting of human GRB10 in placental trophoblast and brain: Evolutionary conservation of reversed allelic expression. *Human Molecular Genetics*, *18*(16), 3066–3074. https://doi.org/10.1093/hmg/ddp248

Monk, D., Smith, R., Arnaud, P., Preece, M. A., Stanier, P., Beechey, C. V., … Moore, G. E. (2003). Imprinted methylation profiles for proximal mouse Chromosomes 11 and 7 as revealed by methylation-sensitive representational difference analysis. *Mammalian Genome*, *14*(12), 805–816. https://doi.org/10.1007/s00335-003-2287-7

Morrione, A., Valentinis, B., Resnicoff, M., Xu, S., & Baserga, R. (1997). The role of mGrb10alpha in insulin-like growth factor I-mediated growth. *Biological Chemistry*, *272*(42), 26382–26387.

Mulherkar, S. A., & Jana, N. R. (2010). Loss of dopaminergic neurons and resulting behavioural deficits in mouse model of Angelman syndrome. *Neurobiology of Disease*, *40*(3), 586–592. https://doi.org/10.1016/j.nbd.2010.08.002

Müller, A. E., & Thalmann, U. (2000). Origin and evolution of primate social organisation: a reconstruction. *Biological Reviews of the Cambridge*

Philosophical Society, *75*(3), 405–435. https://doi.org/10.1111/j.1469-185X.2000.tb00050.x

Müller, J., Hart, C. M., Francis, N. J., Vargas, M. L., Sengupta, A., Wild, B., … Simon, J. A. (2002). Histone methyltransferase activity of a Drosophila Polycomb group repressor complex. *Cell*, *111*(2), 197–208. https://doi.org/10.1016/S0092-8674(02)00976-5

Nagano, T., Mitchell, J. A., Sanz, L. A., Pauler, F. M., Ferguson-Smith, A. C., Feil, R., & Fraser, P. (2008). The Air Noncoding RNA Epigenetically Silences Transcription by Targeting G9a to Chromatin. *Science*, *322*(5908), 1717–1720. https://doi.org/10.1126/science.1163802

Nakamura, T., Arai, Y., Umehara, H., Masuhara, M., Kimura, T., Taniguchi, H., … Nakano, T. (2007). PGC7/Stella protects against DNA demethylation in early embryogenesis. *Nature Cell Biology*, *9*(1), 64–71. https://doi.org/10.1038/ncb1519

Nantel, A., Mohammad-Ali, K., Sherk, J., Posner, B. I., & Thomas, D. Y. (1998). Interaction of the Grb10 adapter protein with the Raf1 and MEK1 kinases. *Journal of Biological Chemistry*, *273*(17), 10475–10484. https://doi.org/10.1074/jbc.273.17.10475

Ohlsson, R., Renkawitz, R., & Lobanenkov, V. (2001). CTCF is a uniquely versatile transcription regulator linked to epigenetics and disease. *Trends in Genetics*, *17*(9), 520–527. https://doi.org/10.1016/S0168-9525(01)02366-6

Ooi, J., Yajnik, V., Immanuel, D., Gordon, M., Moskow, J. J., Buchberg, A. M., & Margolis, B. (1995). The cloning of Grb10 reveals a new family of SH2 domain proteins. *Oncogene*, *10*(8), 1621–1630. Retrieved from http://www.ncbi.nlm.nih.gov/pubmed/7731717

Orr, H. A. (1995). Somatic mutation favors the evolution of diploidy. *Genetics*, *139*(3), 1441–1447.

Pauler, F. M., Stricker, S. H., Warczok, K. E., & Barlow, D. P. (2005). Long-range DNase I hypersensitivity mapping reveals the imprinted Igf2r and Air promoters share cis-regulatory elements. *Genome Research*, *15*(10), 1379–8. https://doi.org/10.1101/gr.3783805

Pellow, S., Chopin, P., File, S. E., & Briley, M. (1985). Validation of open:closed arm entries in an elevated plus-maze as a measure of anxiety in the rat. *Journal of Neuroscience Methods*, *14*(3), 149–167. https://doi.org/10.1016/0165-0270(85)90031-7

Perez-Pinera, P., Kocak, D. D., Vockley, C. M., Adler, A. F., Kabadi, A. M., Polstein, L. R., … Gersbach, C. A. (2013). RNA-guided gene activation by CRISPR-Cas9-based transcription factors. *Nature Methods*, *10*(10), 973–976. https://doi.org/10.1038/nmeth.2600

Perez, J. D., Rubinstein, N. D., & Dulac, C. (2016). New Perspectives on Genomic Imprinting, an Essential and Multifaceted Mode of Epigenetic Control in the Developing and Adult Brain. *Annual Review of Neuroscience*, *39*, 347–384. https://doi.org/10.1146/annurev-neuro-061010-113708

Plagge, A., Isles, A. R., Gordon, E., Humby, T., Dean, W., Gritsch, S., … Kelsey, G. (2005). Imprinted Nesp55 influences behavioral reactivity to novel

environments. *Molecular and Cellular Biology*, *25*(8), 3019–3026. https://doi.org/10.1128/MCB.25.8.3019-3026.2005
Plasschaert, R. N., & Bartolomei, M. S. (2015). Tissue-specific regulation and function of Grb10 during growth and neuronal commitment. *PNAS*, *112*(22), 6841–6847. https://doi.org/10.1073/pnas.1411254111
Qu, C., Ligneul, R., Van der Henst, J. B., & Dreher, J. C. (2017). An Integrative Interdisciplinary Perspective on Social Dominance Hierarchies. *Trends in Cognitive Sciences*, *21*(11), 893–908. https://doi.org/10.1016/j.tics.2017.08.004
Quenneville, S., Verde, G., Corsinotti, A., Kapopoulou, A., Jakobsson, J., Offner, S., … Trono, D. (2011). In embryonic stem cells, ZFP57/KAP1 recognize a methylated hexanucleotide to affect chromatin and DNA methylation of imprinting control regions. *Molecular Cell*, *44*(3), 361–372. https://doi.org/10.1016/j.molcel.2011.08.032
Ralls, K. (1971). Mammalian Scent Marking. *Science*, *171*(3970), 443–449. https://doi.org/10.1126/science.171.3970.443
Regha, K., Sloane, M. A., Huang, R., Pauler, F. M., Warczok, K. E., Melikant, B., … Barlow, D. P. (2007). Active and Repressive Chromatin Are Interspersed without Spreading in an Imprinted Gene Cluster in the Mammalian Genome. *Molecular Cell*, *27*(3), 353–366. https://doi.org/10.1016/j.molcel.2007.06.024
Reichel, J. M., Bedenk, B. T., Gassen, N. C., Hafner, K., Bura, S. A., Almeida-Correa, S., … Wotjak, C. T. (2016). Beware of your Cre-Ation: lacZ expression impairs neuronal integrity and hippocampus-dependent memory. *Hippocampus*, *26*(10), 1250–1264. https://doi.org/10.1002/hipo.22601
Reik, W. (2007). Stability and flexibility of epigenetic gene regulation in mammalian development. *Nature*, *447*(7143), 425–432. https://doi.org/10.1038/nature05918
Rienecker, K. D. A., Hill, M. J., & Isles, A. R. (2016). Methods of epigenome editing for probing the function of genomic imprinting. *Epigenomics*, *8*(10), 1389–1398. https://doi.org/10.2217/epi-2016-0073
Russo, V. C., Gluckman, P. D., Feldman, E. L., & Werther, G. A. (2005). The insulin-like growth factor system and its pleiotropic functions in brain. *Endocrine Reviews*, *26*(7), 916–943. https://doi.org/10.1210/er.2004-0024
Saavedra-Rodríguez, L., & Feig, L. A. (2013). Chronic social instability induces anxiety and defective social interactions across generations. *Biological Psychiatry*, *73*(1), 44–53. https://doi.org/10.1016/j.biopsych.2012.06.035
Sandel, A. A., Miller, J. A., Mitani, J. C., Nunn, C. L., Patterson, S. K., & Garamszegi, L. Z. (2016). Assessing sources of error in comparative analyses of primate behavior: Intraspecific variation in group size and the social brain hypothesis. *Journal of Human Evolution*, *94*, 126–133. https://doi.org/10.1016/j.jhevol.2016.03.007
Sanz, L. A., Chamberlain, S., Sabourin, J.-C., Henckel, A., Magnuson, T., Hugnot, J.-P., … Arnaud, P. (2008). A mono-allelic bivalent chromatin

domain controls tissue-specific imprinting at Grb10. *The EMBO Journal*, *27*(19), 2523–2532. https://doi.org/10.1038/emboj.2008.142
Schmitz, C., Eastwood, B. S., Tappan, S. J., Glaser, J. R., Peterson, D. A., & Hof, P. R. (2014). Current automated 3D cell detection methods are not a suitable replacement for manual stereologic cell counting. *Frontiers in Neuroanatomy*, *8*(27). https://doi.org/10.3389/fnana.2014.00027
Schonberg, T., Fox, C. R., & Poldrack, R. A. (2011). Mind the gap: Bridging economic and naturalistic risk-taking with cognitive neuroscience. *Trends in Cognitive Sciences*, *15*(1), 11–19. https://doi.org/10.1016/j.tics.2010.10.002
Schubert, M., Brazil, D. P., Burks, D. J., Kushner, J. a, Ye, J., Flint, C. L., … White, M. F. (2003). Insulin receptor substrate-2 deficiency impairs brain growth and promotes tau phosphorylation. *The Journal of Neuroscience : The Official Journal of the Society for Neuroscience*, *23*(18), 7084–7092. https://doi.org/23/18/7084 [pii]
Seuss, D. (1955). *On Beyond Zebra*. New York: Random House.
Sferruzzi-Perri, A. N., Owens, J. A., Standen, P., & Roberts, C. T. (2008). Maternal Insulin-like Growth Factor-II Promotes Placental Functional Development Via the Type 2 IGF Receptor in the Guinea Pig. *Placenta*, *29*(4), 347–355. https://doi.org/10.1016/j.placenta.2008.01.009
Shiura, H., Miyoshi, N., Konishi, A., Wakisaka-Saito, N., Suzuki, R., Muguruma, K., … Kaneko-Ishino, T. (2005). Meg1/Grb10 overexpression causes postnatal growth retardation and insulin resistance via negative modulation of the IGF1R and IR cascades. *Biochemical and Biophysical Research Communications*, *329*(3), 909–916. https://doi.org/10.1016/j.bbrc.2005.02.047
Shiura, H., Nakamura, K., Hikichi, T., Hino, T., Oda, K., Suzuki-Migishima, R., … Ishino, F. (2009). Paternal deletion of Meg1/Grb10 DMR causes maternalization of the Meg1/ Grb10 cluster in mouse proximal Chromosome 11 leading to severe pre- and postnatal growth retardation. *Human Molecular Genetics*, *18*(8), 1424–1438. https://doi.org/10.1093/hmg/ddp049
Singleton, G. R., & Krebs, C. J. (2007). The Secret World of Wild Mice. In J. G. Fox, F. W. Quimby, C. E. Newcomer, M. T. Davisson, S. W. Barthold, & A. L. Smith (Eds.), *The Mouse in Biomedical Research* (2nd Edition, pp. 25–51). Elsevier Inc. https://doi.org/10.1016/B978-012369454-6/50015-7
Siuda, D., Wu, Z., Chen, Y., Guo, L., Linke, M., Zechner, U., … Li, H. (2014). Social isolation-induced epigenetic changes in midbrain of adult mice. *Journal of Physiology and Pharmacology*, *65*(2), 247–255.
Smallwood, S. A., & Kelsey, G. (2012). De novo DNA methylation: A germ cell perspective. *Trends in Genetics*, *28*(1), 33–42. https://doi.org/10.1016/j.tig.2011.09.004
Smith, E. Y., Futtner, C. R., Chamberlain, S. J., Johnstone, K. A., & Resnick, J. L. (2011). Transcription is required to establish maternal imprinting at the Prader-Willi syndrome and Angelman syndrome locus. *PLoS Genetics*, *7*(12), e1002422. https://doi.org/10.1371/journal.pgen.1002422
Smith, F. M., Holt, L. J., Garfield, A. S., Charalambous, M., Koumanov, F.,

Perry, M., … Ward, A. (2007). Mice with a Disruption of the Imprinted Grb10 Gene Exhibit Altered Body Composition, Glucose Homeostasis, and Insulin Signaling during Postnatal Life. *Molecular and Cellular Biology*, *27*(16), 5871–5886. https://doi.org/10.1128/MCB.02087-06

Stanford, M. S., Houston, R. J., Mathias, C. W., Villemarette-Pittman, N. R., Helfritz, L. E., & Conklin, S. M. (2003). Characterizing aggressive behavior. *Assessment*, *10*(2), 183–190. https://doi.org/10.1177/1073191103010002009

Stein, E. G., Ghirlando, R., & Hubbard, S. R. (2003). Structural basis for dimerization of the Grb10 Src homology 2 domain: Implications for ligand specificity. *Journal of Biological Chemistry*, *278*(15), 13257–13264. https://doi.org/10.1074/jbc.M212026200

Strozik, E., & Festing, M. F. W. (1981). Whisker trimming in mice. *Laboratory Animals*, *15*(4), 309–312. https://doi.org/10.1258/002367781780953040

Suetake, I., Shinozaki, F., Miyagawa, J., Takeshima, H., & Tajima, S. (2004). DNMT3L stimulates the DNA methylation activity of Dnmt3a and Dnmt3b through a direct interaction. *Journal of Biological Chemistry*, *279*(26), 27816–27823. https://doi.org/10.1074/jbc.M400181200

Surani, M. A. (1998). Imprinting and the Initiation of Gene Silencing in the Germ Line. *Cell*, *93*(3), 309–312. https://doi.org/10.1016/S0092-8674(00)81156-3

Surani, M. A. (2001). Reprogramming of genome function through epigenetic inheritance. *Nature*, *414*(6859), 122–128. https://doi.org/10.1038/35102186

Surani, M. A. H., & Barton, S. C. (1983). Development of gynogenetic eggs in the mouse: Implications for parthenogenetic embryos. *Science*, *222*(4627), 1034–1036. https://doi.org/10.1126/science.6648518

Tahiliani, M., Koh, K. P., Shen, Y., Pastor, W. A., Bandukwala, H., Brudno, Y., … Rao, A. (2009). Conversion of 5-methylcytosine to 5-hydroxymethylcytosine in mammalian DNA by MLL partner TET1. *Science*, *324*(5929), 930–935. https://doi.org/10.1126/science.1170116

Trivers, R. L. (1974). Parent-offspring conflict. *Integrative and Comparative Biology*, *14*(1), 249–264. https://doi.org/10.1093/icb/14.1.249

Tury, A., Mairet-Coello, G., & Dicicco-Bloom, E. (2011). The cyclin-dependent kinase inhibitor p57Kip2 regulates cell cycle exit, differentiation, and migration of embryonic cerebral cortical precursors. *Cerebral Cortex*, *21*(8), 1840–1856. https://doi.org/10.1093/cercor/bhq254

Úbeda, F., & Gardner, A. (2010). A model for genomic imprinting in the social brain: Juveniles. *Evolution*, *64*(9), 2587–2600. https://doi.org/10.1111/j.1558-5646.2010.01015.x

Úbeda, F., & Gardner, A. (2011). A model for genomic imprinting in the social brain: Adults. *Evolution*, *65*(2), 462–475. https://doi.org/10.1111/j.1558-5646.2010.01115.x

Valzelli, L., & Bernasconi, S. (1979). Aggressiveness by isolation and brain serotonin turnover changes in different strains of mice. *Neuropsychobiology*, *5*(3), 129–135. https://doi.org/10.1159/000117674

van den Berg, W. E., Lamballais, S., & Kushner, S. A. (2015). Sex-Specific

Mechanism of Social Hierarchy in Mice. *Neuropsychopharmacology*. https://doi.org/10.1038/npp.2014.319

van der Kooij, M. A., Hollis, F., Lozano, L., Zalachoras, I., Abad, S., Zanoletti, O., … Sandi, C. (2018). Diazepam actions in the VTA enhance social dominance and mitochondrial function in the nucleus accumbens by activation of dopamine D1 receptors. *Molecular Psychiatry*, *23*(3), 569–578. https://doi.org/10.1038/mp.2017.135

van der Vlag, J., & Otte, A. P. (1999). Transcriptional repression mediated by the human polycomb-group protein EED involves histone deacetylation. *Nature Genetics*, *23*(4), 474–478. https://doi.org/10.1038/70602

Vecchione, A., Marchese, A., Henry, P., Rotin, D., & Morrione, A. (2003). The Grb10/Nedd4 Complex Regulates Ligand-Induced Ubiquitination and Stability of the Insulin-Like Growth Factor I Receptor. *Molecular and Cellular Biology*, *23*(9), 3363–3372. https://doi.org/10.1128/MCB.23.9.3363–3372.2003

Vojta, A., Dobrinic, P., Tadic, V., Bocˇkor, L., Korac, P., Julg, B., … Zoldos, V. (2016). Repurposing the CRISPR-Cas9 system for targeted DNA methylation. *Nucleic Acids Research*, *44*(12), 5615–5628. https://doi.org/10.1093/nar/gkw159

Walf, A. A., & Frye, C. A. (2007). The use of the elevated plus maze as an assay of anxiety-related behavior in rodents. *Nature Protocols*, *2*(2), 322–328. https://doi.org/10.1038/nprot.2007.44

Wang, F., Kessels, H. W., & Hu, H. (2014). The mouse that roared: Neural mechanisms of social hierarchy. *Trends in Neurosciences*, *37*(11), 674–682. https://doi.org/10.1016/j.tins.2014.07.005

Wang, F., Zhu, J., Zhu, H., Zhang, Q., Lin, Z., & Hu, H. (2011). Bidirectional control of social hierarchy by synaptic efficacy in medial prefrontal cortex. *Science (New York, N.Y.)*, *334*(6056), 693–697. https://doi.org/10.1126/science.1209951

Wang, J., Dai, H., Yousaf, N., Moussaif, M., Deng, Y., Boufelliga, A., … Riedel, H. (1999). Grb10, a positive, stimulatory signaling adapter in platelet-derived growth factor BB-, insulin-like growth factor I-, and insulin-mediated mitogenesis. *Molecular and Cellular Biology*, *19*(9), 6217–6228. https://doi.org/10.1128/MCB.19.9.6217

Watson, F. M. C., Henry, J. P., & Haltmeyer, G. C. (1974). Effects of Early Experience on Emotional and Social Reactivity in CBA Mice. *Physiology and Behavior*, *13*(1), 9–14.

Werner, H., & LeRoith, D. (2014). Insulin and insulin-like growth factor receptors in the brain: Physiological and pathological aspects. *European Neuropsychopharmacology : The Journal of the European College of Neuropsychopharmacology*, *24*(12), 1947–1953. https://doi.org/10.1016/j.euroneuro.2014.01.020

Westbury, J., Watkins, M., Ferguson-Smith, A. C., & Smith, J. (2001). Dynamic temporal and spatial regulation of the cdk inhibitor p57kip2 during embryo morphogenesis. *Mechanisms of Development*, *109*(1), 83–89. https://doi.org/10.1016/S0925-4773(01)00512-3

Wick, K. R., Werner, E. D., Langlais P, Ramos, F. J., Dong, L. Q., Shoelson, S. E.,

& Liu, F. (2003). Grb10 inhibits insulin-stimulated insulin receptor substrate (IRS)-phosphatidylinositol 3–kinase/Akt signaling pathway by disrupting the association of IRS–1/IRS–2 with the insulin receptor. *The Journal of Biological Chemistry*, *278*(10), 8460–8467. https://doi.org/10.1074/jbc.M208518200

Wilkins, J. F. (2013). Phenotypic plasticity, pleiotropy, and the growth-first theory of imprinting. In R. Jirtle & F. Tyson (Eds.), *Environmental Epigenomics in Health and Disease* (pp. 57–72). New York: Springer, Berlin, Heidelberg. https://doi.org/10.1007/978-3-642-36827-1_4

Wilkins, J. F., & Haig, D. (2003). What good is genomic imprinting: The function of parent-specific gene expression. *Nature Reviews Genetics*, *4*(5), 359–368. https://doi.org/10.1038/nrg1062

Williamson, C., Blake, A., Thomas, S., Beechey, C., Hancock, J., Cattanach, B., & Peters, J. (2013). Mouse Imprinting Data and References. Retrieved September 7, 2018, from http://www.har.mrc.ac.uk/research/genomic_imprinting/

Wolf, J. B., & Hager, R. (2006). A maternal-offspring coadaptation theory for the evolution of genomic imprinting. *PLoS Biology*, *4*(12), e380. https://doi.org/10.1371/journal.pbio.0040380

Wood, A. J., & Oakey, R. J. (2006). Genomic imprinting in mammals: Emerging themes and established theories. *PLoS Genetics*, *2*(11), 1677–1685. https://doi.org/10.1371/journal.pgen.0020147

Wood, A. J., Schulz, R., Woodfine, K., Koltowska, K., Beechey, C., Peters, J., … Oakey, R. (2008). Regulation of alternative polyadenylation by genomic imprinting. *Genes Dev*, *22*(9), 1141–1146. https://doi.org/10.1101/gad.473408

Wood, J., LaPalombara, Z., & Ahmari, S. E. (2018). Monoamine abnormalities in the SAPAP3 knockout model of obsessive-compulsive disorder-related behaviour. *Philosophical Transactions of the Royal Society B: Biological Sciences*, *373*(1742). https://doi.org/10.1098/rstb.2017.0023

Woodfine, K., Huddleston, J. E., & Murrell, A. (2011). Quantitative analysis of DNA methylation at all human imprinted regions reveals preservation of epigenetic stability in adult somatic tissue. *Epigenetics and Chromatin*, *4*(1), 1. https://doi.org/10.1186/1756-8935-4-1

Wossidlo, M., Nakamura, T., Lepikhov, K., Marques, C. J., Zakhartchenko, V., Boiani, M., … Walter, J. (2011). 5-Hydroxymethylcytosine in the mammalian zygote is linked with epigenetic reprogramming. *Nature Communications*, *2*(241). https://doi.org/10.1038/ncomms1240

Xu, S., Das, G., Hueske, E., & Tonegawa, S. (2017). Dorsal Raphe Serotonergic Neurons Control Intertemporal Choice under Trade-off. *Current Biology*, *27*(20), 3111–3119.e3. https://doi.org/10.1016/j.cub.2017.09.008

Yamasaki-Ishizaki, Y., Kayashima, T., Mapendano, C. K., Soejima, H., Ohta, T., Masuzaki, H., … Kishino, T. (2007). Role of DNA methylation and histone H3 lysine 27 methylation in tissue-specific imprinting of mouse Grb10. *Molecular and Cellular Biology*, *27*(2), 732–742. https://doi.org/10.1128/MCB.01329-06

Yan, X., Himburg, H. A., Pohl, K., Quarmyne, M., Tran, E., Zhang, Y., … Chute, J.

P. (2016). Deletion of the Imprinted Gene Grb10 Promotes Hematopoietic Stem Cell Self-Renewal and Regeneration. *Cell Reports*, *17*(6), 1584–1594. https://doi.org/10.1016/j.celrep.2016.10.025

Yin, Q. F., Yang, L., Zhang, Y., Xiang, J. F., Wu, Y. W., Carmichael, G. G., & Chen, L. L. (2012). Long Noncoding RNAs with snoRNA Ends. *Molecular Cell*, *48*(2), 219–230. https://doi.org/10.1016/j.molcel.2012.07.033

Zhang, Y., Jurkowska, R., Soeroes, S., Rajavelu, A., Dhayalan, A., Bock, I., … Jeltsch, A. (2010). Chromatin methylation activity of Dnmt3a and Dnmt3a/3L is guided by interaction of the ADD domain with the histone H3 tail. *Nucleic Acids Research*, *38*(13), 4246–4253. https://doi.org/10.1093/nar/gkq147

Zhou, T., Zhu, H., Fan, Z., Wang, F., Chen, Y., Liang, H., … Hu, H. (2017). History of winning remodels thalamo-PFC circuit to reinforce social dominance. *Science*, *357*(6347), 162–168. https://doi.org/10.1126/science.aak9726

11 Appendix I–Histology

11.1 FDR Corrections–Brain and Body Weight

Variable	P value	Rank (m = 67)	B-L: (min, 0.05, 0.05*(m/(m+1-i)^2)	Difference
BW Simple Main Effect of AGE (AGE*GENOTYPE)–WT	6.16E-32	1	7.46E-04	7.46E-04
BW Simple Main Effect of AGE (AGE*GENOTYPE)–*Grb10+/p*	1.21E-30	2	7.69E-04	7.69E-04
BW Simple Main Effect of AGE (AGE*GENOTYPE)–*Grb10+/p* 305-325 vs 75-95	2.28E-30	3	7.93E-04	7.93E-04
BW Simple Main Effect of AGE (AGE*GENOTYPE)–WT 305-325 vs 75-95	1.91E-28	4	8.18E-04	8.18E-04
BW Simple Main Effect of SEX (GENOTYPE*SEX)–*Grb10+/p*	1.68E-23	5	8.44E-04	8.44E-04
BW Simple Main Effect of SEX (GENOTYPE*SEX)–WT	2.90E-23	6	8.71E-04	8.71E-04
BW Simple Main Effect of AGE (AGE*GENOTYPE)–WT 185-205 vs 75-95	1.15E-20	7	9.00E-04	9.00E-04
BW Simple Main Effect of AGE (AGE*GENOTYPE)–*Grb10+/p* 185-205 vs 75-95	6.05E-14	8	9.31E-04	9.31E-04
WWB Simple Main Effect of GENOTYPE–305 to 325 Days	1.14E-10	9	9.62E-04	9.62E-04
BW Simple Main Effect of AGE (AGE*GENOTYPE)–	8.15E-09	10	9.96E-04	9.96E-04

***Grb10+/p* 305-325 vs 185-205**				
WWB Simple Main Effect of GENOTYPE–305 to 325 Days WT vs *Grb10+/p*	1.02E-08	11	1.03E-03	1.03E-03
WWB Simple Main Effect of GENOTYPE–75 to 95 Days WT vs *Grb10+/p*	2.20E-08	12	1.07E-03	1.07E-03
WWB Simple Main Effect of GENOTYPE–75 to 95 Days	5.27E-08	13	1.11E-03	1.11E-03
WWB Simple Main Effect of AGE–WT 185-205 vs 75-95	8.20E-08	14	1.15E-03	1.15E-03
WWB Simple Main Effect of AGE–Wildtype	1.18E-07	15	1.19E-03	1.19E-03
WWB Simple Main Effect of GENOTYPE–305 to 325 Days *Grb10+/p* vs *Grb10+/m*	2.00E-06	16	1.24E-03	1.24E-03
WWB Simple Main Effect of AGE–*Grb10+/m* 305-325 vs 185-205	0.000117	17	1.29E-03	1.17E-03
BW Simple Main Effect of AGE (AGE*GENOTYPE)–*Grb10+/m* 305-325 vs 75-95	0.000126	18	1.34E-03	1.21E-03
WWB Simple Main Effect of AGE–*Grb10+/m*	0.000128	19	1.40E-03	1.27E-03
BW Simple Main Effect of AGE (AGE*GENOTYPE)–*Grb10+/m*	0.000151	20	1.45E-03	1.30E-03
BW Simple Main Effect of SEX (GENOTYPE*SEX)–*Grb10+/m*	0.000772	21	1.52E-03	7.45E-04
BW Simple Main Effect of AGE (AGE*GENOTYPE)–*Grb10+/m* 305-325 vs 185-205	0.000934	22	1.58E-03	6.49E-04

Whole Wet Brain Weight AGE*GENOTYPE	0.001129	23	1.65E-03	5.25E-04
WWB Simple Main Effect of AGE–WT 305-325 vs 185-205	1.16E-03	24	1.73E-03	5.70E-04
WWB Simple Main Effect of GENOTYPE–185 to 205 Days WT vs *Grb10+/p*	0.002458	25	1.81E-03	-6.46E-04
Body Weight AGE*GENOTYPE	0.002832	26	1.90E-03	-9.33E-04
WWB Simple Main Effect of GENOTYPE–185 to 205 Days	0.003339	27	1.99E-03	-1.35E-03
BW Simple Main Effect of AGE (AGE*GENOTYPE)–WT 305-325 vs 185-205	3.77E-03	28	2.09E-03	-1.68E-03
WWB Simple Main Effect of AGE–*Grb10+/p*	0.006944	29	2.20E-03	-4.74E-03
BW Simple Main Effect of GENOTYPE (AGE*GENOTYPE)–75 to 95 days *Grb10+/p* vs *Grb10+/m*	0.01071	30	2.32E-03	-8.39E-03
BW Simple Main Effect of GENOTYPE (AGE*GENOTYPE)–75 to 95 days	0.011611	31	2.45E-03	-9.16E-03
BW Simple Main Effect of GENOTYPE (AGE*GENOTYPE)–75 to 95 days WT vs *Grb10+/m*	0.014738	32	2.58E-03	-1.22E-02
WWB Simple Main Effect of AGE–*Grb10+/p* 305-325 vs 75-95	0.020392	33	2.73E-03	-1.77E-02
WWB Simple Main Effect of AGE–*Grb10+/p* 185-205 vs 75-95	0.024467	34	2.90E-03	-2.16E-02
BW Simple Main Effect of GENOTYPE (AGE*GENOTYPE)–305 to 325 days	0.038096	35	3.08E-03	-3.50E-02
Body Weight GENOTYPE*SEX	0.045077	36	3.27E-03	-4.18E-02

WWB Simple Main Effect of AGE–*Grb10+/m* 305-325 vs 75-95	**0.061445**	**37**	**3.49E-03**	**-5.80E-02**
WWB Simple Main Effect of AGE–*Grb10+/m* 185-205 vs 75-95	0.071873	38	3.72E-03	-6.82E-02
BW Simple Main Effect of GENOTYPE (AGE*GENOTYPE)–305 to 325 days WT vs *Grb10+/p*	0.074587	39	3.98E-03	-7.06E-02
WWB Simple Main Effect of GENOTYPE–305 to 325 Days WT vs *Grb10+/m*	0.0823	40	4.27E-03	-7.80E-02
Body Weight AGE*SEX	0.104772	41	4.60E-03	-1.00E-01
BW Simple Main Effect of GENOTYPE (GENOTYPE*SEX)–Males	0.178664	42	4.96E-03	-1.74E-01
BW Simple Main Effect of GENOTYPE (AGE*GENOTYPE)–185 to 205 days	0.204054	43	5.36E-03	-1.99E-01
WWB Simple Main Effect of GENOTYPE–75 to 95 Days *Grb10+/p*vs *Grb10+/m*	2.21E-01	44	5.82E-03	-2.15E-01
BW Simple Main Effect of GENOTYPE (AGE*GENOTYPE)–305 to 325 days WT vs *Grb10+/m*	0.289071	45	6.33E-03	-2.83E-01
BW Simple Main Effect of GENOTYPE (AGE*GENOTYPE)–185 to 205 days WT vs *Grb10+/m*	0.319114	46	6.92E-03	-3.12E-01
BW Simple Main Effect of GENOTYPE (GENOTYPE*SEX)–Males *Grb10+/p* vs *Grb10+/m*	0.355957	47	7.60E-03	-3.48E-01
Whole Wet Brain Weight GENOTYPE*SEX	0.382169	48	8.38E-03	-3.74E-01
BW Simple Main Effect of GENOTYPE (GENOTYPE*SEX)–Males WT vs *Grb10+/p*	0.406012	49	9.28E-03	-3.97E-01

WWB Simple Main Effect of GENOTYPE–75 to 95 Days WT vs *Grb10+/m*	4.10E-01	50	1.03E-02	-4.00E-01
Whole Wet Brain Weight AGE*SEX	0.456258	51	1.16E-02	-4.45E-01
WWB Simple Main Effect of AGE–WT 305-325 vs 75-95	4.60E-01	52	1.31E-02	-4.47E-01
WWB Simple Main Effect of GENOTYPE–185 to 205 Days WT vs *Grb10+/m*	0.460367	53	1.49E-02	-4.45E-01
Whole Wet Brain Weight AGE*GENOTYPE*SEX	0.625821	54	1.71E-02	-6.09E-01
BW Simple Main Effect of GENOTYPE (AGE*GENOTYPE)–185 to 205 days WT vs *Grb10+/p*	0.686636	55	1.98E-02	-6.67E-01
BW Simple Main Effect of GENOTYPE (GENOTYPE*SEX)–Females	0.722393	56	2.33E-02	-6.99E-01
Body Weight AGE*GENOTYPE*SEX	0.896875	57	2.77E-02	-8.69E-01
WWB Simple Main Effect of AGE–*Grb10+/p* 305-325 vs 185-205	1	58	3.35E-02	-9.67E-01
WWB Simple Main Effect of GENOTYPE–185 to 205 Days *Grb10+/p* vs *Grb10+/m*	1	59	4.14E-02	-9.59E-01
BW Simple Main Effect of GENOTYPE (GENOTYPE*SEX)–Females WT vs *Grb10+/p*	1	60	5.00E-02	-9.50E-01
BW Simple Main Effect of GENOTYPE (GENOTYPE*SEX)–Females WT vs *Grb10+/m*	1	61	5.00E-02	-9.50E-01
BW Simple Main Effect of GENOTYPE (GENOTYPE*SEX)–Females *Grb10+/p* vs *Grb10+/m*	1	62	5.00E-02	-9.50E-01

BW Simple Main Effect of GENOTYPE (GENOTYPE*SEX)–Males WT vs *Grb10+/m*	1	63	5.00E-02	-9.50E-01
BW Simple Main Effect of AGE (AGE*GENOTYPE)–*Grb10+/m* 185-205 vs 75-95	1	64	5.00E-02	-9.50E-01
BW Simple Main Effect of GENOTYPE (AGE*GENOTYPE)–305 to 325 days *Grb10+/p*vs *Grb10+/m*	1	65	5.00E-02	-9.50E-01
BW Simple Main Effect of GENOTYPE (AGE*GENOTYPE)–185 to 205 days *Grb10+/p* vs *Grb10+/m*	1	66	5.00E-02	-9.50E-01
BW Simple Main Effect of GENOTYPE (AGE*GENOTYPE)–75 to 95 days WT vs *Grb10+/p*	1	67	5.00E-02	-9.50E-01

Ventricles–Alternative Analysis

The assumption of homogeneity of error variances was violated for ventricle area (Levene's test $p < 0.001$). Therefore, we performed alternative analyses to attempt to circumvent the violation. Two way ANOVAs for GENOTYPE and AGE violated the assumption of homogeneity of variance for both males and females. Two way ANOVAs for GENOTYPE and SEX satisfied the assumption of homogeneity of variance for data at 10 weeks and 6 months, but not 10 months. There were no significant interactions or main effects for two-way ANOVAs for GENOTYPE and SEX in any age bin. One-way ANOVAs for GENOTYPE satisfied the assumption, except for females at 10 months ($p = 0.020$) and males at 6 months ($p = 0.021$). These two exceptions were analyzed with Welch's ANOVA. There were no significant main effects of GENOTYPE for these one-way ANOVAs. All one-way ANOVAs for AGE satisfied the assumption of homogeneity of variance. Only *Grb10*$^{+/m}$ males had a significant main effect of AGE, $F(2,6) = 6.022$, $p = 0.037$, partial $\eta^2 = 0.667$. Ventricle area at 10 months (1.083 ± 0.159 mm^2) was significantly larger than at 10 weeks (0.211 ± 0.195 mm^2), mean difference 0.872 (95%CI 0.045 to 1.699) mm^2, $p = 0.040$.

11.3 FDR Corrections–Nissl Bregma 0.74 mm

Variable	P value	Rank (m = 48)	B-L: (min, 0.05, 0.05*(m/(m+1-i)^2)	Difference
Caudate Putamen AGE	9.58E-07	1	1.042E-03	1.041E-03
Caudate Putamen (AGE) 10 mo vs 10 wks	3.000E-06	2	1.086E-03	1.083E-03
Caudate Putamen (AGE) 6 mo vs 10 wks	1.200E-05	3	1.134E-03	1.122E-03
Subcortical (AGE) 10 mo vs 10 wks	2.210E-04	4	1.185E-03	9.642E-04
Subcortical AGE	3.280E-04	5	1.240E-03	9.117E-04
Ventricles AGE	3.740E-04	6	1.298E-03	9.240E-04
Ventricles (AGE) 10 mo vs 10 wks	4.940E-04	7	1.361E-03	8.665E-04
Cortical (SEX*AGE) SEX 6 mo	2.933E-03	8	1.428E-03	-1.505E-03
Ventricles (AGE) 10 mo vs 6 mo	6.726E-03	9	1.500E-03	-5.226E-03
Whole Brain AGE– 10 mo vs 10 wks	0.011311	10	1.578E-03	-9.733E-03
Whole Brain AGE	0.013896	11	1.662E-03	-1.223E-02
Cortical SEX*AGE	0.046741	12	1.753E-03	-4.499E-02
Subcortical (AGE) 10 mo vs 6 mo	0.047065	13	1.852E-03	-4.521E-02
Whole Brain SEX*AGE	**0.063156**	**14**	**1.959E-03**	**-6.120E-02**
Caudate Putamen SEX	0.064025	15	2.076E-03	-6.195E-02
Whole Brain SEX	0.08142	16	2.204E-03	-7.922E-02
Cortical GENOTYPE*SEX	0.124284	17	2.344E-03	-1.219E-01
Subcortical (AGE) 6 mo vs 10 wks	0.127382	18	2.497E-03	-1.249E-01
Subcortical SEX*AGE	0.142289	19	2.667E-03	-1.396E-01
Cortical GENOTYPE*SEX*AGE	0.19677	20	2.854E-03	-1.939E-01
Subcortical SEX	0.20849	21	3.061E-03	-2.054E-01

Ventricles GENOTYPE*SEX	0.212328	22	3.292E-03	-2.090E-01
Cortical (SEX*AGE) SEX 10 mo	0.221294	23	3.550E-03	-2.177E-01
Whole Brain GENOTYPE*SEX	0.279459	24	3.840E-03	-2.756E-01
Whole Brain AGE– 10 mo vs 6 mo	0.291136	25	4.167E-03	-2.870E-01
Whole Brain GENOTYPE*SEX*AGE	0.310532	26	4.537E-03	-3.060E-01
Whole Brain GENOTYPE	0.337248	27	4.959E-03	-3.323E-01
Ventricles GENOTYPE*SEX*AGE	0.340388	28	5.442E-03	-3.349E-01
Subcortical GENOTYPE	0.35331	29	6.000E-03	-3.473E-01
Caudate Putamen SEX*AGE	0.354657	30	6.648E-03	-3.480E-01
Caudate Putamen GENOTYPE*AGE	0.396182	31	7.407E-03	-3.888E-01
Ventricles GENOTYPE*AGE	0.40783	32	8.304E-03	-3.995E-01
Whole Brain AGE– 6 mo vs 10 wks	0.420545	33	9.375E-03	-4.112E-01
Subcortical GENOTYPE*AGE	0.460692	34	1.067E-02	-4.500E-01
Subcortical GENOTYPE*SEX*AGE	0.492638	35	1.224E-02	-4.804E-01
Ventricles GENOTYPE	0.512247	36	1.420E-02	-4.980E-01
Cortical GENOTYPE	0.515709	37	1.667E-02	-4.990E-01
Subcortical GENOTYPE*SEX	0.527528	38	1.983E-02	-5.077E-01
Cortical (SEX*AGE) SEX 10 wks	0.539687	39	2.400E-02	-5.157E-01
Ventricles SEX*AGE	0.566957	40	2.963E-02	-5.373E-01
Whole Brain GENOTYPE*AGE	0.575725	41	3.750E-02	-5.382E-01
Ventricles SEX	0.583402	42	4.898E-02	-5.344E-01
Caudate Putamen GENOTYPE	0.618944	43	5.000E-02	-5.689E-01
Cortical GENOTYPE*AGE	0.646647	44	5.000E-02	-5.966E-01

Caudate Putamen GENOTYPE*SEX*AGE	0.705439	45	5.000E-02	-6.554E-01
Caudate Putamen GENOTYPE*SEX	0.792495	46	5.000E-02	-7.425E-01
Ventricles (AGE) 6 mo vs 10 wks	0.810802	47	5.000E-02	-7.608E-01
Caudate Putamen (AGE) 10 mo vs 6 mo	1	48	5.000E-02	-9.500E-01

12 Appendix II–Social Behaviour

12.1 FDR Corrections–Stranger Encounter Tube Test

Finding	P value	Rank (m=25)	BL = (min 0.05, 0.05*m/(m+1-i)^2	(BL) – P value
Stranger Tube Test 6 months–Barbered Female Mice	**4.181E-03**	**1**	**5.000E-03**	**0.001**
Stranger Tube Test 8-10 weeks–Males	0.087	2	6.173E-03	-0.081
Stranger Tube Test 6 months–Barbered Male Mice	0.180	3	7.813E-03	-0.172
Stranger Tube Test 8-10 weeks–Females	0.263	4	0.010	-0.253
Stranger Tube Test 10 months–Barbered Male Mice	0.359	5	0.014	-0.345
Stranger Tube Test 6 months–Females	0.383	6	0.020	-0.363
Stranger Tube Test 10 months–Males	0.678	7	0.031	-0.646
Stranger Tube Test 10 months–Barbered Female Mice	0.727	8	0.050	-0.677
Stranger Tube Test 6 months–Males	1.000	9	0.050	-0.950
Stranger Tube Test 10 months–Females	1.000	10	0.050	-0.950

12.2 FDR Corrections–Social Tube Test

Finding	P value	Rank (m=10)	BL = (min 0.05, 0.05*m/(m+1-i)^2	(BL) – P value
Social Tube Test 10 months–Males	0.302	1	4.17E-03	-0.298
Average Cage Rank 10 months–Females	0.334	2	4.96E-03	-0.329
Social Tube Test 8-10 weeks–Males	0.350	3	6.00E-03	-0.344
Social Tube Test 6 months–Females	0.471	4	7.41E-03	-0.463

Average Cage Rank 8-10 weeks–Males	0.688	5	9.38E-03	-0.679
Average Cage Rank 6 months–Females	0.727	6	0.012	-0.715
Average Cage Rank 10 months–Males	0.727	7	0.017	-0.710
Social Tube Test 10 months–Females	0.860	8	0.024	-0.836
Social Tube Test 8-10 weeks–Females	0.875	9	0.038	-0.837
Average Cage Rank 8-10 weeks–Females	1.000	10	0.050	-0.950
Social Tube Test 6 months–Males	1.000	11	0.050	-0.950
Average Cage Rank 6 months–Males	1.000	12	0.050	-0.950

12.3 FDR Corrections–Urine Marking Test

Finding	**P value**	**Rank (m=6)**	**BL = (min 0.05, 0.05*m/(m+1-i)^2**	**(BL) – P value**
Urine Test 8-10 weeks–*Grb10+/p* wins	0.010	1	8.33E-03	-1.23E-03
Average Cage Rank 8-10 weeks	0.039	2	0.012	-0.027
Urine Test 6 months–*Grb10+/p* wins	0.488	3	0.019	-0.470
Average Cage Rank 6 months	0.508	4	0.033	-0.475
Urine Test 10 months–*Grb10+/p* wins	0.302	5	0.050	-0.252
Average Cage Rank 10 months	0.473	6	0.050	-0.423

12.4 FDR Corrections–Social Dominance Correlations

Table 12.1 FDR Corrections–Social Dominance Correlations

Finding	**P value**	**Rank (m=25)**	**BL = (min 0.05, 0.05*m/(m+1-i)^2**	**(BL) – P value**
Males 10 months Urine vs Tube Association (Both Genotypes)	0.007	1	2.00E-03	-0.005

Males 10 months Urine vs Tube Association (*Grb10+/p*)	0.017	2	2.17E-03	-0.015
Males 10 months Tube vs Barbering (Wildtypes)	0.043	3	2.36E-03	-0.041
Males 10 months Tube vs Barbering (Both Genotypes)	0.046	4	2.58E-03	-0.043
Males 10 months Urine vs Barbering (Wildtypes)	0.068	5	2.83E-03	-0.065
Females 10 months Tube vs Barbering Association (*Grb10+/p*)	0.127	6	3.13E-03	-0.124
Females 6 months Tube vs Barbering Association (*Grb10+/p*)	0.160	7	3.46E-03	-0.156
Males 6 months Tube vs Barbering (Wildtypes)	0.190	8	3.86E-03	-0.186
Females 10 months Tube vs Barbering Association (Both Genotypes)	0.241	9	4.33E-03	-0.236
Males 10 months Urine vs Tube Association (Wildtype)	0.274	10	4.88E-03	-0.269
Males 6 months Tube vs Barbering (*Grb10+/p*)	0.336	11	5.56E-03	-0.330
Females 6 months Tube vs Barbering Association (Both Genotypes)	0.338	12	6.38E-03	-0.332
Males 10 weeks Urine vs Tube Association (Both Genotypes)	0.404	13	7.40E-03	-0.397
Males 10 weeks Urine vs Tube Association (*Grb10+/p*)	0.474	14	8.68E-03	-0.465
Females 10 months Tube vs Barbering Association (Wildtypes)	0.475	15	0.010	-0.465
Males 6 months Urine vs Tube Association (*Grb10+/p*)	0.559	16	0.013	-0.547
Males 6 months Urine vs Barbering (*Grb10+/p*)	0.579	17	0.015	-0.564
Males 6 months Urine vs Tube Association (Both Genotypes)	0.583	18	0.020	-0.564

Males 6 months Urine vs Barbering (Both Genotypes)	0.680	19	0.026	-0.654
Males 10 months Urine vs Barbering (Both Genotypes)	0.775	20	0.035	-0.741
Males 6 months Urine vs Tube Association (Wildtype)	0.845	21	0.050	-0.795
Males 10 weeks Urine vs Tube Association (Wildtype)	0.852	22	0.050	-0.802
Males 6 months Urine vs Barbering (Wildtypes)	0.861	23	0.050	-0.811
Females 6 months Tube vs Barbering Association (Wildtypes)	0.969	24	0.050	-0.919
Males 6 months Tube vs Barbering (Both Genotypes)	1.000	25	0.050	-0.950

12.5 FDR Corrections–Social Isolation Stranger Encounter Tube Test

Finding	**P value**	**Rank (m=6)**	**BL = (min 0.05, 0.05*m/(m+1-i)^2**	**(BL) – P value**
Isolated Males–Stranger Encounter Days 1-3	5.93E-03	1	8.33E-03	2.41E-03
Isolated Females–Stranger Encounter Days 1-3	9.48E-03	2	0.012	0.003
Isolated Females–Stranger Encounter Day 1	0.065	3	0.019	-0.047
Isolated Females–Oestrus	0.267	4	0.033	-0.234
Isolated Males–Stranger Encounter Day 1	0.289	5	0.050	-0.239
Isolated Males and Females–Stranger Encounter Days 1-3	0.902	6	0.050	-0.852

13 Appendix III–Compulsive and Anxiety Behaviours

13.1 Marble Burying Ethovision Measures–Data Screening

The following table summarizes data screening of all marble burying ethovision data sets prior to statistical analysis.

Table 13.1 Marble Burying Ethovision Measures–Data Screening

	Normality	**Homogeneity**	**SRE > ± 3 SD**	**Boxplot outliers**	**Interaction Sig?**
Velocity	WT 6 mo p = 0.024	Y	C19 P SRE = 3.44	A63 P, C19 P > 1.5 IQ	N; p = 0.352
Total time digging	Y	Y	C13 P SRE = 3.64	A53 P, D22 P > 1.5 IQ	N; p = 0.571
Total time grooming	N; all except WT at 6 mo violate normality	N; p = 0.008	D47 P SRE = 3.79, C41 P SRE = 3.40, A18 P SRE = 3.30, D15 P SRE = 3.08	D35P, D11 P, D47 P, D15 P, D41 P, A61 P > 1.5 IQ C41 P, A15 P, A18 P > 3 IQ	
% Time in "Start"	Y	Y		C11 P, C20 P > 1.5 IQ	N; p = 0.218
% Time in Marbles	Y	Y		C20 P, C11 P > 1.5 IQ	N; p = 0.218
Transitions	Y	Y	A53 P SRE = 3.08	A53 P, A25 P, A63 P, C56 P > 1.5 IQ	N; p = 0.219

13.2 Marbles Buried, Half-Buried, and Displaced–Males 10 weeks Data Screening

The following tables summarize data screening of all data sets for marbles buried, half-buried, and displaced by males at 10 weeks of age prior to statistical analysis.

Table 13.2 Marbles Buried by Males 10 wks–Data Screening

Buried 10 wks	**SRE > ± 3 SD**	**Normality**	**Homogeneity**	**Sphericity**
5 min	D22 P SRE = 4.05 and D18 P SRE = 4.19	Not normal	Y	N; Greenhouse-Geisser ε = 0.708
10 min	D22 P SRE = 3.65 and D7 P SRE = 3.08	Not normal	Y	
15 min		WT normal, *Grb10*$^{+/p}$ not normal	Y	
20 min		Normal	Y	
25 min		Normal	Y	
30 min		Normal	Y	

Table 13.3 Marbles Half Buried by Males 10 wks–Data screening

Half Buried 10 wks	**SRE ± 3SD**	**Normality**	**Homogeneity**
5 min	0	Not normal	Y
10 min	0	Y	Y
15 min	0	WT normal, *Grb10*$^{+/p}$ not	Y
20 min	0	WT normal, *Grb10*$^{+/p}$ not	Y
25 min	0	WT normal, *Grb10*$^{+/p}$ not	Y
30 min	0	Y	Y

Table 13.4 Marbles Displaced by Males 10 wks–Data screening

Displaced 10 wks	**SRE > ± 3 SD**	**Normality**	**Homogeneity**	**Sphericity**
5 min	0	Y	Y	N; Greenhouse-Geisser ε = 0.315
10 min	0	N	Y	
15 min	D21 P SRE = -5.23	N	Y	
20 min	D21 P SRE = -5.35; D42 P SRE = -3.62	N	Y	
25 min	D21 P SRE = -6.71;	N	N	
30 min	All equal, no residuals	N	N	

13.3 Marbles Buried, Half-Buried, and Displaced–Males 6 months Data Screening

The following tables summarize data screening of all data sets for marbles buried, half-buried, and displaced by males at 6 months of age prior to statistical analysis.

Table 13.5 Marbles Buried by Males 6 months–Data screening

Buried 6 mo	**Studentized> ± 3 SD**	**Normality**	**Homogeneity**	**Sphericity**
5 min	C60 P SRE = 5.00	N	N; p = 0.014	
10 min	C3 P SRE = 3.28	N	Y	N; Greenhouse-Geisser ε = 0.738
15 min	0	N	Y	
20 min	0	N	Y	
25 min	0	Y	Y	
30 min	0	Y	Y	

Table 13.6 Marbles Half-Buried by Males 6 months–Data Screening

Half Buried 6 mo	**Studentized > ± 3 SD**	**Normality**	**Homogeneity**	**Sphericity**
5 min	0	N	Y	N; Greenhouse-Geisser applied ε = 0.598
10 min	0	Y	Y	
15 min	0	Y	Y	
20 min	0	Y	Y	
25 min	0	Y	Y	
30 min	0	Y	Y	

Table 13.7 Marbles Displaced by Males 6 months–Data screening

Displaced 6 mo	**Studentized> ± 3 SD**	**Normality**	**Homogeneity**	**Sphericity**
5 min	0	N	Y; Box's M sig.	N; Greenhouse-Geisser ε= 0.320
10 min	C61 P SRE = -3.05	N	Y; Box's M sig.	
15 min	C40 P SRE = -4.38; C61 P SRE = -3.46	N	Y; Box's M sig.	
20 min	C40 P SRE = -4.90; C53 P SRE = -3.68	N	Y; Box's M sig.	
25 min	C53 P SRE = -5.61	N	Y; Box's M sig.	
30 min	C53 P SRE = -6.36	N	Y; Box's M sig.	

13.4 Marbles Buried, Half-Buried, and Displaced–Males 10 months Data Screening

The following tables summarize data screening of all data sets for marbles buried, half-buried, and displaced by males at 10 months of age prior to statistical analysis.

Table 13.8 Marbles Buried by Males 10 months–Data screening

Buried 10 mo	**SRE > ± 3 SD**	**Normality**	**Homogeneity**	**Sphericity**
5 min	A53 P SRE = 3.44; A69 P SRE = 3.35	N	Y	N; Greenhouse-Geisser ε = 0.522
10 min	0	N	Y	
15 min	0	N	Y	
20 min	0	N	Y	
25 min	0	N	Y	
30 min	0	Y	Y	

Table 13.9 Marbles Half-Buried by Males 10 months–Data screening

Half-Buried 10 mo	**Outliers SRE > ± 3SD**	**Normality**	**Homogeneity**	**Sphericity**
5 min	0	WT not normal	Y	N; Greenhouse-Geisser ε = 0.517
10 min	0	Y	Levene's test significant	
15 min	0	WT not normal	Y	
20 min	0	Y	Y	
25 min	0	Y	Y	
30 min	0	WT not normal	Y	

Table 13.10 Marbles Displaced by Males 10 months–Data screening

Displaced 10 mo	**Outliers > ± 3SD**	**Normality**	**Homogeneity of Variance**	**Homogeneity of Covariance**	**Sphericity**
5 min	0	*Grb10$^{+/p}$* data normal; WT not	Y	Box's M not calc;	Mauchly's not calc
10 min	A18 P SRE = -3.50	N	Y		
15 min	A18 P SRE = -5.42; A66 P SRE = -3.06	N	Levene's Test not homogenous;		
20 min	A25 P SRE = -3.03; A15 P	N	Y		

	SRE = -3.03				
25 min	A66 P SRE = -6.93	N	Y		
30 min	A66 P SRE = -6.93	N	Y		

13.5 False Discovery Rate Corrections–Marble Burying

Finding	P value	Rank	(min 0.05, 0.05*m/(m+1-i)^2	(BL) – P value
Cohort D Marbles Buried– Greenhouse-Geisser main effect TIME	5.71E-27	1	2.91E-04	2.91E-04
Cohort C Marbles Buried– Greenhouse-Geisser main effect TIME	1.88E-20	2	2.94E-04	2.94E-04
Cohort A Marbles Buried– Greenhouse-Geisser main effect TIME	8.24E-18	3	2.98E-04	2.98E-04
Cohort A Marbles Displaced– Greenhouse-Geisser main effect of TIME	4.16E-16	4	3.01E-04	3.01E-04
Cohort D Marbles Displaced––Greenhouse-Geisser main effect TIME	3.55E-14	5	3.05E-04	3.05E-04
Cohort C Marbles Displaced— Greenhouse-Geisser main effect TIME	2.44E-13	6	3.08E-04	3.08E-04
Cohort D Marbles Buried –5 to 20 minutes Bonferroni adjusted	6.06E-13	7	3.12E-04	3.12E-04
Cohort D Marbles Buried –5 to 25 minutes Bonferroni adjusted	9.14E-13	8	3.16E-04	3.16E-04
Cohort A Marbles Displaced– 5 to 10 minutes Bonferroni adjusted	5.90E-12	9	3.20E-04	3.20E-04
Cohort C Marbles Buried –5 to 30 minutes Bonferroni adjusted	1.15E-11	10	3.24E-04	3.24E-04

Cohort A Marbles Displaced– 5 to 15 minutes Bonferroni adjusted	1.23E-11	11	3.28E-04	3.28E-04
Cohort A Marbles Displaced– 5 to 25 minutes Bonferroni adjusted	1.64E-11	12	3.32E-04	3.32E-04
Cohort A Marbles Displaced– 5 to 30 minutes Bonferroni adjusted	1.64E-11	13	3.36E-04	3.36E-04
Cohort A Marbles Displaced– 5 to 20 minutes Bonferroni adjusted	1.67E-11	14	3.40E-04	3.40E-04
Cohort D Marbles Buried –5 to 30 minutes Bonferroni adjusted	2.14E-11	15	3.44E-04	3.44E-04
Cohort A Marbles Buried –5 to 25 minutes Bonferroni adjusted	1.13E-10	16	3.49E-04	3.49E-04
Cohort C Marbles Buried –5 to 25 minutes Bonferroni adjusted	1.39E-10	17	3.53E-04	3.53E-04
Cohort D Marbles Displaced– 5 to 30 minutes Bonferroni adjusted	1.91E-10	18	3.58E-04	3.58E-04
Cohort D Marbles Displaced – 5 to 25 minutes Bonferroni adjusted	1.96E-10	19	3.63E-04	3.63E-04
Cohort D Marbles Displaced – 5 to 15 minutes Bonferroni adjusted	2.48E-10	20	3.67E-04	3.67E-04
Cohort D Marbles Displaced – 5 to 20 minutes Bonferroni adjusted	3.08E-10	21	3.72E-04	3.72E-04
Cohort A Marbles Buried –5 to 20 minutes Bonferroni adjusted	3.75E-10	22	3.77E-04	3.77E-04
Cohort A Marbles Buried –5 to 30 minutes Bonferroni adjusted	1.05E-09	23	3.82E-04	3.82E-04
Cohort C Marbles Displaced – 5 to 25 minutes Bonferroni adjusted	1.41E-09	24	3.87E-04	3.87E-04
Cohort C Marbles Displaced – 5 to 20 minutes Bonferroni adjusted	1.76E-09	25	3.93E-04	3.93E-04

Cohort C Marbles Displaced–5 to 30 minutes Bonferroni adjusted	2.11E-09	26	3.98E-04	3.98E-04
Cohort D Marbles Displaced – 5 to 10 minutes Bonferroni adjusted	2.39E-09	27	4.03E-04	4.03E-04
Cohort C Marbles Displaced – 5 to 15 minutes Bonferroni adjusted	2.44E-09	28	4.09E-04	4.09E-04
Cohort D Marbles Buried –10 to 20 minutes Bonferroni adjusted	2.81E-09	29	4.15E-04	4.15E-04
Cohort D Marbles Buried –10 to 25 minutes Bonferroni adjusted	6.56E-09	30	4.21E-04	4.21E-04
Cohort C Marbles Buried –10 to 30 minutes Bonferroni adjusted	1.24E-08	31	4.27E-04	4.26E-04
Cohort D Marbles Buried –10 to 30 minutes Bonferroni adjusted	1.50E-08	32	4.33E-04	4.33E-04
Cohort C Marbles Buried –5 to 20 minutes Bonferroni adjusted	2.48E-08	33	4.39E-04	4.39E-04
Cohort C Marbles Displaced – 5 to 10 minutes Bonferroni adjusted	2.53E-08	34	4.45E-04	4.45E-04
Cohort D Marbles Buried –5 to 15 minutes Bonferroni adjusted	8.34E-08	35	4.52E-04	4.52E-04
Cohort A Marbles Buried –5 to 15 minutes Bonferroni adjusted	1.44E-07	36	4.58E-04	4.58E-04
Cohort C Marbles Buried –10 to 25 minutes Bonferroni adjusted	1.58E-07	37	4.65E-04	4.65E-04
Cohort A Marbles Buried –10 to 25 minutes Bonferroni adjusted	4.53E-07	38	4.72E-04	4.71E-04
Cohort A Marbles Buried –10 to 20 minutes Bonferroni adjusted	1.00E-06	39	4.79E-04	4.78E-04
Cohort A Marbles Buried –10 to 30 minutes Bonferroni adjusted	1.00E-06	40	4.86E-04	4.85E-04

Cohort D Marbles Half-Buried –5 to 10 minutes Bonferroni adjusted	3.00E-06	41	4.94E-04	4.91E-04
Cohort C Marbles Buried –5 to 15 minutes Bonferroni adjusted	6.00E-06	42	5.01E-04	4.95E-04
Cohort D Marbles Half-Buried—Greenhouse-Geisser main effect TIME	6.00E-06	43	5.09E-04	5.03E-04
Cohort C Marbles Half-Buried –5 to 10 minutes Bonferroni adjusted	1.50E-05	44	5.17E-04	5.02E-04
Time Digging–main effect AGE	1.80E-05	45	5.25E-04	5.07E-04
Cohort C Marbles Buried –15 to 30 minutes Bonferroni adjusted	1.80E-05	46	5.33E-04	5.15E-04
Cohort D Marbles Half-Buried –5 to 15 minutes Bonferroni adjusted	2.40E-05	47	5.42E-04	5.18E-04
Cohort A Marbles Buried –5 to 10 minutes Bonferroni adjusted	2.50E-05	48	5.50E-04	5.25E-04
Cohort C Marbles Buried –10 to 20 minutes Bonferroni adjusted	3.60E-05	49	5.59E-04	5.23E-04
Cohort D Marbles Buried –15 to 20 minutes Bonferroni adjusted	5.40E-05	50	5.68E-04	5.14E-04
Cohort D Marbles Buried –15 to 25 minutes Bonferroni adjusted	7.00E-05	51	5.78E-04	5.08E-04
Cohort A Marbles Buried –15 to 25 minutes Bonferroni adjusted	2.57E-04	52	5.87E-04	3.30E-04
Cohort C Marbles Buried –5 to 10 minutes Bonferroni adjusted	3.00E-04	53	5.97E-04	2.97E-04
Cohort C Marbles Buried –15 to 25 minutes Bonferroni adjusted	3.49E-04	54	6.07E-04	2.58E-04
Cohort A Marbles Half-Buried–5 to 10 minutes Bonferroni adjusted	4.16E-04	55	6.18E-04	2.02E-04
Cohort C Marbles Half-Buried—Greenhouse-Geisser main effect TIME	4.77E-04	56	6.28E-04	1.51E-04

Cohort A Marbles Buried –15 to 20 minutes Bonferroni adjusted	8.55E-04	57	6.39E-04	-2.16E-04
Cohort D Marbles Buried –15 to 30 minutes Bonferroni adjusted	0.0010	58	6.50E-04	-3.63E-04
Cohort A Marbles Buried –10 to 15 minutes Bonferroni adjusted	0.0013	59	6.62E-04	-6.23E-04
Cohort D Marbles Buried –5 to 10 minutes Bonferroni adjusted	0.0014	60	6.74E-04	-6.76E-04
Cohort D Marbles Buried –10 to 15 minutes Bonferroni adjusted	0.0015	61	6.86E-04	-8.49E-04
Cohort A Marbles Half-Buried –Greenhouse Geisser main effect TIME	0.0026	62	6.98E-04	-0.002
Cohort D Marbles Displaced– 10 to 30 minutes Bonferroni adjusted	0.0039	63	7.11E-04	-0.003
Cohort D Marbles Displaced– 10 to 25 minutes Bonferroni adjusted	0.0040	64	7.24E-04	-0.003
Cohort D Marbles Half-Buried –15 to 20 minutes Bonferroni adjusted	0.0046	65	7.37E-04	-0.004
Cohort C Marbles Displaced– 10 to 25 minutes Bonferroni adjusted	0.0049	66	7.51E-04	-0.004
Cohort C Marbles Half-Buried –5 to 15 minutes Bonferroni adjusted	0.0051	67	7.65E-04	-0.004
Cohort A Marbles Buried –15 to 30 minutes Bonferroni adjusted	0.0052	68	7.80E-04	-0.004
Cohort D Marbles Displaced – 10 to 20 minutes Bonferroni adjusted	0.0056	69	7.95E-04	-0.005
Cohort C Marbles Displaced – 10 to 20 minutes Bonferroni adjusted	0.0057	70	8.11E-04	-0.005
Cohort C Marbles Displaced– 10 to 30 minutes Bonferroni adjusted	0.0057	71	8.27E-04	-0.005

Cohort D Marbles Displaced –10 to 15 minutes Bonferroni adjusted	0.0062	72	8.43E-04	-0.005
Cohort D Marbles Half-Buried –5 to 30 minutes Bonferroni adjusted	0.0068	73	8.60E-04	-0.006
Cohort C Marbles Displaced –10 to 15 minutes Bonferroni adjusted	0.0069	74	8.77E-04	-0.006
Cohort A Marbles Displaced–10 to 25 minutes Bonferroni adjusted	0.0072	75	8.95E-04	-0.006
Cohort A Marbles Displaced–10 to 30 minutes Bonferroni adjusted	0.0072	76	9.14E-04	-0.006
Cohort A Marbles Half-Buried –5 to 15 minutes Bonferroni adjusted	0.0143	77	9.33E-04	-0.013
Cohort A Marbles Displaced–10 to 20 minutes Bonferroni adjusted	0.0148	78	9.53E-04	-0.014
Cohort A Marbles Displaced–10 to 15 minutes Bonferroni adjusted	0.0307	79	9.73E-04	-0.030
Cohort C Marbles Buried –15 to 20 minutes Bonferroni adjusted	0.0322	80	9.94E-04	-0.031
Cohort C Marbles Buried –10 to 15 minutes Bonferroni adjusted	0.0330	81	0.001	-0.032
Cohort D Marbles Half-Buried –5 to 20 minutes Bonferroni adjusted	0.0483	82	0.001	-0.047
Cohort D Marbles Half-Buried –15 to 25 minutes Bonferroni adjusted	0.0498	83	0.001	-0.049
Percent Time in "start"–main effect AGE	0.0550	84	0.001	-0.054
Cohort D Marbles Half-Buried –5 to 25 minutes Bonferroni adjusted	0.0552	85	0.001	-0.054
Transitions–main effect GENOTYPE	0.0597	86	0.001	-0.059
Cohort C Marbles Buried –20 to 30 minutes Bonferroni adjusted	0.0738	87	0.001	-0.073

Velocity–main effect GENOTYPE	0.0770	88	0.001	-0.076
Transitions–main effect AGE	0.0844	89	0.001	-0.083
Cohort A Marbles Displaced–main effect of GENOTYPE	0.1048	90	0.001	-0.104
Cohort C Marbles Half-Buried –5 to 20 minutes Bonferroni adjusted	0.1142	91	0.001	-0.113
Time Grooming–10 mo	0.1230	92	0.001	-0.122
Cohort A Marbles Half-Buried–5 to 25 minutes Bonferroni adjusted	0.1309	93	0.001	-0.130
Cohort A Marbles Half-Buried–5 to 30 minutes Bonferroni adjusted	0.1397	94	0.001	-0.138
Cohort C Marbles Half-Buried –5 to 30 minutes Bonferroni adjusted	0.1511	95	0.001	-0.150
Cohort A Marbles Half-Buried–5 to 20 minutes Bonferroni adjusted	0.1634	96	0.001	-0.162
Time Grooming– 6 mo	0.1730	97	0.001	-0.172
Cohort C Marbles Buried–main effect GENOTYPE	0.1783	98	0.002	-0.177
Cohort D Marbles Half-Buried –15 to 30 minutes Bonferroni adjusted	0.1835	99	0.002	-0.182
Cohort A Marbles Half-Buried–Greenhouse Geisser Interaction	0.1865	100	0.002	-0.185
Cohort A Marbles Buried–main effect GENOTYPE	0.1996	101	0.002	-0.198
Percent Time in "start"–Interaction	0.2179	102	0.002	-0.216
Transitions–Interaction	0.2191	103	0.002	-0.217
Cohort C Marbles Buried –20 to 25 minutes Bonferroni adjusted	0.2943	104	0.002	-0.292
Percent Time in "start"–main effect GENOTYPE	0.3480	105	0.002	-0.346
Velocity–Interaction	0.3523	106	0.002	-0.350
Cohort A Marbles Displaced–15 to 25 minutes Bonferroni adjusted	0.4328	107	0.002	-0.431

Cohort A Marbles Displaced–15 to 30 minutes Bonferroni adjusted	0.4328	108	0.002	-0.431
Cohort CMarbles Half-Buried –5 to 25 minutes Bonferroni adjusted	0.4444	109	0.002	-0.442
Cohort C Marbles Displaced–15 to 30 minutes Bonferroni adjusted	0.4922	110	0.002	-0.490
Cohort C Marbles Displaced –15 to 25 minutes Bonferroni adjusted	0.5203	111	0.002	-0.518
Time Digging–main effect GENOTYPE	0.5219	112	0.002	-0.520
Time Grooming–10 wks	0.5230	113	0.002	-0.521
Cohort C Marbles Half-Buried –10 to 25 minutes Bonferroni adjusted	0.5271	114	0.002	-0.525
Cohort D Marbles Half-Buried–main effect GENOTYPE	0.5297	115	0.003	-0.527
Cohort C Marbles Half-Buried–Greenhouse-Geisser Interaction	0.5577	116	0.003	-0.555
Time Digging–Interaction	0.5712	117	0.003	-0.569
Velocity–main effect AGE	0.6002	118	0.003	-0.597
Cohort C Marbles Half-Buried–main effect GENOTYPE	0.6391	119	0.003	-0.636
Cohort A Marbles Displaced–20 to 25 minutes Bonferroni adjusted	0.6548	120	0.003	-0.652
Cohort A Marbles Displaced–20 to 30 minutes Bonferroni adjusted	0.6548	121	0.003	-0.652
Cohort C Marbles Displaced–main effect GENOTYPE	0.6850	122	0.003	-0.682
Cohort D Marbles Buried–Greenhouse-Geisser Interaction	0.7085	123	0.003	-0.705
Cohort D Marbles Displaced–15 to 30 minutes Bonferroni adjusted	0.7144	124	0.004	-0.711
Cohort D Marbles Displaced–main effect GENOTYPE	0.7411	125	0.004	-0.737
Cohort D Marbles Displaced–Greenhouse-Geisser Interaction	0.7556	126	0.004	-0.752

Cohort D Marbles Buried–main effect GENOTYPE	0.8234	127	0.004	-0.819
Cohort D Marbles Half-Buried–Greenhouse-Geisser Interaction	0.8359	128	0.004	-0.832
Cohort A Marbles Half-Buried–main effect GENOTYPE	0.8598	129	0.004	-0.855
Cohort A Marbles Buried –20 to 25 minutes Bonferroni adjusted	1	130	0.005	-0.995
Cohort A Marbles Buried –20 to 30 minutes Bonferroni adjusted	1	131	0.005	-0.995
Cohort A Marbles Buried –25 to 30 minutes Bonferroni adjusted	1	132	0.005	-0.995
Cohort A Marbles Half-Buried–10 to 15 minutes Bonferroni adjusted	1	133	0.005	-0.995
Cohort A Marbles Half-Buried–10 to 20 minutes Bonferroni adjusted	1	134	0.006	-0.994
Cohort A Marbles Half-Buried–10 to 25 minutes Bonferroni adjusted	1	135	0.006	-0.994
Cohort A Marbles Half-Buried–10 to 30 minutes Bonferroni adjusted	1	136	0.006	-0.994
Cohort A Marbles Half-Buried–15 to 20 minutes Bonferroni adjusted	1	137	0.007	-0.993
Cohort A Marbles Half-Buried–15 to 25 minutes Bonferroni adjusted	1	138	0.007	-0.993
Cohort A Marbles Half-Buried–15 to 30 minutes Bonferroni adjusted	1	139	0.007	-0.993
Cohort A Marbles Half-Buried–20 to 25 minutes Bonferroni adjusted	1	140	0.008	-0.992
Cohort A Marbles Half-Buried–20 to 30 minutes Bonferroni adjusted	1	141	0.008	-0.992
Cohort A Marbles Half-Buried–25 to 30 minutes Bonferroni adjusted	1	142	0.009	-0.991

Cohort A Marbles Displaced– 15 to 20 minutes Bonferroni adjusted	1	143	0.010	-0.990
Cohort C Marbles Buried –25 to 30 minutes Bonferroni adjusted	1	144	0.010	-0.990
Cohort C Marbles Half-Buried –10 to 15 minutes Bonferroni adjusted	1	145	0.011	-0.989
Cohort C Marbles Half-Buried –10 to 20 minutes Bonferroni adjusted	1	146	0.012	-0.988
Cohort C Marbles Half-Buried –10 to 30 minutes Bonferroni adjusted	1	147	0.013	-0.987
Cohort C Marbles Half-Buried –15 to 20 minutes Bonferroni adjusted	1	148	0.014	-0.986
Cohort C Marbles Half-Buried –15 to 25 minutes Bonferroni adjusted	1	149	0.015	-0.985
Cohort C Marbles Half-Buried –15 to 30 minutes Bonferroni adjusted	1	150	0.016	-0.984
Cohort C Marbles Half-Buried –20 to 25 minutes Bonferroni adjusted	1	151	0.018	-0.982
Cohort C Marbles Half-Buried –20 to 30 minutes Bonferroni adjusted	1	152	0.020	-0.980
Cohort C Marbles Half-Buried –25 to 30 minutes Bonferroni adjusted	1	153	0.022	-0.979
Cohort C Marbles Displaced– 15 to 20 minutes Bonferroni adjusted	1	154	0.024	-0.976
Cohort C Marbles Displaced– 20 to 25 minutes Bonferroni adjusted	1	155	0.027	-0.973
Cohort C Marbles Displaced – 20 to 30 minutes Bonferroni adjusted	1	156	0.030	-0.970
Cohort C Marbles Displaced – 25 to 30 minutes Bonferroni adjusted	1	157	0.034	-0.966

Cohort D Marbles Buried –20 to 25 minutes Bonferroni adjusted	1	158	0.038	-0.962
Cohort D Marbles Buried –20 to 30 minutes Bonferroni adjusted	1	159	0.044	-0.956
Cohort D Marbles Buried –25 to 30 minutes Bonferroni adjusted	1	160	0.050	-0.950
Cohort D Marbles Half-Buried –10 to 15 minutes Bonferroni adjusted	1	161	0.050	-0.950
Cohort D Marbles Half-Buried –10 to 20 minutes Bonferroni adjusted	1	162	0.050	-0.950
Cohort D Marbles Half-Buried –10 to 25 minutes Bonferroni adjusted	1	163	0.050	-0.950
Cohort D Marbles Half-Buried –10 to 30 minutes Bonferroni adjusted	1	164	0.050	-0.950
Cohort D Marbles Half-Buried –20 to 25 minutes Bonferroni adjusted	1	165	0.050	-0.950
Cohort D Marbles Half-Buried –20 to 30 minutes Bonferroni adjusted	1	166	0.050	-0.950
Cohort D Marbles Half-Buried –25 to 30 minutes Bonferroni adjusted	1	167	0.050	-0.950
Cohort D Marbles Displaced– 15 to 20 minutes Bonferroni adjusted	1	168	0.050	-0.950
Cohort D Marbles Displaced – 15 to 25 minutes Bonferroni adjusted	1	169	0.050	-0.950
Cohort D Marbles Displaced– 20 to 25 minutes Bonferroni adjusted	1	170	0.050	-0.950
Cohort D Marbles Displaced – 20 to 30 minutes Bonferroni adjusted	1	171	0.050	-0.950
Cohort D Marbles Displaced – 25 to 30 minutes Bonferroni adjusted	1	172	0.050	-0.950

13.6 Elevated Plus Maze Ethovision Measures

The following table summarizes data screening of all EPM data sets prior to statistical analysis.

13.6.1 EPM Data Screening Table

Table 13.11 EPM All Cohorts—Data Screening

Measure	Normality	Homogeneity	SRE > ± 3 SD	Boxplot outliers	Interaction Sig?
"All entries"	Y	Y	A17 P SRE = 3.26	D24 P, D51 P > 1.5 IQ	N; p = 0.534
"open arm entries"	*Grb10*$^{+/p}$ 10 mo p = 0.008; 6 mo p = 0.004	N; p = 0.010 Ratio:	A17 P SRE = 4.61	A17 P, C44 P, C3 P > 1.5 IQ	N; p = 0.621
"total closed arm entries"	WT 10 wks p = 0.003; *Grb10*$^{+/p}$ 6 mo p = 0.030	Y	D24 P SRE = 3.83	A3 P, C19 P, D24 P, A61 P, C52 P < 1.5 IQ	N; p = 0.164
"total middle entries"	Y	Y	A17 P SRE = 3.20	D24 P, D51 P > 1.5 IQ	N; p = 0.507
"Latency to first open arm entry"	N; All cells < 0.001	N; p = 0.004	C45 P, SRE = 7.95 A66 P SRE = 5.09	A62 P, C19 P, D47 P, A42 P, A74 P, C60 P > 1.5 IQ A66 P, C2 P, C46 P, C45 P, D62 P, A9 P, C41 P, D26 P, D51 P > 3 IQ	N; p = 0.424

"Time spent per open arm entry"	*Grb10*$^{+/p}$ 6 mo p < 0.001	Y	C52 P SRE = 8.22	A61 P > 1.5 IQ C52 P > 3 IQ	N; p = 0.122
"Time spent per closed arm entry"	WT 10 mo p < 0.001, 6 mo p = 0.002, *Grb10*$^{+/p}$ p < 0.001	N; p = 0.002	A3 P SRE = 5.15, C19 P SRE = 3.97, D51 P SRE = 3.86	C19 P, D47 P, A61 P > 1.5 IQ A3 P , D51 P > 3 IQ	N; p = 0.084
"Time spent per middle entry"	WT 10 weeks p = 0.022	N; p = 0.003		A1 P, A53 P, A43 P, A48 P, A18 P, D47 P > 1.5 IQ	N; p = 0.927
"Mean velocity"	Y	Y	A17 P SRE = 3.73	A24 P, D24 P, D59 P, A17 P > 1.5 IQ	N; p = 0.665
"Percent time in open arm"	*Grb10*$^{+/p}$ 10 mo p = 0.026, 6 mo p < 0.001	Y	C52 P SRE = 5.38, A17 P SRE = 3.18	A17 P, D56 P > 1.5 IQ C52 P > 3 IQ	N; p = 0.297
"Percent time in closed arm"	WT 6 mo p = 0.025; *Grb10*$^{+/p}$ 6 mo p = 0.015	**N; p = 0.007**		C52 P, D20 P, D53 P, D56 P > 1 IQ D51 P > 3 IQ	**Not interpreting interaction b/c homogeneity of var violated**
"Percent time in middle zone"	Y	N; p = 0.033		A3 P, D38 P, C51 P, C10 P, C52 P, D51 P > 1.5 IQ	N; p = 0.108

"Percent time in open vs closed arm"	*Grb10*$^{+/p}$ p < 0.001	N; p = 0.035	C52 P SRE = 4.09; A17 P SRE = 3.14	D56 P > 1.5 IQ C52 P > 3 IQ	N; p = 0.234
"Head dip duration"	*Grb10*$^{+/p}$ 10 mo p = 0.026; 6 mo p < 0.001	Y	C52 P SRE = 5.19		N; p = 0.117
"Stretch attend duration"		Y	C52 P SRE = 3.44	A3 P, C52 P, D56 P > 1.5 IQ	N; p = 0.063
"Grooming duration"	WT 10 months p < 0.001; 6 months p = 0.004, 10 weeks p = 0.046; *Grb10*$^{+/p}$ 10 months p = 0.016, 10 weeks p < 0.001	N; p = 0.002	D100 P SRE = 4.45, D51 P SRE = 4.20, A49 P SRE = 3.11	C71 P, C65 P, D43 P, D30 P, D33 P > 1.5 IQ A49 P, D61 P, D51 P, D100 P > 3 IQ	N; p = 0.108

13.6.2 EPM–"Time per middle entry"

"Time per middle entry" was analyzed using separate one-way ANOVAs for each cohort. Data are presented as mean ± standard deviation.

At 10 weeks, the assumption of homogeneity of error variances was violated (Levene's test p = 0.009). Therefore, we interpreted Welch's ANOVA. There was a statistically significant difference between *Grb10*$^{+/p}$ (1.610 $\pm$ 0.324 s) and wildtype (2.045 $\pm$ 0.671 s) trials in time spent per middle zone entry, Welch's F(1, 31.731) = 7.852, p = 0.009. This did not survive FDR correction. At 6 months, "time per middle zone entry" was not statistically different between

Grb10$^{+/p}$ (2.718 ± 0.943 s) and wildtype (3.270 ± 0.919 s) trials, F(1,40) = 3.686, p = 0.062, η^2 = 0.084. At 10 months, there was no statistically significant difference in "time per middle zone entry" between *Grb10*$^{+/p}$ (2.783 ± 0.977 s) and wildtype (3.338 ± 0.972 s) trials, F(1,41) = 3.487, p = 0.069, partial η^2 = 0.078.

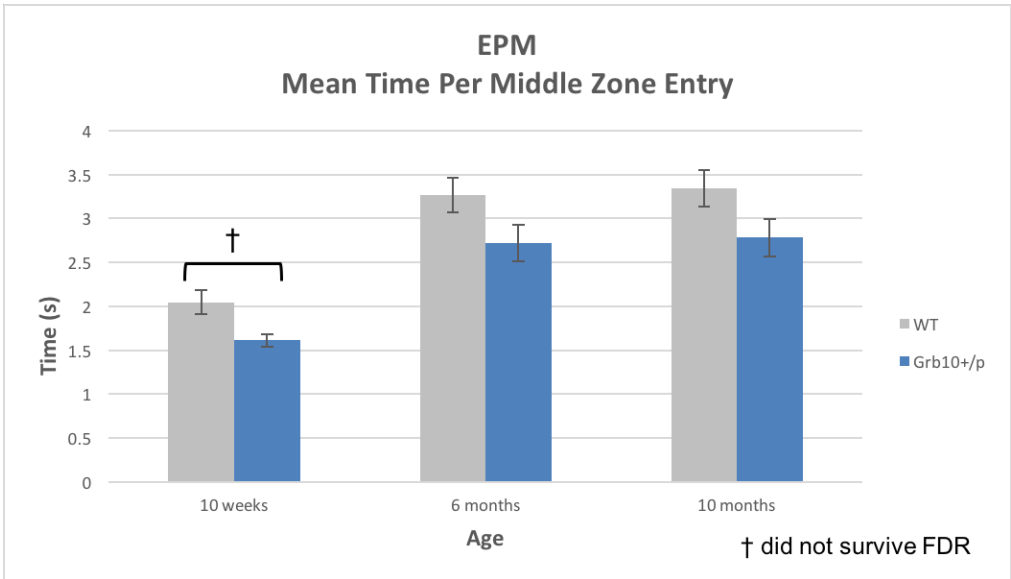

Figure 13.1 EPM Time Per Middle Zone Entry

13.6.3 EPM "Percent time in open vs closed arms"

"Percent time in open vs closed arms" was analyzed using separate one-way ANOVAs for each cohort. Data are presented as mean ± standard deviation. The measure refers to the percent of total time spent on the open arm when time the middle zone is eliminated and open and closed arm are compared directly.

At 10 weeks, the assumption of homogeneity of error variances was violated (Levene's test p = 0.032). Therefore, we interpreted Welch's ANOVA. There was no statistically significant difference between *Grb10*$^{+/p}$ (28.621 ±

10.894%) and wildtype (26.475 ± 14.890%) trials in percent time in open vs closed arms, Welch's F(1, 40.307) = 0.311, p = 0.580. At 6 months, "percent time in open vs closed arms" was statistically different between *Grb10*$^{+/p}$ (28.837 ± 16.431%) and wildtype (15.897 ± 12.637%) trials, F(1,40) = 8.271, p = 0.006, partial η^2 = 0.171. At 10 months, the assumption of homogeneity of error variances was violated (Levene's test p = 0.023). Therefore, we interpreted Welch's ANOVA. There was no statistically significant difference in "percent time in open vs closed arms" between *Grb10*$^{+/p}$ (23.704 ± 20.390%) and wildtype (16.113 ± 11.816%) trials, Welch's F(1,31.769) = 2.204, p = 0.148.

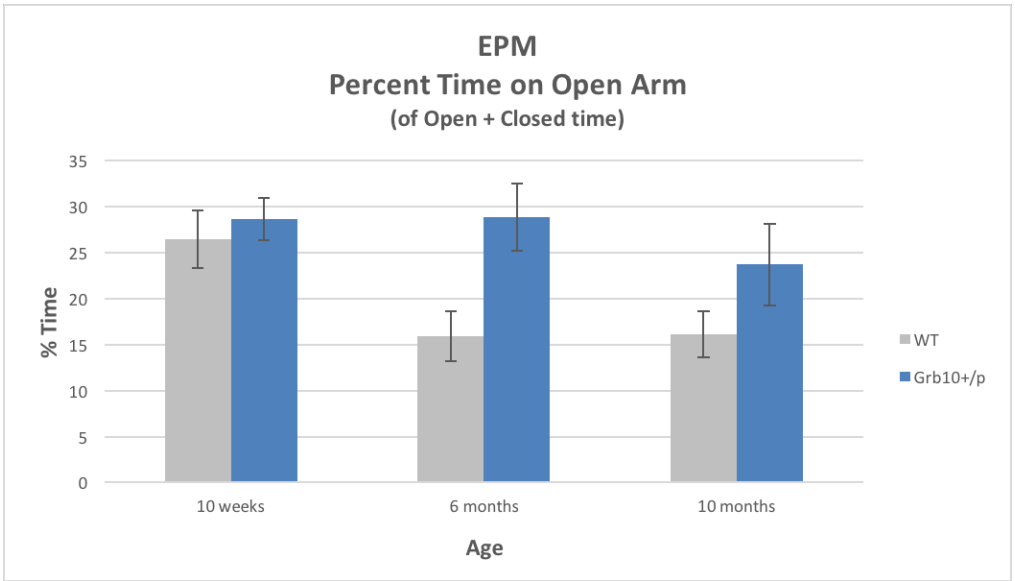

Figure 13.2 EPM Percent Time Open vs Closed

13.6.4 EPM–"Stretch-attend duration"

There was no statistically significant interaction between GENOTYPE and AGE for "stretch-attend duration", F(2,125) = 2.820, p = 0.063, partial η^2 = 0.043. Therefore, analyses for main effects were performed. There was a statistically significant main effect of GENOTYPE on "stretch-attend duration", F(1,125) = 4.532, p = 0.035, partial η^2 = 0.035. *Grb10*$^{+/p}$ mice spent significantly

more time in “stretch-attend” behaviour (124.949 ± 4.000 s) than wildtypes (113.049 ± 3.904 s), mean difference (11.900 (95%CI 0.837 to 22.963) s, p = 0.035).

There was also a significant main effect of AGE on “stretch-attend duration”, F(2,125) = 4.162, p = 0.018, partial η^2 = 0.062. At 10 weeks, mice spent 109.886 ± 4.711 s, at 6 months 117.747 ± 4.936 s, and at 10 months 129.363 ± 4.874 s. There was a significant difference between time spent at 10 weeks and 10 months (-19.477 (95%CI -35.926 to -3.029) s, p = 0.014), but not between 10 weeks and 6 months (-7.861 (95%CI -24.417 to 8.696) s, p = 0.754). There was no significant difference in time spent in stretch-attend between 6 months and 10 months (-11.616 (95%CI -28.448 to 5.215) s, p = 0.289).

When outliers were removed, there was no statistically significant main effect of GENOTYPE on “stretch attend duration”, F(1,115) = 1.604, p = 0.208, partial η^2 = 0.014. There was a statistically significant main effect of AGE on stretch-attend duration, F(2,115) = 5.143, p = 0.007, partial η^2 = 0.082. There was no longer a significant difference between mice 10 weeks (110.683 ± 4.512 s) and 6 months of age (116.615 ± 4.738 s), mean difference -5.933 (95%CI -21.830 to 9.964) s, p = 1.000.

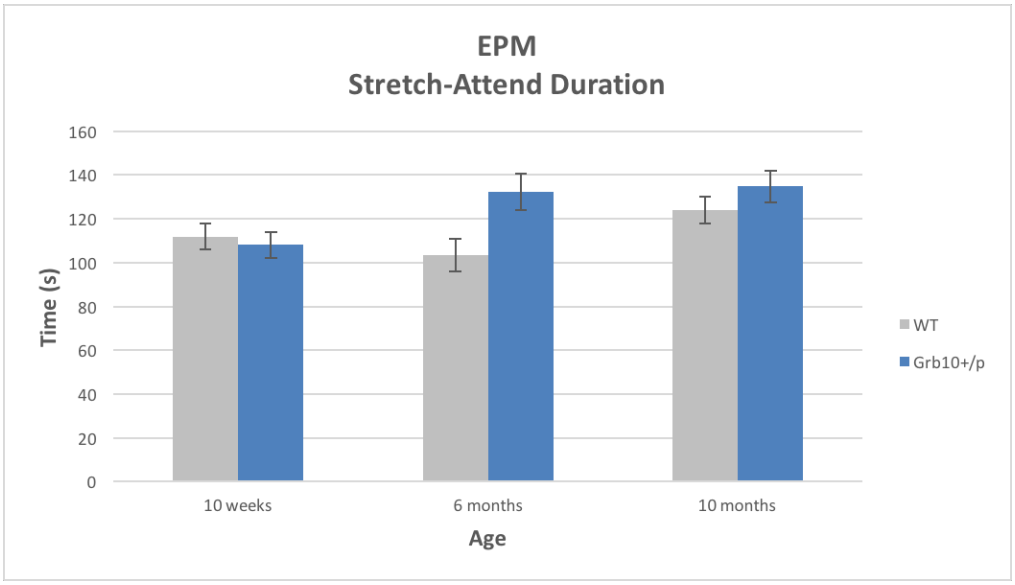

Figure 13.3 EPM Stretch-Attend Duration

13.6.5 EPM–"Grooming duration"

"Grooming duration" was analyzed using separate one way ANOVAs for each cohort. Data are presented as mean ± standard deviation.

At 10 weeks, the assumption of homogeneity of error variances was violated (Levene's test p = 0.027). Therefore, we interpreted Welch's ANOVA. There was no statistically significant difference between *Grb10*$^{+/p}$ (10.014 ± 9.825 s) and wildtype (5.682 ± 4.841s) trials in total time spent grooming, Welch's F(1, 32.088) = 3.599, p = 0.067. At 6 months, "grooming duration" was not statistically different between *Grb10*$^{+/p}$ (4.880 ± 3.871 s) and wildtype (6.087 ± 4.776 s) trials, F(1,40) = 0.800, p = 0.377, partial η^2 = 0.020. At 10 months, the assumption of homogeneity of variance was violated (Levene's test p = 0.043). Therefore, we interpreted Welch's ANOVA. There was no statistically significant difference in "grooming duration" between *Grb10*$^{+/p}$

(7.011 ± 6.142 s) and wildtype (5.595 ± 4.824 s) trials, Welch's F(1,37.952) = 0.703, p = 0.407.

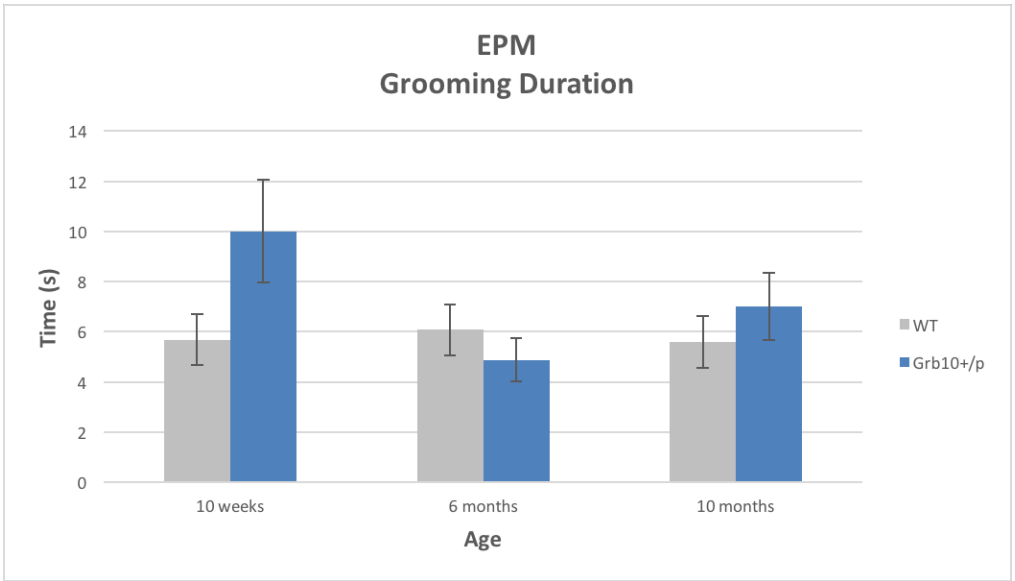

Figure 13.4 EPM Grooming Duration

13.7 False Discovery Rate Corrections–EPM

Finding	P value	Rank m = 63	(min 0.05, 0.05*m/(m+1-i)^2	(BL) – P value
Middle Entries–main effect GENOTYPE	4.00E-05	1	7.94E-04	7.54E-04
All Entries–main effect GENOTYPE	4.40E-05	2	8.19E-04	7.75E-04
Head dip duration–main effect GENOTYPE	2.14E-04	3	8.47E-04	6.33E-04
Velocity–main effect GENOTYPE	2.54E-04	4	8.75E-04	6.21E-04
Closed Entries–main effect GENOTYPE	3.88E-04	5	9.05E-04	5.17E-04
Percent time in closed arms–6 months (Welch)	5.50E-04	6	9.36E-04	3.86E-04
Time per closed entry–6 months (Welch)	7.09E-04	7	9.70E-04	2.61E-04
Middle Entries–main effect AGE	0.001	8	0.0010	-4.26E-04
All Entries–main effect AGE	0.002	9	0.0010	-6.67E-04

Velocity–main effect AGE	0.002	10	0.0011	-1.06E-03
Middle Entries– 10 weeks to 6 months	0.003	11	0.0011	-1.76E-03
All Entries–10 weeks to 6 months	0.004	12	0.0012	-2.37E-03
Percent time in open arms–10 weeks to 10 months	0.004	13	0.0012	-2.68E-03
Percent time in open arms–AGE	0.004	14	0.0013	-2.69E-03
Open Entries–6 months	0.006	15	0.0013	-4.24E-03
Velocity–10 weeks to 6 months	0.006	16	0.0014	-4.76E-03
Percent time in open arms–GENOTYPE	0.006	17	0.0014	-4.86E-03
Percent time in open vs closed arms–6 months	0.006	18	0.0015	-4.94E-03
Time per middle entry–10 weeks (Welch)	0.009	19	0.0016	-7.03E-03
Velocity–10 weeks to 10 months	0.009	20	0.0016	-7.32E-03
Middle Entries–10 weeks to 10 months	0.011	21	0.0017	-8.90E-03
All Entries–10 weeks to 10 months	0.011	22	0.0018	-9.58E-03
Stretch-attend duration–10 weeks to 10 months	0.014	23	0.0019	-1.24E-02
Stretch-attend duration–main effect AGE	0.018	24	0.0020	-1.58E-02
Stretch-attend duration–main effect GENOTYPE	0.035	25	0.0021	-3.32E-02
Percent time in middle zone–6 months	0.040	26	0.0022	-3.83E-02
Time per open entry–main effect AGE	0.055	27	0.0023	-5.25E-02
Closed Entries–main effect AGE	0.059	28	0.0024	-5.64E-02
Time per middle entry–6 months	0.062	29	0.0026	-5.95E-02
Latency to first open entry–6 months (Welch)	0.063	30	0.0027	-6.01E-02
Stretch-attend duration–Interaction	0.063	31	0.0029	-6.05E-02
Percent time in open arms–10 weeks to 6 months	0.063	32	0.0031	-6.03E-02
Grooming duration– 10 weeks	0.067	33	0.0033	-6.36E-02

Time per middle entry–10 months	0.069	34	0.0035	-6.55E-02
Open Entries–10 months (Welch)	0.094	35	0.0037	-9.03E-02
Head dip duration–Interaction	0.117	36	0.0040	-1.13E-01
Time per open entry–Interaction	0.122	37	0.0043	-1.18E-01
Latency to first open entry–10 months	0.138	38	0.0047	-1.34E-01
Latency to first open entry–10 weeks	0.147	39	0.0050	-1.42E-01
Percent time in open vs closed arms–10 months (Welch)	0.148	40	0.0055	-1.42E-01
Closed Entries–Interaction	0.164	41	0.0060	-1.58E-01
Time per closed entry–10 weeks	0.199	42	0.0065	-1.93E-01
Open Entries–10 weeks	0.211	43	0.0071	-2.03E-01
Time per open entry–main effect GENOTYPE	0.276	44	0.0079	-2.68E-01
Time per closed entry–10 months	0.285	45	0.0087	-2.76E-01
Stretch-attend duration–6 months to 10 months	0.289	46	0.0097	-2.80E-01
Percent time in closed arms–10 months	0.295	47	0.0109	-2.84E-01
Percent time in open arms–Interaction	0.297	48	0.0123	-2.85E-01
Grooming duration– 6 months	0.377	49	0.0140	-3.63E-01
Grooming duration– 10 months (Welch)	0.407	50	0.0161	-3.91E-01
Middle Entries–Interaction	0.507	51	0.0186	-4.89E-01
All Entries–Interaction	0.534	52	0.0219	-5.12E-01
Percent time in open vs closed arms– 8 weeks (Welch)	0.580	53	0.0260	-5.54E-01
Percent time in closed arms–10 weeks	0.615	54	0.0315	-5.84E-01
Velocity–Interaction	0.665	55	0.0389	-6.26E-01
Stretch-attend duration–10 weeks to 6 months	0.754	56	0.0492	-7.05E-01
Head dip duration–main effect AGE	0.875	57	0.0500	-8.25E-01

Percent time in middle zone–10 months	0.902	58	0.0500	-8.52E-01
Percent time in middle zone–10 weeks	0.999	59	0.0500	-9.49E-01
All Entries–6 months to 10 months	1.000	60	0.0500	-9.50E-01
Middle Entries–6 months to 10 months	1.000	61	0.0500	-9.50E-01
Velocity–6 months to 10 months	1.000	62	0.0500	-9.50E-01
Percent time in open arms–6 months to 10 months	1.000	63	0.0500	-9.50E-01

14 Appendix IV–Alternative methods of measuring methylation

14.1 Methylation-Sensitive Restriction Enzyme Digestion

Each DNA sample was digested under three parallel conditions in preparation for methylation analysis by southern blot. First, all conditions were digested overnight at 37˚C with HindIII in CutSmart Buffer from New England Biolabs to reduce average fragment size. In the first condition, samples were digested a further hour in the same restriction enzyme; this served as the 0% methylation control. In the second condition, samples were digested for 1 hour in the methylation insensitive MspI as the 100% methylated control. Finally, test samples were digested 1 hour in the methylation sensitive HspII. This sample would be compared to the two control conditions to determine relative digestion as a measure of % methylation. The HspII and MspI restriction enzymes came from the EpiJet Kit from Thermofisher.

14.2 Southern Blot

Restriction Enzyme digested samples were run on a 1.2% agarose gel without Ethidium Bromide overnight at 20V. Once the fragments separated, the gel was soaked in alkaline transfer buffer and assembled in an Alkaline Transfer Southern Blot with a Hybond N+ membrane. The blot was left overnight. After disassembling the blot, the hybond membrane was rinsed in Neutralizing solution. The membrane was pre-hybridized in PerfectHyb–Plus Hybridization Buffer (Sigma) at 37˚C for 5 minutes before the 6-FAM labeled fluorescent probes were added at a concentration of 2nM final concentration

for each probe. The membrane was agitated with the probes for 3 hours at 37˚C. After hybridization, the membrane was washed in low-stringency wash buffer (2X SSC, 0.1% SDS). The membrane was imaged under the ChemiDoc MP system under the Fluorescein setting. Six southern hybridization probes 48-64 base pairs long were designed to cover 11 HspII sites within the CGI2 DMR of GRB10. These probes were synthesized with 6-FAM at Sigma Aldrich.

Table 14.1 Southern Blot GRB10 6-FAM probes

Name	Target	Species	Sequence	Label	HpaII sites
South_GRB10_Probe_1	GRB10 CGI2	Human	GGC CCG GGT AGG GCT TCG GGG CCC GGC CCC CGC AGT GCC CGG CGC GTG GAC	6-FAM	3
South_GRB10_Probe_2	GRB10 CGI2	Human	AGC GCT CCG CAT GGA CAG CGC TCG GAG CCG GGC CGG GCT GGT CCT CCA	6-FAM	2
South_GRB10_Probe_3	GRB10 CGI2	Human	CGG CTC CGC CCC GGC CAG GGG CCT GCG GCG CAG AAA ACC GAC CCG GGG CCT	6-FAM	2
South_GRB10_Probe_4	GRB10 CGI2	Human	CGG GGC CAC CGC	6-FAM	0

			GCG CCA GGC GAA CGC GCT AGC ACG AAA AGC GGG CCA ACG		
South_GRB10_Probe_5	GRB10 CGI2	Human	CCG CCT CTG GGG ACG CCA TCC GGG CGA GGG TGG GAT GCC GCG CCA CCG CCC	6-FAM	1
South_GRB10_Probe_6	GRB10 CGI2	Human	GAG CGT GCC CGG GGG CTC CCA GCG CCA TCA CCA CGC AGG TGC CCG GGG GCC CCT CCG CGG AGC C	6-FAM	3

15 Appendix V–mESCs

15.1 Derivation of mESCs

Animal pairs were selected for mESC derivation to generate maternally and paternally derived KO cells and WT controls. Experienced mating pairs were preferred over new pairs. Females were whittened with activity tubes from male cages two days prior to mating. Four days after successful mating (determined by plug check the morning after pairing), females were sacrificed and the oviducts and uterine horns were dissected out. These were flushed with M2 media (Sigma) under a microscope to harvest the blastocysts and morulae. Harvested cells were washed in M2 and KSOM (Sigma) and cultured overnight in KSOM under oil in an incubator. The following day, blastocysts were split to individual drops of 2iL media (composition described above) with 1% Penicillin-Streptomycin (P/S; Sigma). The blastocysts hatch from the zona pellucida around Day 5 post-mating. 2iL media was partially changed as needed until Day 12, when the sphere of mESCs was split using StemPro Accutase (Thermofisher), dissociated with a finely pulled Pasteur pipette, and plated in 2iL + P/S on 0.1% gelatin in a 4-well plate. This split was marked passage 1 and media was changed as needed for ~10 days. Cells were split using accutase and dissociated with a 200µl micropipette tip to Matrigel hESC-qualified Matrix, LDEV-free (Scientific Laboratory Supplies, SLS). Once the line was established, cells were cultured in 2iL + P/S on matrigel and split every other day using accutase or TrypLE. Cell lines were frozen in KSR + 10% DMSO after a PBS wash.

15.1.1 Mycoplasma Testing

Derived mESC cultures were cultured in an isolation incubator until used media was tested for mycoplasma using the Mycoplasma PCR detection kit (Sigma).

15.1.2 Media and Solutions

15.1.2.1 Fibronectin solution preparation

PBS supplemented with 15µg/ml human plasma fibronectin (Millipore, # FC010, already diluted - stock 1mg/ml). Supplemented PBS was used to coat plates for culture.

15.1.2.2 2iL media

2iL media for mESC culture was prepared first as 2i (2 inhibitor) media with mouse recombinant LIF added to smaller aliquots prior to use.

SFES media 50 ml

Reagent	Source	[Stock]	Amt Stock	[Final]
Neurobasal medium	Thermofisher		24.5 ml	
Advanced DMEM/F12	Thermofisher		24.5 ml	
B27 (w/o retinol)	Thermofisher		500 µl	
Glutamax	Thermofisher	200 mM	500 µl	2 mM
β-mercaptoethanol	Thermofisher		50 µl	

2i media 50 ml

Reagent	Source	[Stock]	Amt Stock	[Final]
SFES media	See Above		50 ml	
PD03259010	Axon MedChem	10 mM	5 µl	1 µM
CHIR99021	ReproCELL	3 mM	50 µl	3 µM

2iL + P/S 50 ml

Reagent	[Stock]	Amt Stock	[Final]
2i media	See Above	50 ml	
Mouse Recombinant LIF		20 µl	1000 U/ml
Penicillin-Streptomycin	50 x	500 ul	0.5x

15.1.3 Murine Grb10 transcript q RT PRC primer targets

Murine qRT PCR primer targets for the major isoform of *Grb10* use primers from Plasschaert 2016, Grb101AF/R_qPCR. The forward primer targets the first exon.

Primer set: mGrb10 Set A or Grb101AF/R_qPCR

Forward primer	CACGAGTCACAACGGAGAAA
Reverse primer	CACGGGAGCACGAAGTTT

Murine qRT PCR primer targets for the neuron-specific transcript amplified a section of exon 1b, described as neuron-specific in Arnaud 2003. Primers to this region were designed using the NCBI primer design tool and the PCR template “AB106541.1 Mus musculus *Grb10* mRNA for growth factor

receptor-bound protein 10, partial cds". Exon 1b is also targeted by a different set of q RT PCR primers in Plasschaert 2016.

Primer Set: nGrb10 Set 1

Forward primer	**CCGCGATCATTCGTCTCTGA**
Reverse primer	GTTACATGCGCCAACACTGG

Expected product size: 107 bp